Remobilització dels contaminants orgànics persistents en els ecosistemes polars costaners

Paulo Casal Rodríguez
Barcelona, 2018

Universitat Politècnica de Catalunya
Programa de Doctorat en Ciències del Mar

UNIVERSITAT POLITÈCNICA
DE CATALUNYA
BARCELONATECH

Remobilització dels contaminants orgànics persistents en els ecosistemes polars costaners

Paulo Casal Rodríguez

ADVERTIMENT La consulta d'aquesta tesi queda condicionada a l'acceptació de les següents condicions d'ús: La difusió d'aquesta tesi per mitjà del repositori institucional UPCommons (http://upcommons.upc.edu/tesis) i el repositori cooperatiu TDX (http://www.tdx.cat/) ha estat autoritzada pels titulars dels drets de propietat intel·lectual **únicament per a usos privats** emmarcats en activitats d'investigació i docència. No s'autoritza la seva reproducció amb finalitats de lucre ni la seva difusió i posada a disposició des d'un lloc aliè al servei UPCommons o TDX. No s'autoritza la presentació del seu contingut en una finestra o marc aliè a UPCommons (*framing*). Aquesta reserva de drets afecta tant al resum de presentació de la tesi com als seus continguts. En la utilització o cita de parts de la tesi és obligat indicar el nom de la persona autora.

ADVERTENCIA La consulta de esta tesis queda condicionada a la aceptación de las siguientes condiciones de uso: La difusión de esta tesis por medio del repositorio institucional UPCommons (http://upcommons.upc.edu/tesis) y el repositorio cooperativo TDR (http://www.tdx.cat/?locale-attribute=es) ha sido autorizada por los titulares de los derechos de propiedad intelectual **únicamente para usos privados enmarcados** en actividades de investigación y docencia. No se autoriza su reproducción con finalidades de lucro ni su difusión y puesta a disposición desde un sitio ajeno al servicio UPCommons No se autoriza la presentación de su contenido en una ventana o marco ajeno a UPCommons (*framing*). Esta reserva de derechos afecta tanto al resumen de presentación de la tesis como a sus contenidos. En la utilización o cita de partes de la tesis es obligado indicar el nombre de la persona autora.

WARNING On having consulted this thesis you're accepting the following use conditions: Spreading this thesis by the institutional repository UPCommons (http://upcommons.upc.edu/tesis) and the cooperative repository TDX (http://www.tdx.cat/?locale-attribute=en) has been authorized by the titular of the intellectual property rights **only for private uses** placed in investigation and teaching activities. Reproduction with lucrative aims is not authorized neither its spreading nor availability from a site foreign to the UPCommons service. Introducing its content in a window or frame foreign to the UPCommons service is not authorized (framing). These rights affect to the presentation summary of the thesis as well as to its contents. In the using or citation of parts of the thesis it's obliged to indicate the name of the author.

Remobilització dels contaminants orgànics persistents en els ecosistemes polars costaners

Paulo Casal Rodríguez

Departament de Química Ambiental

Institut de Diagnosi Ambiental i Estudis de l'Aigua (IDAEA-CSIC)

Programa de doctorat:

CIÈNCIES DEL MAR

Tesi per compendi de publicacions

Memòria presentada per optar al grau de Doctor per la Universitat Politècnica de Catalunya

Director:	Tutor:
Dr. Jordi Dachs	Dr. Manuel Espino
IDAEA-CSIC	UPC

“There’s so much pollution in the air now that if it weren´t for our lungs there’d be no place to put it all”
Robert Orben

“SCIENCE: a way of finding things out and then making them work. Science explains what is happening around us the whole time. So does RELIGION, but science is better because it comes up with more understandable excuses when it’s wrong”
GNU Terry Pratchett

ÍNDEX

ABSTRACT (English)

Persistent Organic Pollutants (POPs) constitute a heterogenic group of chemical substances of environmental concern. Their persistence, bioaccumulation, long range transport potential and negative health and environmental effects, have led to their study and international regulation. As a consequence, there has been a decrease of the primary sources of some of these substances, notably legacy POPs. However, this decrease in primary emissions of some of these compounds, and the consequent decrease of their concentrations in the atmospheric compartment, favors the re-emission of POPs from soils, ice, snow and water to become secondary sources in the environment.

The Arctic and Antarctica are two remote regions on Earth, but they are nevertheless polluted by POPs. In Polar Regions, persistence is enhanced due to low temperatures. Atmospheric deposition can also be enhanced at low temperatures due to snow scavenging of atmospheric chemicals, and lower air-water and air-soil partition coefficients (a process called cold trapping). Biogeochemical controls, such as changing vegetation cover, degradation or the biological pump, have also been described as driving the trapping of POPs in polar ecosystems. All these processes promote the accumulation of POPs in soils, seawater and ice/snow in Polar Regions. Thus, these matrices have become reservoirs of legacy and emerging POPs in the polar environment. However, the aforementioned decrease in atmospheric concentrations coupled with increasing temperatures induced by the anthropogenic climate change can reverse the role of these compartments that previously acted as sinks. Furthermore, the ice retreat acts unequivocally as a source from an environmental compartment that is reducing its size on a global scale.

This process, known as remobilization, has received recent attention on the scientific community as it impacts the cycling and environmental fate of POPs. In the Arctic, recent studies have shown the influence of increasing temperatures and sea-ice retreat in atmospheric concentrations of several banned POPs, including polychlorinated biphenyls (PCBs), hexacyclochlorohexanes (HCHs) and DDT. In Antarctica, volatilization of PCBs and polycyclic aromatic hydrocarbons (PAHs) from snow and soil have been observed during the austral summer and linked to temperature and soil organic matter. Nevertheless, the quantification and prediction of these processes under an scenario of environmental change are limited to our current understanding of POP cycling during long-time periods at coastal regions.

Although previous observations confirm the occurrence of this process under certain circumstances, the cascading changes in the different environmental compartments and its effects in other cycling processes, on the local biota, and further along in human health, remain poorly understood. The relevance in the characterization of this process goes beyond these studied compounds, as there is a myriad of pollutants, “legacy” and emergent, that present a range of physical chemical properties with various transport pathways to remote regions and multimedia partitioning.

In the present thesis, remobilization processes were studied on rellevant environmental compartments from an Arctic and Antarctic coastal sites and for chemicals with a wide range of physico-chemical properties.

In the arctic site (Tromsø, Norway), the soil/snow-air exchange of PCBs, PAHs and organochlorine pesticides (OCPs) was evaluated over a 14-month sampling period. In general, atmospheric concentrations and the diffusive exchange with soil/snow followed seasonal patterns closely linked to air temperature, with net-volatilization occurring during the warmer months. However, notable differences were observed between the different POP families, which are discussed in detail.

At coastal Livingston Island (Antarctica), the remobilization of perfluoroalkyl substances (PFASs), PAHs, OCPs and PCBs were assessed from the samples and measurements performed during a 3-month multicompartmental sampling campaign. This sampling effort included, for the first time, concurrent sampling of plankton, seawater, snow (including snowmelt and freshly deposited snow), air and the determination of several fugacities, diffusive exchange fluxes and mass balances, among other analyses. Snow deposition and seasonal snow melting were established as key factors for all the studied compounds in the cycling of POPs in coastal polar environments. Ice and snow melting, linked to temperature changes, influenced coastal seawater POPs concentrations, and as a result induced the re-emission of the most volatile POPs to the atmosphere. Even PFASs, which were thought to be primarily controlled by oceanic transport, proved to be heavily influenced by the marine aerosol scavenging during snow deposition and land to seawater snow-melt fluxes. Dissolved phase concentrations or volatilization fluxes showed correlations with temperature, further supporting the pivotal role of snow melting supporting the concentrations in the coastal zone. The resulting plankton concentrations in the Antarctic coastal environment were determined for all the target families, as it constitutes a key element in the biological pump process and the first step in the bioaccumulation and trophic transfer in marine food webs.

RESUM (català)

Els contaminants orgànics persistents (POPs) constitueixen un grup heterogeni de substàncies químiques de gran rellevància ambiental. La seva persistència, bioacumulació, potencial de transport de llarg abast i efectes negatius en salut i medi ambient, han conduït al seu estudi i regulació internacional. Com a conseqüència, s'ha produït una disminució de les fonts primàries d'algunes d'aquestes substàncies, especialment els "legacy" POP. No obstant això, aquesta disminució de les emissions primàries d'alguns d'aquests compostos i la conseqüent disminució de les seves concentracions en el compartiment atmosfèric, afavoreix la reemissió de POPs procedents de sòls, gel, neu i aigua per convertir-se en fonts secundàries en el medi ambient.

L'Àrtic i l'Antàrtida són dues regions remotes de la Terra, no obstant estan contaminades per POPs. A les regions polars, la persistència es veu incrementada a causa de les baixes temperatures. La deposició atmosfèrica també és incrementada a baixes temperatures gràcies a la recollida de compostos químics presents a l'atmosfera per la deposició de neu, i als baixos coeficients de partició aire-aigua i aire-sòl (un procés conegut com a "cold trapping"). També s'ha descrit controls biogeoquímics, com el canvi en la coberta vegetal, la degradació o la bomba biològica, que dirigeixen la captura de POPs en els ecosistemes polars. Tots aquests processos promouen l'acumulació de POPs en sòls, aigua de mar i gel/neu a les regions polars. Per tant, aquestes matrius s'han convertit en reservoris de POPs "legacy" i emergents en l'ecosistema polar. No obstant això, l'esmentada disminució en les concentracions atmosfèriques, juntament amb l'augment de les temperatures induït pel canvi climàtic antropogènic, pot revertir el paper d'aquests compartiments que prèviament van

actuar com a embornals. A més, la retirada de les glaceres actua inequívocament com una font d'un compartiment ambiental que està reduint la seva mida a escala global.

Aquest procés, conegut com remobilització, ha rebut una atenció recent a la comunitat científica, ja que té un impacte en la compartimentació i la destinació ambiental dels POPs. A l'Àrtic, estudis recents han demostrat la influència de l'augment de les temperatures i del retrocés del gel marí a les concentracions atmosfèriques de diversos POPs, inclosos policlorobifenils (PCBs), hexaclorociclohexans (HCHs) i DDT. A l'Antàrtida, durant l'estiu austral s'ha observat la volatilització de PCBs i hidrocarburs aromàtics policíclics (PAHs) de la neu i el sòl, associada als canvis en la temperatura i la matèria orgànica del sòl. No obstant això, la quantificació i predicció d'aquests processos sota un escenari de canvi ambiental es limitat a la nostra comprensió actual del cicle dels POPs durant períodes prolongats en les regions costaneres.

Tot i que observacions prèvies confirmen l'ocurrència d'aquest procés sota certes circumstàncies, els canvis en cascada en els diferents compartiments ambientals i els seus efectes en altres processos, en la biota local i en la salut humana, segueixen sent poc coneguts. La rellevància en la caracterització d'aquest procés va més enllà d'aquests compostos estudiats, ja que hi ha una gran quantitat de contaminants, "legacy" i emergents, amb una àmplia gamma de propietats físico-químiques, rutes de transport a regions remotes i compartimentació ambiental pròpies .

En la present tesi, es van estudiar els processos de eliminació en compartiments ambientals rellevants d'una zona costanera ártica i una antàrtica, per a compostos amb una àmplia gamma de propietats físico-químiques.

A l'àrea de mostreig àrtica (Tromsø, Noruega), es va avaluar l'intercanvi sòl/neu-aire de PCBs, PAHs i pesticides organoclorats (OCPs) durant un període de mostreig de 14 mesos. En general, les concentracions atmosfèriques i l'intercanvi difusiu amb sòl/neu van seguir patrons estacionals estretament relacionats amb la temperatura de l'aire, i es va observar volatilització neta durant els mesos més càlids. No obstant això, es van observar notables diferències entre les diferents famílies de POPs, que són discutides en detall.

A la costa de l'illa de Livingston (Antàrtida), la remobilització de substàncies de perfluoroalquilades (PFASs), PAHs, OCPs i PCBs es van avaluar a partir de mostres i mesuraments realitzats durant una campanya de mostreig multicompartimental de 3 mesos. Aquest esforç de mostreig va incloure, per primera vegada, el mostreig simultani de plàncton, aigua de mar, neu (incloent neu fosa i neu recent dipositada), aire i la determinació de diverses fugacitats, fluxos d'intercanvi difusiu i balanços de massa, entre d'altres anàlisi. La deposició de neu i el desglaç estacional van ser establerts com a factors clau per a tots els compostos estudiats en el cicle dels POPs en els ambients polars costaners. La fusió del gel i la neu, vinculat als canvis de temperatura, va influir en les concentracions de POPs en l'aigua costanera, i com a resultat va induir la reemissió dels POPs més volàtils a l'atmosfera. Fins i tot els PFAS, que es considerava que eren controlats principalment pel transport oceànic, van demostrar estar fortament influenciats per la recol·lecció d'aerosols marins durant la deposició de neu i els fluxos de fusió de neu de terra a aigua de mar. Les concentracions de fase dissolta o els fluxos de volatilització van mostrar correlacions amb la temperatura, la qual cosa dóna encara més suport al paper fonamental de la fusió de la neu que dirigeix les concentracions a la zona costanera. Les concentracions resultants de plàncton en el medi costaner antàrtic es van determinar per a totes les famílies objectiu, ja que constitueixen un element clau en el procés de bomba biològica i són el primer pas en la bioacumulació i la transferència a les xarxes tròfica marines.

Capítol 1: Introducció

Capítol 1: Introducció

1.1 Els contaminants orgànics persistents

A l'actualitat es produeixen i utilitzen més de 200.000 substàncies químiques sintètiques amb fins industrials, agrícoles i domèstics (Muir i Howard 2006). Milers d'aquestes substàncies s'alliberen al medi ambient i s'han descrit efectes nocius a escala ecosistèmica, de comunitat i d'organisme de part d'elles. Malgrat tot, per una vasta majoria d'aquestes substàncies no es disposen estudis que valorin els seus efectes en el medi ambient. La presència d'aquesta ingent quantitat de substàncies químiques sintètiques, unides a les ja creades amb anterioritat i que encara persisteixen en els nostres ecosistemes constitueix una de les característiques pròpies del antropocè, atesos els canvis que aquestes indueixen en la composició química de la biosfera (Dachs i Méjanelle 2010).

Entre aquestes substàncies es troben els anomenats contaminants orgànics persistents (“persistent organic pollutants” o POPs) que constitueixen un grup divers de compostos orgànics, tòxics, persistents, i propensos a la bioacumulació i al transport a llargues distàncies. Degut a la preocupació internacional relacionada amb aquests productes químics, l’any 2001 el Programa de les Nacions Unides per al Medi Ambient (PNUMA) va promoure l'adopció del Conveni d'Estocolm per protegir la salut humana i el medi ambient dels POPs. Aquest conveni recollia el compromís de reduir o eliminar la producció, ús i/o alliberament de 12 POPs prioritaris, als quals es van anar sumant altres a posteriori, fins arribar a 25 compostos actualment (Taula 1.1). A més d'aquesta llista de POPs, el 2003 amb el Conveni sobre la Contaminació Atmosfèrica Transfronterera a Gran Distància (CLRTAP) de la Comissió Econòmica de les Nacions

Unides per a Europa (UNECE) es van adoptar prohibicions similars d'una llista de 16 POPs que també va ser ampliada posteriorment (Taula 1.1).

Conveni d'Estocolm			
Annex A. Eliminació		**Annex B. Prohibició**	**Annex C. Producció inintencionada**
Aldrín Clordà Clordecona Dieldrina Èter de Pentabromodifenil Endrina Endosulfan Heptaclor	Hexaclorobenzè Hexaclorociclohexans Lindà Mirex PBB PBDE PCBs Pentaclorobenzè Toxafè	Àcid sulfònic de perfluorooctà, les seves sals i fluorur de sulfonil perfluorooctà DDT	Dioxines i furans Hexaclorobenzè PCBs

Conveni sobre la Contaminació Atmosfèrica Transfronterera a Gran Distància		
Àcid sulfònic de perfluorooctà, les seves sals, i fluorur de sulfonil perfluorooctà Aldrín Clordà Clordecona DDT 9Dieldrina Èter de hexabromodifenil	Endosulfan Endrina Hexaclorociclohexans Heptaclor Hexabromobifenil Hexaclorobenzè Hexaclorobutadiè Lindà Toxafè	Mirex PBDE PCB Pentaclorobenzè Naftalens policlorats Parafines clorades de cadena curta

Taula 1.1. Llista de contaminants orgànics persistents inclosos en el Conveni d'Estocolm i el Conveni sobre la Contaminació Atmosfèrica Transfronterera a Gran Distància.

Aquestes llistes, que recullen i defineixen els POPs regulats, en base a unes característiques fisicoquímiques comuns, són llistes incompletes ja que hi ha molts altres POPs amb característiques semblants però que encara han estat poc estudiats (Muir i Howard 2006). Així mateix, malgrat que puguin no complir tots els requisits per ser considerats POPs, alguns compostos s'inclouen en aquestes regulacions. Aquest últim és el cas dels hidrocarburs aromàtics policíclics (PAHs), que s'inclouen al Protocol d’Aarhus de la UNECE i en el Conveni sobre la Contaminació Atmosfèrica Transfronterera a Gran Distància (CLRTAP) malgrat que no presenten la mateixa persistència que altres POPs. L'Agència de Protecció Ambiental dels Estats Units (EPA) també ha assenyalat la necessitat de mesurar en mostres ambientals els nivells de 16 PAHs prioritaris: naftalè, acenaftilè, acenaftè, fluorè, fenantrè, antracè, fluorantrè, benzo[a]antracè, crisè, pirè, benzo[b]fluorantè, benzo[k]fluorantè, benzo[a]pirè, dibenzo[a, h]antracè, benzo[g,h,i]perilè, indeno[1,2,3-c,d]pirè. Tenint en compte aquestes consideracions en aquesta tesi es fa referència als PAHs com a POPs excepte quan s'especifica d'una altra manera.

1.2 Propietats fisicoquímiques dels POPs i els coeficients de partició

Els POPs tenen unes característiques fisicoquímiques comuns dins d'un rang (Taula 1.2). Aquestes propietats fisicoquímiques juguen un paper fonamental en el seu transport a llarga distància, la seva persistència i els seus processos de bioacumulació i algunes d'elles constitueixen un criteri per a classificar-los com a POPs (Taula 1.2).

Propietat	Criteri per a ser definit com POP
Potencial per a transport atmosfèric a llarga distància	Pv^a < 1000 Pa Vida mitjana a l'aire > 2 dies Presència en regions remotes
Persistència	Vida mitjana a l'aigua > 2 mesos Vida mitjana en sòls > 6 mesos Vida mitjana en sediments > 6 mesos
Bioacumulació	Log $K_{OW}{}^b > 5$ $BCF^c > 5000$ Evidència d'alta toxicitat

Taula 1.2. Característiques definitòries de POPs segons la UNECE. [a]Pressió de vapor [b]Coeficient de partició octanol - aigua [c] Factor de bioconcentració

-Pressió de vapor (Pv): La pressió de vapor és la pressió exercida per gas sobre les seves formes condensades (sòlid o líquid) en una temperatura determinada en un sistema tancat. Es relaciona amb la tendència de les partícules a escapar del líquid (o sòlid) i es mesura en pascals (Pa). Els compostos orgànics amb Pv més elevada tenen una major tendència a la partició a l'atmosfera i al transport atmosfèric a llarga distància.

-Solubilitat en aigua (S_W): la solubilitat en aigua és la concentració màxima d'una substància química a l'aigua quan es troba en contacte amb el compost pur (sòlid, líquid o gas). Els compostos orgànics no iònics tendeixen a tenir baixes solubilitats a l'aigua, i el seu valor depèn de la polaritat del solut i de la temperatura. Les seves unitats en el sistema internacional són mol m^{-3}. Els compostos amb solubilitat elevada són comparativament més propensos a la partició a l'aigua, i al transport oceànic.

-Solubilitat en octanol (S_{OCT}): La solubilitat en la matèria orgànica és la concentració saturada del solut dissolt l'orgànica matèria orgànica (absorció) quan està en equilibri amb el compost pur. El octanol s'utilitza com a "surrogate" de la matèria orgànica, atès que la composició de la matèria orgànica presenta una variabilitat que dificulta tabularla. La majoria dels POPs són altament hidrofòbics, és a dir, tenen una alta tendència a la partició a la matèria orgànica i lípids de partícules i organismes.

-Bioacumulació: La bioacumulació es coneix com un procés en el qual la concentració d'un compost en un organisme arriba a un nivell que excedeix el del mig respiratori (per exemple, aigua per a un peix o aire per a un mamífer), mitjançant la difusió directa del compost, la dieta, o tots dos (Gobas et al., 2009). El grau en què els POPs es bioacumulen s'expressa generalment mitjançant el factor de bioconcentració (BCF) si la incorporació del contaminant es per difusió passiva o el factor de bioacumulació (BAF) si la incorporació del compost és per dieta i difusió.

Aquestes propietats fisicoquímiques són a més determinants en la distribució preferencial dels POPs entre la fase gas, aigua i octanol, és a dir, en la compartimentació ambiental (Figura 1.1). La compartimentació dels POP entre els diferents compartiments ambientals es pot expressar mitjançant coeficients de partició com K_{AW} (aire-aigua), K_{OA} (octanol-aire) o K_{OW} (octanol-aigua) (Figura 1.1), on s'expressa el quocient entre les concentracions d'un determinat component presents en dues fases en equilibri ($K_{ij} = C_i / C_j$).

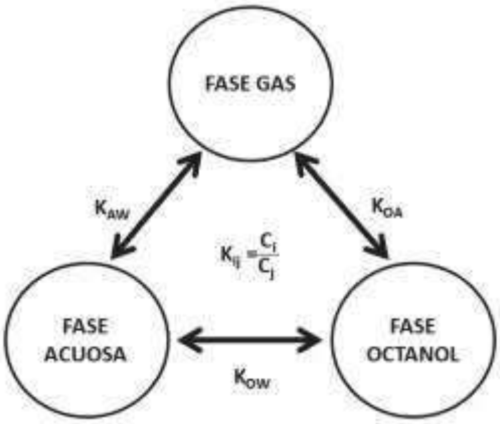

Figura 1.1. Diagrama dels coeficients de partició K_{AW}, K_{OA} i K_{OW} i la seva relació entre la compartimentació dels contaminants entre l'aire, l´aigua i l´octanol (matèria orgànica).

Hi ha diverses formes d'obtenir o calcular els coeficients de partició: i) es poden obtenir a partir de la mesura de les concentracions de camp del compost en cada fase si es compleixen les condicions d'equilibri; ii) poden ser mesurats directament sota condicions controlades en estudis de laboratori; o iii) en absència de dades empíriques, es poden estimar a partir de models empírics o teòrics.

Aquests coeficients de partició constituïen una mesura de la volatilitat (K_{AW}) i l'hidrofobicitat tant medi aquàtic (K_{OW}) com terrestre (K_{OA}). En termes generals, els POPs considerats en aquesta tesi presenten una correlació directa entre el seu pes molecular (MW) i la seva hidrofobicitat, i un correlació inversa amb la seva volatilitat. De manera que els compostos més lleugers tendeixen a trobar-se preferencialment en el compartiment atmosfèric i presenten un major potencial per al transport atmosfèric a llarga distància, mentre que els més pesats tenen una tendència major a la seva unió a partícules i a la bioacumulació. La majoria dels POPs regulats presenten valors de K_{AW} entre 10^{-1} i 10^{-4}, K_{OW} entre 10^{3} i 10^{8}, i de K_{OA} entre 10^{5} i 10^{12} (Figura 1.2, Wania i Mackay, 1999). La compartimentació de POPs en fases orgàniques és, per tant, de 3 a 8 ordres de magnitud més elevat que a l'aigua i de 5 a 12 ordres de magnitud superior que a l'atmosfera. Malgrat això, hi ha algunes famílies de POPs com les substàncies perfluoradas (PFAs) que estan fora d'aquest rang de propietats fisico-químiques.

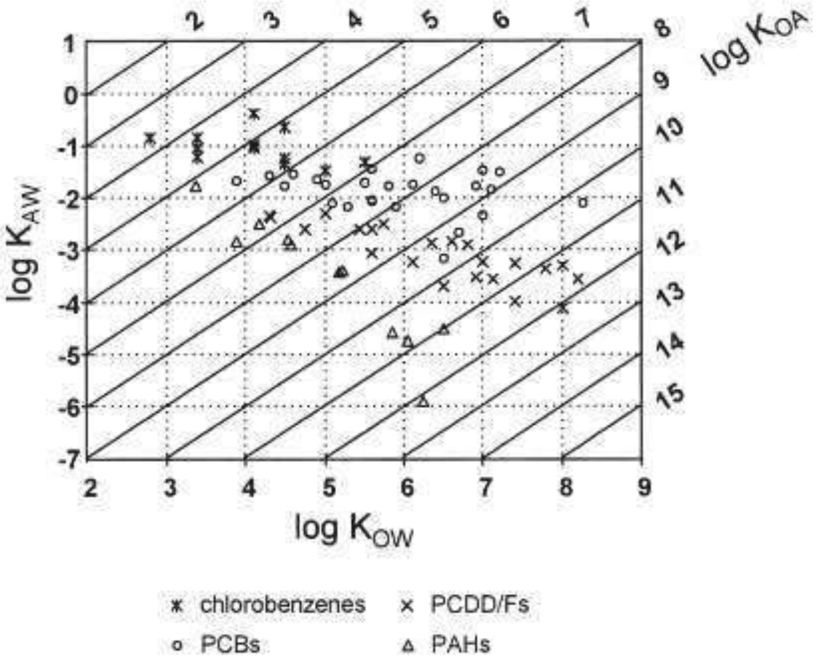

Figura 1.2. L'espai de partició K_{OW} (eix x), K_{AW} (eix y) i K_{OA} (diagonal) (Wania i Mackay 1999)

1.3 Fonts, vies i distribució global dels POPs

En funció del seu origen podem distingir entre fonts primàries i secundàries dels POPs. L'emissió directa constitueix la font primària, per exemple l'emissió a l'aire de compostos volàtils (o semivolàtils) en zones industrials o l'aplicació en camp de pesticides organoclorats. Després de la seva emissió, els POPs es poden acumular en diferents dipòsits globals com els sòls, els glaciars o els oceans, en funció del punt en què van ser alliberats inicialment, els processos transport dominants i les propietats específiques dels POPs (volatilitat, persistència, hidrofobicitat, etc.). Posteriorment, aquests dipòsits poden reemetre els POPs per al seu transport, constituint així una font secundària. Per exemple, contaminants que han estat acumulats en sòls poden ser revolatilitzats (o **remobilitzats**) sempre que es donin unes condicions que afavoreixin la volatilització d'aquests compostos, com ara un augment en la temperatura i/o un descens en les concentracions atmosfèriques. També en aquesta remobilització influeixen els paràmetres fisicoquímics del compost, sent més propensos a la volatilització els compostos amb menor pes molecular. La regulació de POPs com els PCBs, normalment referenciats com "legacy POPs", va comportar una important disminució de les seves fonts primàries a escala global. No obstant, l'elevada persistència dels POPs i la seva acumulació en aquests dipòsits durant dècades fa que les fonts secundàries cobrin importància al llarg del temps. Aquestes fonts secundàries retarden així les tendències de disminució de concentracions atmosfèriques de POPs, que a més presenten variacions en funció del a ubicació, el període de temps i els compostos específics (Hung et.al. 2005, Nizzeto et al., 2010a, 2010b).

Els prèviament descrits coeficients de partició son determinants en el transport global dels POPs, en funció aquests coeficients, un compost serà més o menys propens a trobar-se en una fase en concret i a ser transportat preferencialment en aquesta fase (Figura 1.3).

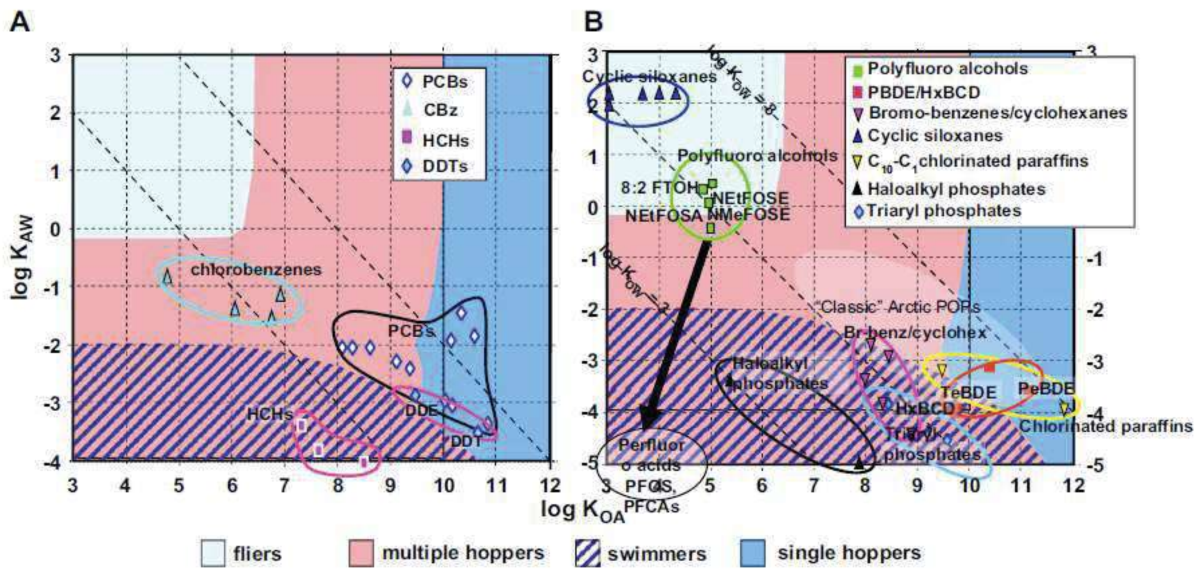

Figura 1.3. Espai de fases (K_{AW} versus K_{OA}) de diverses famílies de contaminants orgànics històrics (A) i emergents (B).

Pels compostos volàtils i semivolàtils, la principal via de transport a llarga distància és el transport atmosfèric. A escala global, la distribució dels POPs semivolàtils es van explicar inicialment per les teories de destil·lació global i de l 'efecte "Grasshopper" (Wania i Mackay, 1993, 1996). La teoria de destil·lació global explicaria que aquells compostos amb una major mobilitat serien preferencialment acumulats en zones polars, degut a que arribarien a aquestes amb una major facilitat i sent la absorció/evaporació un procés dependent de la temperatura, tendirien en el temps a acumular-se en aquestes zones més fredes a una taxa més accelerada que compostos amb una menor mobilitat, que presentarien una tendència major a quedar-se prop de la seva font primària (Figura 1.4). Aquest procés a més es veuria facilitat per l'efecte "Grasshopper", segons el qual els compostos semivolàtils passarien per una sèrie de successius cicles de deposició i reemissió, que també afavoriria preferencialment el desplaçament i acumulació en zones fredes dels compostos més mòbils (Figura 1.4).

Malgrat que el procés de “grasshopping” permet explicar el transport a llarga distancia, i fluxes de volatilitizació i absorció s’han mesurat en nombrosos estudis (Lohmann et al., 2007), hi ha poca evidencia experimental de que la distribució global dels POPs semivolátils segueixin aquesta distribució amb una major abundancia dels compostos menys volàtils a les zones polars. Diversos estudis teòrics i experimentals han sugerit altres procesos com a responsables de les concentracions i distribucions dels contaminants orgànics a diferents latituds.

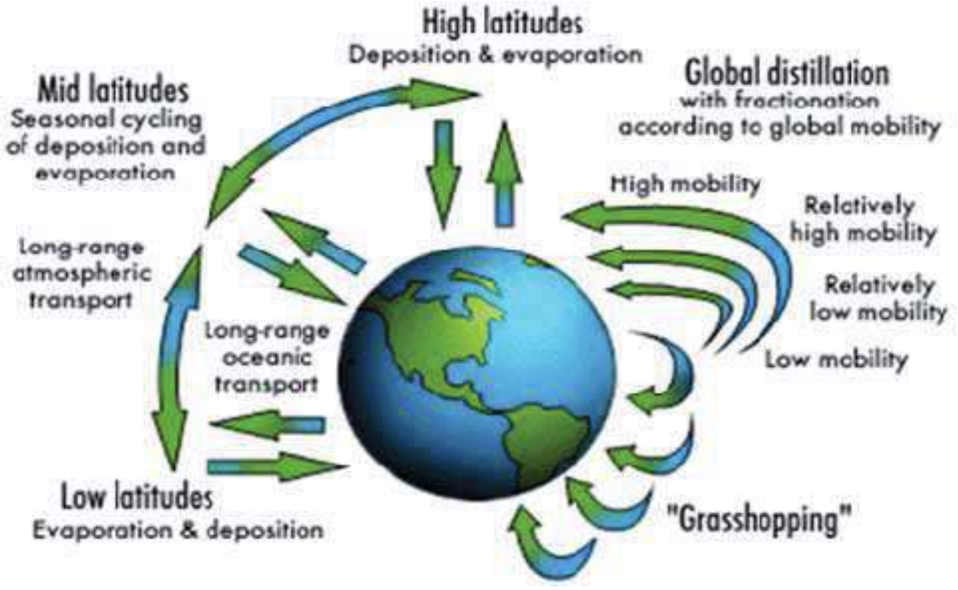

Figura 1.4. Processos de migració global dels POPs segons Wania i Mackay (1996).

Els contaminants també són transportats a escala global per les corrents oceàniques. Tot i que el transport oceànic és comparativament molt més lent que el transport atmosfèric, pot ser important per aquells compostos que es compartimenten preferencialment cap a l'aigua, com per exemple les substàncies perfluoroalquilades (PFASs) iòniques (Nash et al., 2010). La dependència dels corrents oceànics presenta certes limitacions en aquesta forma de transport, per exemple, la Corrent Circumpolar

Antàrtica que flueix d'oest a est al voltant de l'Antàrtida, presenta un transport molt limitat en direcció nord-sud, actuant així de barrera física en el transport de POPs al continent (Nash et al., 2010, 2011).

Els oceans a més constitueixen un dels principals dipòsits dels POPs (Jurado et al., 2004, Lohmann et al., 2006), especialment si tenim en compte el transport vertical de POPs a les zones profundes (Dachs et al., 2002, Lohmann et al., 2013). Aquest transport vertical es veu mediat per factors biòtics i abiòtics. D'una banda la formació d'aigües oceàniques profundes, que es produeix com a part de la circulació termohalina global, deguda als gradients en la salinitat i la temperatura, actua com a "bomba física" dels POPs cap a aigües profundes (Lohmann et al., 2006). D'altra banda, atès que la hidrofobicitat dels pops els fa propensos a la seva unió a la matèria orgànica, l'enfonsament de la matèria orgànica particulada comporta un altre mecanisme de transport vertical POPs, especialment efectiu en zones d'elevada productivitat (Dachs et al., 1999, 2000 Lipiatou et al., 2003, Jurado i Dachs, 2008). Aquest flux descendent de POPs lligats a la matèria orgànica pot disminuir les concentracions de POPs en la superfície de l'oceà, modificant així la magnitud de l'intercanvi difusiu aire-aigua, en el procés conegut com "bomba biològica" (Galbán-Malagón et al., 2012, Nizzetto et al., 2012).

Un decreixement de les concentracions en la fase dissolta, modificant els fluxes de deposició atmosfèrica, també pot ser degut a la degradació biòtica i abiòtica en la zona fòtica. Aquest procés, conegut com a bomba degradativa, ha estat descrit pels PAHs i els hexaclorociclohexans (HCHs) (Castro-Jiménez et al., 2012, Galbán-Malagón et al., 2013).

En les zones polars, tant la bomba biològica com la degradativa juguen un paper important en els fluxes de deposició atmosfèrica de contaminants a mar obert. A més, en les zones polars, hi ha altres controls físics y biogeoquímics. Un d'ells es el paper poc estudiat de la neu com a amplificadora de concentracions (Meyer i Wania 2008), i els canvis dels continguts de materia orgànica en els sols costaners com a reserva de POPs (Cabrerizo et al., 2012, 2013). Es el conjunt de tots aquestes variables i processos físics i biogeoquímics que poden explicar la distribució complexa dels POPs a escala global i regional.

1.4 Contaminants orgànics

1.4.1 Els policlorobifenils (PCBs)

Els policlorobifenils (PCBs) són una sèrie de compostos organoclorats que es van començar a sintetitzar en els anys 20 i que van arribar al seu màxim de producció a finals de la dècada de 1970. Van ser emprats en una àmplia gamma de productes industrials i de consum com fluids de transferència de calor en transformadors i condensadors, en plastificants, adhesius, tints, segelladors i recobriments per a superfícies (Vallack et al., 1998). La seva estructura química general és un bifenil amb entre un i deu àtoms de clor (Figura 1.5).

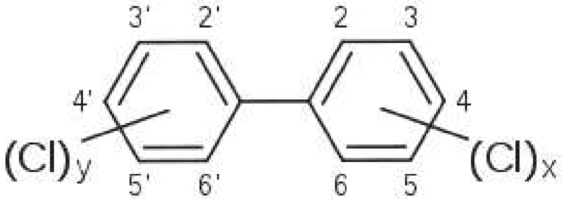

Figura 1.5. Estructura general d'un PCB.

Aquesta estructura permet la possibilitat de 209 congèneres, i es coneix ús comercial d'uns 100 d'ells. El nombre d'àtoms de clor així com les seves diferents posicions determinen un ampli rang de propietats fisicoquímiques (Taula 1.3) que alhora determinen la compartimentació ambiental de cada un dels congèneres (Vallack et al., 1998).

Compost	Estructura química	Pv (Pa)	Log K_{OW}	Log K_{OA}
PCB18	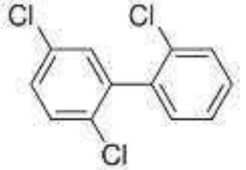	0.0904[a]	5.6[a]	7.6[b]
PCB28	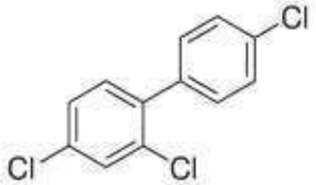	0.0277[a]	5.6[a]	8.2[b]
PCB52	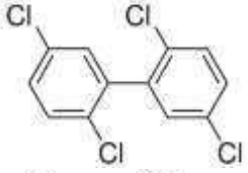	0.0192[a]	5.8[a]	8.3[b]
PCB70	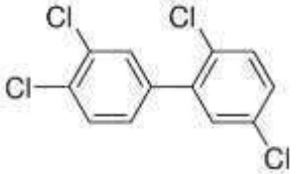	0.0052[a]	5.9[a]	9.2[b]
PCB110	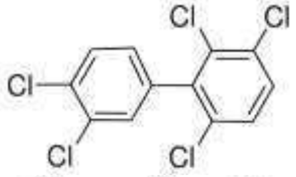	0.0023[a]	6.5[a]	9.3[b]
PCB138	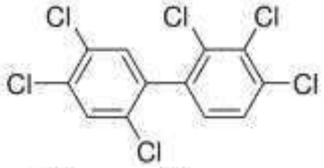	0.00049[a]	6.6[a]	9.8[b]
PCB153	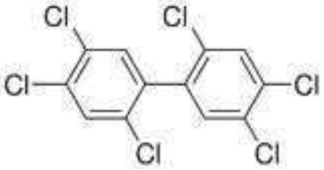	0.00066[a]	6.9[a]	9.7[b]
PCB180	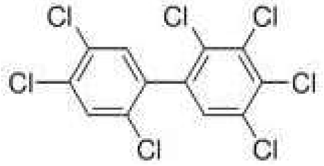	0.000506[a]	7.2[a]	10.5[b]

Taula 1.3. Estructura molecular i propietats fisicoquímiques dels PCBs. [a](Mackay et al. 1992) [b](Jonker i Koelmans 2001,2002)

L'enllaç carboni-clor és molt estable enfront de la hidròlisi de manera que com més gran és el nombre de substitucions de clor més gran és la resistència a la degradació biològica i fotolítica d’aquests compostos (Kannan et al., 1988). En conseqüència, els congèneres altament clorats tendeixen a bioacumular en major mesura que els menys clorats (Kannan et al., 1988). Així mateix, solubilitat en aigua i la pressió de vapor disminueixen amb l'augment de substitucions de clor, mentre que la hidrofobicitat i tendència de sorció va en augment.

La toxicitat dels PCBs també varia en un ampli rang segons els congèneres, sent especialment tòxics els PCBs coplanars ja que poden presentar propietats similars a les de les dioxines (Van den Berg et al., 1998). Els seus efectes tòxics són d'un ampli espectre, sent símptomes comuns de l'exposició aguda les lesions oculars i dermals, immunodepressió o irregularitat menstrual entre d'altres (Takamatsu et al., 1985), a més d'estar reconegut com carcinogènic (EPA 2013).

1.4.2 Pesticides organoclorats (OCPs)

1.4.2.2 Hexaclorobencè (HCB)

L' HCB es va introduir per primera vegada el 1933 com un fungicida sobre les llavors de ceba i cultius com el blat, l'ordi, la civada i el sègol (Barber et al., 2005). L'ús agrícola de HCB dominava les seves emissions durant les dècades de 1950 i 1960 i va arribar al seu màxim de producció, per sobre de les 100000 tones per any, en els anys 70 (Barber et al., 2005). També es generat com a subproducte de la fabricació d'una gran quantitat de productes químics clorats, es troba com a impuresa en molts pesticides i pot ser alliberat accidentalment en processos de combustió incompleta, per exemple en la incineració d'abocadors (Jacoff et al., 1986).

L'HCB té una volatilitat elevada i valors moderats de K_{OA} i K_{OW} en comparació amb altres POPs (Taula 1.4). Aquestes propietats determinen que l'HCB pot considerar-se un "multiple hopper" i pot distribuir-se globalment en una sèrie de cicles de volatilització-deposició (Wania i Mackay, 1996). A més, l'HCB és altament persistent en el medi ambient, té una llarga vida mitjana en l'aire, l'aigua i els sediments i un potencial de bioacumulació relativament alt (Mackay et al., 1992).

Compost	**Estructura química**	**Pv (Pa)**	**Log K_{OA}**	**Log K_{OW}**
HCB	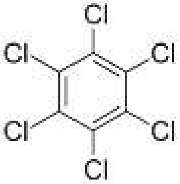	0.303^{a}	5.64^{b}	6.78^{c}

Taula 1.4. Estructura molecular i propietats fisicoquímiques del HCB. [a](Hincley et al., 1990), [b](Shen i Wania, 2005), [c](Harner i Mackay, 1995)

1.4.2.3 Hexaclorociclohexans (HCHs)

El HCH està disponible en dues mescles tècniques: i) l'HCH "tècnic" una que conté els diferents isòmers, inclosos α-, β-, γ- i δ-HCH (la barreja pot variar entre 55.70% de α-HCH, 5-14% de β -HCH i 10-18% de γ-HCH amb una quantitat menor de δ-HCH i altres impureses) i ii) una altra que conté exclusivament γ-HCH, també conegut com lindà. Al voltant de 10 milions de tones d'HCH tècnic han estat alliberades en els últims 60 anys, arribant al màxim de producció als anys 1970 i 1980, i sent més del 80% emès per països de l'Hemisferi Nord (Li, 1999). Tot i que el HCH avui dia està en desús, les aplicacions de lindà encara continuen en molts països i les seves emissions s'han estimat en 720.000 tones durant els últims 40 anys (Voldner, 1995).

Va ser utilitzat com a pesticida per tot el món, sent el lindà l'isòmer més actiu con insecticida d'ampli espectre.

Des de la seva regulació, hi ha hagut una tendència clara en la reducció d'emissions primàries i es correlaciona amb una disminució de les concentracions atmosfèriques d'HCH (Li i Bidleman, 2003, Li i Macdonald, 2005).

En comparació amb altres OCPs, els HCHs exhibeixen una solubilitat en aigua i pressions de vapor relativament altes i són molt menys lipofílics (Taula 1.5). Per tant, els HCH generalment són presents en l'ambient en la fase gas o en la fase aquosa, amb només un petit percentatge adsorbit sobre partícules, el que promou el seu transport atmosfèric i la seva distribució mundial (Walker et al., 1999).

Compost	**Estructura química**	**Pv (Pa)**	**Log K_{OW}**	**Log K_{OA}**
α-HCH	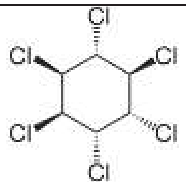	0.1^{a}	3.94^{b}	7.464^{b}
β-HCH	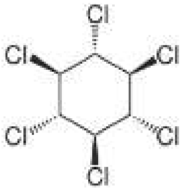	0.053^{b}	3.92^{b}	8.74^{b}
γ-HCH	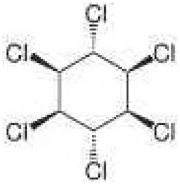	0.3^{a}	4.14^{c}	8.848^{d}
δ-HCH	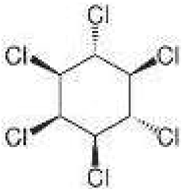	0.073^{c}	3.83^{b}	7.74^{b}

Taula 1.5. Estructura molecular i propietats fisicoquímiques del HCHs. [a](Mackay et al., 1992), [b](Xiao et al., 2004), [c](Hansch et al., 1995), [d](Shoeib i Harner, 2002)

1.4.3 Hidrocarburs aromàtics policíclics (PAHs)

Els hidrocarburs aromàtics policíclics (PAHs) són compostos químics constituïts per àtoms de C i H formant anells benzènics. Aquests contaminants poden tenir des d'estructures simples de dos anells, com el naftalè, fins a estructures de 6 anells com el benzo[g,h,i]perilè. Així mateix, posseeixen un rang ampli de característiques fisicoquímiques (Taula 1.6) amb compostos altament volàtils com el naftalè, que es troben principalment en la fase gas, i altres més pesats com el Benzo[g,h,i]perilè, que tendeixen a trobar-se associats a partícules atmosfèriques, matèria orgànica del sòl, carboni condensat ("soot carbon" o "Black carbon"), o lípids.

Provenen principalment de la combustió incompleta dels combustibles fòssils i de la matèria orgànica, tot i que també es poden arribar a generar a partir de processos biogènics (Wickström i Tolonen, 1987, Laflamme i Hites, 1978, Wilcke 2007). Hi ha processos de combustió naturals com els incendis forestals o les emissions volcàniques que contribueixen a l'emissió de PAHs, però la principal font d'emissions d'aquests compostos és el consum de biocarburants. La magnitud d'aquestes emissions els converteix en els compostos carcinògens més abundants i àmpliament distribuïts a la Terra (Harvey, 1991).

En comparació amb altres POPs, la vida mitjana dels PAHs és més reduïda, sent en els PAHs de menor pes molecular una vida mitjana des de minuts fins a unes poques hores a la fase gas, atès que poden ser degradats per processos de fotooxidació per radicals hidroxil . A més els PAHs poden ser biodegradats per microorganismes presents en sòl i aigua (Head et al., 2006, Zhang et al., 2006).

Compost	Estructura química	Pv (Pa)	Log K_{OW}	Log K_{OA}
Naftalè		11^{e}	3.3^{e}	
Acenaftilè		1.5^{a}	3.92^{a}	$6.4^{a,b}$
Acenaftè		4.1^{a}	3.94^{a}	
Fluorè		0.72^{a}	4.18^{a}	6.68^{c}
Fenantrè	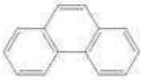	0.11^{a}	4.57^{a}	7.45^{c}
Antracè	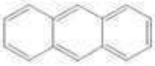	0.078^{a}	4.54^{a}	$6.94^{a,b}$
Fluorantrè		0.0087^{a}	5.22^{a}	8.84^{d}
Pirè		0.012^{a}	5.18^{a}	8.43^{c}
Benzo[a] antracè		0.00061^{a}	5.91^{a}	$10.80^{a,b}$
Crisè		0.00011^{a}	5.80^{a}	$10.40^{a,b}$
Benzo[b] fluorantè		$4.1x10^{-6a}$	5.78^{a}	$10.02^{a,b}$
Benzo[k] Fluorantè			6.40^{a}	$10.35^{a,b}$
Benzo[e] Pirè		$2.25x10^{-5a}$		
Dibenzo[a,h] Antracè	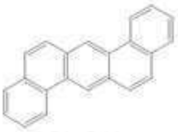	$9.2x10^{-8a}$	6.75^{a}	$13.91^{a,d}$
Benzo[g,h,i] Perilè		$1.39x10^{-8a}$	6.90^{a}	$13.07^{a,b}$

Taula 1.6. Propietats fisicoquímiques dels PAHs. [a](Mackay et al. 1992), [b](Bamford et al. 1999), [c](Harner i Bidleman, 1998), [d](Hulscher et al. 1992), [e](Shiu y Mackay 1997)

1.4.4 Substàncies perfluoroalquilades (PFASs)

Les substàncies perfluoroalquilades (PFASs), incloent els àcids perfluoroalquilcarboxílics (PFCAs) i perfluoroalquilsulfònics (PFSAs) (Taula 1.7), són compostos amb una cadena de carbonis perfluorada, on tots els hidrògens son substituïts per fluor, en que la molècula conté almenys un grup funcional diferent. Són molècules amb característiques amfipàtiques, és a dir, que tenen un extrem hidròfil i un altre d'hidròfob. Aquesta característica, unida a la seva elevada estabilitat, ha afavorit que s'usessin tant per a ús industrial i com en productes de consum en forma d'adhesius, revestiments, repel·lents a l'aigua o escumes ignífugues (DEFRA 2004).

Aquests compostos són persistents contra els processos típics de degradació ambiental i ja han estat trobats en aigua (Yamashita et al., 2005), aire (Jahnke et al., 2007), aliments (Ostertag et al., 2009), fauna (Giesy i Kannan, 2001) i en l'ésser humà (Kannan et al., 2004). Tant PFCAs com PFSAs presenten la capacitat per a la bioacumulació (Casal et al., 2017) i s'han descrit efectes adversos tant per éssers humans com pel medi ambient (Hekster et al., 2003).

A causa d' aquests efectes, l'àcid perfluorooctanosulfònic (PFOS) va ser agregat a la llista de contaminants orgànics persistents (POPs) del Conveni d'Estocolm al maig de 2009, que comporta la restricció mundial de la seva producció (UNEP 2009). A més, donada la pressió de la Environmental Protection Agency (EPA), la indústria va abandonar voluntàriament la producion de PFOS i de l'àcid perfluorooctanoic (PFOA) en els Estats Units (Carloni et al., 2009). No obstant això, la producció d'altres PFASs segueix encara avui dia. Entre aquests s'inclouen els PFASs "neutres" com per exemple els alcohols de fluorotelomers (FTOHs).

Els PFASs iònics (PFCAs i PFSAs) són altament persistents i tenen una alta solubilitat en aigua. En canvi els PFASs neutres, són menys persistents, poden ser transformats per hidròlisi, fotòlisi i biodegradació (Martin et al., 2006, Rhoads et al., 2008), i presenten major pressió de vapor i baixa solubilitat en aigua. A escala global, la majoria dels estudis indiquen que la via de transport dominant de PFASs iònics és el transport oceànic (Armitage et al., 2006, Wania, 2007), mentre que per als PFASs neutres o és el transport atmosfèric (Ellis et al., 2004, Martin et al., 2003). No obstant això, alguns PFAS neutres (per exemple, els FTOHs) formen PFAS iònics a com a productes de la seva degradació, actuant així com un mecanisme de transport que permet l'arribada de PFAS iònics a zones fora de l'abast del transport oceànic (Ellis et al., 2004, Loewen et al., 2008, Ahrens et al., 2010, Young et al., 2007).

Compost	**Acrònim**	**Cadena C (n)**	**Log K_{OA}**	**Log K_{OW}**
Àcid perfluorobutanoic	PFBA	3	6.04	2.82
Àcid perfluoropentanoic	PFPeA	4	6.33	3.43
Àcid perfluorohexanoic	PFHxA	5	6.63	4.06
Àcid perfluoroheptanoic	PFHpA	6	6.92	4.67
Àcid perfluorooctanoic	PFOA	7	7.23	5.30
Àcid perfluorononaanoic	PFNA	8	7.50	5.92
Àcid perfluorodecanoic	PFDA	9	7.77	6.50
Àcid perfluoroundecanoic	PFUnA	10	8.08	7.15
Àcid perfluorododecanoic	PFDoA	11	8.36	7.77
Àcid perfluorotridecanoic	PFTrA	12	8.63	8.25
Àcid perfluorotetradecanoic	PFTeA	13	8.87	8.90

Àcid perfluorohexanosulfònic	PFHxS	6	7.55	5.17
Àcid perfluorooctanosulfònic	PFOS	8	8.07	6.43
Àcid perfluorodecanosulfònic	PFDS	10	8.82	7.66

Taula 1.7. Propietats fisicoquímiques dels PFASs iònics (Wang et al., 2011).

1.5 Compartimentació ambiental dels POPs a les regions polars costaneres

Les regions polars estan delimitades pels paral·lels 66° Nord i 58° Sud per a les regions àrtica i antàrtica, respectivament. La seva posició geogràfica dota a aquestes regions de climes que es caracteritzen en general per temperatures extremadament fredes, glaciació i presència de gel permanent en aquelles zones en què hi ha precipitacions i una marcada estacionalitat amb estius de vint-i-quatre hores de llum diürna i completa foscor a durant l'hivern.

Les regions polars contenen alguns dels ecosistemes més remots del planeta. Malgrat aquesta condició d'ecosistemes a priori pristins i de la gran distància que els separa de les grans fonts primàries d'altres latituds, aquestes regions no estan exemptes de la contaminació per POPs (Mackay i Wania, 1995, Macdonald et al., 2000, Letcher et al., 2010, Riget et al., 2008). L'Antàrtida i l'Àrtic han acumulat POPs en sòls, aigua de mar, biota i gel/neu a causa de l'efecte de "cold-trapping" o de "condensació freda", mitjançant el qual les temperatures més baixes promouen un desplaçament de l'equilibri de partició dels POPs en la fase de vapor cap a les fases "condensades", aquest procés afavoreix l'acumulació de aquests compostos en ambients freds com les regions polars i els ecosistemes d'alta muntanya (Wania et al., 1998, Lei i Wania, 2004, Macdonald et al., 2000, Grimalt et al., 2001, Letcher et al., 2010). Però a més les precipitacions en forma de neu, comuns en les regions polars, resulten especialment eficients a l'hora de recollir aquests POPs de l'atmosfera i dipositar-los en altres compartiments (Lei i Wania, 2004). Malgrat que l'amplificació de les concentracions de POPs per la neu ha estat descrita, no es coneix la importància que té en el cicle dels POPs en zones polars, específicament en la zona costanera.

L'Àrtic i l'Antàrtida presenten notables diferències tant en la seva distància pel que fa a les fonts primàries de POPs com en nombre d'estudis d'aquests compostos a la regió. Hi ha molts estudis que descriuen la variabilitat espacial i temporal de POPs com els PCBs, HCHs, PFASs i molts altres contaminants orgànics persistents a l'Àrtic (Macdonald et al., 2000, Riget et al., 2008, Nash 2011), incloent llargues sèries temporals de mesures que han permès dilucidar les tendències a llarg termini d'algunes famílies de POPs (Hung et al., 2001). En canvi, donades les dificultats logístiques que representa el mostreig, els estudis disponibles sobre POPs a l'Antàrtida sovint es limiten a reportar concentracions d'un petit nombre de mostres, amb concentracions normalment baixes en comparació amb l'Àrtic (Nash 2011). A causa aquestes limitacions, la majoria d'estudis es centren en compartiments ambientals individuals, o en algunes ocasions en dos dels compartiments i la interacció que es produeix entre ells, sense avaluar altres processos que tenen lloc simultàniament i podrien impactar directament o indirectament el seu objecte d'estudi (Figura 1.6).

Figura 1.6. Diagrama dels principals compartiments ambientals de les regions polars costaneres

1.5.1 Processos atmosfèrics

L'arribada de POPs a regions polars, i en concret de POPs semivolàtils, ve donada principalment pel transport atmosfèric, tenint en compte que les fonts primàries locals són comparativament limitades. PCBs, OCPs i PAHs presenten concentracions atmosfèriques detectables tant a l'Àrtic com a la Antàrtida (Halsall et al., 1997, 1998, Kallenborn et al., 1998, 2013, Cabrerizo et al., 2013, 2014, Hung et al., 2016,).També els PFASs neutres, que poden actuar com a precursors de PFAS iònics, presenten concentracions notables a les regions polars costaneres (Del Vento et al., 2012, Wang et al., 2015, Xie et al., 2015). La transferència de POPs des del compartiment atmosfèric a la resta de compartiments es produeix per processos de deposició seca, deposició humida i per intercanvi difusiu amb la superfície de la resta de compartiments en contacte (sòl, neu, aigua, etc) i la importància relativa d'aquestes formes de deposició depèn dels coeficients de partició característics de cada POP, i dels diversos controls físics i biogeoquímics de les concentracions en l’aire, aigua, sòls i neu.

La deposició seca és la deposició de contaminants units a aerosols en absència de precipitació. Aquestes partícules atmosfèriques estan en intercanvi difusiu amb la fase gas i els POPs hidrofòbics i són dipositades generant un flux unidireccional de deposició seca (Baker i Hites, 1999, Jurado et al., 2004). Aquests fluxos són dependents no només de les característiques i concentracions dels POPs en l'aire, sinó a més de la composició i grandària de les partícules, i també de variables ambientals com la velocitat del vent o l'estabilitat atmosfèrica (Jurado et al., 2004). A diferència d'altres àrees d'estudi, la deposició seca no és un procés dominant a l’Antàrtida degut a la baixa concentració de partícules atmosfèriques d'aquesta zona remota.

La deposició humida és un procés que inclou la deposició de contaminants incorporats a la pluja o les nevades (Bidleman et al., 1988). Les precipitacions recullen els POPs que es troben a la fase de gas i als aerosols de l'atmosfera amb una elevada eficiència, però amb una intensitat intermitent (Lei i Wania, 2004, Herbert et al., 2005, 2006). Aquest procés depèn de la concentració del compost a l'atmosfera, el coeficient de partició entre l'aigua de pluja (o la neu) i la fase gas, i la taxa de precipitació. Però a més és depenent del tipus de precipitació, sent la neu significativament més eficient que la pluja a l'hora de recollir POPs de l'atmosfera, per la seva elevada superfície de contacte (Figura 1.7, Lei i Wania, 2004). Aquest procés de deposició especialment efectiu de la neu, es coneix com "snow scavenging" i constitueix una de les principals entrades de POPs en zones remotes fredes com les zones d'alta muntanya i zones polars (Lei i Wania, 2004, Herbert et al., 2006). La compartimentació cap a la fase aquosa es veu afavorida a baixes temperatures, aquest factor conjuntament amb l'elevada superfície específica de la neu, fa que aquest procés de deposició sigui encara més eficient i particularment important per a les regions polars (Lei i Wania, 2004, Herbert et al., 2006). La neu un cop dipositada, pot constituir un compartiment ambiental altament dinàmic amb propietats fisicoquímiques i concentracions de POPs en constant canvi (Herbert et al., 2005, 2006).

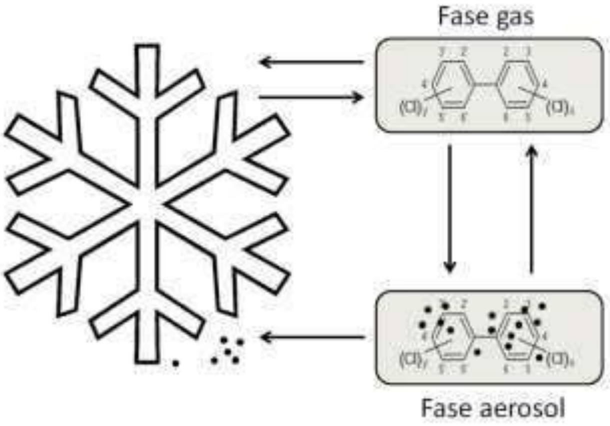

Figura 1.7. Diagrama de la deposició atmosfèrica de POPs per "snow scavenging". La neu arrasta tant compostos presents a la fase gas, com aquells adsorbits als aerosols.

L'intercanvi difusiu és un procés bidireccional entre l'atmosfera i un altre compartiment amb el qual tingui un contacte directe. En aquest intercanvi, podem distingir fluxos de deposició, en els quals el compost difon de l'atmosfera a una superfície i és retingut allà, fluxos de volatilització, en què el compost és reemès a l'atmosfera, i els fluxos d'intercanvi nets resultants de aquests dos processos oposats.

La direcció de l'intercanvi gasós net és des de la fase (és a dir, superfície o atmosfera) amb més potencial químic (o **fugacitat**) a la fase en què és més baixa. La **fugacitat** (f_i, en Pa) és un concepte àmpliament utilitzat per investigar la compartimentació ambiental de substàncies químiques orgàniques, tant en condicions d'equilibri com fora de l'equilibri (Mackay et al., 1979). La paraula fugacitat prové de la paraula llatina "fugere" i descriu la tendència específica d'un compost a escapar d'una fase en un moment determinat. De manera que les fugacitats d'un compost en dues fases en contacte indiquen la direcció d'intercanvi entre aquestes. En altres paraules, els compostos químics tendeixen a moure de les fases on tenen alta fugacitat a aquelles en que tenen poca fugacitat, i presenten fugacitats iguals al trobar-se en equilibri (tot i que presentin concentracions molt dispars entre les dues fases).

La fugacitat es defineix com:

$$\mathrm{f_i} = \frac{\mathrm{C_i}}{\mathrm{Z_i\ MW}}$$

on C_I és la concentració (mol m^{-3}), MW és la massa molecular (g mol^{-1}) i el valor de Z_i és la capacitat de fugacitat (mol m^{-3} Pa^{-1}), que descriu el potencial d'una fase (aire, aigua, sòl) per retenir un compost químic, i depèn dels paràmetres fisicoquímics i les característiques de sorció de la fase.

La capacitat de fugacitat en el aire (Z_A) es:

$$\mathrm{Z_A} = \frac{1}{\mathrm{RT}}$$

on R és la constant del gas i T és la temperatura a Kelvin. De manera que la fugacitat en el aire (f_a) es calcula com:

$$\mathrm{f_a} = \mathrm{C_A RT/MW}$$

on C_A es la concentració del POP a la fase gas.

Assumint que la major part de les substàncies químiques s'associa amb el contingut de la matèria orgànica del sòl, la capacitat de fugacitat del sòl (Z_S) ve donada per:

$$\mathrm{Z_S} = \frac{\mathrm{foc}}{\mathrm{RT}} \mathrm{K_{OA}}$$

on f_{oc} és les fracció de carboni orgànic al sòl i K_{OA} el coeficient de partició octanol-aire. Per tant, la fugacitat al sòl (f_S) es pot calcular com:

$$\mathrm{f_s} = \frac{\mathrm{C_S RT}}{\mathrm{f_{oc} K_{OA} MW}} = \frac{\mathrm{C_S RT}}{\mathrm{K_{SA} MW}}$$

on C_S es la concentració del POP al sòl i K_{SA} es el coeficient de partició sòl-aire.

De la ràtio (f_s/f_a) entre aquestes dues fugacitats podem establir la direcció d'intercanvi difusiu sòl-atmosfera. D'aquesta manera, $f_s/f_a > 1$ indicaria volatilització, $f_s/f_a < 1$ indicaria deposició i $f_s/f_a = 1$ indicaria equilibri entre els dos compartiments.

Aquesta aproximació a la fugacitat del sòl però, depèn de l'assumpció de que $\mathrm{K_{SA}} \approx \mathrm{f_{oc}K_{OA}}$, de la fiabilitat de la mesura de la f_{oc} i de les estimacions de K_{OA}, que a més de ser altament dependents de la temperatura ambiental (Harner i Mackay, 1995, Shoeib i Harner, 2002) no estan exemptes d'una elevada incertesa en la seva aplicació directa en dades de camp. A més, la capa de sòl en contacte directe amb l'atmosfera és d'1 cm de profunditat, o fins i tot menys segons alguns models (Dalla Valle et al., 2005, Harner et al., 2001), mentre que per determinar les concentracions en sòl acostumen a mostrejar-se els primers 5 o 10 cm. El recent desenvolupament de mostrejadors de fugacitat permet una altra aproximació amb un grau d'incertesa considerablement menor (Cabrerizo et al., 2009). Aquests captadors prenen una mesura directa de l'aire equilibrat in situ amb el terra (C_{SA}) al mateix temps que mostregen el compartiment atmosfèric (C_A) en paral·lel (Cabrerizo et al., 2009).

D'aquesta manera la fugacitat en el sòl (f_s) es pot calcular directament com:

$$\mathrm{f_s} = \mathrm{C_{SA}RT/MW}$$

Aquesta mateixa aproximació, que permet també establir les ràtios de fugacitat aire-neu, i ha sigut utilitzada amb anterioritat per confirmar els processos de revolatilització de PCBs i PAHs de sòl i neu a l'Antàrtida i la relació d'aquests amb variables ambientals com la temperatura o la f_{oc} del sòl (Cabrerizo et al., 2013, 2014). En aquest sentit, tot i que aquesta determinació de la f_s no requereix la mesura de la f_{oc} del sòl, el contingut en matèria orgànica del sòl actua com a control biogeoquímic en l'intercanvi aire-sòl. Per exemple, a l'Antàrtida, un augment en la temperatura de 1 °C, comportaria un augment de les concentracions atmosfèriques de PCBs en un 21-45% per volatilització, però alhora es produiria un conseqüent augment que en el SOM, que seria capaç de contrarestar aquest efecte tan sols amb superar el 0.5% del SOM, degut a la reducció que suposaria a la fugacitat del sòl (Cabrerizo et al., 2013).

La fugacitat de l'aigua (f_w) també pot ser estimada per a l'estudi de les ràtios de fugacitat, seguint:

$$\mathrm{f_w = C_W H' RT/MW}$$

on C_W es la concentració del compost a l'aigua i H' es la constant de Henry adimensional.

Els fluxos difusius s'estimen a partir d'un gradient de fugacitat i un coeficient de transferència de massa, que depenen d'una àmplia gamma de paràmetres ambientals. Per exemple, el flux d'aire-neu (F_{Snow}) pot calcular-se a partir de la concentració de POP en l'aire i en la neu de la següent manera:

$$\mathrm{F_{Snow} = v\left(\frac{C_S}{K_{SA}} - C_A\right)}$$

on v és la velocitat d'intercanvi entre les fases (m d^{-1}), calculada seguint el mètode de resistència de dos capes de Whitman (Hansen et al., 2006), i K_{SA} és el coeficient de partició neu-aire (C_{SA}/C_A). La velocitat d'intercanvi te una component que de l'aire, que depèn de paràmetres com la velocitat del vent, i una component per la neu que depèn de paràmetres com la densitat de la neu.

De manera similar, el fluxos difusius aire-aigua s’estimen seguint un model de resistència de dues capes (Jurado et al., 2005)

$$\mathrm{F_{AW}} = \mathrm{k_{AW}} \left(\frac{\mathrm{C_G}}{\mathrm{H'}} - \mathrm{C_W}\right)$$

on $\mathrm{k_{AW}}$ es la taxa de transferència de massa d'aire-aigua (m $\mathrm{d^{-1}}$) (Jurado et al., 2004).

1.5.2 Els POPs a la neu i el gel glacial

La neu com a compartiment ambiental passa per una sèrie de processos d'envelliment post-deposició atmosfèrica que influeixen tant a les seves concentracions de POPs com a les dels compartiments adjacents.

La neu recent dipositada es caracteritza per una elevada superfície de contacte i una reduïda densitat (Wania et al., 1997, 1998), acompanyades normalment d'una elevada concentració de POPs a causa del procés de “snow scavenging” (Figura 1.7). Durant els primers dies després de la deposició, la neu experimenta un procés de fusió i compactació, durant el qual la seva superfície de contacte disminueix exponencialment i la seva densitat es redueix des de valors propers a 50-100 kg $\mathrm{m^{-3}}$, cap als 500-650 kg $\mathrm{m^{-3}}$ (Wania et al., 1997, Domine et al., 2002). Aquest procés d'envelliment de la neu, que depèn en la seva velocitat de les condicions ambientals, es veu acompanyat per un descens significatiu en les concentracions de POPs a la neu (Gregor i Gummer, 1989; Wania et al., 1997, 1998, Herbert et al., 2005, 2006). Per exemple, Herbert et al., (2005) van observar un descens de 2500 fins a 340 pg $\mathrm{L^{-1}}$ de ∑PCBs en neu del àrtic, amb una caiguda d'aproximadament el 75% de la concentració durant les primeres 96 hores. Aquests ràpids canvis en la concentració de POPs a la neu poden ser responsables, almenys en part, dels amplis rangs de concentracions en neu reportats en alguns estudis (Herbert et al., 2006). La fugida de contaminants durant l'envelliment de la neu, pot explicar-se principalment per processos d'intercanvi difusiu amb l'atmosfera i per fusió de la neu amb el seu transport posterior a altres compartiments, i en menor magnitud per processos de fotòlisi a la superfície de la neu (Herbert et al., 2006). La neu fosa és inicialment retinguda sota la neu per efecte de la capil·laritat però se separa d'aquesta en assolir una massa crítica (Wania et al., 1997). La destinació dels POPs de l'aigua de neu depèn de les seves propietats fisicoquímiques, podent revolatilizarse, adherir-se a partícules o romandre lliure en l'aigua de neu en funció d'aquestes (Wania et al., 1997). L'efecte de la descàrrega d'aquesta aigua de neu carregada de POPs en els ecosistemes costaners és pràcticament inexplorat a dia d'avui.

La neu no estacional continua la seva compactació fins a formar neu “Firn”, que significa literalment "de l'any passat", amb densitats properes a 800 kg m^{-3} (Petrenko i Whitworth, 1999, Domine et al., 2002), i la compactació successiva del Firn al llarg del temps forma els glaciars. També el gel glacial pot contenir quantitats significatives de substàncies químiques dipositades en èpoques anteriors que s'han emmagatzemat durant dècades en les capes més profundes. El desglaç i el retrocés de les glaceres comporta com a resultat un alliberament substancial de químics d'aquest tipus de reservori (Bogdal et al., 2009). D'aquesta manera, els ecosistemes es poden veure afectats per l'alliberament retardat de POPs que han vist les seves fonts primàries reduïdes en l'actualitat (Bogdal et al., 2009). Diversos estudis demostren que en les regions polars, les glaceres i, en general, el gel i la neu poden ser font de POPs per a l'aigua de mar (Geisz et al., 2007; Meyer et al., 2008) i però també per a la atmosfera (Gioia et al., 2008).

1.5.3 Processos a la columna d'aigua

L'arribada de POPs a la columna d'aigua es realitza de manera general pels 3 processos atmosfèrics anteriorment explicats, i en el cas dels ecosistemes costaners s'hi afegeix la contribució de descàrregues fluvials i/o glacials.

Un cop ingressats en el compartiment marí, els POPs presents en les aigües marines poden existir lliurement en forma dissolta, adherits a diferents tipus de partícules, o incorporat en els éssers vius. La compartimentació entre aquests diferents components dins de l'aigua de mar és una consideració important ja que les rutes de transport, la biodisponibilitat, els processos de degradació, la sedimentació, el temps de residència i el destí ambiental dels diferents compostos són determinats per aquesta compartimentació.

La incorporació dels POPs en el compartiment biològic marí, i en concret en el plàncton, és un focus d'estudi important de cara a entendre el destí ambiental d'aquests compostos en el medi marí, atès que afecta les seves concentracions i distribució a la columna de aigua, és el primer pas en les xarxes tròfiques marines i és un factor determinant en la a bomba biològica (Dachs et al., 1996; Dachs et al., 1997a, Dachs et al., 1997b, Dachs et al., 2002, Jurado i Dachs, 2008, Galbán-Malagón et al., 2012, 2013, Russell et al., 1999). El factor de bioacumulació (BAF) que avalua aquesta incorporació en condicions de camp es calcula com:

$$\mathrm{BAF} = \frac{\mathrm{C_P}}{\mathrm{C_W}}$$

on C_P es la concentració del compost a l’aigua.

El BAF dóna una mesura de la magnitud en què una substància química és absorbida en un organisme per totes les vies d'exposició, incloses les fonts alimentàries i ambientals (Arnot i Gobas, 2006). Per tant, és el resultat net dels processos d'absorció en els organismes en la superfície respiratòria i de la dieta i al mateix temps de l'eliminació del compost de l'organisme, sigui a través de la superfície respiratòria, per via fecal i per biotransformació metabòlica del compost original (Arnot i Gobas, 2006). El K_{OW} de cada compost és determinant en la bioacumulació, però a més hi ha una sèrie de factors biològics que influeixen en la transferència dels POP en les cadenes tròfiques (Borga et al., 2004). Entre aquests s'inclouen les condicions d'exposició, els organismes involucrats, el nivell tròfic, el contingut lipídic, l'estacionalitat, factors reproductius, la mida, edat, sexe, cicle de vida, ús del hàbitat, o les migracions, entre d'altres (Borga et al., 2004).

Per a aigües obertes oceàniques, hi ha evidències que mostren que la bomba biològica juga un paper important en el segrest de POP atmosfèrics i d'aigua de mar, controlant les concentracions en aigua i fitoplàncton (Dachs et al., 2002, Jurado i Dachs 2008, Galbán-Malagón et al., 2012, 2013). No obstant, la rellevància d'aquesta bomba biològica de POPs per a un lloc costaner polar on a més influeix l'entrada de contaminants de les glaceres, així com de nutrients i altres materials associats a les descàrregues fluvials, no ha estat determinada.

1.6 Objectius de la tesi

L'objectiu general d'aquesta tesi doctoral és **l'estudi de la rellevància dels processos de remobilització de contaminants orgànics persistents en zones polars costaneres**. Els objectius específics són:

1. Determinar les concentracions d'un ampli ventall de famílies de POPs, “legacy” i emergents, en els principals compartiments dels ecosistemes polars costaners.

2. Quantificar els fluxos d'intercanvi entre l'atmosfera i els diferents compartiments característics de les zones polars.

3. Avaluar el destí dels contaminants orgànics persistents durant la fusió de la neu / gel i determinar l'entrada d'aquests contaminants en el sistema aquàtic costaner, incloent el plàncton, per la seva importància com a primer pas en les cadenes tròfiques.

4. Establir el paper de les variables climatològiques principals, temperatura i precipitacions, en els processos de remobilizació de contaminants orgànics persistents.

5. Elucidar els controls biogeoquímics en el destí ambiental dels POPs en zones costaneres polars

Capítol 2: Seasonal soil/snow-air exchange of semivolatile organic pollutants at a coastal arctic site (Tromsø, 69°N)

Paulo Casal, Javier Castro-Jiménez, Mariana Pizarro, Athanasios Katsoyiannis,

Jordi Dachs

Publicat a Science of the Total Environment 636, 1109-1116, 2018

ATENCIÓ ¡

Les pàgines 48 a 56 de la tesi contenen aquest article, que cal consultar a la web de l'editor
https://www.sciencedirect.com/science/article/pii/S0048969718315080
https://doi.org/10.1016/j.scitotenv.2018.04.330

Capítol 3: Role of Snow Deposition of Perfluoroalkylated Substances at Coastal Livingston Island (Maritime Antarctica).

Paulo Casal, Yifeng Zhang, Jonathan W. Martin, Marina Pizarro, Begoña Jimenez,

Jordi Dachs

Publicat a Environmental Science and Technology 51, 8460-8470, 2017

Capítol 4: Pivotal role of snow deposition and melting driving fluxes of Policyclic Aromatic Hydrocarbons at Coastal Livingston Island (Antarctica).

Paulo Casal, Ana Cabrerizo, Maria Vila-Costa, Mariana Pizarro, Begoña Jiménez,

Jordi Dachs

En revisió a Environmental Science and Technology

Submitted to *Environmental Science & Technology*

PIVOTAL ROLE OF SNOW DEPOSITION AND MELTING DRIVING FLUXES OF POLYCYCLIC AROMATIC HYDROCARBONS AT COASTAL LIVINGSTON ISLAND (ANTARCTICA)

Paulo Casal[1], Ana Cabrerizo[1], Maria Vila-Costa[1], Mariana Pizarro[1], Begoña Jiménez[2], Jordi Dachs[1]*

[1]Institute of Environmental Assessment and Water Research, Spanish National Research Council (IDAEA-CSIC), Barcelona, Catalonia 08034, Spain

[2]Department of Instrumental Analysis and Environmental Chemistry, Institute of Organic Chemistry, Spanish National Research Council (IQOG-CSIC), Madrid 28006, Spain

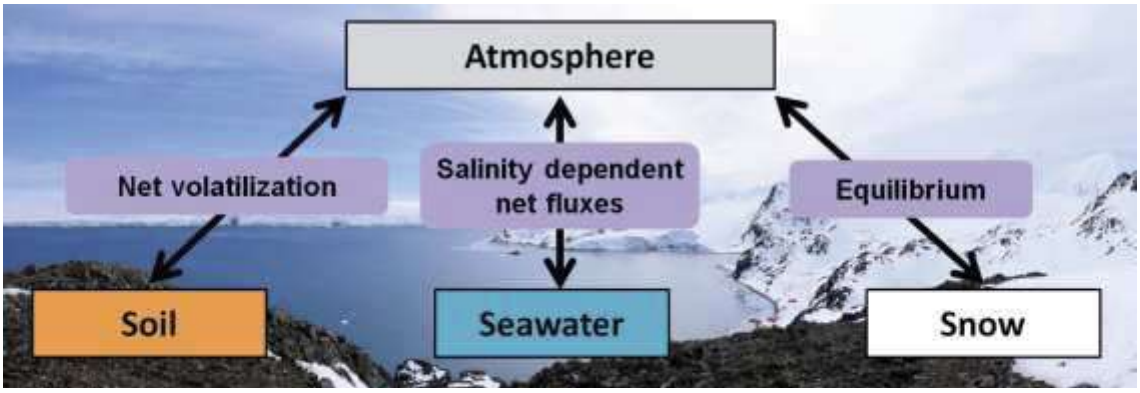

ABSTRACT

The atmosphere-land-ocean dynamics of semivolatile organic compounds has been generally omitted, also for the abundant and ubiquitous polycyclic aromatic hydrocarbons (PAHs). We report the concentrations and fluxes of PAHs in a polar coastal ecosystem (Livingston Island, Antarctica). From late spring (December 2014) to late summer (February 2015), we sampled air, snow, coastal seawater, plankton, and the fugacity in soils and snow. The concentrations of PAHs in seawater were low but increased during the austral summer. The PAH concentrations in snow were significantly higher than in coastal seawater. Soil-air fugacity ratios showed a net volatilization of PAH when soils were covered with lichens, and close to air-soil equilibrium for bare soils. Concentrations in surface snow were also close to equilibrium with atmospheric PAHs. Conversely, there was a net diffusive deposition of PAHs to coastal seawater during late spring, but a net volatilization from seawater during late summer. Volatilization fluxes were correlated with seawater temperature and salinity, consistent with a key role of snow-melt to the fluxes and dissolved phase concentrations during the austral summer. The comprehensive assessment provided here shows that the fugacity amplification in snow is transferred to soils and coastal seawater supporting PAH concentrations and fluxes.

INTRODUCTION

Polycyclic aromatic hydrocarbons (PAHs) are semivolatile organic compounds (SVOCs), mainly generated from the incomplete combustion of fossil fuels and organic matter, being ubiquitously found in the global environment.[1-3] PAHs are under international regulation by the United Nations Economic Commission for Europe Convention on Long-Range Transboundary Air Pollution, due to their widely reported harmful and carcinogenic effects.[4,5] PAHs can be found even in remote regions such as Antarctica[1,2] due to their susceptibility for long-range atmospheric transport (LRAT) coupled with deposition favoured by cold trapping[6] and air-seawater disequilibrium in the open ocean.[2] Additionally, tourism and research stations have been suggested as a significant local source of PAHs, especially in Antarctic soils.[7,8]

Nevertheless, there are few studies on the occurrence of PAHs in Antarctic snow, soils, air, seawater, sediments and biota.[1, 2, 9-14] Notwithstanding, the Antarctic region is still understudied in comparison to other remote areas such as the Arctic.[15] The dynamic coupled fluxes between the different Antarctic compartments is poorly understood as it requires a multimedia approach comprising the analysis of different environmental matrices, and the assessment of fluxes between air, water, snow and soils. Conversely, previous Antarctic SVOCs assessments tended to focus on individual compartments or processes. The few multi-compartmental works on PAHs include the determination of volatilization of 3-4 ring PAHs from soils and snow during a short period of the austral summer.[1] Particularly, there is a lack of integrated assessments of PAH dynamics at the interface between land and ocean, not only at coastal Antarctica, but also for other regions. The study of the coupling between the atmosphere, land and ocean requires an ambitious sampling strategy and the comprehensive assessment of the multiple interactions between the different compartments, including air-snow, air-soil, air-water and land-ocean coupled fluxes. Furthermore, microbially driven processes such as the degradative and biological pumps may also play a role sequestering PAHs in the coastal waters and sediments as for other organic pollutants.[16,17] The atmosphere-seawater cycling of PAHs is also of particular biogeochemical relevance due to the important role that the large pool of semivolatile aromatic-like compounds has in the marine carbon cycle.[3] While the behaviour of PAHs in terms of atmospheric inputs and fate in the open ocean water column has been comprehensively studied recently,[3,18] its dynamics in remote coastal regions remains uncharacterized. There are no previous concurrent assessments of air and seawater PAHs for the coastal Maritime Antarctica, and atmosphere-seawater fluxes have not been determined for this region.

The objectives of this work were: i) to provide, for the first time, concurrent multimedia concentrations in the Maritime Antarctica, including several relevant matrices (air, snow, seawater, plankton), ii) to assess the air-soil, air-snow and air-water PAHs dynamics at coastal Antarctica, and iii) to elucidate the main biogeochemical and climatic drivers of PAHs fluxes and remobilization on land and in the water column.

MATERIALS AND METHODS

Site description and sampling

A three-month intensive sampling campaign (1st December 2014 to 1st March 2015) was performed at Livingston Island (62° 39′ S, 60° 23′ W), in the South Shetlands Archipelago, Antarctica. With two seasonal and small research stations located at South Bay of Livingston Island (Figure 1), this coastal area is under a lower anthropogenic pressure in comparison to other South Shetland Islands such as King's George.

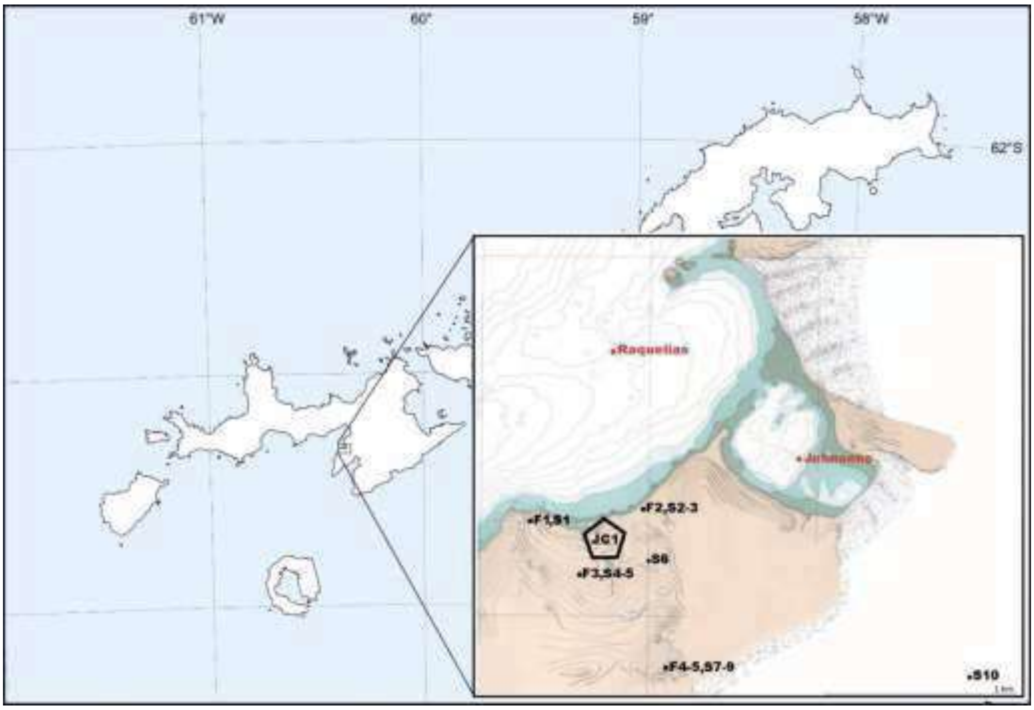

Figure 1. Sampling sites at Livingston Island. Five fugacity samplers were deployed to collect gas phase and gas phase equilibrated with snow/soil at F1-5 sites. Seawater and plankton samples were taken at Raquelias site (62° 39,438' S, 60° 23,306' W) and Johnsons site (62° 39,556' S, 60° 22,132' W). Snow samples were collected at S1-10 sites.

Plankton and seawater sampling was conducted from a rigid inflatable boat at two sampling sites: Johnsons and Raquelias (Figure 1). Johnsons site (62° 39,556'S, 60° 22,132'W, 14 m depth) is located inside a shallow cove under the influence of several thawing rivers, 200 m away from the Johnsons glacier. Raquelias site (62° 39,438'S, 60° 23,306'W, 40m depth) is open to the South Bay of Livingston Island, at 1 km from the coast. CTD (Conductivity, Temperature, Density) depth profiles were taken immediately before sample collection and presented significant differences between sampling sites (Table S1, SI). Concurrent samples for seawater nutrient and bacterial biomass determination were also taken at the same sampling locations and dates, and stored at -20 °C until their determination in the laboratory.

Twenty-six 100-120 L surface seawater samples (0.5-1 m depth) were collected in 20 L aluminum jerry cans and transported to the research station for their immediate filtration and extraction (Table S2, SI) as previously described.[3] Briefly, seawater was filtered through pre-combusted GF/F glass fiber Whatmann filters (0.7 µm) before passing through pre-cleaned XAD-2 (Supelco) packed stainless steel columns. This extraction was performed outside the laboratory in order to avoid potential contamination from indoor air, and for keeping the temperature at ambient levels (ranging from 0 to 4 °C), thus not affecting the particle-water partitioning of PAHs. XAD-2 columns were stored at 4 °C for refrigerated transport until further analysis, while GFF filters were wrapped in pre-combusted aluminum foil, and stored at -20 °C in air-tight plastic bags until their analysis in the laboratory.

Twenty-six plankton samples were collected using a conical plankton net with a 50 µm mesh size by vertical hauls from bottom to surface (Table S3, SI). The sampling depth at Johnsons and Raquelias was of 14 and 30 m (close to water column depth), respectively. The collected samples were filtered with pre-combusted and pre-weighted GF/D glass fiber Whatman filters (2.7 µm), and the filters were subsequently wrapped in pre-combusted aluminum foil, and stored at -20 °C in air-tight plastic bags until their analysis in the laboratory.

Ten surface (top 1-2 cm) snow samples were collected with a stainless steel shovel into Teflon bottles (Figure 1) and allowed to melt at 4-6 °C for 24 - 48 h (Table S4, SI). Snow water samples followed the same procedure as surface seawater samples, also filtered outdoors to minimize temperature changes and/or contact with air from the research station.

52 ambient air and 51 surface fugacity samples were collected by means of a previously described fugacity sampler,[19] deployed at 5 sampling sites (Figure 1, Table S5-S7, SI). The fugacity sampler forces air to flow below a stainless-steel chamber separated 3 cm from the soil/snow surface allowing the air to equilibrate with the surface (soil or snow), thus providing a measure of the soil or snow fugacity. The fugacity sampler was initially developed for soils, and the air-soil equilibration assessed by comparison of the concentrations using different flow-rates.[19] The comparison of the concentrations in air-equilibrated with the snow surface at flow rates of 6 and 8 L per minute with a second sampler operating at 10 L per minute, showed comparable concentrations,[1] with a variability for 3-4 ring PAHs concentrations of 16% (n=4, phenanthrene to pyrene). This variability is comparable to the variability of the concentrations obtained from side-by-side samplers over snow operating at the same flowrate (10 L per minute). These results are consistent with PAHs in air and surface snow reaching equilibrium when the air is forced to flow below the fugacity sampler. The ambient air samples were collected simultaneously at 1.5 m height. Ambient air and surface fugacity samples were taken by passing the air through pre-combusted quartz fibber filters (GF/F) to remove dust particles, and through 10 × 2 cm pre-cleaned polyurethane foam plugs (PUFs), where the compounds from the gas phase were retained. Sampling flow rates were slow (8-10 L per minute) to allow air-surface

equilibrium conditions below the sampler,[19] with average sampled air volumes of 86 m^3. The PUFs were subsequently stored at -20 °C in air-tight pre-combusted glass vials.

Analytical Procedures

Plankton samples were Soxhlet extracted with dichlorometane:hexane (1:1, v:v) during 24 h. Extracts were concentrated and fractionated with 25 ml of hexane and 40 ml of dichlorometane:hexane (1:3, v:v) on a 5g of silica gel column (silica 60-200 mesh, activated at 250 °C for 24h) and 3g of 3% deactivated neutral alumina column (aluminium oxide 90, activated at 250°C for 12h). The dichlorometane:hexane fraction containing the PAHs was concentrated and solvent exchanged to iso-octane with a final volume of 100 µl.

XAD-2 columns were sequentially eluted with 200 mL of methanol, followed by 200 mL of dichlorometane and 100 mL of hexane using an axial piston pump with a 2 mL min^{-1} flow rate. The methanol fraction was concentrated and liquid-liquid extracted with 50 mL of hexane for three times. The hexane extracts were dried over anhydrous sodium sulphate and combined with the dichloromethane and hexane fractions. After reducing the volume, the extract followed the same fractionation process than the plankton samples. PUFs were Soxhlet extracted with acetone:hexane (3:1, v:v) during 24 h. PUFs fractionation details can be found elsewhere.[20, 21]

PAH quantification was performed with an Agilent 6890 Series gas chromatograph coupled to a mass spectrometer Agilent 5973 (GCMS) operating in selected ion monitoring (SIM) and electron impact mode (EI). A 30 m capillary column (HP-5MS, 0.25mm x 0.25um film thickness) was used. The oven temperature was increased to 90 °C (held for 1 min), then increased to 175 °C at 6 °C/min (held for 4 min), increased to 235 °C at 3 °C/min, increased to 300 °C at 8 °C/min (held for 8 min), and finally to 315

°C for 5 min (held for 8 min). Injector and transfer line temperatures were 280 and 300 °C, respectively. 2 µl of sample were injected in split less mode.

The following parent and alkylated PAHs were analysed: acenaphtylene (Act), acenaphthene (Ace), fluorene (Flu), phenanthrene (Phe), anthracene (Ant), dibenzonthiophene (DBT), fluoranthrene (Flt), pyrene (Pyr), benzo[a]anthracene (B[a]ant), chrysene (Cry), benzo[b]fluoranthene (B[b]f), benzo[k]fluoranthene (B[k]f), benzo[e]pyrene (B[e]pyr), benzo[a]pyrene (B[a]pyr), perylene (Pery), dibenzo[a,h]anthracene (Dib[a,h]ant), benzo[g,h,i]perylene (B[g,h,i]pery), indeno[1,2,3-cd]pyrene (In[1,2,3-cd]pyr), Benzo[ghi]fluoranthrene (B[g,h,i]f), methylphenanthrenes (ΣMP, sum of 4 isomers), dimethylphenanthrenes (ΣDMP, sum of 7 isomers), methyldibenzonthiophenes (ΣMDBT, sum of 3 isomers), dimethyldibenzonthiophenes (ΣDMDBT, sum of 5 isomers), methylpyrenes (ΣMPyr, sum of 5 isomers), dimethylpyrenes (ΣDMPyr, sum of 8 isomers), methylchrysenes (ΣMCry, sum of 2 isomers).

Nutrients (phosphate, nitrate plus nitrite, and ammonia) were analysed by continuous flow analysis on a Bran+Luebbe (currently Seal Analytical) autoanalyzer following standard colometric methods.[22]

Bacterial abundance was estimated from the gene copy numbers of the 16S gene by quantitative real-time polymerase chain reaction (qPCR) as described elsewhere.[23] Briefly, DNA was extracted from 47-mm-diameter, 0.2 µm pore-size PTFE filters (Millipore) where we collected the biomass of 2 liters of seawater pre-filtered by GF/D (Whatmann) filters. Filters were soaked with lysis buffer (50 mM Tris HCl, 40 mM EDTA, 0.75 M Sucrose), incubated with lysozyme, proteinase K and sodium dodecyl sulphate (SDS), and then nucleic acids were phenol-extracted as previously described.[24] Partial bacterial 16S gene fragments were quantified with SYBR Green (Thermo Scientific, Inc.) in one 96-well plate using primers 331F/518R in a Lightcycler 480 II (A.F. Hoffmann-La Roche AG, Inc). The reaction mixture was thermocycled at 95 °C for 7 minutes, 40 cycles at 95 °C for 10 s, 60 °C for 30s, and 68 °C for 90s, followed by a final extension of 5 min at 68 °C. The plasmid vector pNORM was used as standard to normalize quantified genes. Each assay was run in triplicates including no template controls and standard curves spanning from 101 to 108 copies of standard 16S genes. Melting curves were obtained to confirm amplification specificity.

Quality Assurance/Quality Control

All recipients, tubes and connections used during sampling and chemical analysis were of stainless steel, glass or PTFE, and they had been pre-cleaned with acetone prior use in order to avoid contamination.

To minimize contamination, all filters were precombusted at 450 °C over 4 hours. XAD-2 was Soxhlet extracted in methanol:dichlorometane (1:1) before column packing, the columns were pre-eluted with methanol, dichloromethane and hexane and the extracts were concentrated and injected to check for residual contamination. PUFs were precleaned with acetone/hexane (3:1, v:v) over 24 hours and stored in in air-tight pre-combusted glass vials.

Field blanks consisted of GF/D filters, PUFs and XAD-2 columns that followed the same process as the samples albeit without the pass of plankton, air or water. Procedural and/or field blanks were analysed with each batch of 4-6 samples to monitor potential contamination during sampling and extraction. The limits of quantification (LOQs) were defined as the mean concentration of field or procedural blanks plus three times the standard deviation of the blank response. For the analytes which were not found in procedural blanks, LOQ were derived from the lowest standard in the calibration curve.

Recoveries were monitored by a spike of pre-deuterated PAHs standards (acenaphthene-d10, phenanthrene-d10, crysene-d12 and perylene-d12) prior to the extraction process and are resumed in Table S8 (supplementary material).

The measure of the copies of the 16S genes were done in triplicates. The standard deviation of the triplicate measurements was of 5%.

Statistical Analysis

All statistical analyses were performed with SPSS Statistics version 22.0 (IBM Corp.), and significance was set to $p < 0.05$. Correlations among concentrations and environmental variables were performed by Spearman rank-order analysis. Microbial controls on seawater and plankton concentrations were explored by multiple linear least squares regressions.

RESULTS AND DISCUSSION

Soil-air exchange of PAHs

Average ∑PAHs gas phase concentrations (150 ± 140 pg m^{-3}) were generally in the lower range (Table S5, SI) than in a previous atmospheric assessment in this region.[1] Similar gas phase ∑PAH concentrations have been reported in the Arctic,[25-28] even though with a large variability mainly due to differences in the number of targeted PAHs.

Although temperature constitutes one of the main drivers of gas phase semivolatile organic compound concentrations,[21, 29] neither ∑PAHs, nor the individual PAH gas phase concentrations were correlated with air temperature, as previously reported in semiurban/rural regions and over the ocean.[30-32] The lack of temperature-dependent gas phase concentrations is consistent with air and surface (sea) at non-equilibrium and with an important contribution of atmospheric long-range transport in comparison to local sources.[29, 30] Potential PAH sources at coastal Antarctica are in-situ emissions from local research stations and scientific/tourism cruises,[8] revolatilization from soils and snow,[1] and biogenic sources related to organic matter degradation.[1, 33, 34] The lower persistence of 2-4 ring PAHs than other SVOCs[30, 31] could also mask the influence of temperature on gas phase concentrations.

PAH profiles in the gas phase were dominated by the lower molecular weight 3-ring PAHs, which accounted for 87 ± 9.8% of ∑PAHs , with Phe being the highest contributor (30 ± 8.2%) to ∑PAHs (Figure 2), consistent with previous studies in polar regions.[1, 21]

The air fugacity (f_a, Pa) and the soil fugacity (f_s, Pa) of individual PAHs were calculated by:

$$f_a = 10^{-9} C_A RT/MW \qquad [1]$$

$$f_s = 10^{-9} C_{SA} RT/MW \qquad [2]$$

where C_A is the measured ambient air concentration at 1.5 m height (ng m^{-3}), R is the gas constant (8.314 Pa m^3 mol^{-1} K^{-1}), MW is the chemical molecular weight (g mol^{-1}), and C_{SA} (ng m^{-3}) is the gas phase concentration that had been equilibrated with the soil/snow surface (Tables S6, SI), as measured using the soil fugacity sampler. With this approach, C_{SA} is directly proportional to the surface fugacity.

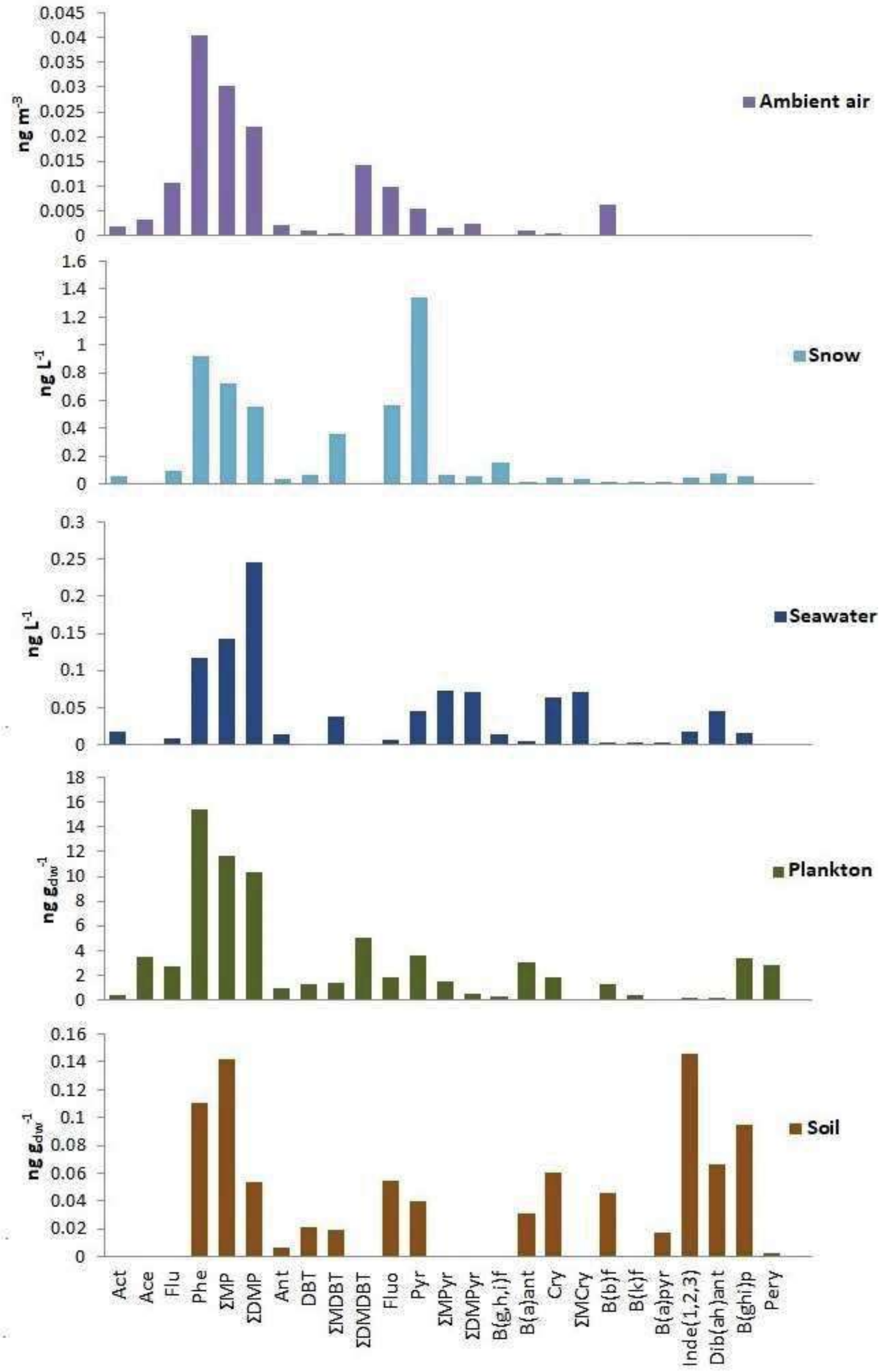

Figure 2. PAH average profiles in air, snow, seawater, plankton and soil matrices. Soil concentrations taken from Cabrerizo et al.,[8].

C_{SA} PAHs profiles had a higher proportion of low MW PAHs than C_A. 3-rings PAHs contributed 95 ± 2.1% to ∑PAHs, and the average Phe contribution to ∑PAHs was 40 ± 11%. This is consistent with the low concentrations of aerosol black carbon and associated PAHs in the region,[1] as black carbon is especially enriched in high MW PAHs. Furthermore, previous studies reported soils as a source of volatile PAHs on polar regions.[1, 21, 34] C_{SA} was not correlated with the inverse of temperature, as for ambient air. This contrasts with the influence of temperature observed for the soil fugacity of some PAHs in an arctic urban and coastal site.[21] This lack of correlation is likely due to the narrow range of the mean ambient temperatures at this region of the Maritime Antarctica during summer (averages ranging from 0.26 to 2.6 °C) (Table S7, SI).

The least squares linear regression of Log f_s versus Log f_a showed that the PAHs fugacity in air and soils were closely correlated (Figure 3). This correlation confirms a close coupling of air and soil PAH fugacities, and is consistent with previous reports in temperate and European polar regions.[1, 21, 34, 35]

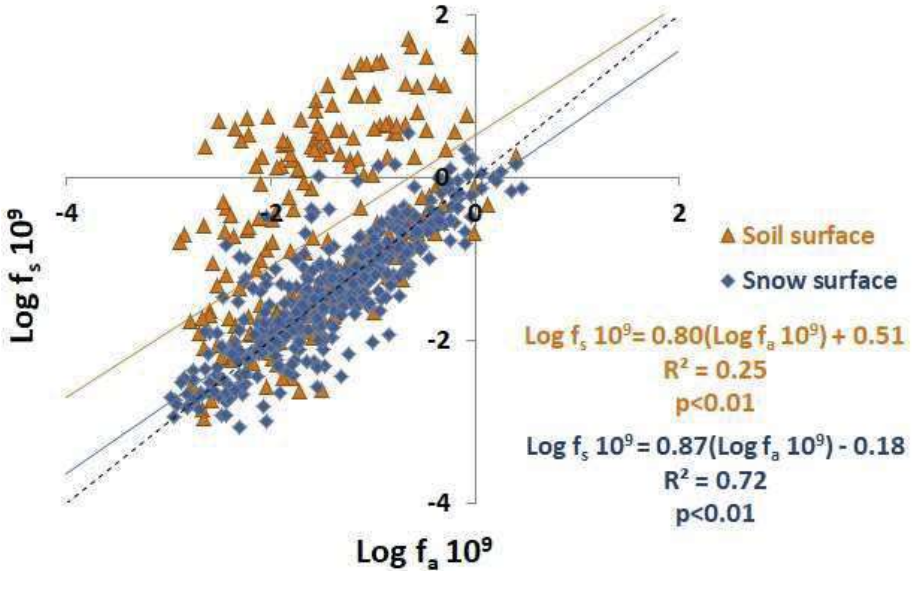

Figure 3. PAHs fugacity in air (f_a, Pa) versus fugacity in soil or snow (f_s, Pa).

f_s/f_a ratios were evaluated to determine the direction of soil-air exchanges of PAHs (Figure 4, Table S9, SI), where values higher and lower than 1 indicate net volatilization and deposition of the chemical, respectively. 72% of f_s values were higher than the simultaneously measured f_a, which indicates a dominance of PAH volatilization processes on the air-soil exchange. Due to uncertainty in the measurements, equilibrium is considered for Ln f_s/f_a values between -1.2 and 0.53.[20] Bare soil and soil with vegetation presented notable differences in f_s/f_a ratios (Figure 4), with bare soil-air coupling being close to equilibrium during the sampling campaign. Conversely, net volatilization from soil with vegetation was observed for most of the target compounds (Figure 4). These differences are likely related with higher soil organic matter (SOM) content in soil with vegetation cover. Furthermore, the statistically significant least squares linear regressions of Ln f_s/f_a versus Log K_{OA} showed higher volatilization for the less hydrophobic compounds (Figure 4). The fact that soils covered with vegetation showed a higher volatilization fluxes than bare soils could be due to a number of factors. There is a potential biogenic production of the more volatile PAHs contributing to PAHs volatilization by degradation of diterpenes and enhanced SOM digestion by fungal acids, which have been suggested as mechanisms that would mediate in this process.[1,20,33] Indeed, terpens from plant detritus can aromatize during ageing, converting to low MW PAHs.[36,37] The fugacity amplification of PAHs in snow melt is retained in the soil organic carbon, as soils covered with vegetation have higher SOM, this is translated to higher soil concentrations of PAHs. The high soils concentrations can be translated to a high soil fugacity in the case that there is a decrease of the fugacity capacity of soils. This fugacity capacity is related to the soil organic carbon content. Soil respiration converts soil organic carbon to CO_2.

Soil respiration is an example of a solvent depletion amplifying the fugacity, as has been described by other processes such as snow melting.[38] In the South Shelland regions, it has been shown that soil respiration in soils covered by lichens is significantly higher than in bare soils, and that soil respiration is significantly increased after snow melting.[39] This solvent depletion mechanism is consistent with the higher PAH fugacity in soils covered with lichens than in soils without vegetation (lower SOM and solvent depletion by respiration).

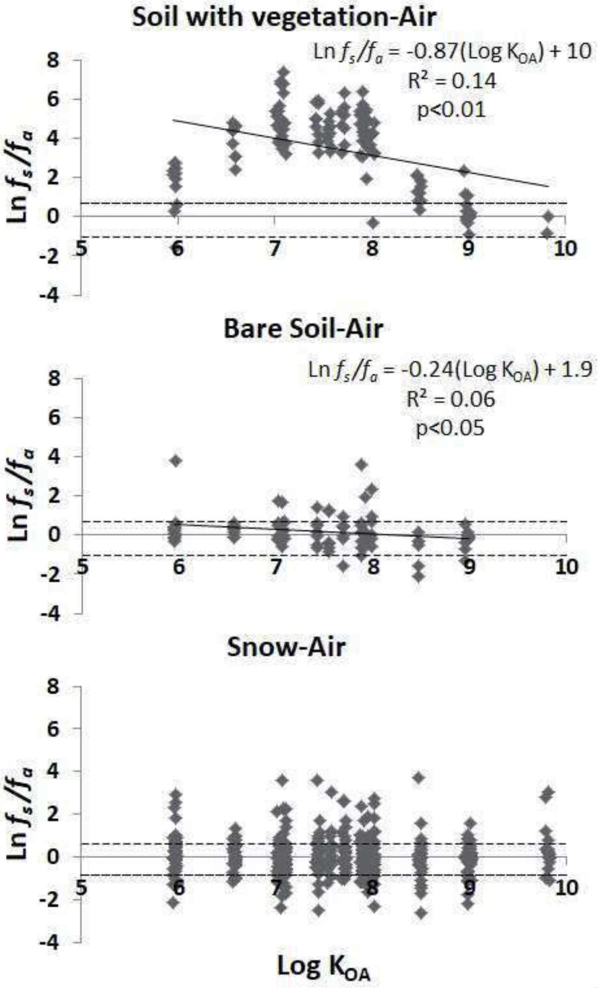

Figure 4. Variation of the soil/snow-air fugacity ratios (Ln f_s/f_a) versus the octanol-air partition coefficient (K_{OA}). The horizontal dashed lines mark ratios −1.2 and 0.53, interval for air-surface equilibrium.

Snow-air partitioning of PAHs

∑PAHs average concentrations in snow ranged from 0.39 to 9.2 ng L^{-1} (Table S4, SI), and were not significantly correlated to the snow density or age. Similar ∑PAHs concentrations have been previously reported in coastal surface snow from the Northern Victoria Land,[14] and in snow/firn cores at Talos Dome.[10]

One to two orders of magnitude higher PAHs concentrations were observed in King George Island,[13] which is likely due to a higher presence of local sources in the Fildes Peninsula, such as 9 permanent research stations, a small airport and a high incidence of cruise tourism, which is residual at Livingston Island. Similarly, high levels of PAHs have been reported in snow from Victoria Land (140 ng L^{-1}), particularly high for naphthalene (125 ng L^{-1}), which was attributed to local contamination from a Twin Otter (aircraft) refuelling point.[14] These examples of the presence of local contamination in soils or snow was suggested as evidence that LRAT did not contribute significantly to recent snow contamination in other regions.[40] However, at Livingston island, there was no significant correlation between PAH snow concentrations and the distance to JC1 Station. On the other hand, PAH snow concentrations reported on the Arctic and remote regions from the northern hemisphere are generally one or two orders of magnitude higher than in Antarctica, which has been suggested as a result of limited inputs of air masses from lower latitudes due to the atmospheric dynamics of the Antarctic region.[41] However, PAH atmospheric concentrations reported here and by Cabrerizo et al.[1] are comparable to those reported for the Arctic,[25-28] which is due to preferential air mass transport from South America and northern latitudes affecting primarily the northern Antarctic Peninsula and South Shetland islands during the Austral summer.[42] As we have shown in a companion paper reporting the dynamics for perfluoroalkyl substances during the same sampling campaign,[43] the back trajectories for snow deposition events are from air masses from northern latitudes and South America. The rest of the Antarctic continent has a strong influence of katabatic winds. Snow-Air partitioning constants (K_{SA}) were calculated as:

$$K_{SA} = \frac{C_S}{C_{SA}} \qquad [3]$$

where C_S (ng m^{-3}) is the individual PAH concentration in surface snow and C_{SA} (ng m^{-3}) is the gas phase concentration that has been equilibrated with the snow surface as measured using the soil-snow fugacity sampler (Table S6, SI). PAHs Log K_{SA} presented a statistically significant correlation with its Log vapour pressure (r^2_s= -0.21, $p < 0.001$), consistent with a lower MW PAHs profile in the gas phase equilibrated with the snow surface than in its correspondent snow sample (Figure 2). Furthermore, as with soil fugacity, snow fugacity was closely correlated to air fugacity and the significant least squares regression between them explained 72% of the variability (Figure 3).

However, f_s/f_a ratios presented no correlation with K_{OA} nor with vapour pressure, and no clear tendency towards volatilization or net-deposition could be established for PAHs regardless of its hydrophobicity (Figure 4), showing close to snow-air equilibrium. This result contrasts with the PAHs net-volatilization from snow observed in for a short period in 2009 at the same region.[1] Even though the temperature ranges in the 2008-2009 and 2014-15 sampling campaigns were overlapping (0.5 to 3.5 °C), during the 2014-15 campaign there was a much larger snow cover of the coastal zone, and a larger number of snow deposition events. Snowflakes may equilibrate with the gas phase in terms of PAH fugacity during their fall[38] and thus, the several snow deposition events during the 2014-15 campaign may have contributed to keep the surface snow fugacity close to equilibrium with the atmosphere. Conversely, in the absence of snow events, and due to melting/freezing occurring daily, it is likely that surface snow losses part of its fugacity capacity, inducing a larger surface snow fugacity than in ambient air, as observed in the 2008-09 campaign. These differences between the two campaigns reflected in the behaviour and fluxes of PAHs are likely due to the amount of snowfall and the timing of snowmelt between the two campaigns.

PAHs in the coastal water column

Average ∑PAHs seawater and plankton concentrations were 1.0 ± 0.82 ng L^{-1} and 80 ± 46 ng g_{dw}^{-1}, respectively (Tables S2-3, SI), with no significant differences between the two sampling sites. PAHs seawater and plankton profiles were dominated by the lower molecular weight compounds, 3-rings PAHs represented on average 50 ± 17% and 73 ± 9.0% of the profile, respectively, with Phe the average highest contributor to ∑PAHs in both matrices (Figure 2). The high predominance of low MW PAHs is consistent with the low aerosol black carbon concentrations and thus low concentrations of high MW PAHs in the atmosphere.[1] The profile in the dissolved and plankton phase reflects the gas phase.

These PAHs seawater concentrations and profiles are comparable to previous reports on Prydz Bay[2] and Terra Nova Bay.[12] Similar low PAHs seawater concentrations can be found in the open ocean.[3] To our knowledge, there are no previous reports of PAHs in plankton for the maritime Antarctica. PAHs concentrations reported in suspended particle matter and biota from Potter Cove (King George Island) are not significantly different.[11]

PAHs concentrations in plankton were not significantly correlated with those in seawater. This is likely due to the fact that while seawater was sampled from the surface, plankton samples integrated the water column from 14 and 30 m depth for the Johnsons and Raquelias sampling sites, respectively. A concurrent sampling on perfluoroalkylated substances concentrations in seawater and plankton also did not show a significant correlation.[43]

∑PAHs concentrations in seawater increased over the sampling campaign period, from late spring to late summer, and were significantly correlated with seawater temperature (Figure 5). This increase in ∑PAHs concentrations is consistent with an increase of fresh water discharge from ice and snow melt during the austral summer, as ambient temperature fluctuated from below freezing temperatures to few positive Celsius degrees (Figure 5). Snow ∑PAHs concentrations were significantly higher than seawater, and fugacity ratios showed no net volatilization from snow, as there was close to equilibrium conditions for air-snow exchange (Figure 4), suggesting that most PAHs in snow are transferred to coastal water through snow-melt.

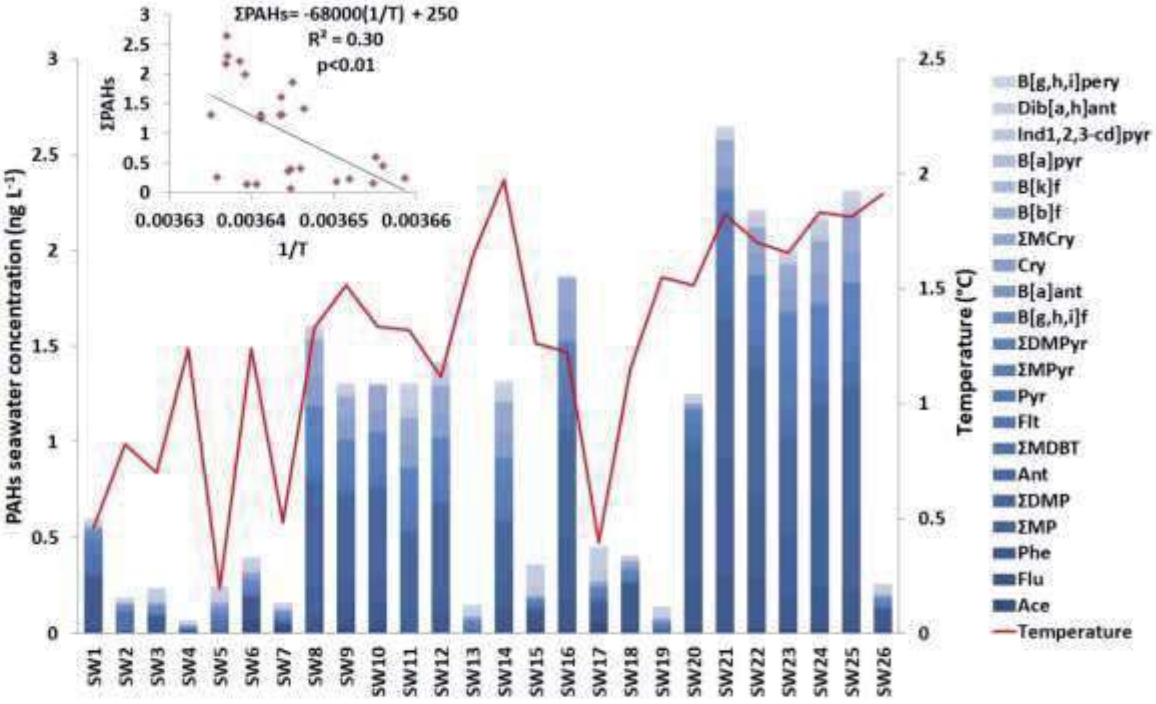

Figure 5. PAHs seawater concentrations (ng L^{-1}) at coastal Livingston Island, and ambient temperature during the austral summer. The sampling for seawater started on December – (sample SW1) and lasted until February – (sample SW26).

Furthermore, 4-5 ringed ∑PAHs concentrations in seawater also were correlated with seawater temperature (Figure S1, SI). This is consistent with the role of fresh water (snowmelt) discharge removing previously deposited aerosol phase PAHs scavenged by wet (snow and rain) deposition. However, ∑PAHs concentrations in coastal seawater were not significantly correlated with salinity, which is likely due to its narrow range (33−34 PSU, Table S1, SI), the tidal dynamics renewing and mixing the top seawater in South Bay, or that the increase of concentration of PAHs in surface waters due to snow-melt inputs is lost due to volatilization, the biological pump, or degradation.

Diffusive air-water fluxes are the main driver for light (2-4 rings) PAHs in the gas and dissolved phase exchange.[3,31] Diffusive air-water fluxes (F_{AW}) were calculated following the two-film resistance model:[44]

$$F_{AW} = F_{AWabs} - F_{AWvol} = k_{AW}\left[\frac{C_A}{H'} - C_W\right] \qquad [4]$$

Where C_W is the dissolved phase PAH concentration (ng m^{-3}), respectively, H' is the temperature and salinity corrected dimensionless Henry's law constant,[45] and k_{AW} is the air-water mass transfer rate (m d^{-1}).[46]

Gross absorption fluxes (F_{AWabs}) ranged from 6.0 to 170 ng m^{-2} d^{-1} (Table S10, SI), and, although H' is temperature dependent, they did not present a significant correlation with seawater or air temperature. On the other hand, as seawater PAH concentrations did present a significant correlation with seawater temperatures (Figure 5), so did the gross volatilization fluxes F_{AWvol}, which ranged from 0.79 to 260 ng m^{-2} d^{-1} (Table S11, SI). Furthermore, gross volatilization fluxes presented significant inverse correlations with salinity (Table S14, SI), consistent with snow-melt driving an increase of the losses due to volatilization.

The resulting net air-water fluxes (F_{AW}, Table S12, SI) followed a remarkable shift during the sampling campaign, from the net deposition of 150 ng m^2 d^{-1} during the late spring, to the net volatilization of 220 ng m^2 d^{-1} during the late summer. The net air-water fluxes showed significant correlations with seawater salinity and temperature (Table S13-14, SI). This net volatilization contrasts with the dominance of absorption fluxes observed in open sea regions such as the tropical and subtropical Atlantic, Pacific and Indian oceans,[3] as well as the Mediterranean and Black seas.[18]

The least squares linear regression of F_{AW} versus salinity (Figure 6), indicates that volatilization is enhanced by the freshwater discharge due to snow/ice melting, which is consistent with the high PAHs concentrations in snow contributing to increase the concentrations in seawater during the snow-melt season. As there is no net volatilization from snow (Figure 3), PAHs are transferred to soil organic matter or coastal seawater. Similar latitudinal and seasonal shifts in the air-seawater water exchange have been previously reported and linked to the contributions from ice/snow-melt for other SVOCs in Antarctica.[47-49] Indeed, glacier snowmelt has also been recently highlighted as a secondary source of SVOCs to the Antarctic marine ecosystem.[50, 51]

Therefore, the overall dynamics of PAHs in coastal Antarctica is consistent with an important role of snow deposition of PAHs, which are accumulated in the snow pack during winter. Surface snow is close to equilibrium with the gas phase concentrations. The concentrations of aerosols are extremely low in this region, especially for black carbon aerosols,[52] dry deposition does not drive high concentrations of high MW PAHs to coastal soils, snow and seawater. Nevertheless, their low concentrations in seawater are correlated with salinity (Figure S1, SI). During the austral summer melting, the PAHs in snowmelt will be either accumulated in the soil organic matter (especially in soils covered by vegetation), and if not retained in soils, PAHs will be transferred to coastal seawater. Glacier melting will also introduce historic PAHs burden to seawater and contribute to salinity decrease. Either in soil organic matter, or in coastal seawater, the fugacity amplification of the original snow results in a fugacity amplification in soil organic matter or surface seawater, and thus it results in a volatilization of PAHs back to the atmosphere.

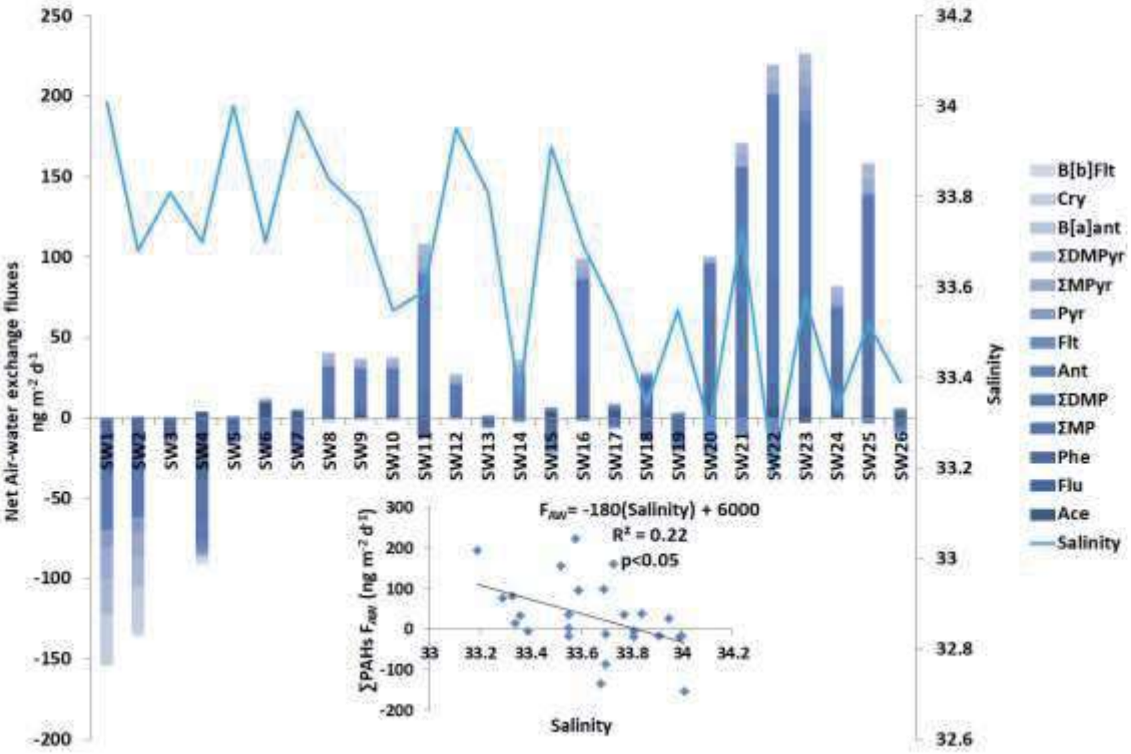

Figure 6. PAHs net air-water exchange fluxes (F_{AW}, ng m^{-2} d^{-1}) and salinity during the three months sampling campaign. Inner panel shows the correlations of F_{AW} with surface seawater salinity.

The main Antarctic sinks will be the transfer of PAHs to coastal sediments due to the biological pump, as well as microbial degradation in seawater and soils,[53] and potential increasing concentrations in the different Antarctic matrixes. Nitrate showed a decrease of concentrations during the austral summer, with direct correlations with salinity and temperature (Figure S2, SI), consistent with an increase of primary productivity that fueled bacterial activities.[54] Phosphate concentrations also increased during high turbidity periods, maybe related to inputs of glacier derived material (Figure S3, SI). Bacterial abundances were concurrently measured with the PAHs and nutrient concentrations in seawater, and the rates of increase/decrease of bacterial cells estimated from consecutive measurements of bacterial biomass. Bacterial abundance was correlated with ammonium concentrations ($r^2=0.47$, $p<0.01$), that increased from the low values during the first sampling periods, to higher levels for most of the rest of the austral summer (Table S1, SI). Ammonium may have originated from organic matter inputs from land, which is consistent with its co-variability with bacteria, and the direct correlation between ∑PAHs in the dissolved phase and ammonium concentrations (Figure S4, SI). Previous reports have shown that the concentrations of 2-3 ring PAHs in plankton (as surrogates of the levels in the water column) decrease with the planktonic biomass, which has been suggested as evidence of microbial degradation.[52] PAH concentrations of lower MW PAHs at coastal Antarctic plankton also decreased with biomass as in previous reports (Figure S5, SI). In addition, the concentrations of 2-3 ring PAHs in plankton were correlated by means of a multiple linear least squares regression with the bacterial abundance for the previous time period, temperature and the interaction of both ($r^2=0.57$, $p<0.5$). These results provide evidence that microbial degradation and temperature play key roles by controlling the water column concentrations through snow-melting enhanced inputs to the coastal zone (temperature driven) and consumption of lighter PAHs in the water column. Polar marine bacteria has been described to have the potential for degrading PAHs using these chemicals as a source of carbon.[56, 57] It is unclear, to which degree the Antarctica is a net sink of PAHs, as the integrated fluxes to the sediment, and of degradation in the water column could not be constrained. Microbial degradation of PAHs in coastal soils is feasible, but experiments have shown that this is an extremely slow process at low temperatures.[58] Therefore, the marine biological and degradative pumps will account for the major Antarctic sinks, as the temperature driven net volatilization of PAHs described here will recycle an important fraction of PAHs back to the atmosphere, and thus susceptible of further transport and deposition. In this case, Antarctica would just be one stop in the grass hopping journey.

REFERENCES

(1) Cabrerizo, A.; Galbán-Malagón, C.; Del Vento, S.; Dachs, J. Sources and fate of polycyclic aromatic hydrocarbons in the Antarctic and Southern Ocean atmosphere. *Glob. Biogeochem. Cycles*, **2014**, 28, 1424–1436.

(2) Cai, M.; Liu, M.; Hong, Q.; Lin, J.; Huang, P.; Hong, J.; Wang, J.; Zhao, W.; Chen, M.; Cai, M.; Ye, J. Fate of Polycyclic Aromatic Hydrocarbons in Seawater from the Western Pacific to the Southern Ocean (17.5°N to 69.2°S) and Their Inventories on the Antarctic Shelf. *Environ. Sci. Technol*. **2016**, 50(17), 9161-9168.

(3) Gonzalez-Gaya, B.; Fernandez-Pinos, M.-C.; Morales, L.; Mejanelle, L.; Abad, E.; Pina, B.; Duarte, C. M.; Jimenez, B.; Dachs, J. High atmosphere-ocean exchange of semivolatile aromatic hydrocarbons. *Nat. Geosci*. **2016**, 9(6), 438−442.

(4) Bostrom, C. E.; Gerde, P.; Hanberg, A.; Jernström, B.; Johansson, C.; Kyrklund, T.; Rannug, A.; Törnqvist, M.; Victorin, K.; Westerholm, R. Cancer risk assessment, indicators, and guidelines for polycyclic aromatic hydrocarbons in the ambient air. *Environ. Health Perspect.* **2002**, 110:451–488.

(5) Hylland, K. Polycyclic aromatic hydrocarbon (PAH) ecotoxicology in marine ecosystems. J*. Toxicol. Environ Health* **2006**, A, 69, 109–123.

(6) Lei, Y. D.; Wania, F. Is rain or snow a more efficient scavenger of organic chemicals? *Atmos. Environ*. **2004**, 38(22), 3557-3571.

(7) Tin, T.; Fleming, Z.L.; Hughes, K.A.; Ainley, D.G.; Convey, P.; Moreno, C.A.; Pteiffer, S.; Scott, J.; Snape, I. Impacts of local human activities on the Antarctic environment. *Antarct. Sci*. **2008**, 21 (01), 3–33.

(8) Cabrerizo, A.; Dachs, J.; Barceló, D.; Jones, K. C. Influence of organic matter content and human activities on the occurrence of organic pollutants in Antarctic soils, lichens, grass, and mosses. *Environ. Sci. Technol*. **2012**, 46(3), 1396-1405.

(9) Fuoco, R.; Giannarelli, S.; Wei, Y.; Abete, C.; Francesconi, S.; Termine, M. Polychlorobiphenyls and polycyclic aromatic hydrocarbons in the sea-surface micro-layer and the water column at Gerlache Inlet (Antarctica), *J. Environ. Monit*. **2005**, 1313–1319.

(10) Fuoco, R.; Giannarelli, S.; Onor, M.; Ghimenti, S.; Abete, C.; Termine, M.; Francesconi, S. A snow/firn four-century record of polycyclic aromatic hydrocarbons (PAHs) and polychlorobiphenyls (PCBs) at Talos Dome (Antarctica). *Microchem. J.* **2012**, 105, 133–141, http://dx.doi.org/10.1016/j.microc.2012.05.018.

(11) Curtosi, A.; Pelletier, E.; Vodopivez, C. L.; Mac Cormack, W. P. Distribution of PAHs in the water column, sediments and biota of Potter Cove, South Shetland Islands, Antarctica. *Antarct. Sci.* **2009**, 21(4), 329-339.

(12) Stortini, A. M.; Martellini, T.; Del Bubba, M.; Lepri, L.; Capodaglio, G.; Cincinelli, A. n-Alkanes, PAHs and surfactants in the sea surface microlayer and sea water samples of the Gerlache Inlet sea (Antarctica). *Microchem. J*. **2009**, 92(1), 37-43

(13) Na, G.; Liu, C.; Wang, Z.; Ge, L.; Ma, X.; Yao, Z. Distribution and characteristic of PAHs in snow of Fildes Peninsula, *J. Environ. Sci*. **2011**, 23, 1445–1451.

(14) Vecchiato, M.; Argiriadis, E.; Zambon, S.; Barbante, C.; Toscano, G.; Gambaro, A.; Piazza, R. Persistent Organic Pollutants (POPs) in Antarctica: occurrence in continental and coastal surface snow. *Microchem. J*. **2015**, 119, 75-82.

(15) Bengtson Nash S. Persistent organic pollutants in Antarctica: current and future research priorities. *J. Environ. Monit.* **2011**, 13, 497-504.

(16) Galbán-Malagón, C. J.; Del Vento, S.; Cabrerizo, A.; Dachs, J. Factors affecting the atmospheric occurrence and deposition of polychlorinated biphenyls in the Southern Ocean. *Atmos. Chem. Phys*. **2013**, 13(23), 12,029–12,041.

(17) Galbán-Malagón, C.; Cabrerizo, A.; Caballero, G.; Dachs, J. Atmospheric occurrence and deposition of hexachlorobenzene and hexachlorocyclohexanes in the Southern Ocean and Antarctic Peninsula. *Atmos. Environ.* **2013,** 80, 41–49.

(18) Castro-Jiménez, J.; Berrojalbiz, N.; Wollgast, J.; Dachs, J. Polycyclic aromatic hydrocarbons (PAHs) in the Mediterranean Sea: atmospheric occurrence, deposition and decoupling with settling fluxes in the water column. *Environ. Pollut*. **2012**, 166, 40-47.

(19) Cabrerizo, A.; Dachs, J.; Barcelo, D. Development of a Soil Fugacity Sampler for Determination of Air−Soil Partitioning of Persistent Organic Pollutants under Field Controlled Conditions. *Environ. Sci. Technol*. **2009**, 43 (21), 8257−8263.

(20) Cabrerizo, A.; Dachs, J.; Moeckel, C.; Ojeda, M. J.; Caballero, G.; Barceló, D.; Jones, K. C. Ubiquitous net volatilization of polycyclic aromatic hydrocarbons from soils and

parameters influencing their soil-air partitioning. *Environ. Sci. Technol*. **2011**, 45 (11), 4740–4747.

(21) Casal, P.; Castro-Jiménez, J.; Pizarro, M.; Katsoyiannis, A.; Dachs, J. Seasonal soil/snow-air exchange of semivolatile organic pollutants at a coastal arctic site (Tromsø, 69° N). *Sci. Total Environ*. **2018**, 636, 1109-1116.

(22) Grasshoff, K.; Armstrong, F. A. J.; Sterns, C.R.; Strickland, J. D. H. The measurement of upwelling and subsequent biological processes by means of the Technicon AutoAnalyzer and associated equipment. *Deep Sea Res*. **1967**, 14, 381-389.

(23) Tamminen, M.; Karkman, A.; Lõhmus, A.; Muziasari, W. I.; Takasu, H.; Wada, S.; Suzuki, S.; Virta, M. Tetracycline resistance genes persist at aquaculture farms in the absence of selection pressure. *Environ. Sci. Technol*. **2010**, 45(2), 386-391.

(24) Vila-Costa, M., Barberan, A.; Auguet, J. C.; Sharma, S.; Moran, M. A.; Casamayor, E. O. Bacterial and archaeal community structure in the surface microlayer of high mountain lakes examined under two atmospheric aerosol loading scenarios. *FEMS microbiology ecology*, **2013**, 84(2), 387-397.

(25) Halsall, C. J.; Barrie, L. A.; Fellin, P.; Muir, D. C. G.; Billeck, B. N.; Lockhart, L.; Rovinsky, F. Y.; Kononov, E. Y.; Pastukhov, B. Spatial and temporal variation of polycyclic aromatic hydrocarbons in the Arctic atmosphere, *Environ. Sci. Technol*. **1997**, 31(12), 3593–3599.

(26) Hung, H.; Blanchard, P.; Halsall, C. J.; Bidleman, T. F.; Stern, G. A.; Fellin, P.; Muir, D.G.C.; Barrie, L.A.; Jantunen, L.M.; Helm, P.A.; Ma, J. Temporal and spatial variabilities of atmospheric polychlorinated biphenyls (PCBs), organochlorine (OC) pesticides and

polycyclic aromatic hydrocarbons (PAHs) in the Canadian Arctic: Results from a decade of monitoring. *Sci. Total Environ*. **2005**, 342(1-3), 119-144.

(27) Wang, R.; Tao, S.; Wang, B.; Yang, Y.; Lang, C.; Zhang, Y. X.; Hu, J.; Ma, J. M.; Hung, H. Sources and pathways of polycyclic aromatic hydrocarbons transported to alert, the Canadian High Arctic, *Environ. Sci. Technol*. **2010**, 44(3), 1017–1022.

(28) Ma, Y.; Xie, Z.; Yang, H.; Möller, A.; Halsall, C.; Cai, M.; Sturm,R.; Ebinghaus, R. Deposition of polycyclic aromatic hydrocarbons in the North Pacific and the Arctic. *J. Geophys. Res.* **2013**, 118 (11), 5822−5829.

(29) Wania, F.; Haugen, J.-E.; Lei, Y. D.; Mackay, D. Temperature Dependence of Atmospheric Concentrations of Semivolatile Organic Compounds. *Environ. Sci. Technol*. **1998**, 32, (8), 1013-1021-

(30) Gigliotti, C. L.; Dachs, J.; Nelson, E. D.; Brunciak, P. A.; Eisenreich, S. J. Polycyclic aromatic hydrocarbons in the New Jersey coastal atmosphere. *Environ. Sci. Technol*. **2000**, 34(17): 3547-3554.

(31) Gigliotti, C. L.; Brunciak, P. A.; Dachs, J.; Glenn, T. R.; Nelson, E. D.; Totten, L. A.; Eisenreich, S. J. Air—water exchange of polycyclic aromatic hydrocarbons in the New York—New Jersey, USA, Harbor Estuary. *Environ. Toxicol. Chem.* **2002**, 21(2), 235-244.

(32) Nizzetto, L.; Lohmann, R.; Gioia, R.; Jahnke, A.; Temme, C.; Dachs, J.; Herckes, P.; Guardo, A. D.; Jones, K. C. PAHs in air and seawater along a northsouth atlantic transect: trends, processes and possible sources. *Environ. Sci. Technol*. **2008**, 42 (5), 1580–1585.

(33) Wilcke, W. Global patterns of polycyclic aromatic hydrocarbons (PAHs) in soil. *Geoderma* **2007**, 141 (34), 157–166.

(34) Cabrerizo, A.; Tejedo, P.; Dachs, J.; Benayas, J. Anthropogenic and biogenic hydrocarbons in soils and vegetation from the South Shetland Islands (Antarctica). *Sci. Total Environ.* **2016**, 569, 1500-1509.

(35) Degrendele, C.; Audy, O.; Hofman, J.; Kučerik, J.; Kukučka, P.; Mulder, M. D.; Přibylová, P.;Prokeš, R.; Šáňka, M.; Schaumann, G. E.; Lammel, G. Diurnal variations of air-soil exchange of semivolatile organic compounds (PAHs, PCBs, OCPs, and PBDEs) in a central European receptor area. *Environ. Sci. Technol*. **2016**, 50(8), 4278-4288.

(36) Kukučka, P.; Lammel, G.; Dvorská, A.; Klánová, J.; Möller, A.; Fries, E. Contamination of Antarctic snow by polycyclic aromatic hydrocarbons dominated by combustion sources in the polar region. *Environ. Chem.* **2010**, 7, 504, http://dx.doi.org/10.1071/EN10066.

(37) Keyte, I. J.; Harrison, R. M.; Lammel, G. Chemical reactivity and long-range transport potential of polycyclic aromatic hydrocarbons — a review. *Chem. Soc. Rev*. **2013**, 42, 9333–9391, http://dx.doi.org/10.1039/c3cs60147a.

(38) Stohl, A.; Sodemann, H. Characteristics of atmospheric transport into the Antarctic troposphere. *J. Geophys. Res*. **2010**, 115, D02305, doi: 10.1029/2009JD012536.

(39) Macdonald, R.; Mackay, D.; Hickie, B. Contaminant amplification in the environment *Environ. Sci. Technol*. **2002**, 36, 456A– 462A DOI: 10.1021/es022470u

(40) Casal, P.; Zhang, Y.; Martin, J. W.; Pizarro, M.; Jiménez, B.; Dachs, J. Role of Snow Deposition of Perfluoroalkylated Substances at Coastal Livingston Island (Maritime Antarctica). *Environ. Sci. Technol*. **2017**, 51(15), 8460-8470.

(41) Jurado, E.; Jaward, F.; Lohmann, R.; Jones, K. C.; Simó, R.; Dachs, J. Wet deposition of persistent organic pollutants to the global oceans. *Environ. Sci. Technol*. **2005**, 39, 2426-2435.

(42) Bamford, H. A.; Poster, D. L.; Baker, J. E. Temperature dependence of Henry's law constants of thirteen polycyclic aromatic hydrocarbons between 4 C and 31 C. *Environ. Toxicol. Chem.* **1999**, 18(9), 1905-1912.

(43) Jurado, E.; Lohmann, R.; Meijer, S.; Jones, K. C.; Dachs, J. Latitudinal and seasonal capacity of the surface oceans as a reservoir of polychlorinated biphenyls. *Environ. Pollut*. **2004**, 128, 149-162.

(44) Dickhut, R. M.; Cincinelli, A.; Cochran, M.; Ducklow, H. W. Atmospheric concentrations and air− water flux of organochlorine pesticides along the Western Antarctic Peninsula. *Environ. Sci. Technol*. **2005**, 39(2), 465-470.

(45) Bigot, M.; Muir, D. C.; Hawker, D. W.; Cropp, R.; Dachs, J.; Teixeira, C. F.; Bengtson Nash, S. Air–seawater exchange of organochlorine pesticides in the southern ocean between Australia and Antarctica. *Environ. Sci. Technol*. **2016**, 50(15), 8001-8009.

(46) Bigot, M.; Hawker, D. W.; Cropp, R.; Muir, D. C.; Jensen, B.; Bossi, R.; Bengtson Nash, S. M. Spring melt and the redistribution of organochlorine pesticides in the sea-ice environment: A comparative study between Arctic and Antarctic regions. *Environ. Sci. Technol*. **2017**, 51(16), 8944-8952.

(47) Geisz, H. N.; Dickhut, R. M.; Cochran, M. A.; Fraser, W. R.; Ducklow, H. W. Melting glaciers: a probable source of DDT to the Antarctic marine ecosystem. *Environ. Sci. Technol*. **2008**, 42(11), 3958-3962.

(48) Khairy, M. A.; Luek, J. L.; Dickhut, R.; Lohmann, R. Levels, sources and chemical fate of persistent organic pollutants in the atmosphere and snow along the western Antarctic Peninsula. *Environ. Pollut*. **2016**, 216, 304-313.

(49) Maskey, S.; Geng, H.; Song, Y. C.; Hwang, H.; Yoon, Y. J.; Ahn, K. H.; Ro, C. U. Single-particle characterization of summertime antarctic aerosols collected at King George island using quantitative energy-dispersive electron probe X-ray microanalysis and attenuated total reflection Fourier transform-infrared imaging techniques. *Environ. Sci. Technol*. **2011**, 45 (15), 6275−6282.

(50) Haritash, A. K.; Kaushik, C. P. Biodegradation aspects of polycyclic aromatic hydrocarbons (PAHs): a review. *J. Hazard. Mater*. **2009**, 169(1-3), 1-15.

(51) Goldberg, S. J.; Nelson, C. E.; Viviani, D. A.; Shulse, C. N.; Church, M. J. Cascading influence of inorganic nitrogen sources on DOM production, composition, lability and microbial community structure in the open ocean. *Environ. Microbiol*. **2017**, 19, 9, (3450-3464).

(52) Berrojalbiz, N.; Dachs, J.; Ojeda, M. J.; Valle, M. C.; Castro-Jimenez, J.; Wollgast, J.; Ghiani, M.; Hanke, G.; Zaldivar, J. M. Biogeochemical and physical controls on concentrations of polycyclic aromatic hydrocarbons in water and plankton of the Mediterranean and Black Seas. *Global Biogeochem. Cycles* **2011**, 25.

(53) Garneau, M. È.; Michel, C.; Meisterhans, G.; Fortin, N.; King, T. L.; Greer, C. W.; Lee, K. Hydrocarbon biodegradation by Arctic sea-ice and sub-ice microbial communities during microcosm experiments, Northwest Passage (Nunavut, Canada). *FEMS Microbiology Ecology*, **2016**, 92(10)

(54) Vergeynst, L.; Wegeberg, S.; Aamand, J.; Lassen, P.; Gosewinkel, U.; Fritt-Rasmussen, J.; Gustavson, K.; Mosbech, A. Biodegradation of marine oil spills in the Arctic with a Greenland perspective. *Sci. Total. Environ.* **2018**; 626: 1243–1258.

(55) Okere, U. V.; Cabrerizo, A.; Dachs, J.; Jones, K. C.; & Semple, K. T. Biodegradation of phenanthrene by indigenous microorganisms in soils from Livingstone Island, Antarctica. *FEMS microbiology letters*, **2012**, 329(1), 69-77.

ACKNOWLEDGEMENTS

Inorganic nutrient analyses were performed by Mrs. M. I. Abad in coordination with Dr. E. Berdalet (Head of the Service) at the “Nutrient Analysis Service” of the ICM (CSIC). We thank F Cerqueria and A Martinez for support with DNA analysis. This work was supported by Spanish Ministry of science to PC through a predoctoral fellowhip, by Fundación BBVA award to MVC, European Commission to AC through a Marie Curie international outgoing fellowship, and by the Spanish MINECO through projects REMARCA (CTM2012-34673) and ISOMICS (CTM2015-65691-R). The research group of Global Change and Genomic Biogeochemistry is supported by the Catalan Government (2017SGR800).

Capítol 5: Snow deposition enhances the net volatilization of Polychlorinated Biphenyls and Organochlorine Pesticides from Antarctic coastal soils and waters

Paulo Casal, Ana Cabrerizo, Maria Vila-Costa, Mariana Pizarro, Begoña Jiménez,

Jordi Dachs

Enviat a Environmental Science and Technology

Submitted to *Environmental Science & Technology*

SNOW DEPOSITION ENHANCES THE NET VOLATILIZATION OF POLICHLORINATED BIPHNYLS AND ORGANOCHLORINE PESTICIDES FROM ANTARCTIC COASTAL SOILS AND WATERS

Paulo Casal[1], Ana Cabrerizo[1], Maria Vila-Costa[1], Mariana Pizarro[1], Begoña Jiménez[2], Jordi Dachs[1]*

[1]Institute of Environmental Assessment and Water Research (IDAEA-CSIC), Barcelona, Catalonia 08034, Spain.

[2]Department of Instrumental Analysis and Environmental Chemistry, Institute of Organic Chemistry (IQOG-CSIC), Madrid 28006, Spain.

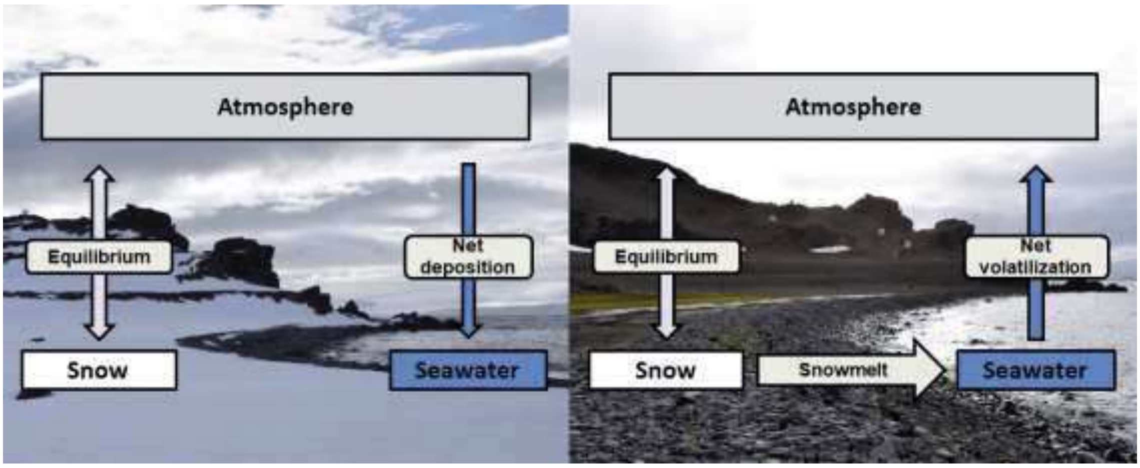

Abstract

Polar Regions are considered global sinks and reservoirs of persistent organic pollutants (POPs), such as polychlorinated biphenyls (PCBs) and organochlorine pesticides (OCPs). However, recent studies have shown a remobilization of semivolatile POPs from soils, snow and glaciers. Nevertheless, the cycling of POPs between the atmosphere, land and ocean remain under-characterized, especially for coastal Antarctica. A three-month sampling campaign was carried out at Livingston Island, Antarctica, to assess the dynamics of POPs and its environmental driving factors. Air, snow, the fugacity of POPs in soils and snow, coastal seawater and plankton were sampled concurrently from late spring (December 2014) to late summer (February 2015). POPs snow concentrations were significantly correlated with snow density consistent with snow aging affecting the concentrations in the snowpack, and driving the transfer of POPs to air, soils and seawater. Air-snow fugacity ratios and net diffusive fluxes showed a high variability, but with air and snow concentrations close to equilibrium. The air-soil fugacity ratios also indicated concentrations close to air-soil equilibrium for bare soils. However, a significant net volatilization of POPs was observed for soils covered with vegetation, which presented a higher content in organic matter, probably retaining POPs from the snow-melt. For all sampling periods, POP concentrations in snow were higher than in seawater. Furthermore, PCBs seawater concentrations increased during the austral summer, consistent with snow-melt as a source of POPs, which also affected PCBs seawater-air diffusive fluxes. While air to seawater net deposition fluxes were dominant during the late spring, net volatilization fluxes were dominant during the late summer. The resulting net air-water diffusive fluxes were correlated with the decrease in seawater salinity, consistent with snow-melt driving a discharge of POPs to seawater over the austral summer. All these observations are consistent with the role of snow amplifying concentrations and fugacities of POPs, an amplification that is transferred to soils and seawater. The study presented here provides evidence of a key role of snow deposition and melting driving the re-volatilization of POPs from Antarctic coastal soils and waters.

Introduction

Persistent organic pollutants (POPs), including polychlorinated biphenyls (PCBs) and organochlorine pesticides (OCPs), such as hexachlorocyclohexanes (HCHs) and hexachlorobenzene (HCB), are under international regulation by the Stockholm Convention of the United Nations Environment Programme.[1] POPs have raised concern due to their toxicity, bioaccumulation and biomagnification potential and their low degradability.[2]

These semivolatile POPs reach remote regions due to their persistence and long-range atmospheric transport (LRAT) potential. Nevertheless, oceanic transport of POPs to Antarctica is hindered by the Antarctic Circumpolar Current, which minimizes the north-south exchange of dissolved POPs.[3] Despite this, POPs have been detected in water masses south of the Antarctic circumpolar current due to atmospheric transport and deposition.[4-7] Local sources have also been reported from research stations,[8, 9] although represent a comparable limited impact due to a low population.

Dry and wet deposition, particularly the later due to the effectiveness of snow scavenging,[10] contribute as a unidirectional air to seawater/soil/snow flux of POPs. Partitioning from the atmosphere to seawater, soils, and snow is generally enhanced at low temperatures, a process known as “cold-trapping”.[11] Diffusive exchanges occur in both directions, and snow and soil reemission of POPs to the atmosphere can occur as a consequence of declining atmospheric concentrations and/or climate change induced temperature increases in Polar Regions.[12-14] A temperature increase and consequent glacial retreat has been well documented for the Western Antarctic Peninsula,[15-17] which may drive POPs remobilization to air.[12, 13] Seasonal volatilization during warm periods of previously deposited POPs may, however, dominate the observed fluxes in Antarctica, as annual variations in temperature and precipitation are larger than long-term perturbations in climate. Snow and ice melting has been also suggested to contribute to the release of POPs and impact local freshwaters and coastal seawater.[18, 19]

Legacy POPs, such as PCBs, HCHs and HCB have already been reported in the Antarctic atmosphere, seawater, soils and snow,[5, 6, 12, 13, 20-23] however, previous assessments focused on individual air to surface processes such as air-soil and air-water exchange. Even for these extensively studied POPs, there is a lack of works with comprehensive assessments of the atmosphere-land-seawater concentrations and fluxes at coastal Antarctica, as well for other coastal environments. The relative importance of these different partitioning and transport processes, as well as the effect of climatic and seasonal drivers, such as temperature, snow deposition, and biogeochemical controls on them still remain understudied.

Therefore, the objectives of this work are: i) to report the largest multi-compartment data set for HCHs, HCB and PCBs in the coastal Antarctica ii) to evaluate the POPs air-snow, air-soil and air-seawater exchanges and iii) to assess the environmental drivers of POPs fluxes at coastal Antarctica, with an special emphasis of the study of drivers of seawater concentrations.

Materials and methods

Site description and sampling.

The sampling campaign was carried out at Livingston Island (62° 39′ S, 60° 23′ W), in the South Shetland Archipelago, Antarctica, from December 1st, 2014 to March 1st, 2015.

Surface snow samples (n=10) were collected with a stainless steel shovel (Figure 1) and left to melt into Teflon bottles for 24 - 48 h at 4-6 °C. The melted snow was filtered through pre-combusted GF/F glass fiber filters (Whatmann 0.7 µm) before passing through a pre-cleaned XAD-2 (Supelco) packed stainless steel columns. The filtration and extraction of melted snow was performed outdoors in order to maintain environmental temperatures and avoid contamination from indoors air. The XAD-2 columns were stored at 4 °C for refrigerated transport until further analysis.

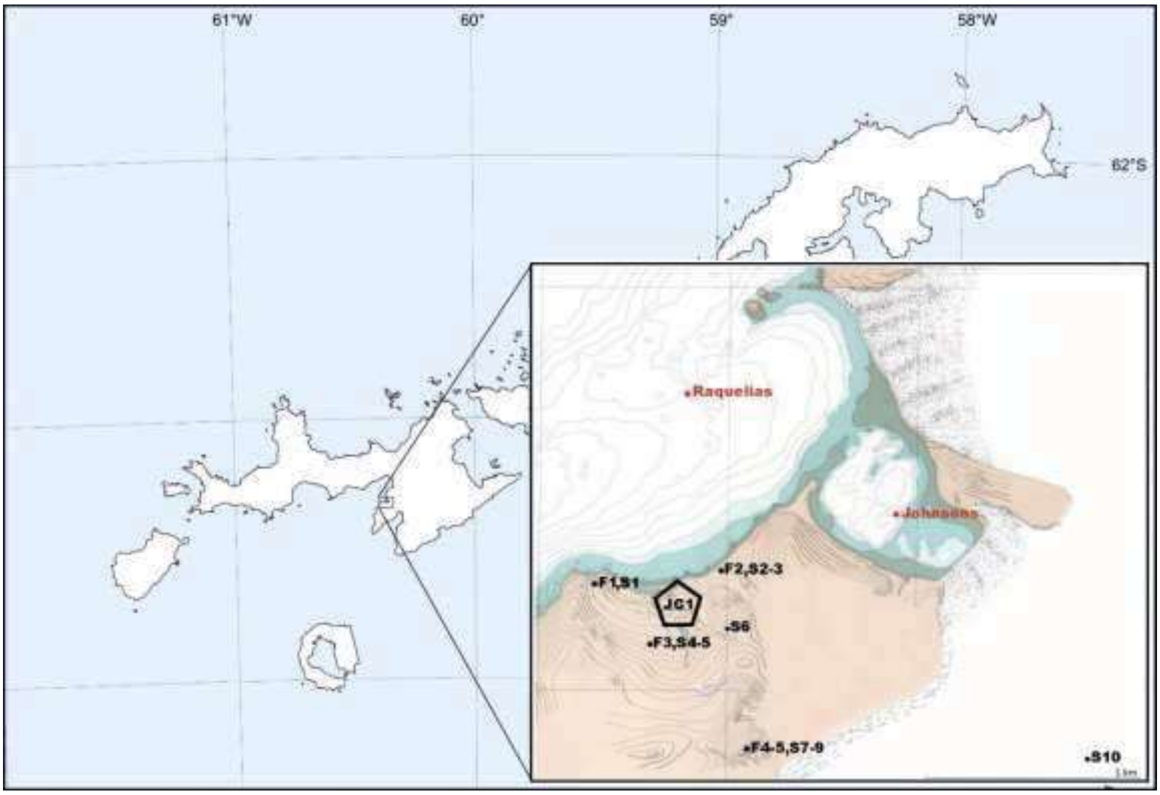

Figure 1. Sampling sites at Livingston Island. Five fugacity samplers were deployed to collect gas phase and gas phase equilibrated with snow/soil at F1-5. Seawater and plankton samples were taken at Raquelias site (62° 39,438’ S, 60° 23,306’ W) and Johnsons site (62° 39,556’ S, 60° 22,132’ W). Snow samples were collected at S1-10.

26 seawater and 26 plankton samples were collected from a rigid inflatable boat at two sampling sites: Johnsons (62° 39,556’S, 60° 22,132’W, 14m depth) and Raquelias (62° 39,438’S, 60° 23,306’W, 30m depth) (Figure 1). CTD (Conductivity, Temperature, Density) depth profiles were taken before sample collection over the sampling campaign (Table S1, SI). 100-120 L surface seawater samples (1 m depth) were collected in 20 L aluminum jerry cans and transported to the Juan Carlos I station (JC1) where they were further processed (Tables S2, SI). Seawater samples followed the

same filtration and extraction method as for snow samples, also carried out outdoors. Plankton samples were collected by vertical hauls with a conical plankton net with a 50 µm mesh. Plankton samples were filtered with pre-combusted and pre-weighted GF/D glass fiber filters (Whatmann 2.7 µm mesh size, 47 mm diameter), subsequently wrapped in pre-combusted aluminum foil, and stored at -20°C in air-tight plastic bags.

Five soil/snow fugacity samplers[24] where deployed during the sampling campaign (Figure 1) to collect ambient air and air in-situ equilibrated with the soil/snow surface (51 pairs of samples). These two simultaneous samplers were taken on a weekly basis (Table S3, SI), and allowed to estimate the POP ambient air and soil/snow fugacity, and thus the direction of the air-snow/soil exchange. The five samplers were deployed at different altitudes (10, 70, 125, 275 meters above sea level) and different distances from the research station (Figure 1). The average sampled air volume was 86 m^3. Both the ambient air and the air equilibrated with the soil/snow were pre-filtered through pre-combusted glass fibber filters (GF/F) to remove dust particles, and subsequently through 10 × 2 cm pre-cleaned polyurethane foam plugs (PUFs) in which the gas phase compounds were retained. After sample collection the PUFs were stored at -20°C in air-tight pre-combusted glass vials.

Analytical Procedures.

Snow and seawater samples collected on XAD-2 columns were eluted with 200 mL of methanol, 200 mL of dichloromethane and 100 mL of hexane at a flow rate of 2 mL min^{-1} using an axial piston pump. The methanol fraction was concentrated and then followed three consecutive liquid-liquid extractions with 50 mL of hexane as reported elsewhere.[25] Extracts were filtered through anhydrous sodium sulphate and combined with the previous dichloromethane and hexane fractions. After reducing the volume, the extracts followed the fractionation method reported elsewhere.[25]

Plankton samples were Soxhlet extracted with dichlorometane:hexane (1:1, v:v) for 24h, and followed a previously described fractionation method.[26] Briefly, extracts were fractionated on a 5g of silica gel (silica 60, 200 mesh, activated at 250 °C for 24h) and 3g of 3% deactivated neutral alumina (aluminium oxide 90, activated at 250 °C for 12h) column, with 25 ml of hexane and 40 ml of dichlorometane:hexane (1:3, v:v). The hexane fraction, which contained the PCBs and OCPs, was concentrated in iso-octane and transferred to an injection vial with a final volume of 100 µl.

PUFs were Soxhlet extracted with acetone:hexane (3:1, v:v) during 24 h. PUFs fractionation details can be found elsewhere.[12, 24]

Hexachlorobenzene (HCB), hexachlorocyclohexane HCH isomers (α-HCH, β-HCH, γ-HCH, δ-HCH) and PCB congeners were analysed by a gas chromatograph equipped with a µ-electron capture detector (GC-µ-ECD, Agilent Technologies, model 7890N) with a 60 m (0.25 mm i.d x 0.25µm film thickness) DB-5 capillary column. The instrument was operated in splitless mode (closed for 1.5 min) and the oven temperature program started at 90 °C to 190 °C at 15 °C/min, then to 203 °C at 3 °C/min (held for 5 min), to 290 °C at 3 °C/min, and finally to 310 °C at 5 °C/min (held for 10 min). Injector and detector temperatures were 280 and 320 °C, respectively. Helium and nitrogen were used as carrier (1.5 mL/min) and makeup (60 mL/min) gases, respectively, and 2 µL of sample were injected. The following PCB congeners were analysed: tri-PCB 18, 17, 31, 28, 33; tetra-PCB 44, 49, 52, 70, 74; penta-PCB 87, 95, 99/101, 105, 110, 118; hexa-PCB, 128, 132, 138, 149, 151, 153, 156, 158, 169; hepta-PCB, 170, 171, 177, 180, 183, 187, 191; octa-PCB 194, 195, 201/199, 205; nona-PCB 206, 208; deca-PCB 209.

Nutrients (phosphate, nitrate plus nitrite, and ammonia) were analysed by continuous flow analysis on a Bran+Luebbe (currently Seal Analytical) autoanalyzer following standard colometric methods.[27]

Bacterial abundance was estimated from the gene copy numbers of the 16S gene by quantitative real-time polymerase chain reaction (qPCR) as described elsewhere.[28] Briefly, DNA was extracted from 47-mm-diameter, 0.2 µm pore-size PTFE filters (Millipore) where we collected the biomass of 2 L of seawater pre-filtered by GF/D (Whatmann) filters. Filters were soaked with lysis buffer (50 mM Tris HCl, 40 mM EDTA, 0.75 M Sucrose), incubated with lysozyme, proteinase K and sodium dodecyl sulphate (SDS), and then nucleic acids were phenol-extracted as previously described.[29] Partial bacterial 16S gene fragments were quantified with SYBR Green (Thermo Scientific, Inc.) in one 96-well plate using primers 331F/518R in a Lightcycler 480 II (A.F. Hoffmann-La Roche AG, Inc). The reaction mixture was thermocycled at 95 °C for 7 minutes, 40 cycles at 95 °C for 10 s, 60 °C for 30s, and 68 °C for 90s, followed by a final extension of 5 min at 68 °C. The plasmid vector pNORM was used as standard to normalize quantified genes. Each assay was run in triplicates including no template controls and standard curves spanning from 101 to 108 copies of standard 16S genes. Melting curves were obtained to confirm amplification specificity.

Quality Assurance/Quality Control

All recipients, tubes and connections used from the sampling to the chemical analysis were made of stainless steel, glass or PTFE. These were pre-cleaned with acetone prior use in order to avoid contamination. All filters were precombusted at 450 °C over 4 hours. XAD-2 was Soxhlet extracted in methanol:dichlorometane (1:1) before packing in columns, the columns were pre-eluted with methanol, dichloromethane and hexane and the extracts were concentrated and injected to check for potential contaminations. PUFs were pre-cleaned with acetone/hexane (3:1, v:v) over 24 hours and stored in air-tight pre-combusted glass jars.

Field blanks consisted of GF/D filters, PUFs and XAD-2 columns that followed the same process as the samples albeit without the pass of plankton, air, snow or seawater. Procedural and/or field blank were analysed with each batch of 4-6 samples to monitor potential contamination during sampling and extraction. The limits of quantification (LOQs) were defined as the mean concentration of field or procedural blanks (the highest) plus three times the standard deviation of the blank response. For the analytes not detected in procedural blanks, LOQ were derived from the lowest standard in the calibration curve. Surrogate recoveries for the different types of samples are resumed in Table S4 (SI).

RESULTS AND DISCUSSION

Soil-air exchange of PCBs and HCB

Atmospheric concentrations of individual PCBs and $\sum_{41}$PCBs (41 ± 24 pg m^{-3}) were within the range of concentrations previously reported for the Antarctic atmosphere (Table S5, SI).[5, 9, 12, 30-36] There were no significant differences in the atmospheric PCB concentrations between sampling stations at different altitudes and at different distances to the research station.

Gas phase HCB concentrations (11 ± 3.5 pg m^{-3}) were also comparable to previous studies in the Antarctic region (Table S5, SI).[6, 22, 37, 38] $\sum_4$HCHs were detected in less than 10% of air samples, with concentrations ranging from <LOQ to 22 pg m^{-3} (Table S5, SI).

This low detection frequency is consistent with the long term decline of HCHs concentrations in Antarctic air over the last decades[6, 21, 22, 30, 37, 39] following the reduction of HCHs primary sources.[40] Due to the low detection frequency of HCHs in air samples, these compounds were not included in the assessment of air-soil/snow/seawater exchange.

PCBs and OCPs atmospheric concentrations were generally not correlated with air temperature (T), with the exception of PCB-149 and PCB-187 (Figure S1, SI). A lack of temperature dependence of atmospheric concentrations have been described before for the maritime atmosphere of the southern ocean[5, 7] and elsewhere.[41, 42] Gas phase concentrations not correlated with ambient temperatures are consistent with a lack of equilibrium between air and the surface[5-7] which suggests an important contribution of LRAT from distant sources. These observations contrast with a previous report in the Antarctic Peninsula[12] that found a temperature dependence of atmospheric concentrations at sampling station F1 (Figure 1) performed during a one month period. However, the narrower range of the temperatures registered during this sampling campaign (0.26 to 2.6 °C) can also hinder the significance of such correlation, especially as it not included the 0 °C, when frozen-soil melting can liberate POPs trapped in surface soil.

To further establish the potential of soils as local secondary sources to ambient air, the fugacity in air (f_a, Pa) and in soil (f_s, Pa) were calculated for HCB and the individual PCB congeners as:

$$f_a = 10^{-9} C_A RT/MW$$

$$f_s = 10^{-9} C_{SA} RT/MW$$

where C_A is the measured ambient air concentration at 1.5 m height (ng m^{-3}), R is the gas constant (8.314 Pa m^3 mol^{-1} K^{-1}), MW is the chemical's molecular weight (g mol^{-1}), and C_{SA} (ng m^{-3}) is the gas phase concentration that has been equilibrated with the soil surface (Tables S6, SI) as measured using the soil fugacity sampler.

C_{SA} PCBs concentrations and profiles were similar to those of C_A (Table S6, SI). Gas phase concentrations of PCB-149 and PCB-187 also presented significant correlations with air temperature (Figure S1, SI).

There was a significant least squares linear regression of Log f_s versus Log f_a for PCBs (Figure 2), consistent with a close coupling of PCBs between the soil and the atmosphere. This close coupling has been described previously for polar and temperate regions.[12, 26]

The net direction of air-soil exchange of PCBs and HCB was evaluated by comparison of f_a and f_s. Where f_s/f_a ratios higher than 1 indicate net volatilization, while net deposition occurs when f_s/f_a ratios are lower than 1. Due to the uncertainty of these measurements as previously quantified,[12, 24] values of Ln f_s/f_a between -1.2 and 0.53 indicate concentrations too close to equilibrium to discern a significant net volatilization or deposition.

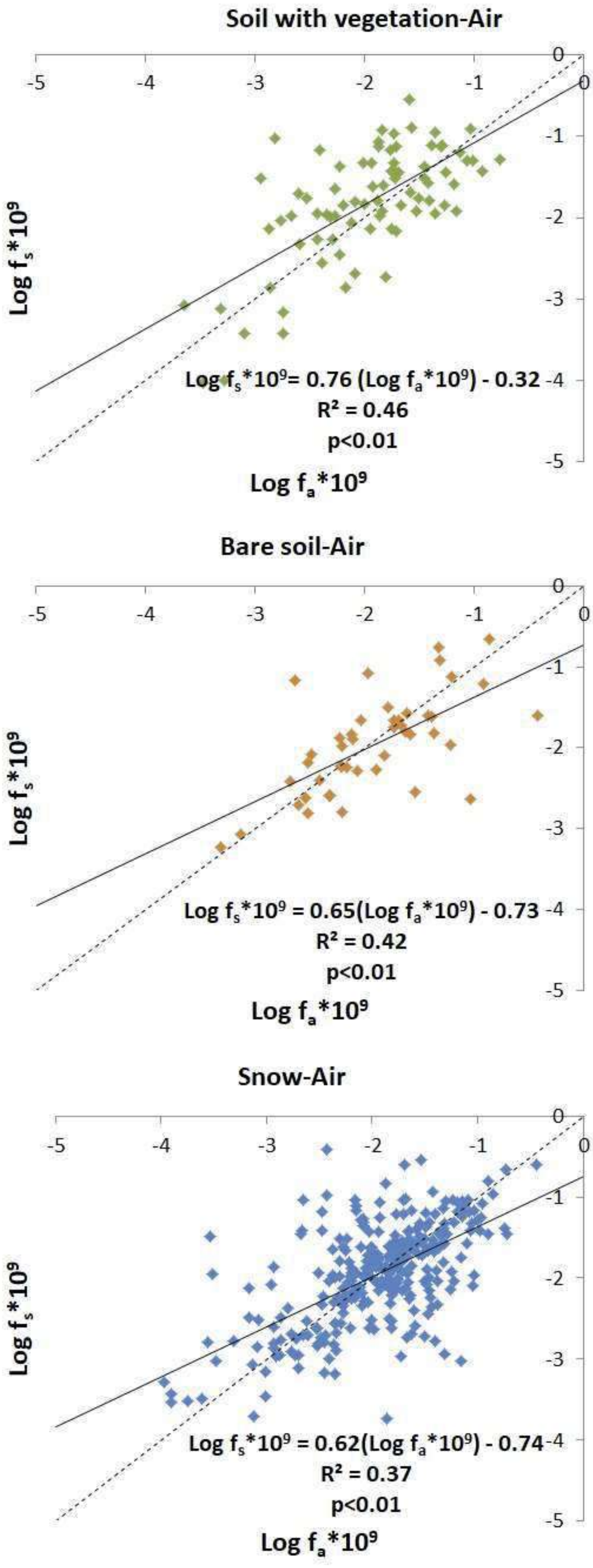

Figure 2. PCB fugacity in air (f_a) versus fugacity in soil/snow (f_s).

PCBs Ln f_s/f_a ratios and Log K_{OA} were significantly correlated (Figure 3), even though this least squares linear regression explained only 10% of the variability. For PCBs with Log K_{OA} below a value of 10.5, Ln f_s/f_a ratios ranged between -1.02 and 4.1 (Figure 3, Table S7, SI), with more than 57% of ratios indicating net-volatilization. On the other hand, more hydrophobic PCBs showed air-soil equilibrium to net deposition for most congeners and sampling events. No differences were observed between sampling sites with bare soil or soil with vegetation (Figure S2, SI).

For HCB, Ln f_s/f_a ratios were not correlated with Log K_{OA} (Figure S3, SI) probably due to the narrow temperature range, however, HCB showed significant differences between sampling sites. While Ln f_s/f_a ratios in bare soils indicated concentrations close to air-soil equilibrium, there was a net-volatilization from soil with a vegetation cover. Probably, these differences are related to the different content in organic matter for the latter, which may retain the high concentrations of HCB in snow (see below).

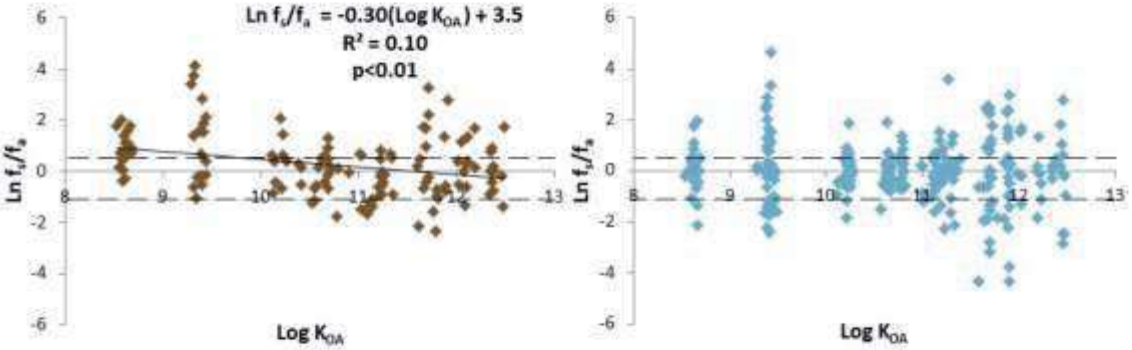

Figure 3. Soil-air fugacity ratios (Ln f_s/f_a) versus the octanol-air partition coefficient (K_{OA}) (left panel), and snow-air fugacity ratios versus K_{OA} (right panel).

Snow-air partitioning of PCBs and OCPs

Snow $\sum_{41}$PCBs concentrations (190 ± 100 pg L^{-1}, Table S8, SI) and the predominance of low MW congeners, mostly tetra and penta-PCBs (39 ± 10% and 35 ± 7.1%, respectively), were similar to those reported in previous studies from the Antarctic Peninsula,[13, 43] and Northern Victoria Land.[44]

Average snow concentrations for HCB and $\sum_{4}$HCHs were of 8.4 ± 3.5 pg L^{-1} and 18 ± 10 pg L^{-1}, respectively (Table S8, SI). These concentrations of OCPs in snow are also in agreement with recent studies,[13, 43] but two to three orders of magnitude lower than those reported in field assessments performed between 1960 and 1980.[30]

Changes in snow properties, particularly the increase in snow density during snow ageing after the snow deposition event, are a dominant factor in PCBs and OCPs snowpack concentrations.[45, 46] Even though snow samples S1-10 were taken in different sampling sites and the snow deposition events occurred over the austral summer (Table S8, SI), $\sum_{41}$PCBs and $\sum_{5}$OCPs snow concentrations presented significant inverse correlations with snow density (Figure 4), these correlations were observed also for individual PCB congeners and OCPs (Table S9, SI). These results are consistent with a previous study performed in the Antarctic Peninsula,[13] where the sample with lowest snow density presented significantly higher concentrations for all POPs. Furthermore, $\sum_{5}$OCPs ($\sum_{4}$HCHs + HCB) and 14 of the target PCBs in that study also presented significant correlations between snow concentrations and snow density (Table S9, SI), even though these correlations were not reported in the original publication.

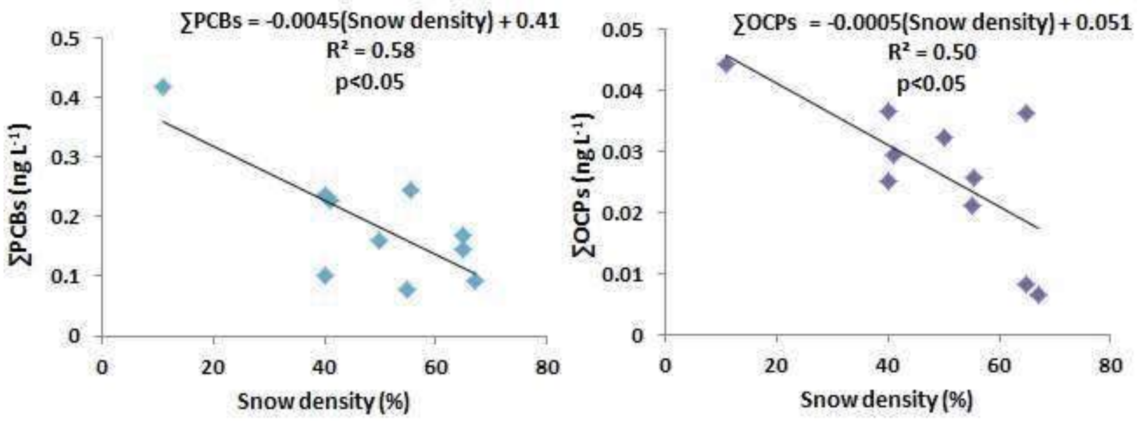

Figure 4. Least squares linear regressions of snow density vs surface $\sum_{41}$PCBs and $\sum_{5}$OCPs snow concentrations (ng L^{-1})

The dependence of snow concentrations with density is consistent with the role of gas and particle phase scavenging of snow during deposition, amplifying the concentrations in snow[47] due to the high specific surface area of fresh snow. This high surface area decreases during aging, concurrently with a snow density increase.[45, 46] Snow aging, and eventually snow-melting, drives a leaching of POPs to water and soils, as well as snow-air gaseous exchange.

Fugacity of PCBs in snow was significantly correlated to air fugacity (Figure 2), consistent with previous reports in this and other polar regions (12, 26), and with a close coupling of the snow and air compartments as observed for soil-air exchange.

The Ln f_s/f_a ratios showed a wide range of variability for all PCB congeners and no significant correlation with Log K_{OA} (Figure 3), nor with vapour pressure (results not shown). A similar variability was observed for HCB (Table S7, SI). There was not a discernible trend on the dominant deposition, equilibrium or volatilization for the different compounds and sampling events. This result is consistent with the correlations between PCBs and OCPs snow concentrations and the rapidly changing snow properties such as snow density (Figure 4). The fugacity sampler integrated seven days for each sample, which included highly variable snow deposition events over the course of each sampling event. Therefore, snow-air gaseous exchanges may have been heavily influenced by these successive changes in snow conditions.

The air-snow diffusive exchange fluxes (F_{Snow}) where calculated for PCBs and HCB by:

$$F_{Snow} = v\left(\frac{C_S}{K_{SA}} - C_A\right)$$

where v is the exchange velocity (m d^{-1}), calculated following the Whitman two-layer resistance method,[48] and K_{SA} is the Snow-Air partition coefficient calculated from the concentrations in air equilibrated with snow and snow ($\frac{C_{SA}}{C_S}$). See Supplementary Information for more details on the flux calculations (Text S1, SI).

Net exchange fluxes ranged from a deposition of 0.22 ng m^{-2} d^{-1} to a volatilization of 0.90 ng m^{-2} d^{-1} for $\sum_{41}$PCBs (Figure 5, Table S10, SI), and from a deposition of 0.14 ng m^{-2} d^{-1} to a volatilization of 0.04 ng m^{-2} d^{-1} for HCB (Table S10, SI). The variability in the fluxes is consistent with the variability of Ln f_s/f_a (Figure 3) together with the snow concentrations dependence on changing snow properties (Figure 4). These results highlight the difficulties in establishing a clear volatilization/deposition pattern between the snow and the atmosphere over long sampling periods, as POPs concentrations are rapidly changing with changing snow properties during aging. Although previous assessments indicate re-volatilization of some POPs in the Antarctic Peninsula,[12, 13] these studies were based on a smaller number of samples covering a shorter sampling period.

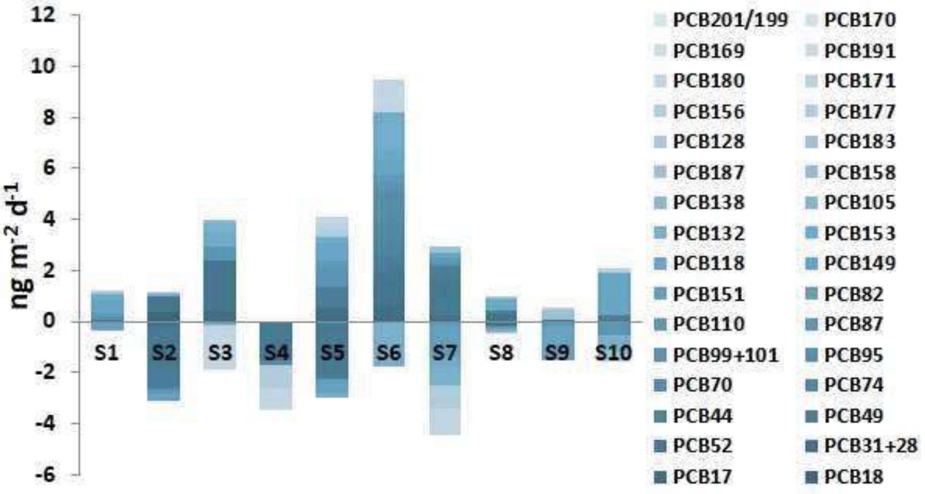

Figure 5. PCBs snow-air diffusive gas fluxes (ng m^{-2} d^{-1})

PCBs, HCHs and HCB in coastal seawater during the austral summer

Average $\sum_{41}$PCBs concentrations in seawater and plankton were 59 ± 26 pg L^{-1} and 26 ± 29 ng g_{dw}^{-1}, respectively (Tables S2, S11, SI). Seawater and plankton PCBs concentrations reported here are comparable with previous studies in the Southern Ocean and Antarctic coastal sites.[5, 23, 30, 49, 50]

OCPs were detected in all seawater and plankton samples (Tables S2, S11, SI). Average HCB concentrations in seawater (2.6 ± 1.7 pg L^{-1}) and plankton (0.28 ± 0.17 ng g_{dw}^{-1}) were within the range of previous studies.[6, 22] Previously reported HCHs concentrations in seawater presented a wide range of values, influenced by the high seawater concentrations reported in the 80s.[30, 49] However, the average $\sum_4$HCHs concentrations in seawater (1.3 ± 1.6 pg L^{-1}) measured here were comparable to recent studies.[6, 22, 37, 51, 52] Plankton phase $\sum_4$HCHs concentrations (1.5 ± 0.7 ng g_{dw}^{-1}) were also within the range of previous reports in Antarctic plankton.[6, 53]

PCBs and OCPs concentrations in seawater and plankton at the Raquelias and Johnsons sampling sites were not significantly different. Furthermore, there were no significant correlations of PCBs or OCPs concentrations with CTD ancillary data (temperature, salinity, photosynthetic active radiation, fluorescence, turbidity) (Table S1, SI). This can be either due to the narrow range in temperature or salinity, and the covariability of these with other biogeochemical and physical controls. Potential inputs of PCBs and OCP due to snow melting can be dissipated by volatilization, settling or degradation.

Air-seawater diffusive fluxes have a dominant role in the transfer of PCBs and OCPs between the atmosphere and oceans.[5, 6, 25, 54] In the open Southern Ocean, these net diffusive fluxes of PCBs and OCPs from air to water are 2-3 orders of magnitude higher than dry deposition fluxes.[5, 6] Diffusive air-water fluxes were calculated following a two-film resistance model:[54]

$$F_{AW} = F_{AWabs} - F_{AWvol} = k_{AW} \left[\frac{C_A}{H'} - C_W\right]$$

Where C_W is the dissolved phase PCBs and HCB concentrations (ng m^{-3}), H' is the temperature corrected and dimensionless Henry's law constant, and k_{AW} is the air-water mass transfer velocity (m d^{-1}).[54]

PCBs gross absorption (F_{AWabs}) and volatilization fluxes (F_{AWvol}) ranged from 0.14 to 6.5 ng m^{-2} d^{-1} , and from 0.45 to 24 ng m^{-2} d^{-1}, respectively (Table S12-13, SI). The resulting net air-water diffusive flux ranged from a net deposition of 0.55 ng m^{-2} d^{-1}, to a net volatilization of 21 ng m^{-2} d^{-1} (Figure 6, Table S14, SI). This net volatilization of PCBs contrasts with the deposition fluxes observed in the open Southern Ocean.[5] High deposition fluxes in the open ocean were explained by the biological pump depleting dissolved phase concentrations, however, it was also noted that for sampling sites near land, concentrations were close to air-water equilibrium.[5] The net volatilization observed in this study at coastal Livingston Island is likely due to the run-off of PCBs from land. A least squares linear regression of PCBs F_{AW} versus salinity (Figure 6) showed a significant correlation. This result is consistent with an increase of snow-melting stream discharge to seawater, increasing PCB concentrations (and subsequent decrease in seawater salinity) as PCB concentrations in snow were higher than in seawater. Increasing PCB concentrations enhance net PCBs coastal seawater-air diffusive fluxes.

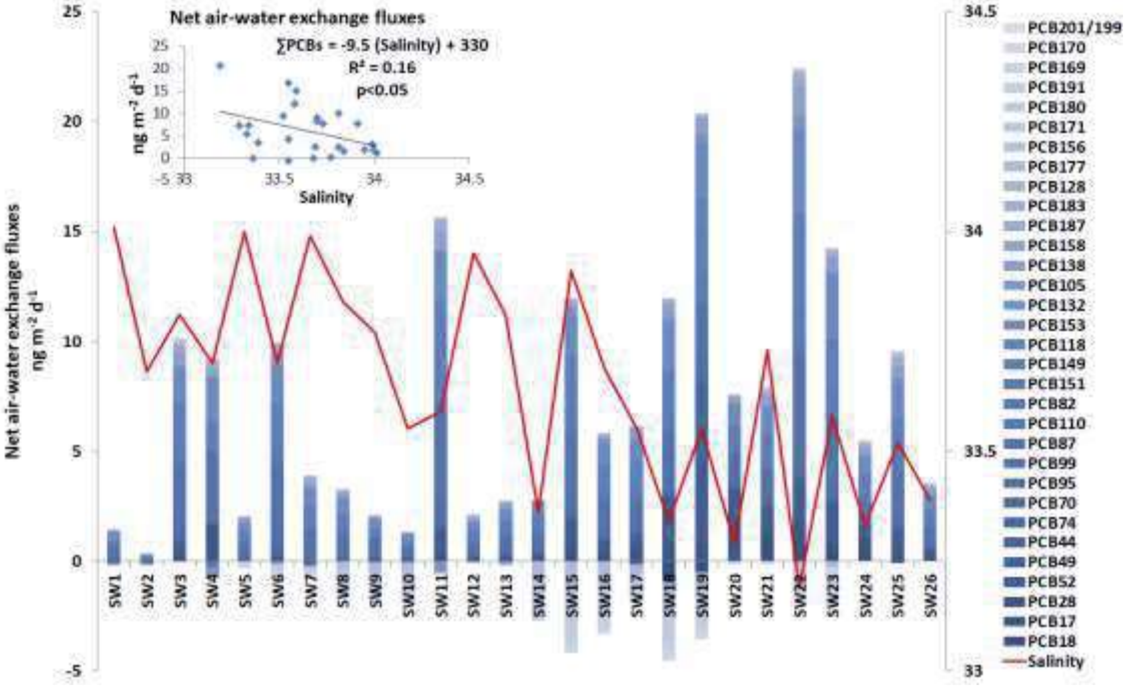

Figure 6. PCBs seawater-air diffusive gas fluxes (ng m^{-2} d^{-1}).

HCB gross absorption (F_{AWabs}) and volatilization fluxes (F_{AWvol}) ranged from 0.091 to 0.94 ng m^{-2} d^{-1} and from 0.075 to 1.4 ng m^{-2} d^{-1}, respectively (Table S12-13, SI). HCB mean net air-water diffusive flux was 0.0084 ± 0.34 ng m^{-2} d^{-1} (Table S14, SI) with no clear dominance of volatilization or absorption fluxes during the sampling campaign and no correlations with seawater temperature or salinity. Air-water fugacity ratios were close to one for most sampling periods. These results are consistent with previous reports from the Southern Ocean and Antarctic Peninsula that show close to equilibrium conditions in the air-water exchange of HCB.[6, 22]

Biotic and abiotic degradation is another sink that may contribute to decrease the concentrations of chemicals such as HCH from the water column, as it has been suggested previously for the marine environment.[6, 55] ∑HCHs concentrations in plankton were inversely correlated with the biomass ($r^2=0.18$, $p<0.05$), and a higher correlation coefficient was found when only α-HCH was considered ($r^2=0.64$, $p<0.001$). Such inverse correlation has been attributed to degradation of HCHs in the water column as reported previously in the Mediterranean Sea[56] and the open Southern Ocean.[6] In addition, a multi-parametric regression analysis of the concentrations of HCH in seawater versus environmental variables including bacterial abundance, showed that the bacterial abundance of the previous time period interacting with seawater temperature explained part of the variability of the concentrations of α-HCH in seawater ($r^2=0.22$, $p<0.05$) and plankton ($r^2=0.25$, $p<0.05$). Bacterial abundance was correlated with ammonia concentrations ($r^2=0.47$, $p<0.01$), which increased from the low values during the first sampling periods to higher levels for most of the rest of the austral summer indicating an increase of productivity. Such influence of bacterial abundances was not found for the more persistent HCB, a chemical with similar hydrophobicity and properties than HCHs. The diffusive air-water exchange of HCHs was not estimated due to the low detection frequency in air (due to low sampling volumes using the fugacity samplers), but the fact that HCHs may be degrading at coastal Antarctica suggests that microbial degradation is likely an important sink for chemicals with moderate persistence, such as low MW PAHs,[26] while re-volatilization and settling to the sediments (not quantified), may dominate the fate of the more persistent compounds, such as PCBs. Future research should assess the relative importance of biogeochemical controls (degradation and biological pump) versus remobilization as the processes governing the fate of POPs with different properties.

ACKNOWLEDGEMENTS

Inorganic nutrient analyses were performed by Mrs. M. I. Abad in coordination with Dr. E. Berdalet (Head of the Service) at the “Nutrient Analysis Service” of the ICM (CSIC). We thank F. Cerqueria and A. Martinez for support with DNA analysis. This work was supported by Spanish Ministry of science to PC through a predoctoral fellowhip, by Fundación BBVA award to M.V.C., European Commission to A.C. through a Marie Curie international outgoing fellowship, and by the Spanish MINECO through projects REMARCA (CTM2012-34673) and ISOMICS (CTM2015-65691-R). The research group of Global Change and Genomic Biogeochemistry is supported by the Catalan Government (2017SGR800).

REFERENCES

1. UNEP, 2016. pops.int [WWWDocument]. Stockh. Conv. Persistent Org. Pollut. URL http://www.pops.int

2. Lohmann, R.; Breivik, K.; Dachs, J.; Muir, D. Global fate of POPs: current and future research directions. *Environ. Pollut*. **2007**, 150(1), 150-165.

3. Bengtson Nash S. Persistent organic pollutants in Antarctica: current and future research priorities. *J. Environ. Monit.* **2011**, 13, 497-504.

4. Risebrough, R. W.; Walker II, W.; Schmidt, T. T.; De Lappe, B. W.; Connors, C. W. Transfer of chlorinated biphenyls to Antarctica. *Nature*, **1976**, 264(5588), 738.

5. Galbán-Malagón, C.; Del Vento, S.; Cabrerizo, A.; Dachs, J. Factors affecting the atmospheric occurrence and deposition of polychlorinated biphenyls in the Southern Ocean. *Atmos. Chem. Phys.* **2013a**, 13(23), 12029-12041.

6. Galbán-Malagón, C.; Cabrerizo, A.; Caballero, G.; Dachs, J. Atmospheric occurrence and deposition of hexachlorobenzene and hexachlorocyclohexanes in the Southern Ocean and Antarctic Peninsula. *Atmos. Environ*. **2013b**, 80, 41-49.

7. Bigot, M.; Muir, D. C.; Hawker, D. W.; Cropp, R.; Dachs, J.; Teixeira, C. F.; Bengtson Nash, S. Air–seawater exchange of organochlorine pesticides in the southern ocean between Australia and Antarctica. *Environ. Sci. Technol*. **2016**, 50(15), 8001-8009.

8. Hale, R. C.; Kim, S. L.; Harvey, E.; La Guardia, M. J.; Mainor, T. M.; Bush, E. O.; Jacobs, E. M. Antarctic research bases: local sources of polybrominated diphenyl ether (PBDE) flame retardants. *Environ. Sci. Technol*. **2008**, 42(5), 1452-1457.

9. Larsson, P.; Järnmark, C.; Södergren, A. PCBs and chlorinated pesticides in the atmosphere and aquatic organisms of Ross Island, Antarctica. *Mar. Pollut. Bull*. **1992**, 25, 281-287.

10. Lei, Y.D.; Wania, F. Is rain or snow a more efficient scavenger of organic chemicals? *Atmos. Environ*. **2004**, 38(22), 3557-3571.

11. Wania, F.; Mackay, D. Tracking the distribution of persistent organic pollutants, *Environ. Sci. Technol*. **1996**, 30, 390A–397A.

12. Cabrerizo, A.; Dachs, J.; Barceló, D.; Jones, K.C. Climatic and biogeochemical controls on the remobilization and reservoirs of persistent organic pollutants in Antarctica. *Environ. Sci. Technol*. **2013a**, 47(9), 4299-4306.

13. Khairy, M. A.; Luek, J. L.; Dickhut, R.; Lohmann, R. Levels, sources and chemical fate of persistent organic pollutants in the atmosphere and snow along the western Antarctic Peninsula. *Environ. Pollut*. **2016**, 216, 304-313.

14. Ma, J.; Hung, H.; Tian, C.; Kallenborn, R. Revolatilization of persistent organic pollutants in the Arctic induced by climate change. *Nature Clim. Change*, **2011**, 1, 255–260.

15. Chapman, W. L.; Walsh, J. E. A synthesis of Antarctic temperatures. *J. Clim*. **2006**, 20, 4096−4117.

16. Cook, A. J.; Fox, A. J.; Vauhan, D. G.; Ferrigno, J. G. Retreating glacier fronts on the Antarctic Peninsula over the past half century. *Science*, **2005**, 308 (5721), 541−544.

17. Turner, J.; Colwell, S. R.; Marshall, G. J.; Lachlan-Cope, T. A.; Carleton, A. M.; Jones, P. D.; Lagun, V.; Reid, P. A.; Iagovkina, S. Antarctic climate change during the last 50 years. *Int. J. Climatol*. **2005**, 25 (3), 279−294.

18. Burniston, D.A.; Strachan, W.J.M.; Hoff, J.T.; Wania, F. Changes in surface area and concentrations of semivolatile organic contaminants in aging snow*. Environ. Sci. Technol*. **2007**, 41, 4932e4937. http://dx.doi.org/10.1021/es0706450.

19. Geisz, H. N.; Dickhut, R. M.; Cochran, M. A.; Fraser,W. R.; Ducklow, H. W. Melting glaciers: a probable source of DDT to the antarctic marine ecosystem. *Environ. Sci. Technol*. **2008**, 42, 3958-3962.

20. Cabrerizo, A.; Dachs, J.; Barceló, D.; Jones, K. C. Influence of organic matter content and human activities on the occurrence of organic pollutants in Antarctic soils, lichens, grass, and mosses. *Environ. Sci. Technol*. **2012**, 46(3), 1396-1405.

21. Bidleman, T. F.; Walla, M. D.; Roura, R.; Carr, E.; Schimidt, S. Organochlorine pesticides in the atmosphere of the Southern Ocean and Antarctica, January-March 1990. *Mar. Pollut. Bull.* **1993**, 26, 258-262.

22. Cincinelli, A.; Martellini, T.; Del Bubba, M.; Lepri, L.; Corsolini, S.; Borghesi, N.; King, M.D.; Dickhut, R. M. Organochlorine pesticide air-water exchange and bioconcentration in krill in the Ross sea. *Environ. Pollut*. **2009**, 157(7), 2153-2158.

23. Fuoco, R.; Giannarelli, S.; Wei, Y.; Ceccarini, A.; Abete, C.; Francesconi, S.; Termine, M. Persistent organic pollutants (POPs) at Ross sea (Antarctica). *Microchem. J*. **2009**, 92 (1), 44−48.

24. Cabrerizo, A.; Dachs, J.; Barcelo, D. Development of a Soil Fugacity Sampler for Determination of Air−Soil Partitioning of Persistent Organic Pollutants under Field Controlled Conditions. *Environ. Sci. Technol*. **2009**, 43 (21), 8257−8263.

25. Galbán-Malagón, C.; Berrojalbiz, N.; Ojeda, M.J.; Dachs, J. The oceanic biological pump modulates the atmospheric transport of persistent organic pollutants to the Arctic. *Nature comm*. **2012**, 3, 862.

26. Casal, P.; Castro-Jiménez, J.; Pizarro, M.; Katsoyiannis, A.; Dachs, J. Seasonal soil/snow-air exchange of semivolatile organic pollutants at a coastal arctic site (Tromsø, 69° N). *Sci. Total Environ*. **2018**, 636, 1109-1116.

27. Grasshoff, K.; Armstrong, F. A. J.; Sterns, C.R.; Strickland, J. D. H. The measurement of upwelling and subsequent biological processes by means of the Technicon AutoAnalyzer and associated equipment. *Deep Sea Res*. **1967**, 14, 381-389.

28. Tamminen, M.; Karkman, A.; Lõhmus, A.; Muziasari, W. I.; Takasu, H.; Wada, S.; Suzuki, S.; Virta, M. Tetracycline resistance genes persist at aquaculture farms in the absence of selection pressure. *Environ. Sci. Technol*. **2010**, 45(2), 386-391.

29. Vila-Costa, M., Barberan, A.; Auguet, J. C.; Sharma, S.; Moran, M. A.; Casamayor, E. O. Bacterial and archaeal community structure in the surface microlayer of high mountain lakes examined under two atmospheric aerosol loading scenarios. *FEMS microbiology ecology*, **2013**, 84(2), 387-397.

30. Tanabe, S.; Hidaka, H.; Tatsukawa, R. PCBs and chlorinated hydrocarbon pesticides in Antarctic atmosphere and hydrosphere. *Chemosphere*, **1983**, 12, 277-288.

31. Iwata, H.; Tanabe, S.; Sakai, N.; Tatsukawa, R. Distribution of persistent organochlorines in the oceanic air and surface seawater and the role of ocean on their global transport and fate. *Environ. Sci. Technol*. **1993**, 27, 1080-1089.

32. Montone, R. C.; Taniguchi, S.; Weber, R. R. PCBs in the atmosphere of king George Island, Antarctica. *Sci. Total Environ*. **2003**, 308, 167-173.

33. Baek, S. Y.; Choi, S. D.; Chang, Y. S. Three-year atmospheric monitoring of organochlorine pesticides and polychlorinated biphenyls in polar regions and the South Pacific. *Environ. Sci. Technol.* **2011**, 45(10), 4475-4482.

34. Li, Y.; Geng, D.; Liu, F.; Wang, T.; Wang, P.; Zhang, Q.; Jiang, G. Study of PCBs and PBDEs in King George Island, Antarctica, using PUF passive air sampling. *Atmos. Environ*. **2012**, 51, 140-145.

35. Kallenborn, R.; Oehme, M.; Wynn-Williams, D.D.; Schlabach, M.; Harris, J. Ambient air levels and atmospheric long-range transport of persistent organochlorines to Signy Island, Antarctica. *Sci. Total Environ*. **1998**, 220, 167-180

36. Kallenborn, R.; Breivik, K.; Eckhardt, S.; Lunder, C.R.; Manø, S.; Schlabach, M.; Stohl, A. Long-term monitoring of persistent organic pollutants (POPs) at the Norwegian Troll station in Dronning Maud Land, Antarctica. *Atmos. Chem. Phys*. **2013**, 13, 6983-6992.

37. Dickhut, R. M.; Cincinelli, A.; Cochran, M.; Ducklow, H. W. Atmospheric concentrations and air− water flux of organochlorine pesticides along the Western Antarctic Peninsula. *Environ. Sci. Technol*. **2005**, 39(2), 465-470.

38. Montone, R. C.; Taniguchi, S.; Boian, C.; Weber, R.R. PCBs and chlorinated pesticides (DDTs, HCHs and HCB) in the atmosphere of the southwest Atlantic and Antarctic oceans. *Mar. Pollut. Bull*. **2005**, 50, 778-782.

39. Weber, R. R.; Montone, R. C. Distribution of organochlorines in the atmosphere of the South Atlantic and Antarctic Oceans. In Long-Range Transport of Pesticides; Kurtz, D. A., Ed.; Lewis Publishing: Chelsea, MI, **1990**; pp 185-197.

40. Breivik, K.; Alcock, R.; Li, Y. F.; Bailey, R. E.; Fiedler, H.; Pacyna, J. M. Primary sources of selected POPs: Regional and global scale emission inventories. *Environ. Pollut.* **2004**, 128(1-2), 3-16. DOI: 10.1016/j.envpol.2003.08.031

41. Gioia, R.; Lohmann, R.; Dachs, J.; Temme, Lakaschus, S.; Schulz-Bull, D.; Hand, I.; Jones, K.C. Polychlorinated biphenyls in air and water of the North Atlantic and Arctic Ocean. *J. Geophys. Res*. **2008**, 113, D19302

42. Gioia, R.; Li, J.; Schuster, J.; Zhang, Y.; Zhang, G.; Li, X.; Spiro, B.; Bhatia, R.S.; Dachs, J.; Jones, K. C. Factors affecting the occurrence and transport of atmospheric organochlorines in the China Sea and the Northern Indian and South East Atlantic Oceans. *Environ. Sci. Technol.* **2012**, 46(18), 10012-10021.

43. Cipro, C. V.; Taniguchi, S.; Montone, R. C. Organic Pollutants in Snow and Seasonal Melting Water from King George Island, Antarctica. *Water, Air, Soil Pollution*, **2017**, 228(4), 149.

44. Vecchiato, M.; Argiriadis, E.; Zambon, S.; Barbante, C.; Toscano, G.; Gambaro, A.; Piazza, R. Persistent organic pollutants (POPs) in Antarctica: occurrence in continental and coastal surface snow. *Microchem. J.* **2015**, 119, 75-82.

45. Herbert, B. M. J.; Halsall, C. J.; Villa, S.; Jones, K. C.; Kallenborn, R. Rapid changes in PCB and OC pesticide concentrations in Arctic snow. *Environ. Sci. Technol*. **2005**, 39, 2998-3005.

46. Herbert, B. M. J.; Villa, S.; Halsall, C. J. Chemical interactions with snow: understanding the behavior and fate of semi-volatile organic compounds in snow. *Ecotoxicol. Environ. Saf*. **2006**, 63, 3-16.

47. Macdonald, R.; Mackay, D.; Li, Y. F. Why Do Contaminants Concentrate in the Environment?. *The State of Ecological and Earth Sciences in Mountain Areas*, **2002**, 20.

48. Hansen, K. M.; Halsall, C. J.; Christensen, J. H. A dynamic model to study the exchange of gas-phase persistent organic pollutants between air and a seasonal snowpack. *Environ. Sci. Technol*. **2006**, 40, 2644-2652.

49. Sen Gupta, R. S.; Sarkar, A.; Kureishey, T. W. PCBs and organochlorine pesticides in krill, birds and water from Antarctica. *Deep-Sea. Res. Pt. II*. **1996**, 43 (1), 119−126.

50. Fuoco, R.; Giannarelli, S.; Wei, Y.; Abete, C.; Francesconi, S.; Termine, M. Polychlorobiphenyls and polycyclic aromatic hydrocarbons in the sea-surface micro-layer and the water column at Gerlache Inlet (Antarctica). *J. Environ. Monit*. **2005**, 7, 1313–1319.

51. Lakaschus, S.; Weber, K.; Wania, F.; Bruhn, R.; Schrems, O. The air− sea equilibrium and time trend of hexachlorocyclohexanes in the Atlantic Ocean between the Arctic and Antarctica. *Environ. Sci. Technol.* **2002**, 36(2), 138-145.

52. Xie, Z.; Koch, B. P.; Möller, A.; Sturm, R.; Ebinghaus, R.; Herndl, G. Transport and fate of hexachlorocyclohexanes in the oceanic air and surface seawater. *Biogeosciences*, **2011**, 8(9).

53. Chiuchiolo, A. L.; Dickhut, R. M.; Cochran, M. A.; Ducklow, H. W. Persistent organic pollutants at the base of the antartic marine food web. *Environ. Sci. Technol*. **2004**, 38 (13), 3551−3557.

54. Jurado, E.; Jaward, F. M.; Lohmann, R.; Jones, K. C.; Simó, R.; Dachs, J. Atmospheric dry deposition of persistent organic pollutants to the Atlantic and inferences for the global oceans. *Environ. Sci. Technol*. **2004**, 38(21), 5505-5513.

55. Harner, T.; Jantunen, L.M.M.; Bidleman, T.F.; Barrie, L.A.; Kylin, H.; Strachan, W.M.J.; Macdonald, R.W. Microbial degradation is a key elimination pathway of hexachlorocyclohexanes from the arctic ocean. *Geophys. Res. Lett*. **2000**, 27 (8), 1155-1158.

56. Berrojalbiz, N.; Dachs, J.; Del Vento, S.; Ojeda, M.J.; Valle, M.C.; Castro-Jiménez, J.; Mariani, G.; Wollgast, J.; Hanke, G. Persistent organic pollutants in Mediterranean seawater and processes affecting their accumulation in plankton. *Environ. Sci. Technol*. **2011**, 45 (10), 4315e4322.

Capítol 6: Discusió

Capítol 6: Discussió

Els resultats obtinguts en aquesta tesi són una contribució rellevant al coneixement de la presència, la compartimentació ambiental, els processos de bescanvi i el destí dels PCBs, OCPs, PAHs i PFASs en els principals compartiments ambientals de les regions polars costaneres. Tot i que les principals conclusions es detallen a cada article d'aquest compendi, aquí es presenta una discussió general de la tesi:

En l'estudi del bescanvi gasós entre el sòl/neu-aire realitzat a l'Àrtic (Tromsø), es va observar un paper clau de la temperatura com a regulador dels processos de remobilització de POPs de les fonts secundàries com el sòl i la neu a les regions polars. Cal aclarir però, que part de la determinació d'aquest factor es deu al disseny experimental d'aquest estudi, atès que en estudiar la fugacitat del sòl/neu en un sol punt al llarg de 14 mesos la temperatura presenta una gran variabilitat al llarg del mostreig, mentre que la matèria orgànica del sòl, que és un factor dominant en la compartimentació aire-sòl, presenta una variació molt limitada durant l'any.

Al llarg del mostreig les concentracions atmosfèriques de ∑PCBs i ∑OCPs van mostrar una clara estacionalitat amb concentracions elevades en els mesos càlids i baixes durant l'hivern. Aquesta estacionalitat es va veure a més reflectida en correlacions significatives amb la temperatura de l'aire. Els ∑PAHs, en canvi, no van presentar aquesta estacionalitat en les concentracions atmosfèriques, la qual cosa indica la influencia de fonts primàries, especialment a l'hivern. En canvi, als sòls les concentracions dels compostos avaluats es van mantenir constants al llarg de l'any, degut a que la capacitat de fugacitat del sòl es centenars de vegades més gran que a la fase gas. A la fase gas equilibrada amb el sòl i la neu, que és proporcional a la fugacitat del sòl/neu, les concentracions de ∑PAHs, ∑PCBs i ∑OCPs van presentar una clara estacionalitat i correlacions significatives amb la temperatura, consistents amb el paper de la temperatura com a control primari en la compartimentació i el bescanvi sòl-aire i neu-aire dels POPs. A més, les fugacitats del sòl i la neu de PAHs, PCBs i OCPs, es van correlacionar amb la fugacitat de l'aire, la qual cosa constitueix evidència la rellevància d'aquests compartiments com a fonts locals d'aquests compostos en l'atmosfera, i demostra que hi ha un fort acoplament aire-sòl/neu dels compostos semi-volàtils.

Els POPs van presentar ràtios de fugacitat (f_s/f_a) d'acord amb la seva K_{OA}, de manera que els compostos més hidròfobs estaven prop de l'equilibri o presentaven una deposició neta i aquells amb valors de K_{OA} més baixos van presentar una major predisposició a la volatilització.

Les ràtios de fugacitat (f_s/f_a) de PCB i HCHs no van presentar grans variacions al llarg de l'any, donat l'estret acoplament entre els compartiments atmosfèric i sòl/neu, les dues fugacitats augmentaven en els mesos càlids i disminuïen en els mesos freds. En canvi, PAHs i HCB van mostrar una clara estacionalitat en les ràtios de fugacitat (f_s/f_a) donant-se condicions d'equilibri durant els mesos d'hivern i volatilització neta durant la resta de l'any, evidenciant així la rellevància dels sòls com a fonts secundàries i ressaltant el paper de la temperatura a l'intercanvi dels POPs entre sòl/neu-aire (Figura 6.1).

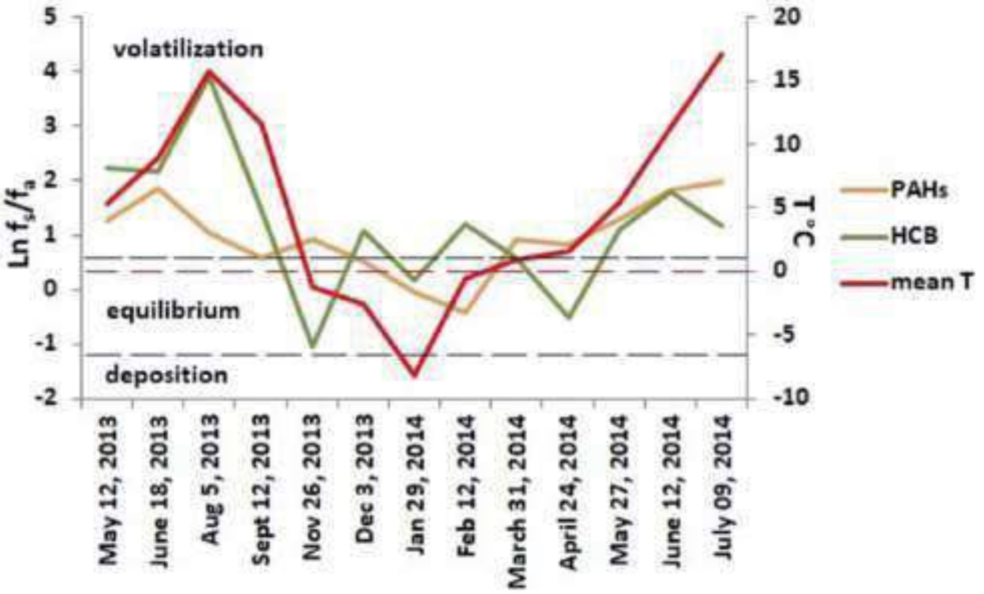

Figura 6.1. Estacionalitat de les ràtios de fugacitat (f_s/f_a) de PAHs i HCB a Tromsø, Noruega

En el cas de la campanya Antàrtica, anàlogament a l'Àrtic i que en estudis anteriors a l'Antàrtida, les fugacitats de PAHs i PCBs al sòl i la neu es van correlacionar amb la fugacitat a l'aire, demostrant una vegada més la seva rellevància com a fonts secundàries. No obstant, les ràtios de fugacitat (f_s/f_a) van presentar diferències notables en funció del substrat (Figura 6.2). El sòl amb vegetació, amb un contingut en matèria orgànica més elevat, va presentar una dominància dels processos de volatilització, especialment significatiu per als compostos més volàtils (amb menor K_{OA}). En canvi, en els sòls sense vegetació i en la neu es van donar condicions d'equilibri.

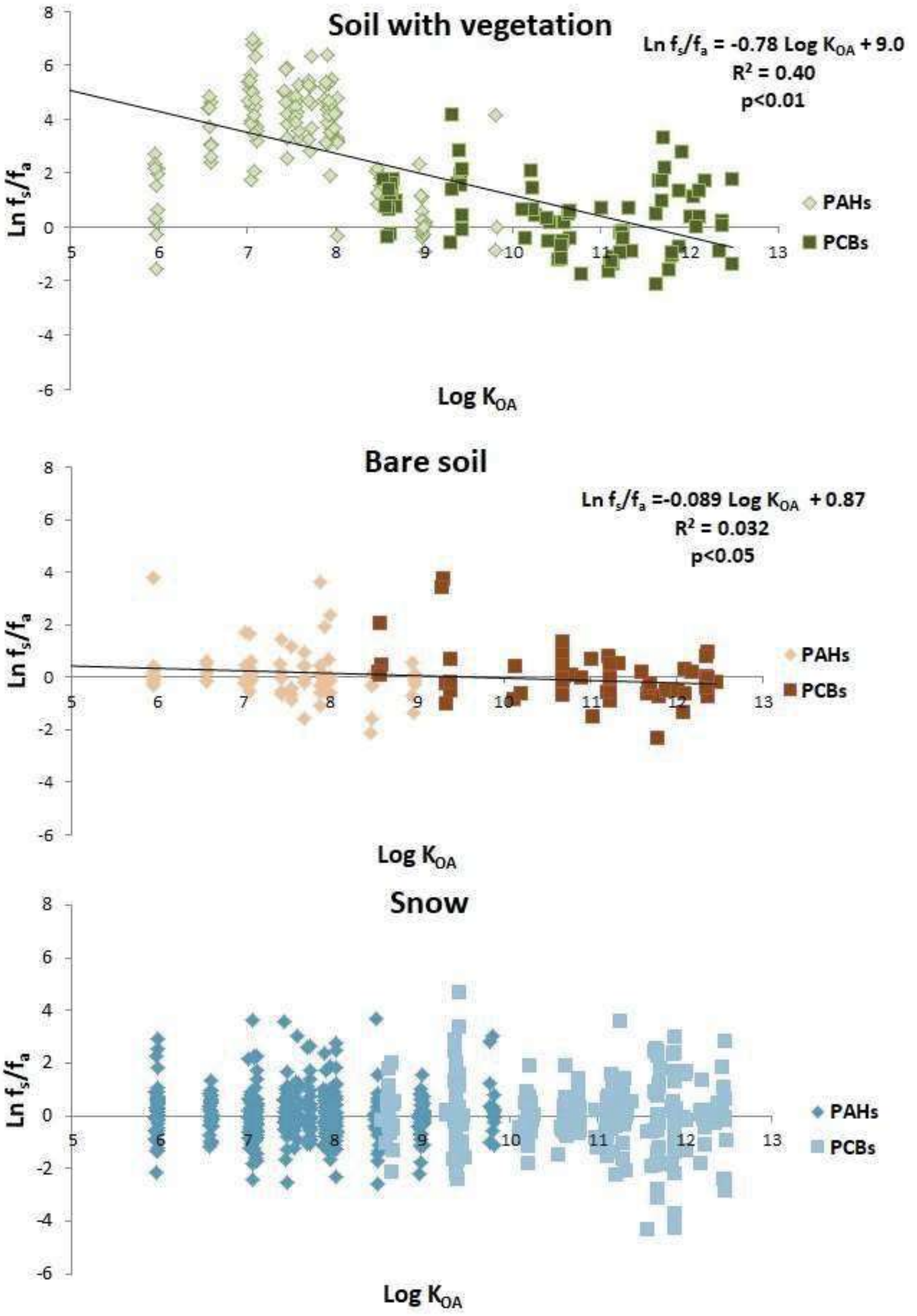

Figura 6.2. Ràtios de fugacitat (Ln f_s/f_a) versus Log K_{OA} de PAHs i PCBs a l'Antàrtida.

Part d'aquesta elevada fugacitat del sòl amb vegetació es pot explicar per l'efecte de la fusió de la neu sobre el sòl. Després de la seva deposició, la neu està carregada de POPs recollits en el procés de snow-scavenging. La neu és un amplificador de concentracions i de fugacitat dels contaminants semi-volàtils. Durant l'envelliment de la neu, no només per la fusió, sinó també per la perdua de superfície específica, la neu perd la seva capacitat de fugacitat (Z), i aquesta passa a ser la de l'aigua (neu fosa) o intermitja entre la de l'aigua i la neu fresca (neu envellida). Al reduir-se el valor de Z, la fugacitat que és el quocient de la concentració i Z, augmenta. Aquest augment de la fugacitat es pot compensar en sols amb valors elevats de carboni orgànic (alta capacitat Z), o transmetres a les escorrenties que porten els contaminants al mar. Pels compostos més hidrofòbics (valor elevat de K_{OA}), els ratios de fugacitat mostren que el sol i l'aire estan prop de l'equilibri. Per compostos amb K_{OA} menor (alguns PAH de 2-4 anells), la capacitat de fugacitat del sòl no és suficient, i l'amplificació de la concentració de la neu fresca original, es reflexa en una major fugacitat en el sòl. Els sols sense vegetació, al ser el contingut en materia orgànica molt reduït, no retenen els POPs, i els POPs alliberats de la neu es perden per volatilització o escorreties. L'alliberament d'aquests compostos, principalment per lixiviació i volatilització, és el que explicales correlacions entre concentracions de ∑PCBs i ∑OCPs i la densitat de neu (Figura 6.3).

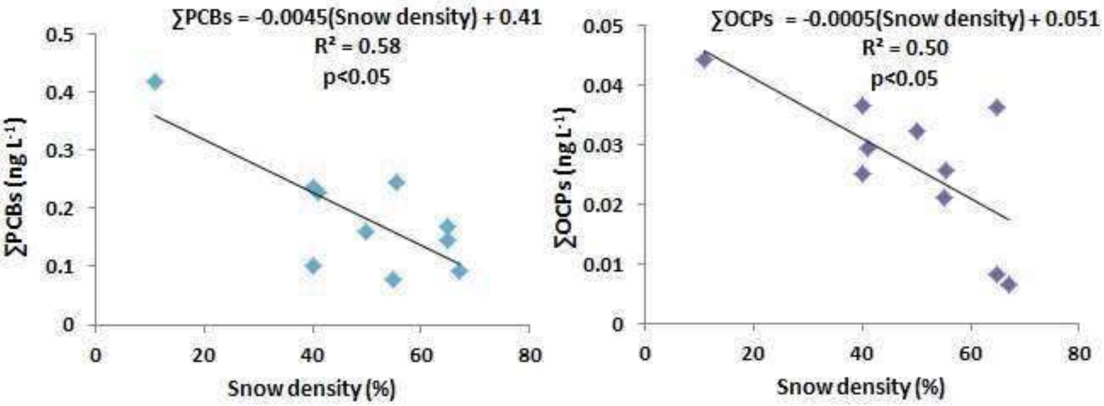

Figura 6.3. Correlacions entre concentracions de ∑PCBs i ∑OCPs i la densitat de neu.

L'alliberament d'aquests compostos capturats a la neu, produeix una amplificació de la fugacitat del sòl, que seria de major efecte en els sòls amb major contingut de matèria orgànica per retenció preferencial dels compostos hidrofòbics. Malgrat això, en el cas dels PAHs volàtils (2-4 anells aromàtics), també podria ser deguda a la potencial producció biogènica de PAH en el sòl amb vegetació, degut a la degradació de diterpens, que ja havia estat prèviament hipotetizada a la regió. L'absència de volatilització de PCBs, OCPs i PAHs des de la neu indica que durant la fusió els POPs emmagatzemats són preferencialmente transferits al sòl i/o al mar per escorrentia.

L'efecte de l'escorrentia a la costa de Livingston és notable pel descens de la salinitat observat al llarg de l’estiu austral. Simultàniament, els fluxos difusius aire-aigua també van mostrar un canvi significatiu al llarg de la campanya de mostreig. A l'inici de l'estiu austral van dominar els fluxos de deposició i al final els de volatilització de PCBs i PAHs. Els fluxos nets es van correlacionar de manera inversa amb la salinitat de l'aigua. Aquestes correlacions són consistents amb l'aportació de POPs de l'aigua de la neu fosa, que presenta concentracions significativament més elevades que l'aigua de mar.

Aquesta volatilització de POPs en l'aigua, vinculada al desgel, constitueix una evidència clara del procés de remobilització en els ecosistemes polars costaners, però a més, contradiu el paradigma de les teories de destil·lació global i de l 'efecte “Grasshopper" de Wania i Mackay, segons el qual, a les regions fredes del planeta dominen el processos de deposició degut al paper regulador de la temperatura a la compartimentació dels POPs. Malgrat que el propi desglaç sigui un procés regulat per la temperatura, l'efecte és l'oposat, induïnt una volatilització de POPs en les zones polars costaneres. En aquest cas la volatilització es depenent del fet que les temperatures a l’estiu austral de l’illa Livingston estan al voltant de la temperatura de fusió de la neu, fet que amplifica l’efecte de la temperatura. En aquest mateix sentit, els nostres resultats confirmen la prèviament observada volatilització de PCBs i PAHs des del sòl. No obstant això, el vincle d'aquest altre procés de volatilització amb el contingut en matèria orgànica en el sòl, que al seu torn també depèn directament de la temperatura, es desvia encara més de la idea base d'aquestes teories inicials sobre la destil·lació global de compostos semivolàtils.

A diferència dels POPs volàtils com PAHs i PCBs, en els PFASs iònics el principal mecanisme de distribució global és el transport marí. Aquesta forma de transport presenta certes limitacions, com l'arribada a zones terrestres allunyades de la costa i, en el cas de l’Antàrtida, a zones en què el transport marí està dificultat per les corrents oceàniques dominants. Malgrat el reduït transport nord-sud del corrent circumpolar oceànic, PFSAs i PFCAs es troben en l'aigua de la costa antàrtica, en concentracions de picograms per litre. En canvi, en aigües obertes de l'oceà glacial antàrtic les concentracions de PFASs reportades són significativament més baixes, majoritàriament per sota dels límits de detecció, la qual cosa indica que el transport marí no pot ser el principal mecanisme de transport a la costa Antàrtica. En canvi, les concentracions atmosfèriques de PFASs neutres (precursors de PFASs iònics) no mostren aquestes diferències a la literatura, la qual cosa donaria suport a la arribada de PFASs a la costa Antàrtica mitjançant el transport i deposició atmosfèrica en lloc del transport oceànic.

Els nivells de PFASs detectats a les mostres ambientals (aigua de mar, neu i plàncton) de l'illa Livingston són significativament més baixos que en altres illes de l'Antàrtida amb una presència humana més elevada, la qual cosa ens indica que podem considerar-les com a referència de processos a llarga escala més que de fonts locals. Les mostres de neu recollides dins i fora de la base JC1 indiquen que tot i que la base constitueix una font de PFASs, aquesta té un efecte espaialment molt limitat.

Igual que en els POPs semivolàtils, en la compartimentació dels PFASs la neu va exercir un paper dominant (Figura 6.4). La neu recentment dipositada presenta concentracions de PFASs significativament més elevats que a la neu ja assentada, la qual cosa és coherent amb estudis previs i indica una elevada importància de la deposició de neu en la arribada de PFASs a la costa antàrtica. A més, l'anàlisi de les masses d'aire indica la seva influència en la deposició, ja que en l'únic cas de deposició en que la massa d'aire provenia del continent americà les concentracions detectades van ser 3 vegades més elevades que a la resta.

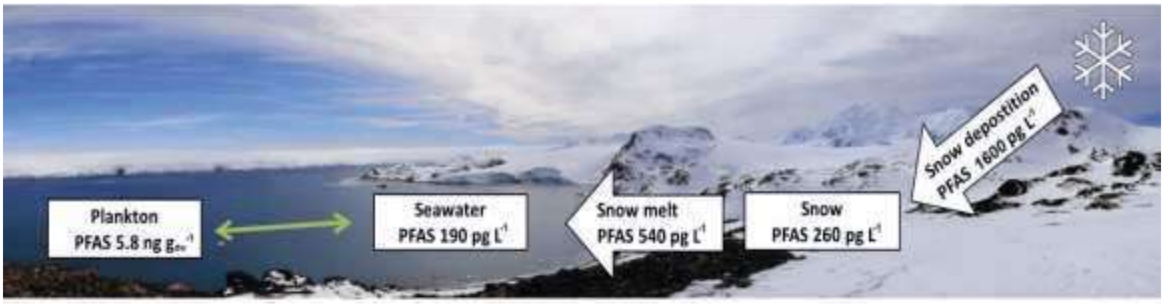

Figura 6.4. Diagrama de les fases de deposició de neu, neu superficial, desglaç, aigua de mar i plàncton.

L'estudi entre les ràtios de concentracions de PFASs en els compartiments de neu recentment depositada (C_{SD}), respecte a la neu superficial (C_{SD}/C_{Snow}), a l'aigua produïda pel desglaç (C_{SD}/C_{SM}) i l'aigua de mar (C_{SD}/C_{SW}) va presentar diferències notables en relació al nombre de carbonis dels PFCAs. Els PFCAs de cadena més llarga i, per tant, menys solubles, van presentar ràtios elevats, que són coherents amb un retard en l'elució de PFCAs menys solubles durant la fusió de la neu i amb l’adhesió preferencial d'aquests compostos al material particulat i al sòl. Mentre que PFCAs de cadena més curta van presentar ràtios més propers a 1, que indiquen una elevada eficiència entre la deposició atmosfèrica i l'arribada a l'aigua de mar. L'elevada abundància de PFCAs de cadena llarga en C_{SD} pel que fa a C_{Snow}, és consistent amb els perfils de PFAS obtinguts en la formació d'esprai marí en condicions de laboratori. Això indica que una fracció important dels PFCAs trobats a la deposició atmosfèrica provenen de la formació i transport d'aerosols marins des d'altres regions oceàniques.

Finalment, el balanç de masses a la columna d'aigua va demostrar que és plausible que la deposició atmosfèrica sostingués les concentracions en aigua de mar costanera de PFCAs, atès que els temps per arribar a aquestes concentracions serien d'entre 0.5 i 10 anys com a màxim, sense tenir en compte la aportació de PFASs recollida sobre terra i posteriorment arrossegada a la costa. Per PFOS, però, el temps neceseri seria de 67 anys, la qual cosa indica que un altre procés de transport com la deposició atmosfèrica de precursors neutres i posterior transformació o el transport oceanic han de ser de major rellevància pels PFSAs.

Aquests resultats confirmen la importància del transport atmosfèric i de la deposició de neu de PFASs a la costa antàrtica.

PCBs, OCPs, PAHs i PFASs van ser detectats a totes les mostres de plàncton costaner de l'Antàrtida, confirmant així l'entrada d'aquests compostos en les cadenes tròfiques polars. Aquesta contribució constitueix la major base de dades de concentracions de POPs en plàncton de la regió antàrtica, i és de gran importància per entendre no només la incidència d'aquests compostos en les cadenes tròfiques sinó també la importància relativa del procés de la bomba biològica en aigües antàrtiques.

Resumint breument, l’estudi realitzat a la costa de l’illa Livingston mostra que la neu juga una paper important com a entrada de contaminants semivolàtils (PAHs, PCBs...), però sorprenentment, també de compostos iònics com els PFASs. En el futur, caldrà estudiar fins a quin punt aquest fet és important per altres contaminants orgànics amb propietats similars o diferents a les famílies estudiades aquí.

Capítol 7: Conclusions generals

Capítol 7: Conclusions generals

El treball presentat constitueix la major base de dades de concentracions de POPs en compartiments múltiples (aire, aigua, neu, plàncton, fugacitat) registrada a la regió antàrtica.

Els resultats obtinguts confirmen la presència de processos de remobilització de PCBs, PAHs, OCPs i PFASs en els ecosistemes polars costaners.

En aquests processos, la temperatura actua amb una variable reguladora de concentracions i fluxes, atès que influeix directament sobre la deposició i revolatilització de compostos prèviament acumulats en el sòl, l'aigua o la neu/gel. Aquest efecte és degut tan a la influència de la temperatura en al compartimentació aire-superficie, com al fet que les temperatures al voltant de 0°C impliquen la fusió de la neu i la re-mobilització dels contaminants.

L'estacionalitat de les concentracions de POPs en la atmosfera i de l'intercanvi de la fase gas amb el sòl i la neu a l'Àrtic (Tromsø, Noruega) confirma aquest efecte dels canvis en la temperatura al llarg de l'any.

A l'Antàrtida, la deposició de neu és un dels factors principals en la compartimentació ambiental dels POPs, tant "legacy" com emergents, amb concentracions de tots els contaminants estudiats superiors a l'aigua de mar.

En el cas dels PFASs iònics, el transport atmosfèric associat a l'aerosol marí i la posterior deposició amb la neu van ser establerts com a principal mecanisme de transport en l'arribada d'aquests compostos a la costa Antàrtica, en lloc del transport oceànic que prèviament es considerava el principal mecanisme de transport a escala global.

Les concentracions de PCBs i OCPs a la neu estaven correlacionades amb la densitat de la neu, consistent amb la pèrdua de superfície específica de la neu durant l’envelliment, i per tant la seva menor capacitat per retenir POPs.

En els POPs semivolàtils (PAHs, PCBs i OCPs) es va observar una clara influència de l'aportació d'aigua de neu a les aigües costaneres en els fluxos difusius aire-aigua. Concretament, es va observar una major volatilització al final de l’estiu Antàrctic, coincidint amb el final del període de fusió de la neu i salinitats de l’aigua de mar menors. A més, en els sols, s’ha observat una amplificació de la fugacitat dels sòls després de la fusió de la neu, especialment en els sòls carregats de matèria orgànica.

Les concentracions i fluxes dels contaminants orgànics en les zones costaneres antàrtiques són la conseqüència d’interaccions diverses entre els procesos de transport, compartimentació, i de controls biogeoquímics (degradació,...) que ocorren en l’atmòsfera, els sòls i la neu, i la columna d’aigua. La recerca futura haurà de delimitar la rellevància d’aquests processos diversos segons les propietats fisico-químicas i persistència dels contaminants orgànics.

Annexos

8.1 Capítol 2. Supporting Information

SEASONAL SOIL/SNOW-AIR EXCHANGE OF SEMIVOLATILE ORGANIC POLLUTANTS AT A COASTAL ARCTIC SITE (TROMSØ, 69^{O}N)

SUPPLEMENTARY INFORMATION

Paulo Casal[a], Javier Castro-Jiménez[a,b], Mariana Pizarro[a], Athanasios Katsoyiannis[c], Jordi Dachs[a]*

[a] Department of Environmental Chemistry (IDAEA-CSIC), Barcelona, Catalunya, Spain.

[b] Aix Marseille University, University de Toulon, CNRS, IRD, MIO UM 110, Marseille, France

[c] NILU - Norwegian Institute for Air Research, Tromsø, Norway.

Table S11. Soil/snow-air fugacity ratios (Ln f_s/f_a) for PAHs.

Table S12. Soil/snow-air fugacity ratios (Ln f_s/f_a) for OCPs and PCBs.

Table S13. Spearman's correlations between the soil/snow-air fugacity ratios (Ln f_s/f_a) and the inverse of the mean temperature (T).

Figure S1. PAHs concentration profiles in the air (C_A), air equilibrated with the soil/snow surface (C_{SA}) and soil (C_S)

Figure S2. PCBs concentration profiles in the air (C_A), air equilibrated with the soil/snow surface (C_{SA}) and soil (C_S)

Figure S3A. 72-hour air mass back-trajectories for the 14 sampling events. Each panel shows the back trajectories starting at 100m height every 12 hours as samples integrate a time period of 5 or 6 days

Figure S3B. 72-hour air mass back-trajectories for the 14 sampling events. Each panel shows the back trajectories starting at 100m height every 12 hours as samples integrate a time period of 5 or 6 days

Figure S4. Soil/snow-air partition constants (K_{SA}) versus the octanol-air partition constant (K_{OA}) for HCB and HCHs.

Figure S5. Seasonality of the concentrations in air equilibrated with the soil/snow surface (C_{SA}) for ∑OCPs, ∑PCBs and ∑PAHs.

Figure S6. Soil/snow-air fugacity ratios (Ln f_s/f_a) for OCP versus K_{OA}.

Table S1. Sampling event dates, air temperatures and fraction of organic carbon in soil (f_{OC}).

Sampling start	07/05/13	05/06/13	13/06/13	31/07/13	06/09/13	21/11/13	27/11/13	23/01/14	12/02/14	25/03/14	22/04/14	21/05/14	06/06/14	03/07/14
Sampling end	13/05/13	10/06/13	18/06/13	05/08/13	12/09/13	26/11/13	03/12/13	29/01/14	16/02/14	31/03/14	24/04/14	27/05/14	12/06/14	09/07/14
min. T.(°C)	0.4	3.8	3.2	8.9	4.9	-3.7	-9.0	-10.6	-4.2	-4.3	-2.5	1.4	7.6	8.8
mean T.(°C)	5.4	12.6	9.0	15.8	11.6	-1.2	-2.6	-8.2	-0.5	1.0	1.6	5.4	11.4	17.1
max. T.(°C)	12.2	22.3	16.4	23.9	18.4	3.4	3.2	-4.6	1.9	5.1	5.8	11.2	21.0	27.7
f_{OC} (%)	6.51	6.86	9.6	10.04	9.5	Snow covered	Snow covered	Snow covered	Snow covered	Snow covered	Snow covered	8.94	9.22	8.2

Table S2. Surrogate recoveries for the air and soil samples.

Surrogate	**PUFs**	**Soil**
acenaphthene-d10	58±20%	58±16%
phenanthrene-d10	73±30%	97±21%
crysene-d12	110±22%	97±5.1%
perylene-d12	90±32%	110±11%
PCB65	70±28%	74±22%
PCB200	80±29%	81±10%

Table S3. Ambient air (gas phase) concentrations of individual OCPs and PCBs, listed by the date of sampling end.

ng m^{-3}	**13/05/13**	**10/06/13**	**18/06/13**	**05/08/13**	**12/09/13**	**06/11/13**	**03/12/13**	**29/01/14**	**16/02/14**	**31/03/14**	**24/04/14**	**27/05/14**	**12/06/14**	**09/07/14**
Σ_5OCPs	0.134	0.053	0.260	0.187	0.306	0.279	0.068	0.046	0.083	0.078	0.169	0.170	0.090	0.154
Σ_4HCH	0.018	0.026	0.030	0.035	0.042	0.005	0.003	0.011	0.008	0.011	0.014	0.030	0.022	0.014
α-HCH	<loq	0.009	0.002	0.003	0.004	0.002	0.003	0.003	<loq	0.002	<loq	0.004	0.003	<loq
β-HCH	0.007	0.018	<loq	<loq	<loq	<loq	<loq	<loq	<loq	<loq	<loq	<loq	<loq	<loq
γ-HCH	0.002	<loq	0.024	0.011	0.008	0.002	<loq	0.002	0.003	0.002	0.005	0.019	0.005	0.014
δ-HCH	0.009	<loq	0.004	0.020	0.031	<loq	<loq	0.006	0.005	0.007	0.009	0.007	0.013	<loq
HCB	0.098	<loq	0.199	0.117	0.221	0.269	0.063	0.025	0.064	0.056	0.141	0.110	0.047	0.125
Σ_{40}PCBs	0.083	0.236	0.264	0.183	0.457	0.080	0.215	0.114	0.085	0.094	0.064	0.273	0.385	0.230
PCB18	<loq	<loq	0.030	<loq	0.010	0.013	<loq	<loq	<loq	0.003	0.006	<loq	0.002	0.010
PCB17	<loq	<loq	<loq	<loq	0.001	<loq	<loq	0.002	0.001	0.001	0.007	<loq	0.008	0.005
PCB31+28	<loq	0.002	0.002	0.001	<loq	0.005	<loq	<loq	<loq	<loq	0.005	0.001	0.007	0.001
PCB52	0.023	<loq	<loq	0.036	0.0.74	0.018	0.002	<loq	0.001	<loq	0.002	0.007	0.011	0.007
PCB49	<loq	<loq	0.002	0.005	0.123	0.035	<loq	<loq	<loq	0.001	0.015	0.018	0.013	0.067
PCB44	0.006	<loq	0.014	0.015	0.021	0.011	0.011	0.020	0.013	0.006	0.023	0.011	0.004	0.013
PCB74	0.004	0.042	0.035	0.006	0.003	<loq	0.016	0.013	0.012	0.007	<loq	0.002	<loq	0.003
PCB70	<loq	0.032	0.005	<loq	0.006	0.008	<loq	<loq	<loq	<loq	<loq	<loq	0.016	<loq
PCB95	<loq	0.011	0.011	0.003	<loq	<loq	<loq	<loq	<loq	<loq	<loq	0.003	<loq	0.004
PCB99+101	0.002	0.053	0.025	0.005	0.008	0.001	0.004	<loq	<loq	<loq	0.005	0.005	0.035	0.006
PCB87	<loq	<loq	0.011	<loq	<loq	<loq	<loq	<loq	0.001	<loq	<loq	<loq	0.002	<loq
PCB110	<loq	<loq	<loq	<loq	0.001	<loq	<loq	<loq	<loq	<loq	<loq	0.002	0.007	<loq
PCB82	<loq	<loq	0.003	<loq	<loq	<loq	0.010	<loq	<loq	<loq	<loq	0.027	<loq	<loq
PCB151	<loq	<loq	<loq	0.002	0.004	<loq	0.002	<loq	<loq	0.001	<loq	<loq	<loq	0.001
PCB149	0.043	0.002	0.030	0.073	0.150	<loq	0.016	0.004	0.008	0.007	<loq	0.028	0.054	0.087
PCB118	<loq	<loq	<loq	<loq	0.003	0.010	<loq	<loq	<loq	<loq	<loq	0.020	0.008	<loq

PCB153	<loq	<loq	<loq	<loq	0.005	<loq	<loq	0.032	<loq	<loq	<loq	<loq	<loq	0.005
PCB132	0.002	<loq	<loq	0.030	0.038	<loq	0.002	0.028	0.007	0.035	<loq	0.005	0.083	0.016
PCB105	<loq	<loq	<loq	<loq	<loq	<loq	0.002	<loq	<loq	<loq	<loq	<loq	0.001	<loq
PCB138	<loq	<loq	<loq	<loq	<loq	<loq	0.007	<loq	<loq	<loq	<loq	<loq	<loq	<loq
PCB158	<loq	<loq	<loq	<loq	0.001	<loq	0.009	<loq	<loq	<loq	<loq	0.004	<loq	<loq
PCB187	<loq	<loq	<loq	0.003	0.006	<loq	<loq	<loq	<loq	0.001	<loq	0.003	<loq	0.003
PCB183	<loq	<loq	<loq	<loq	<loq	<loq	0.020	<loq	<loq	0.009	<loq	0.005	0.007	<loq
PCB128	<loq	<loq	<loq	<loq	<loq	<loq	0.005	<loq	0.001	<loq	<loq	<loq	<loq	<loq
PCB177	<loq	<loq	<loq	<loq	<loq	<loq	0.041	0.006	0.032	<loq	<loq	0.019	0.010	<loq
PCB156	<loq	<loq	<loq	<loq	<loq	<loq	0.002	<loq	<loq	0.007	<loq	<loq	0.001	<loq
PCB171	<loq	<loq	<loq	<loq	<loq	<loq	<loq	<loq	<loq	0.007	<loq	<loq	<loq	<loq
PCB180	0.002	<loq	0.019	0.003	<loq	<loq	0.048	<loq	<loq	<loq	<loq	0.025	0.024	<loq
PCB191	<loq	<loq	<loq	<loq	0.004	<loq	0.009	<loq	<loq	<loq	<loq	0.009	0.028	<loq
PCB169	<loq	0.016	0.003	<loq	<loq	<loq	0.008	0.007	0.007	<loq	<loq	<loq	0.037	<loq
PCB170	<loq	0.078	0.039	<loq	<loq	<loq	<loq	0.003	<loq	0.007	<loq	0.063	0.015	<loq
PCB201/199	<loq	<loq	0.034	<loq	<loq	<loq	<loq	<loq	0.001	<loq	<loq	0.015	0.012	<loq
PCB208	<loq	<loq	<loq	<loq	<loq	<loq	<loq	<loq	<loq	<loq	<loq	<loq	<loq	<loq
PCB195	<loq	<loq	<loq	<loq	<loq	<loq	<loq	<loq	<loq	<loq	<loq	<loq	<loq	<loq
PCB194	<loq	<loq	<loq	<loq	<loq	<loq	<loq	<loq	<loq	<loq	<loq	<loq	<loq	<loq
PCB205	<loq	<loq	<loq	<loq	<loq	<loq	<loq	<loq	<loq	<loq	<loq	<loq	<loq	<loq
PCB209	<loq	<loq	<loq	<loq	<loq	<loq	<loq	<loq	<loq	<loq	<loq	<loq	<loq	<loq
ΣTri-PCBs	<loq	0.002	0.032	0.001	0.011	0.018	<loq	0.002	0.001	0.004	0.018	0.001	0.017	0.016
ΣTetra-PCBs	0.033	0.074	0.056	0.062	0.227	0.052	0.029	0.033	0.026	0.014	0.041	0.038	0.045	0.090
ΣPenta-PCBs	0.002	0.064	0.050	0.009	0.012	0.012	0.016	<loq	0.001	<loq	0.005	0.057	0.053	0.011
ΣHexa-PCBs	0.046	0.018	0.034	0.106	0.198	<loq	0.051	0.071	0.023	0.052	<loq	0.038	0.175	0.110
ΣHepta-PCBs	0.002	0.078	0.058	0.006	0.009	<loq	0.118	0.008	0.032	0.024	<loq	0.124	0.083	0.003
ΣOcta-PCBs	<loq	<loq	0.034	<loq	<loq	<loq	<loq	<loq	0.001	<loq	<loq	0.015	0.012	<loq

Bellow limits of quantification (<loq)

Table S4. Ambient air (gas phase) concentrations of individual PAHs.

ng m^{-3}	**13/05/13**	**18/06/13**	**05/08/13**	**12/09/13**	**06/11/13**	**03/12/13**	**29/01/14**	**16/02/14**	**31/03/14**	**24/04/14**	**27/05/14**	**12/06/14**	**09/07/14**
Act	0.012	0.024	0.049	0.012	0.038	0.007	0.040	0.385	0.027	0.030	0.017	0.006	0.015
Ace	1.479	0.783	1.119	0.445	0.235	0.370	1.979	1.017	0.265	0.322	<loq	<loq	<loq
Flu	3.424	2.459	8.426	4.167	0.516	1.320	3.446	4.207	0.662	0.447	2.272	1.955	2.656
Phe	4.284	3.602	9.911	8.026	0.879	2.073	7.700	5.663	1.031	0.868	4.291	1.859	8.395
ΣMP	1.952	1.178	6.134	4.095	0.319	0.769	1.599	2.276	0.356	0.892	6.820	1.620	3.535
ΣDMPD	0.730	0.485	3.680	1.756	0.101	0.303	0.420	0.917	0.128	0.108	4.478	0.654	1.940
Ant	0.089	0.088	0.224	0.239	0.047	0.112	0.548	0.420	0.028	0.035	0.118	0.036	0.284
DBT	0.305	0.226	0.809	0.565	0.024	0.039	0.056	0.124	0.025	0.026	0.277	0.100	0.624
ΣMDBT	0.223	0.122	0.768	0.540	0.030	0.078	0.050	0.142	0.036	0.018	0.650	0.172	0.487
ΣDMDBT	0.080	0.044	0.713	0.416	<loq	0.357	0.121	0.115	<loq	<loq	0.842	<loq	0.393
Pyr	0.403	1.931	1.108	0.989	0.169	0.565	2.623	1.695	0.665	5.748	0.674	0.422	0.691
ΣMPyr	<loq	<loq	<loq	<loq	<loq	<loq	<loq	<loq	<loq	<loq	<loq	<loq	<loq
ΣDMPyr	0.018	<loq	0.068	0.018	<loq	<loq	0.143	0.033	0.002	0.009	0.016	0.020	0.017
Flt	0.554	0.832	1.380	1.327	0.194	0.778	3.138	2.067	0.428	1.220	0.882	<loq	1.228
Cry	0.022	0.008	0.030	0.017	0.006	0.015	0.281	0.056	0.008	<loq	0.018	0.006	0.025
ΣMCry	<loq	<loq	<loq	<loq	<loq	<loq	<loq	<loq	<loq	<loq	<loq	<loq	<loq
B[*a*]ant	0.010	0.012	<loq	<loq	0.005	0.021	0.202	0.034	0.002	0.291	0.008	<loq	<loq
B[*e*]pyr	0.006	<loq	<loq	<loq	<loq	<loq	0.085	0.010	0.005	<loq	<loq	<loq	<loq
B[*a*]pyr	0.009	<loq	0.009	<loq	0.007	0.009	0.083	0.016	<loq	<loq	0.006	0.012	0.005
B[*g,h,i*]pery	<loq	<loq	<loq	<loq	<loq	<loq	0.047	0.007	<loq	<loq	<loq	<loq	<loq
In[1,2,3-*cd*]pyr	0.007	<loq	<loq	<loq	<loq	<loq	0.075	0.010	<loq	<loq	<loq	<loq	<loq
B[*g,h,i*]f	<loq	0.081	<loq	<loq	<loq	<loq	0.162	0.066	<loq	0.286	<loq	<loq	<loq
B[*b*]f	<loq	0.012	0.044	0.040	0.036	0.086	0.108	<loq	<loq	<loq	<loq	<loq	<loq
B[*k*]f	0.011	<loq	<loq	<loq	<loq	<loq	0.113	0.023	<loq	0.017	0.081	<loq	0.007
Dib[*a,h*]ant	<loq	<loq	<loq	<loq	<loq	<loq	<loq	<loq	<loq	<loq	<loq	<loq	<loq

Pery	<loq	<loq	<loq	<loq	<loq	<loq	<loq	<loq	<loq	<loq	<loq	<loq	<loq
$\sum_{53}$PAHs	13.619	11.886	34.473	22.651	2.607	6.901	23.018	19.282	3.668	10.315	21.450	6.862	20.301

Bellow limits of quantification (<loq)

Table S5. Air concentration correlations with the inverse of the mean temperature.

	C_A	Spearman's rho	1/T
HCHs	**γ-HCH**	Correlation Coefficient	-0.741**
		p-value	0.006
		N	12
	δ-HCH	Correlation Coefficient	-0.673*
		p-value	0.033
		N	10
	Σ_4HCHs	Correlation Coefficient	-0.793**
		p-value	0.001
		N	14
PCBs	**PCB99+101**	Correlation Coefficient	-0.664*
		Sig. (2-tailed)	0.026
		N	11
	PCB149	Correlation Coefficient	-0.601*
		p-value	0.039
		N	12
	ΣTetra-PCBs	Correlation Coefficient	-0.767**
		P-value	0.001
		N	14
	Σ_{40}PCBs	Correlation Coefficient	-0.547*
		p-value	0.043
		N	14
PAHs	**DBT**	Correlation Coefficient	-0.780**
		P-value	0.002
		N	13
	ΣMDBT	Correlation Coefficient	-0.725**
		p-value	0.005
		N	13
	ΣMP	Correlation Coefficient	-0.648*
		P-value	0.017
		N	13
	ΣDMPD	Correlation Coefficient	-0.676*
		p-value	0.011
		N	13
	ΣMePAHs	Correlation Coefficient	-0.626*
		p-value	0.022
		N	13

**. Correlation is significant at the 0.01 confidence level (2-tailed).

*. Correlation is significant at the 0.05 confidence level (2-tailed).

Table S6. Soil concentrations of individual OCPs and PCBs.

ng g_{dw}^{-1}	13/05/2013	10/06/2013	18/06/2013	05/08/2013	12/09/2013	06/11/2013	03/12/2013	29/01/14
Σ_5OCPs	0.701	1.478	0.947	1.021	0.675	1.123	1.115	1.392
α-HCH	<loq	<loq	<loq	<loq	<loq	0.001	<loq	0.002
β-HCH	0.027	<loq	0.069	0.078	0.059	<loq	<loq	<loq
γ-HCH	<loq	<loq	<loq	<loq	<loq	<loq	0.001	<loq
δ-HCH	0.001	0.001	0.001	0.001	0.001	0.001	0.001	0.002
HCB	0.673	1.477	0.877	0.943	0.616	1.121	1.114	1.388
Σ_{40}PCBs	0.422	0.648	0.753	0.799	0.308	0.954	0.681	0.635
PCB18	<loq	<loq	<loq	0.005	0.003	<loq	<loq	<loq
PCB17	<loq	0.003	0.003	<loq	<loq	<loq	<loq	<loq
PCB31+28	<loq	<loq	<loq	<loq	<loq	<loq	0.001	<loq
PCB52	0.036	0.008	0.009	0.013	0.015	0.009	0.016	0.012
PCB49	<loq	<loq	<loq	<loq	<loq	0.003	0.008	<loq
PCB74	<loq	<loq	<loq	<loq	<loq	0.002	<loq	<loq
PCB70	0.001	<loq	0.006	0.008	0.003	0.005	0.008	0.002
PCB95	<loq	<loq	<loq	<loq	<loq	0.006	0.015	<loq
PCB99+101	0.051	0.102	0.109	0.166	<loq	0.198	0.120	0.102
PCB87	0.020	0.028	0.031	0.036	0.010	0.054	0.021	0.025
PCB110	<loq	0.001	<loq	<loq	0.003	0.005	0.009	<loq
PCB82	<loq	<loq	<loq	<loq	<loq	0.001	0.005	<loq
PCB151	0.010	0.019	0.020	0.029	0.011	0.017	0.016	0.021
PCB149	0.030	0.041	0.040	0.076	0.016	0.070	0.064	0.047
PCB118	0.020	0.030	0.038	0.049	0.002	0.079	0.042	0.033
PCB153	0.096	0.158	0.168	0.141	0.084	0.195	0.102	0.136
PCB132	<loq	<loq	<loq	<loq	<loq	<loq	0.005	<loq

PCB105	<loq	<loq	<loq	<loq	<loq	0.003	0.004	0.001
PCB138	0.011	0.036	0.024	0.038	0.007	0.103	0.058	0.021
PCB158	0.024	0.010	0.048	<loq	0.002	0.016	0.009	0.039
PCB187	0.024	0.038	0.042	0.031	0.021	0.026	0.027	0.035
PCB183	0.012	0.021	0.023	0.024	0.019	0.014	0.013	0.021
PCB128	<loq	<loq	<loq	<loq	<loq	<loq	0.003	0.002
PCB177	0.003	<loq	0.007	0.008	<loq	0.010	0.008	0.007
PCB156	0.001	0.002	0.004	0.005	<loq	0.004	0.003	0.003
PCB171	0.002	0.005	0.006	0.009	<loq	0.015	0.006	0.005
PCB180	0.054	0.077	0.091	0.068	0.044	0.065	0.053	0.067
PCB191	<loq	<loq	<loq	<loq	<loq	<loq	<loq	<loq
PCB169	<loq	<loq	<loq	<loq	<loq	0.006	0.010	0.008
PCB170	0.010	0.017	0.022	0.022	0.003	0.022	0.021	0.018
PCB201/199	0.006	0.010	0.013	0.008	0.0072	0.007	0.007	0.010
PCB208	0.001	0.003	0.002	0.002	0.005	0.002	0.002	0.003
PCB195	<loq	<loq	0.002	0.001	<loq	0.001	0.001	0.001
PCB194	0.004	0.008	0.010	0.007	0.005	0.006	0.006	0.008
PCB205	<loq	<loq	<loq	<loq	<loq	<loq	<loq	<loq
PCB206	0.003	0.005	0.003	0.002	0.003	0.003	0.003	0.003
PCB209	0.003	0.001	0.002	0.001	0.001	0.004	0.003	0.004
ΣTri-PCBs	<loq	0.003	0.003	0.005	0.003	<loq	0.001	<loq
ΣTetra-PCBs	0.037	0.008	0.015	0.021	0.018	0.018	0.032	0.015
ΣPenta-PCBs	0.092	0.161	0.178	0.251	0.016	0.347	0.216	0.160
ΣHexa-PCBs	0.171	0.266	0.304	0.288	0.120	0.405	0.261	0.268
ΣHepta-PCBs	0.105	0.160	0.191	0.162	0.088	0.153	0.129	0.154
ΣOcta-PCBs	0.015	0.028	0.031	0.021	0.020	0.020	0.019	0.025

Bellow limits of quantification (<loq)

Table S7. Soil concentrations of individual PAHs.

ng g_{dw}^{-1}	**13/05/2013**	**10/06/2013**	**18/06/2013**	**05/08/2013**	**12/09/2013**	**06/11/2013**	**03/12/2013**	**29/01/14**
Act	0.30	0.21	0.17	0.17	0.20	0.34	0.38	0.37
Ace	0.20	0.48	0.17	0.15	0.51	0.23	0.26	0.19
Flu	0.32	0.83	0.23	0.23	0.71	0.19	0.51	0.45
Phe	8.04	12.09	2.64	4.85	8.24	2.20	6.66	11.81
ΣMP	12.60	10.56	5.12	11.14	13.36	3.47	12.32	15.23
ΣDMPD	11.38	6.67	4.41	12.75	13.46	2.92	14.63	17.57
Ant	1.18	3.85	0.42	0.70	1.52	0.34	1.11	2.19
DBT	0.37	0.47	0.45	1.74	1.82	0.34	2.49	1.60
ΣMDBT	<loq	<loq	<loq	<loq	<loq	<loq	<loq	<loq
ΣDMDBT	0.26	0.24	0.77	0.26	0.27	0.09	0.26	0.51
Pyr	37.06	20.70	7.11	8.97	16.11	6.68	15.86	30.15
ΣMPyr	9.35	6.99	2.23	4.29	6.29	1.90	4.39	7.00
ΣDMPyr	2.89	2.24	1.42	3.04	3.30	1.17	3.08	4.09
Flt	54.07	31.96	8.69	11.31	23.01	7.22	20.67	36.62
Cry	20.91	12.85	5.04	5.38	8.67	5.28	8.50	14.49
ΣMCry	6.24	5.14	3.40	4.09	5.04	2.80	4.96	6.99
B[*a*]ant	21.07	14.58	3.80	4.47	8.92	3.34	6.79	13.26
B[*e*]pyr	21.40	11.05	6.05	6.44	8.77	6.98	9.20	16.27
B[*a*]pyr	20.77	11.51	3.77	4.23	7.45	3.75	7.50	13.42
B[*g,h,i*]pery	12.54	5.84	4.16	3.88	4.77	4.15	5.88	10.67
In[1,2,3-*cd*]pyr	15.05	7.20	3.66	3.33	4.84	3.83	5.84	10.36
B[*g,h,i*]f	3.84	2.69	1.32	1.37	1.77	1.47	1.51	3.54
B[*b*]f	19.57	11.36	4.99	5.11	7.55	4.99	6.67	14.02
B[*k*]f	11.93	6.83	1.92	2.29	3.83	2.39	4.26	6.85
Dib[*a,h*]ant	3.19	2.21	0.83	0.91	1.31	0.87	1.30	2.21

Pery	<loq	<loq	<loq	<loq	<loq	<loq	<loq	<loq
$\sum_{53}$PAHs	295	189	72.8	101	152	66.9	145	240

Bellow limits of quantification (<loq)

Table S8. Concentrations in the gas equilibrated with the soil/snow surface (C_{SA}) of individual OCPs and PCBs.

ng m^{-3}	13/05/13	10/06/13	18/06/13	05/08/13	12/09/13	26/11/13	03/12/13	29/01/14	16/02/14	31/03/14	24/04/14	27/05/14	12/06/14	09/07/14
Σ_5OCPs	1.201	0.425	1.893	6.003	1.019	0.136	0.265	0.102	0.276	0.135	0.376	0.474	0.389	0.609
Σ_4HCH	0.148	0.071	0.077	0.061	0.044	0.022	0.039	0.036	0.030	0.017	0.146	0.069	0.052	0.104
α-HCH	0.065	0.050	0.058	0.033	0.033	0.005	0.018	0.025	0.009	0.009	<loq	0.023	0.027	0.055
β-HCH	<loq	<loq	<loq	0.012	<loq	<loq	0.013	<loq	<loq	<loq	0.079	<loq	<loq	<loq
γ-HCH	0.008	0.007	0.006	0.004	0.004	0.002	0.005	0.002	0.006	0.002	0.054	0.017	0.003	0.010
δ-HCH	0.075	0.014	0.012	0.013	0.007	0.015	0.004	0.009	0.016	0.006	0.014	0.029	0.022	0.039
HCB	0.905	0.284	1.740	5.881	0.932	0.093	0.187	0.030	0.215	0.101	0.084	0.336	0.284	0.400
Σ_{40}PCBs	0.386	0.575	0.336	0.387	0.233	0.081	0.390	0.055	0.219	0.082	0.539	0.262	0.199	0.859
PCB18	0.067	0.050	0.054	0.046	0.020	0.009	0.007	0.004	0.007	0.002	0.288	0.020	0.020	0.076
PCB17	0.006	0.005	0.007	0.005	0.002	0.006	0.003	0.006	0.004	0.001	0.020	0.001	0.003	0.012
PCB31+28	0.017	0.029	0.025	0.021	0.014	<loq	0.005	<loq	0.003	0.004	0.035	0.038	0.026	0.115
PCB52	0.091	0.080	0.048	0.028	0.018	0.018	0.011	0.001	0.013	0.003	<loq	0.043	0.018	0.169
PCB49	0.099	0.100	0.108	0.115	0.035	0.001	0.016	0.001	0.008	0.010	0.003	0.063	0.051	0.258
PCB44	0.047	0.036	0.023	0.049	0.014	0.003	0.018	0.021	0.042	0.016	<loq	0.025	0.030	0.079
PCB74	0.004	0.012	0.010	0.012	0.010	<loq	0.037	0.015	0.027	0.005	0.066	0.005	0.006	0.020
PCB70	0.005	0.007	0.005	0.005	0.010	0.003	0.015	<loq	<loq	<loq	0.015	0.038	0.013	0.018
PCB95	0.011	0.007	0.010	0.004	<loq	<loq	<loq	<loq	<loq	<loq	0.021	0.006	0.003	0.011
PCB99+101	0.021	0.011	0.012	0.010	0.039	<loq	0.002	<loq	0.004	0.023	0.010	0.007	0.007	0.019
PCB87	<loq	0.001	<loq	0.001	<loq	<loq	<loq	<loq	0.004	0.019	0.014	<loq	0.003	0.002
PCB110	0.002	0.002	0.001	0.003	<loq	<loq	0.003	<loq	<loq	<loq	<loq	0.001	0.001	0.003
PCB82	0.001	<loq	<loq	<loq	<loq	<loq	<loq	0.001	<loq	<loq	0.007	<loq	<loq	0.002
PCB151	0.001	<loq	<loq	0.002	<loq	<loq	0.002	0.003	<loq	<loq	<loq	<loq	<loq	0.004
PCB149	<loq	0.026	0.022	0.017	0.002	0.012	0.001	<loq	0.001	0.001	0.030	0.006	0.005	0.023
PCB118	0.008	0.024	0.007	0.013	<loq	<loq	<loq	0.004	<loq	<loq	0.006	0.001	<loq	0.020

PCB153	0.001	0.003	<loq	<loq	<loq	<loq	<loq	<loq	<loq	<loq	0.005	<loq	<loq	0.003
PCB132	0.002	0.002	0.002	0.002	<loq	0.029	0.002	<loq	<loq	<loq	0.032	<loq	0.007	<loq
PCB105	0.001	0.002	<loq	<loq	<loq	<loq	<loq	<loq	<loq	<loq	0.013	<loq	<loq	0.001
PCB138	<loq	<loq	<loq	<loq	<loq	<loq	<loq	<loq	<loq	<loq	0.016	<loq	<loq	0.002
PCB158	<loq	0.002	<loq	<loq	<loq	<loq	<loq	<loq	<loq	<loq	0.017	<loq	<loq	0.001
PCB187	<loq	0.003	<loq	<loq	0.002	<loq	0.004	<loq	<loq	<loq	0.014	<loq	0.002	0.003
PCB183	<loq	<loq	<loq	<loq	<loq	<loq	0.032	<loq	<loq	<loq	<loq	<loq	<loq	<loq
PCB128	<loq	0.001	<loq	<loq	<loq	<loq	0.006	<loq	<loq	<loq	0.014	<loq	<loq	0.001
PCB177	<loq	0.044	<loq	0.006	0.020	<loq	0.062	<loq	<loq	<loq	<loq	<loq	<loq	0.006
PCB156	<loq	<loq	<loq	<loq	<loq	<loq	<loq	<loq	<loq	<loq	0.143	<loq	<loq	<loq
PCB171	<loq	<loq	<loq	<loq	<loq	<loq	0.011	<loq	0.008	<loq	0.093	<loq	<loq	<loq
PCB180	<loq	0.070	<loq	<loq	0.025	<loq	0.070	<loq	0.067	<loq	<loq	0.004	0.004	0.007
PCB191	<loq	0.027	0.002	0.017	0.004	<loq	0.014	<loq	0.013	<loq	<loq	0.002	<loq	0.002
PCB169	<loq	0.028	<loq	0.024	<loq	<loq	0.007	<loq	0.012	<loq	0.009	<loq	<loq	<loq
PCB170	<loq	<loq	<loq	<loq	0.018	<loq	<loq	<loq	0.003	<loq	0.057	<loq	<loq	<loq
PCB201/199	<loq	0.006	<loq	0.008	<loq	<loq	0.063	<loq	0.004	<loq	0.013	<loq	<loq	<loq
PCB208	<loq	<loq	<loq	<loq	<loq	<loq	<loq	<loq	<loq	<loq	<loq	<loq	<loq	<loq
PCB195	<loq	<loq	<loq	<loq	<loq	<loq	<loq	<loq	<loq	<loq	<loq	<loq	<loq	<loq
PCB194	<loq	<loq	<loq	<loq	<loq	<loq	<loq	<loq	<loq	<loq	<loq	<loq	<loq	<loq
PCB205	<loq	<loq	<loq	<loq	<loq	<loq	<loq	<loq	<loq	<loq	<loq	<loq	<loq	<loq
PCB209	<loq	<loq	<loq	<loq	<loq	<loq	<loq	<loq	<loq	<loq	<loq	<loq	<loq	<loq
ΣTri-PCBs	0.090	0.083	0.087	0.073	0.035	0.015	0.014	0.009	0.014	0.007	0.084	0.059	0.049	0.204
ΣTetra-PCBs	0.247	0.235	0.194	0.208	0.087	0.026	0.097	0.038	0.090	0.033	0.083	0.174	0.117	0.545
ΣPenta-PCBs	0.044	0.046	0.029	0.031	0.039	<loq	0.005	0.001	0.008	0.042	0.071	0.016	0.015	0.059
ΣHexa-PCBs	0.005	0.061	0.024	0.045	0.002	0.041	0.018	0.003	0.013	0.001	0.124	0.006	0.012	0.033
ΣHepta-PCBs	<loq	0.172	0.002	0.047	0.069	<loq	0.200	<loq	0.102	<loq	0.173	0.006	0.006	0.019
ΣOcta-PCBs	<loq	0.006	<loq	0.008	<loq	<loq	0.063	<loq	0.004	<loq	0.013	<loq	<loq	<loq

Bellow limits of quantification (<loq)

Table S9. Concentrations in the gas phase equilibrated with the soil/snow surface (C_{SA}) of individual PAHs.

ng m^{-3}	**13/05/13**	**10/06/13**	**18/06/13**	**05/08/13**	**12/09/13**	**06/11/13**	**03/12/13**	**29/01/14**	**16/02/14**	**31/03/14**	**24/04/14**	**27/05/14**	**12/06/14**	**09/07/14**
Act	0.061	0.046	0.058	0.032	0.047	0.030	0.062	0.035	0.386	0.022	0.019	0.017	0.038	0.011
Ace	0.498	0.349	0.278	0.223	0.238	0.186	0.294	2.037	0.859	0.238	<loq	<loq	<loq	<loq
Flu	11.541	10.524	7.933	6.451	3.208	2.027	1.978	4.069	3.776	1.757	1.185	3.435	3.508	4.685
Phe	50.367	108.514	72.879	97.606	18.466	11.391	10.567	9.092	7.377	7.414	6.755	37.985	32.579	166.019
ΣMP	17.773	39.069	27.002	39.907	7.125	3.667	3.717	2.130	2.775	2.422	2.016	16.358	13.844	64.411
ΣDMPD	7.392	18.418	11.177	17.155	2.776	0.972	1.247	0.629	1.085	0.701	0.597	5.900	4.257	29.683
Ant	7.030	16.633	10.857	13.146	2.235	1.261	1.016	0.609	0.563	0.375	0.341	3.323	3.519	16.024
DBT	4.811	9.495	6.366	7.351	1.621	0.979	0.837	0.095	0.360	0.607	0.584	2.982	2.577	11.878
ΣMDBT	3.402	7.539	5.141	7.352	1.345	0.746	0.637	0.099	0.354	0.460	0.423	3.157	2.630	11.857
ΣDMDBT	2.181	4.229	3.194	4.477	0.572	0.291	0.292	<loq	0.192	0.113	0.087	1.479	1.222	5.645
Pyr	3.876	7.969	5.210	7.943	1.333	0.438	1.052	3.673	1.598	0.466	0.289	2.712	1.687	13.087
ΣMPyr	<loq	<loq	<loq	<loq	<loq	<loq	<loq	<loq	<loq	<loq	<loq	<loq	<loq	<loq
ΣDMPyr	0.148	0.550	0.305	0.544	0.058	<loq	<loq	0.221	0.014	0.003	<loq	0.057	0.015	0.563
Flt	5.390	12.329	7.738	12.215	2.012	0.871	1.415	4.396	1.978	0.954	0.635	4.068	3.120	21.123
Cry	0.041	0.208	0.124	0.207	0.024	0.005	0.008	0.216	0.034	0.015	0.009	0.025	0.018	0.158
ΣMCry	<loq	<loq	<loq	<loq	<loq	<loq	<loq	<loq	<loq	<loq	<loq	<loq	<loq	<loq
B[*a*]ant	0.011	0.035	0.027	0.033	0.005	<loq	0.005	0.140	0.011	0.005	<loq	<loq	<loq	0.014
B[*e*]pyr	0.004	0.002	0.005	<loq	<loq	<loq	<loq	0.071	0.002	<loq	<loq	<loq	<loq	<loq
B[*a*]pyr	0.008	<loq	<loq	0.005	0.012	<loq	<loq	0.066	0.006	<loq	0.022	<loq	0.013	<loq
B[*g,h,i*]pery	<loq	<loq	<loq	<loq	<loq	<loq	<loq	0.043	<loq	<loq	<loq	<loq	<loq	<loq
In[1,2,3-*cd*]pyr	<loq	<loq	<loq	0.005	<loq	<loq	<loq	0.064	0.004	<loq	<loq	<loq	<loq	<loq
B[*g,h,i*]f	<loq	<loq	<loq	0.056	<loq	<loq	<loq	0.125	0.071	<loq	<loq	<loq	<loq	<loq
B[*b*]f	<loq	0.025	0.083	0.282	0.055	0.016	0.076	0.097	<loq	<loq	<loq	<loq	<loq	<loq
B[*k*]f	<loq	0.005	<loq	0.010	<loq	<loq	<loq	0.119	0.005	<loq	<loq	<loq	<loq	<loq
Dib[*a,h*]ant	<loq	<loq	<loq	<loq	<loq	<loq	<loq	<loq	<loq	<loq	<loq	<loq	<loq	<loq

Pery	<loq	0.226	<loq	1.218	0.570	<loq	0.715	0.602	0.234	0.546	0.904	<loq	<loq	<loq
$\sum_{53}$PAHs	114.533	236.166	158.377	216.218	41.703	22.881	23.917	28.627	21.685	16.098	13.868	81.497	69.028	345.158

Bellow limits of quantification (<loq)

Table S10. Spearman's correlations between the concentrations equilibrated with the soil/snow surface (C_{SA}) and the inverse of the mean temperature (T).

	C_{SA}	**Spearman's rho**	**1/T**
OCPs	**HCB**	Correlation Coefficient	-0.758**
		p-value	.002
		N	14
	α-HCH	Correlation Coefficient	-0.626*
		p-value	.022
		N	13
	Σ_4HCHs	Correlation Coefficient	-0.547*
		p-value	.043
		N	14
	Σ_5OCPs	Correlation Coefficient	-0.785**
		p-value	.001
		N	14
PCBs	**PCB18**	Correlation Coefficient	-0.626*
		p-value	.017
		N	14
	PCB31+28	Correlation Coefficient	-0.587*
		p-value	.045
		N	12
	PCB52	Correlation Coefficient	-0.747**
		p-value	.003
		N	13
	PCB49	Correlation Coefficient	-0.855**
		p-value	.000
		N	14
	PCB44	Correlation Coefficient	-0.555*
		p-value	.049
		N	13
	ΣTri-PCBs	Correlation Coefficient	-0.670**
		p-value	.009
		N	14
	ΣTetra-PCBs	Correlation Coefficient	-0.710**
		p-value	.004
		N	14
	Σ_{40}PCBs	Correlation Coefficient	-0.560*
		p-value	.037
		N	14
PAHs	**Phe**	Correlation Coefficient	-0.789**
		p-value	.001
		N	14
	Ant	Correlation Coefficient	-0.785**

		p-value	.001
		N	14
	DBT	Correlation Coefficient	-0.851**
		p-value	.000
		N	14
	ΣMP	Correlation Coefficient	-0.815**
		p-value	.000
		N	14
	ΣMDBT	Correlation Coefficient	-0.851**
		p-value	.000
		N	14
	Pyr	Correlation Coefficient	-0.644*
		p-value	.013
		N	14
	Flt	Correlation Coefficient	-0.675**
		p-value	.008
		N	14
	ΣDMPD	Correlation Coefficient	-0.815**
		p-value	.000
		N	14
	ΣDMDBT	Correlation Coefficient	-0.797**
		p-value	.001
		N	13
	ΣDMDBT	Correlation Coefficient	-0.655*
		p-value	.029
		N	11
	Σ_{53}PAHs	Correlation Coefficient	-0.767**
		p-value	.001
		N	14
	ΣMePAHs	Correlation Coefficient	-0.833**
		p-value	.000
		N	14

**. Correlation is significant at the 0.01 confidence level (2-tailed).

*. Correlation is significant at the 0.05 confidence level (2-tailed).

Table S11. Soil/snow-air fugacity ratios (Ln f_s/f_a) for PAHs.

Ln fs/fa	**13/05/13**	**18/06/13**	**05/08/13**	**12/09/13**	**06/11/13**	**03/12/13**	**29/01/14**	**16/02/14**	**31/03/14**	**24/04/14**	**27/05/14**	**12/06/14**	**09/07/14**
Act	1.61	0.90	-0.43	1.38	-0.25	2.24	-0.13	0.00	-0.18	-0.44	0.03	1.88	-0.32
Ace	-1.09	-1.04	-1.61	-0.62	-0.23	-0.23	0.03	-0.17	-0.11				
Flu	1.22	1.17	-0.27	-0.26	1.37	0.40	0.17	-0.11	0.98	0.97	0.41	0.58	0.57
Phe	2.46	3.01	2.29	0.83	2.56	1.63	0.17	0.26	1.97	2.05	2.18	2.86	2.98
Ant	4.37	4.81	4.07	2.24	3.30	2.21	0.11	0.29	2.59	2.28	3.34	4.59	4.03
DBT	2.76	3.34	2.21	1.05	3.70	3.06	0.52	1.06	3.18	3.11	2.37	3.25	2.95
ΣMP	2.21	3.13	1.87	0.55	2.44	1.58	0.29	0.20	1.92	0.82	0.87	2.15	2.90
ΣMDBT	2.73	3.74	2.26	0.91	3.21	2.11	0.69	0.91	2.56	3.17	1.58	2.73	3.19
Pyr	2.26	0.99	1.97	0.30	0.95	0.62	0.34	-0.06	-0.36	-2.99	1.39	1.39	2.94
Flt	2.27	2.23	2.18	0.42	1.50	0.60	0.34	-0.04	0.80	-0.65	1.53		2.84
ΣDMPD	2.31	3.14	1.54	0.46	2.27	1.41	0.40	0.17	1.70	1.71	0.28	1.87	2.73
ΣDMDBT	3.30	4.29	1.84	0.32		-0.20		0.51			0.56		2.66
ΣDMPyr	2.10		2.07	1.15			0.44	-0.88	0.42		1.28	-0.33	3.53
Cry	0.64	2.78	1.94	0.37	-0.05	-0.63	-0.26	-0.49	0.61		0.34	1.02	1.83
B[*a*]ant	0.10	0.86				-1.41	-0.37	-1.08	0.74				
B[*e*]pyr	-0.51						-0.19	-1.43					
B[*a*]pyr	-0.10		-0.57				-0.23	-0.97				0.09	
B[*g,h,i*]pery							-0.09						
In[1,2,3-*cd*]pyr							-0.16	-1.02					
B[*g,h,i*]f							-0.27	0.07					
B[*b*]f		1.94	1.85	0.31	-0.78	-0.13	-0.11						
B[*k*]f							0.05	-1.42					
Σ_{53}PAHs	1.68	2.35	1.45	0.63	1.54	0.88	0.08	-0.21	1.20	1.00	1.24	1.84	2.53

Table S12. Soil/snow-air fugacity ratios (Ln f_s/f_a) for OCPs and PCBs.

Ln f_s/f_a	**13/05/13**	**10/06/13**	**18/06/13**	**05/08/13**	**12/09/13**	**06/11/13**	**03/12/13**	**29/01/14**	**16/02/14**	**31/03/14**	**24/04/14**	**27/05/14**	**12/06/14**	**09/07/14**
α-HCH		1.76	3.17	2.27	2.12	0.61	1.91	2.14	1.90	1.38		1.78	2.11	
β-HCH														
γ-HCH	1.44		-1.32	-1.13	-0.61	0.04		0.09	0.75	-0.21	2.37	-0.13	-0.54	-0.31
HCB	2.22		2.17	3.91	1.44	-1.06	1.09	0.17	1.21	0.58	-0.52	1.11	1.80	1.16
PCB18			0.58		0.65	-0.38				-0.53	3.88		2.12	2.03
PCB17					0.65			1.34	1.45	0.05	0.99		-1.10	0.89
PCB31+28		2.52	2.55	3.75					2.41		2.03	4.06	1.27	4.63
PCB52	1.39			-0.28	-1.39	0.11	1.52		2.52			1.83	0.44	3.20
PCB49			4.01	3.19	-1.25	-2.38				2.08	-1.72	1.22	1.35	1.35
PCB44	2.15		0.51	1.18	-0.40	-1.17	0.52	0.06	1.15	1.03		0.83	2.09	1.81
PCB74	-0.06	-1.21	-1.30	0.65	1.23		0.84	0.09	0.81	-0.39		0.92		1.95
PCB70		-1.46	-0.05		0.55	-0.92							-0.25	
PCB95		-0.46	-0.09	0.08								0.52		1.03
PCB99+101	2.18	-1.58	-0.77	0.65	1.56		-0.80				0.62	0.31	-1.58	1.06
PCB87									1.82				0.51	
PCB110												-0.18	-1.66	2.20
PCB151				-0.07			0.08							1.57
PCB149		2.56	-0.30	-1.46	-4.31		-2.39		-2.27	-2.43		-1.49	-2.34	-1.35
PCB118												-2.62		
PCB153														-0.53
PCB132	-0.05			-2.78			-0.13						-2.55	
PCB187					-1.04								1.54	0.20
PCB183							0.47							
PCB128							0.16							

PCB177							0.42							
PCB180							0.36					-1.90	-1.67	
PCB191					0.16		0.44					-1.26		
PCB169		0.56					-0.11		0.58					
PCB201/199									1.02					

Table S13. Spearman’s correlations between the soil/snow-air fugacity ratios (Ln f_s/f_a) and the inverse of the mean temperature (T).

Ln f_s/f_a	**Spearman's rho**	**1/T**
HCB	Correlation Coefficient	-0.659*
	p-value	0.014
	N	13
γ-HCH	Correlation Coefficient	0.678*
	p-value	0.015
	N	12
PAHs	Correlation Coefficient	-0.582*
	p-value	0.037
	N	13
Ace	Correlation Coefficient	0.783*
	p-value	0.013
	N	9
Phe	Correlation Coefficient	-0.560*
	p-value	0.046
	N	13
Ant	Correlation Coefficient	-0.648*
	p-value	0.017
	N	13
Flt	Correlation Coefficient	-0.594*
	p-value	0.042
	N	12
Cry	Correlation Coefficient	-0.797**
	p-value	0.002
	N	12

**. Correlation is significant at the 0.01 confidence level (2-tailed).

*. Correlation is significant at the 0.05 confidence level (2-tailed).

Figure S1. PAHs concentration profiles in the air (C_A), the air equilibrated with the soil/snow surface (C_{SA}), and soil (C_S).

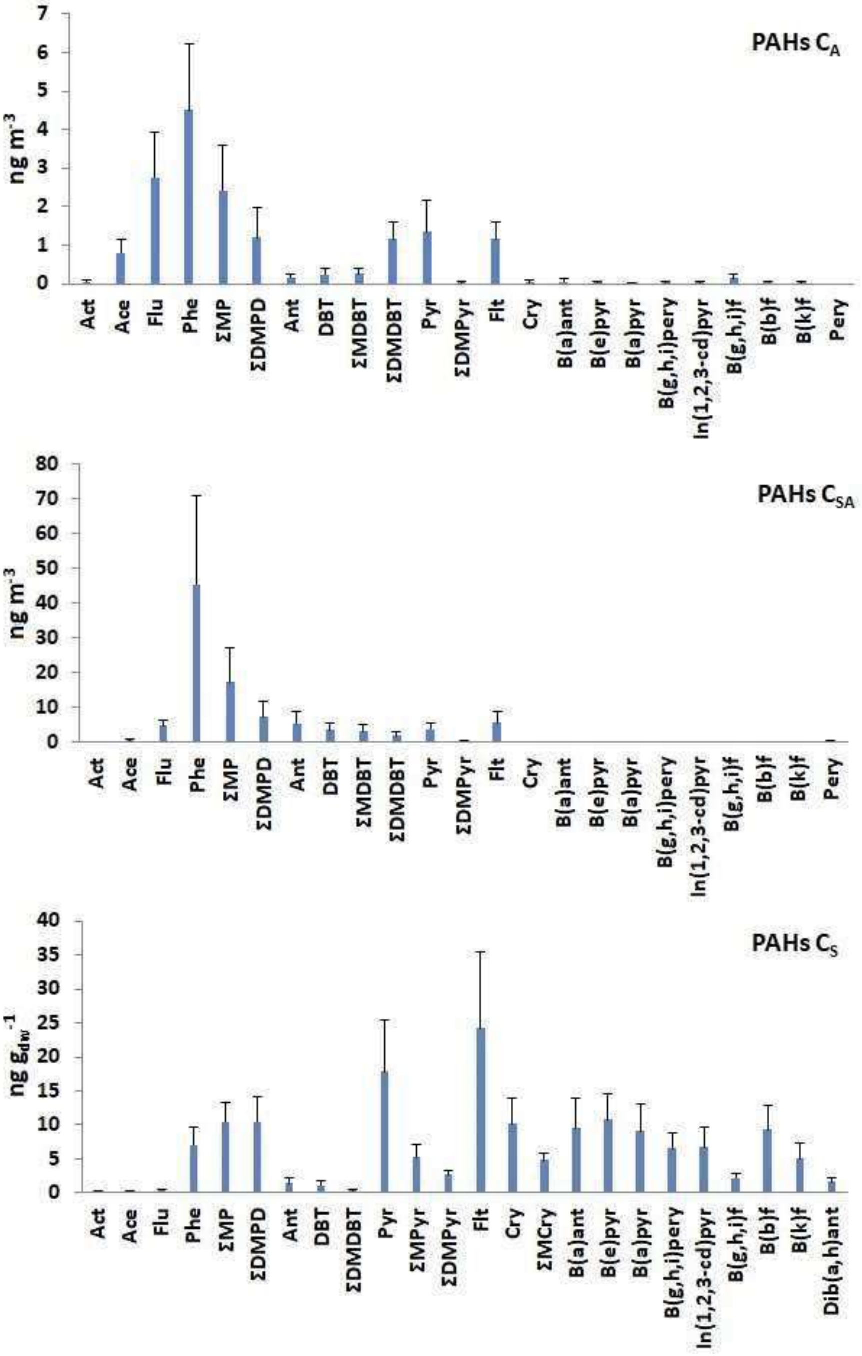

Figure S2. PCBs concentration profiles in the air (C_A), the air equilibrated with the soil/snow surface (C_{SA}), and soil (C_S).

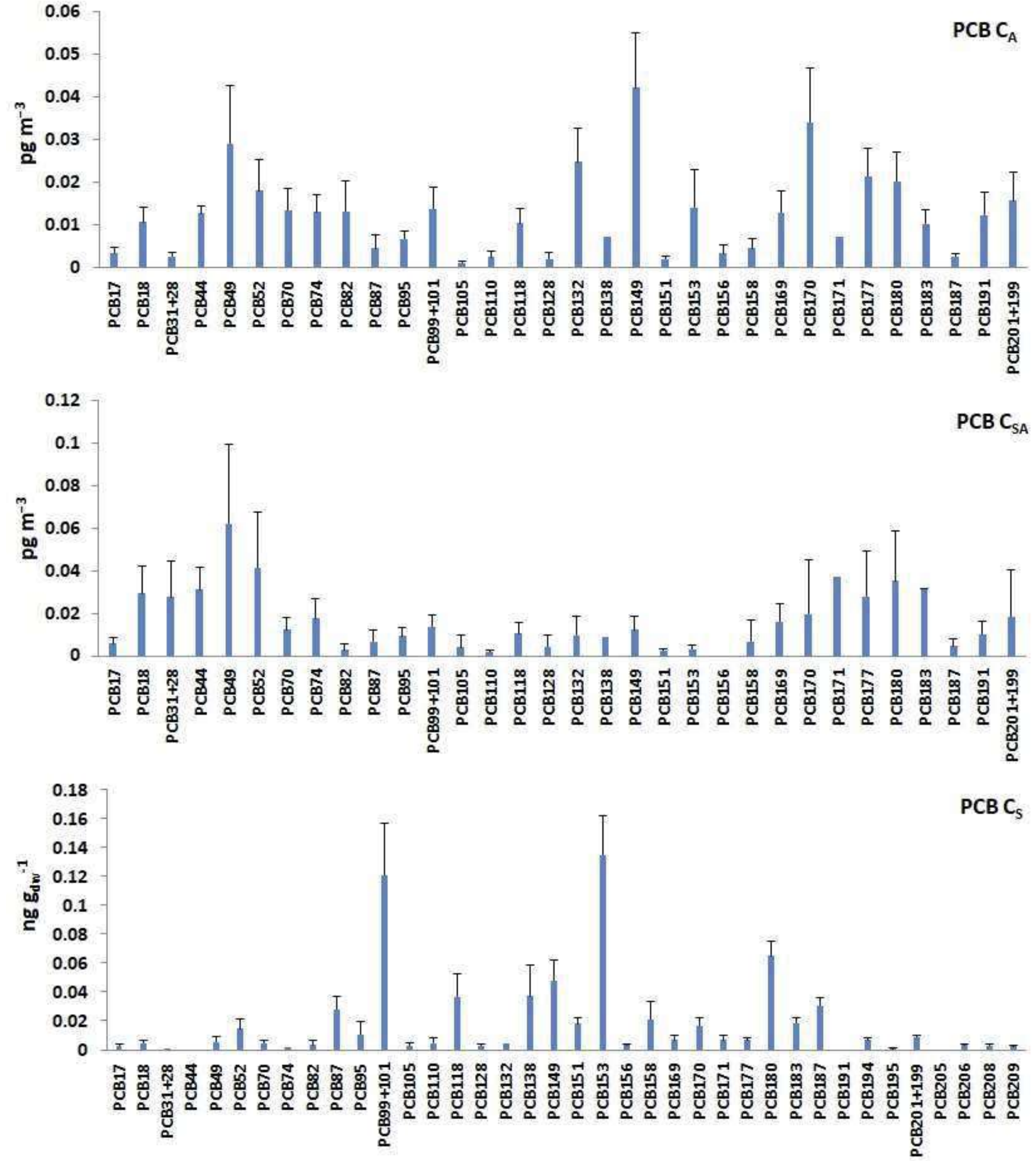

Figure S3A. 72-hour air mass back-trajectories for the 14 sampling events. Each panel shows the back trajectories starting at 100m height every 12 hours as samples integrate a time period of 5 or 6 days.

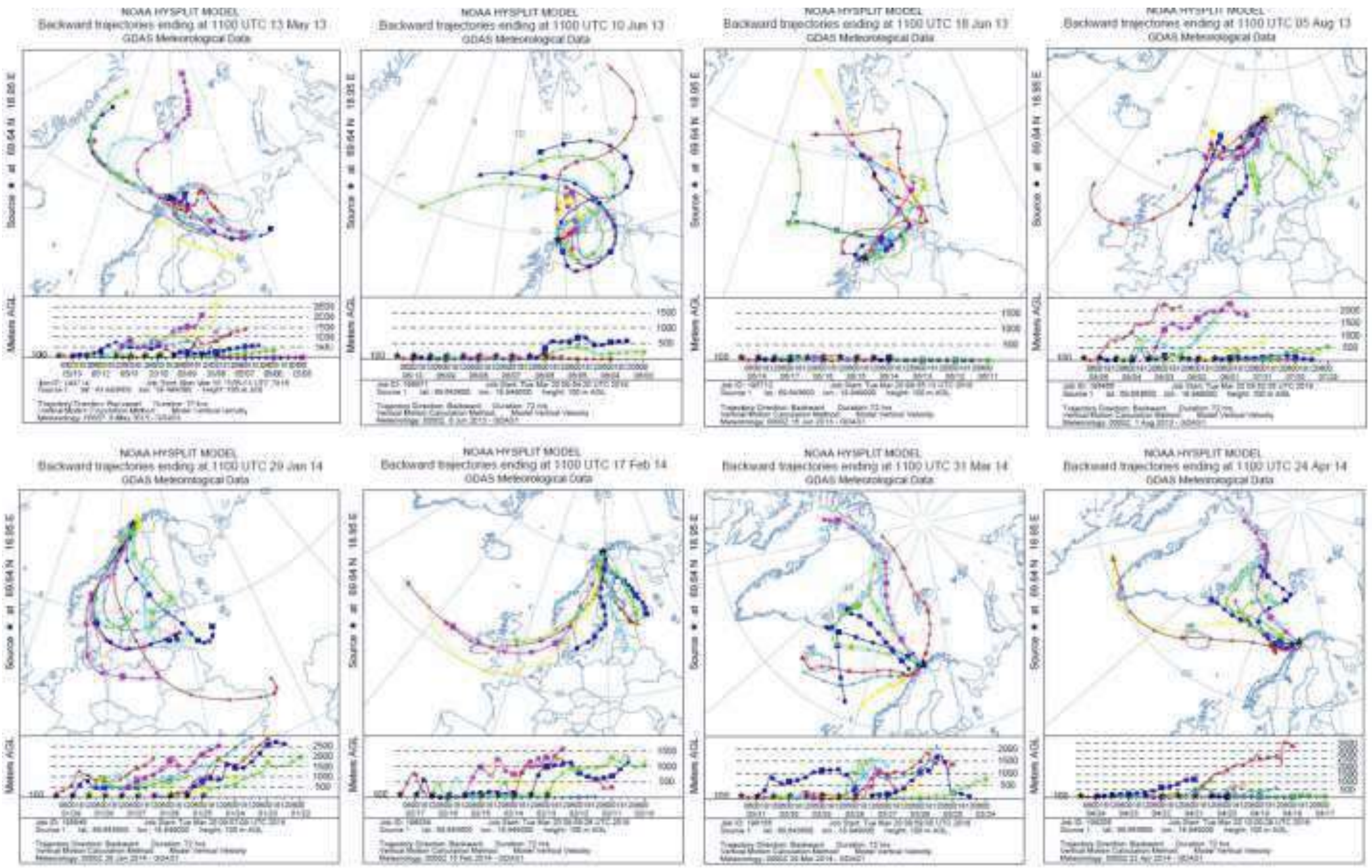

Figure S3B. 72-hour air mass back-trajectories for the 14 sampling events. Each panel shows the back trajectories starting at 100m height every 12 hours as samples integrate a time period of 5 or 6 days.

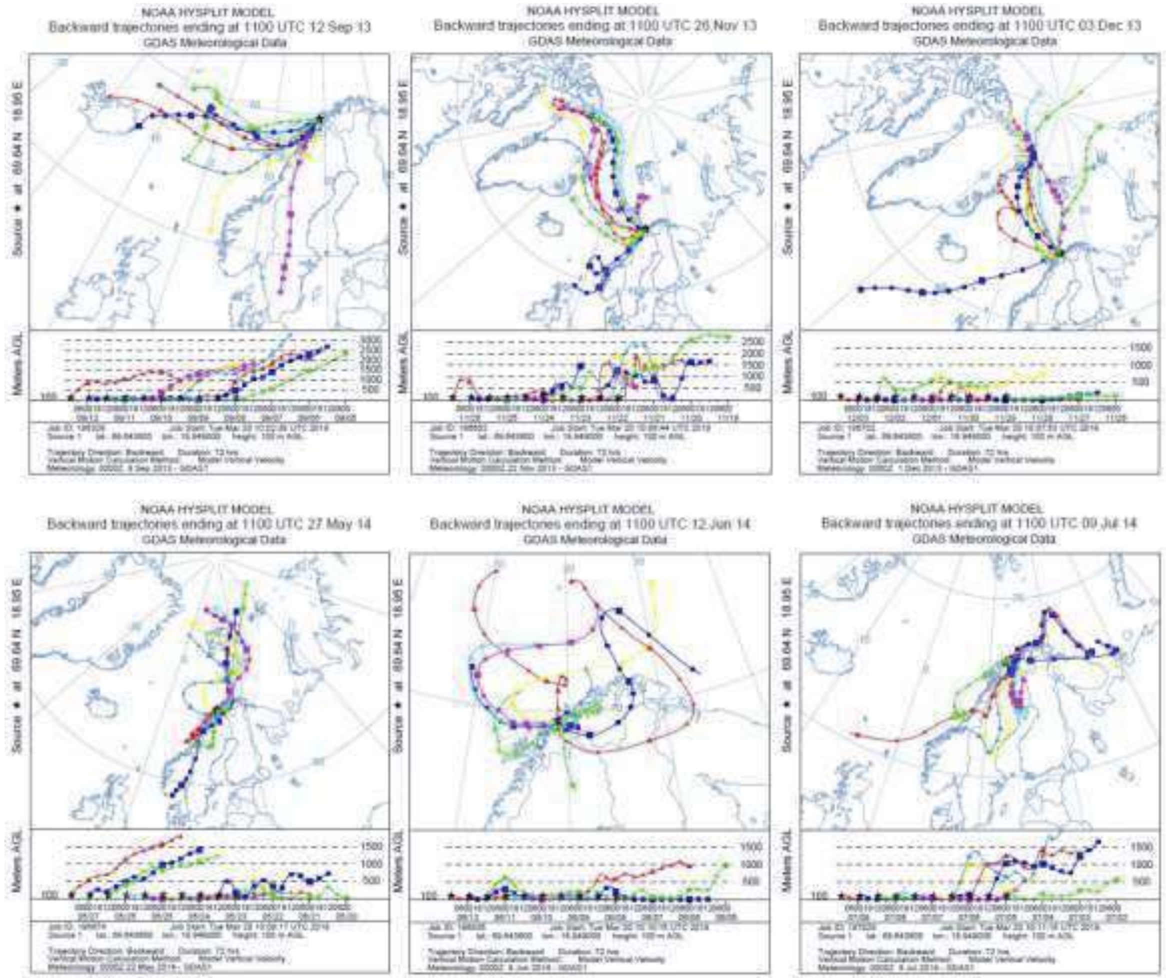

Figure S4. Soil/snow-air partition constants (K_{SA}) versus the octanol-air partition constant (K_{OA}) for HCB and HCHs.

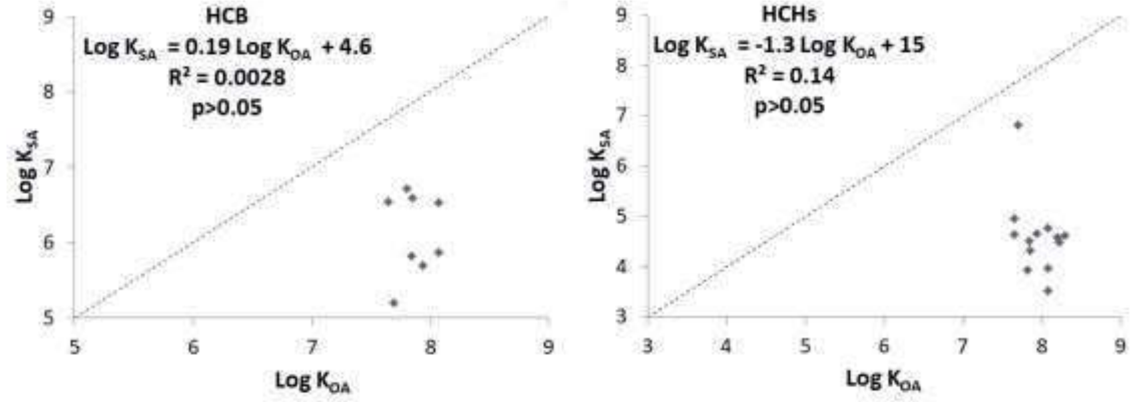

Figure S5. Seasonality of the concentrations in air equilibrated with the soil/snow surface (C_{SA}) for ∑OCPs, ∑PCBs and ∑PAHs.

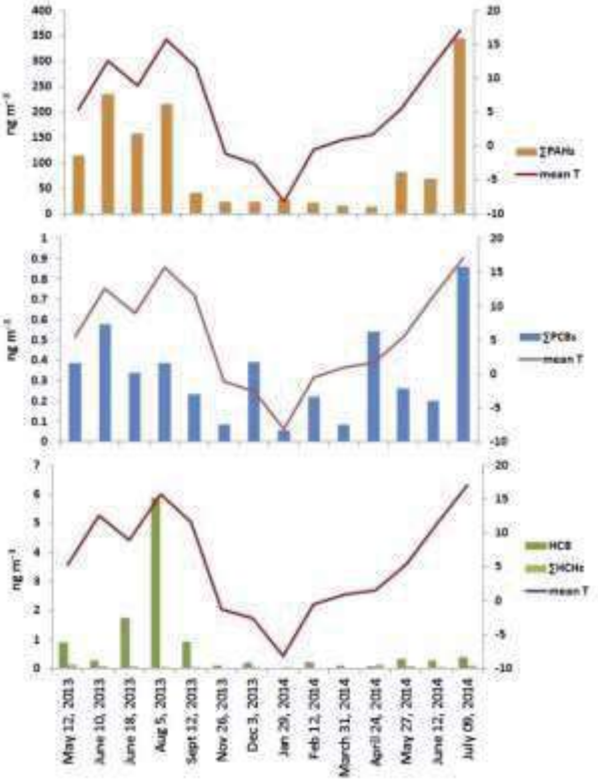

Figure S6. Soil/snow-air fugacity ratios (Ln f_s/f_a) for OCPs versus K_{OA}.

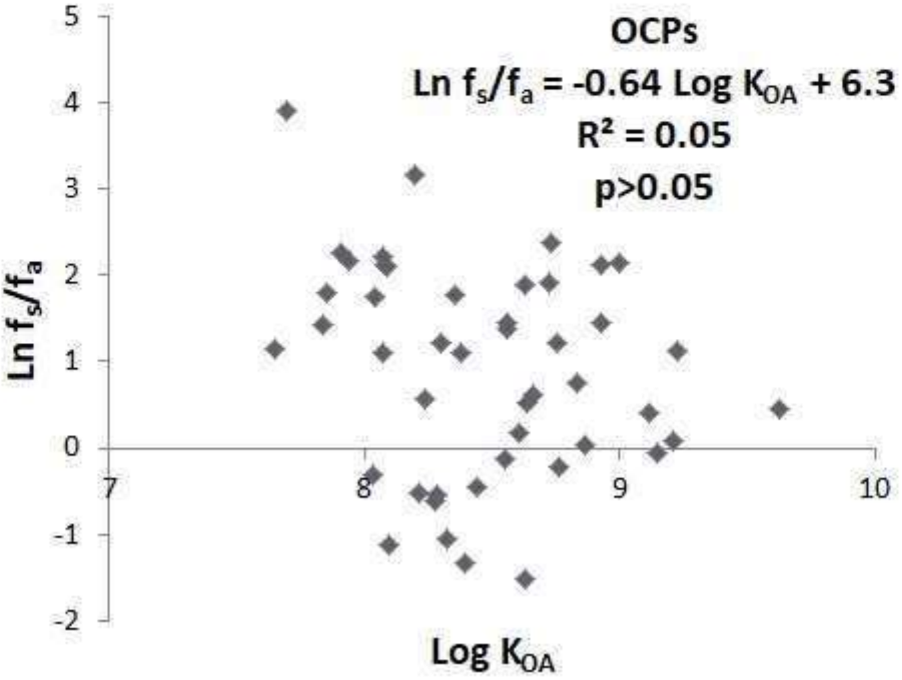

8.3 Capítol 3. Supporting Information

THE ROLE OF SNOW DEPOSITION OF PERFLUOROALKYLATED SUBSTANCES AT COASTAL LIVINGSTON ISLAND (MARITIME ANTARCTICA)

SUPPORTING INFORMATION

Paulo Casal[1], Yifeng Zhang[2], Jonathan W. Martin[2], Mariana Pizarro[1], Begoña Jiménez[3], and Jordi Dachs[1*]

[1]Institute of Environmental Assessment and Water Research, Spanish National Research Council (IDAEA-CSIC), Barcelona, Catalonia, Spain

[2]Division of Analytical and Environmental Toxicology, Department of Laboratory Medicine and Pathology, University of Alberta, Edmonton, Alberta Canada

[3]Department of Instrumental Analysis and Environmental Chemistry, Institute of Organic Chemistry (IQOG-CSIC), Madrid, Spain

* Corresponding author email: jordi.dachs@idaea.csic.es

INDEX

Figure S5. 72 hours air-mass backtrajectories for the four fresh snow deposition samples (SD) analyzed for PFAS.

Figure S6. Least squares linear regression between surface snow PFOS concentration and snow age ($p = 0.025$).

Figure S7. PFOS isomeric composition for the snow samples.

Figure S8. PFOS isomeric composition in the seawater samples. For samplers code refer to Table S5 legend.

Figure S9. PFOS isomeric composition for the plankton samples. For sample code, refer to Table S5 legend.

Figure S10. PFOA isomeric composition for the plankton samples. For sample code, refer to Table S5 legend.

Figure S11. Diagram of ΣPFAS, PFOS and PFOA in snow deposition, surface snow, snow melt, seawater and plankton phases. These schematics allow to see the differences in concentrations of PFAS from fresh snow deposition until PFAS reach coastal seawater in the maritime Antarctica.

Figure S12. Daily mean, minimum and maximum temperatures (°C) during the sampling campaign

Table S1. Average surface (at 0.2 to 5 m depth) CTD data from the Raquelia and Johnson sampling sites.

Date	Sampling station	Temperature (ºC)	Salinity (PSU)	PAR	Fluorescence (RFU)	Turbidity (NTU)
15/12/2014	Raquelia	0.46	34.01	129	0.52	4.86
16/12/2014	Johnson	0.82	33.68	161	0.33	5.97
18/12/2014	Raquelia	0.70	33.81	208	0.68	5.50
23/12/2014	Johnson	1.24	33.70	203	0.50	3.90
24/12/2014	Raquelia	0.20	34.00	367	0.22	3.18
26/12/2014	Johnson	1.24	33.70	203	0.50	3.90
29/12/2014	Raquelia	0.48	33.99	296	0.41	3.59
31/12/2014	Johnson	1.33	33.84	431	0.28	3.92
02/01/2015	Johnson	1.52	33.77	295	0.25	2.65
05/01/2015	Raquelia	1.34	33.55	259	0.59	4.87
07/01/2015	Johnson	1.32	33.59	550	0.43	4.92
09/01/2015	Raquelia	1.12	33.95	126	0.57	2.27
12/01/2015	Raquelia	1.64	33.81	308	0.43	3.13
14/01/2015	Johnson	1.97	33.36	154	1.21	3.68
16/01/2015	Raquelia	1.26	33.91	68	1.91	3.02
19/01/2015	Johnson	1.23	33.69	177	1.01	5.95
21/01/2015	Raquelia	0.40	33.55	180	0.91	5.70
23/01/2015	Johnson	1.15	33.34	50	1.57	6.65
26/01/2015	Raquelia	1.55	33.55	82	1.12	5.79
29/01/2015	Johnson	1.51	33.29	30	1.63	10.55
02/02/2015	Raquelia	1.83	33.73	67	1.21	5.07
05/02/2015	Johnson	1.71	33.19	67	1.04	12.38
10/02/2015	Raquelia	1.66	33.58	46	1.62	7.24
12/02/2015	Johnson	1.83	33.33	42	1.52	10.46
16/02/2015	Raquelia	1.82	33.52	305	0.68	6.15
19/02/2015	Johnson	1.91	33.39	138	0.92	8.23

Table S2. List of the perfluoroalkylated substances monitored in the present study and their acronyms, parent and product ions monitored in the MS/MS.

Compound	**Acronym**	**Parent Ion (m/z)**	**Product Ions (m/z)**
Perfluoroalkyl sulfonic acids	**PFSAs**		
Perfluorohexane sulfonic acid	PFHxS	399	80, 99
Linear perfluorooctane sulfonic acid	PFOS	499	80
Perfluoroisopropyl	*iso*-PFOS	499	80
5-perfluoromethyl	*5m*-PFOS	499	130
4-perfluoromethyl	*4m*-PFOS	499	330
3-perfluoromethyl	*3m*-PFOS	499	130
1-perfluoromethyl	*1m*-PFOS	499	419
Perfluorodecane sulfonic acid	PFDS	599	80, 99
Perfluoroalkyl carboxylic acids	**PFCAs**		
Perfluorobutanoic acid	PFBA	213	169
Perfluoropentanoic acid	PFPeA	263	219
Perfluorohexanoic acid	PFHxA	313	269
Perfluoroheptanoic acid	PFHpA	363	319
Linear perfluorooctanoic acid	PFOA	413	369
Perfluoroisopropyl	*iso*-PFOA	413	369
5-perfluoromethyl	*5m*-PFOA	413	219
4-perfluoromethyl	*4m*-PFOA	413	119
Perfluorononanoic acid	PFNA	463	419, 216
Perfluorodecanoic acid	PFDA	513	469, 219
Perfluoroundecanoic acid	PFUnA	563	519, 219
Perfluorododecanoic acid	PFDoA	613	569, 169
Perfluorotrdecanoic acid	PFTrA	663	619, 269
Perfluorotetradecanoic acid	PFTeA	713	669, 169
Internal Standards			
Perfluoro-($^{13}C_4$)-butanoic acid	^{13}C-PFBA	217	172
Perfluoro-($^{13}C_2$)-hexanoic acid	^{13}C-PFHxA	315	270
Perfluoro-$^{(13}C_4$)-octanoic acid	^{13}C-PFOA	417	372
Perfluoro-$^{(13}C_5$)-nonanoic acid	^{13}C-PFNA	468	423
Perfluoro-($^{13}C_2$)-decanoic acid	^{13}C-PFDA	515	470
Perfluoro-($^{13}C_2$)-undecanoic acid	^{13}C-PFUnA	565	520
Perfluoro-($^{13}C_2$)-dodecanoic acid	^{13}C-PFDoA	615	570
Perfluoro-($^{13}O_2$)-hexane sulfonatic acid	^{18}O-PFHxS	403	84, 103
Perfluoro-($^{13}C_4$)-octane sulfonic acid	^{13}C-PFOS	503	80

*All standards, including brPFOSK, TPFOA, PFAC-MXB and MPFAC-MXA were purchased from Wellington Laboratories (Guelph, ON, Canada)

Table S3. Instrumental limits of quantification (LOD), and experimental recoveries.

	Plankton LOD (pg)	**Plankton Recovery (%)**	**SPE LOD (pq)**	**SPE Recovery (%)**
PFSAs				
PFHxS	0.32	83±34	0.54	82±5.4
PFOS	1.0	120±16	1.3	89±1.6
iso-PFOS	1.0*	87±5.4	1.0*	88±15
5m-PFOS	1.0*	95±49	1.0*	82±5.1
4m-PFOS	1.0*	100±26	1.0*	95±16
3m-PFOS	1.0*	85±10	1.0*	98±25
1m-PFOS	1.0*	110±35	1.0*	86±7.8
PFDS	1.5*	86±18	0.10	83±1.0
PFCAs				
PFBA	35	110±37	6.6*	110.3±2.7
PFPeA	0.61*	110±26	3.7*	90±2.5
PFHxA	1.2*	100±16	0.59	110±2.7
PFHpA	0.5*	130±2.5	1.5	91±2.2
PFOA	11	130±15	3.6	84±1.8
iso-PFOA	1.0*	96±15	1.0*	94±13.7
5m-PFOA	1.1*	96±10	1.0*	85±23
4m-PFOA	0.9*	100±25	1.0*	87±17
PFNA	110	110±20	14.4	96±9.2
PFDA	1.2*	130±17	2.3*	110±31
PFUnA	1.9	100±48	1.5	80±11
PFDoA	1.2*	97±0.9	0.22	73±13
PFTrA	0.90*	110±13	0.60	78±1.0
PFTeA	0.53*	120±8.4	8.5	79±2.0

*not detected in blanks

Table S4. Estimated %brPFOA in snow samples, based on brPFOA LODs.

Snow samples	Estimated %brPFOA
NS1	<1
NS2	<1.2
NS3	<0.44
S1	<4.6
S2	<5.6
S3	<6.6
S4	<6.4
S5	<5.0
S6	<5.0
S7	<4.3
S8	<3.2
S9	<9.4
SD1	<0.9
SD2	<2.3
SD3	<1.0
SD4	<0.2
SM1	<10
SM2	<7.7
SM3	<6.3

Table S5. Estimated %brPFOA in seawater samples, based on brPFOA LODs.

Seawater samples	Estimated %brPFOA
R.15/12/2014	<5.8
R.18/12/2014	<7.7
R.24/12/2014	<6.7
R.29/12/2014	<2.2
R.05/01/2015	<8.0
R.09/01/2015	<5.1
R.12/01/2015	<3.9
R.16/01/2015	<6.9
R.21/01/2015	<7.4
R.26/01/2015	<5.4
R.02/02/2015	<7.3
R.10/02/2015	<2.2
R.16/02/2015	<5.5
J.16/12/2014	<3.6
J.23/12/2014	<4.1
J.26/12/2014	<4.3
J.31/12/2014	<2.6
J.02/01/2015	<4.1
J.07/01/2015	<5.2
J.14/01/2015	<2.8
J.19/01/2015	<5.0
J.23/01/2015	<1.7
J.29/01/2015	<7.7
J.05/02/2015	<13
J.12/02/2015	<7.1
J.19/02/2015	<4.4

Table S6. Snow phase PFAS concentrations (pg L^{-1}), density, age and mm of water equivalents of the snow deposition events. NS accounts for surface snow samples collected within the perimeter of the scientific station (near field snow). S accounts for surface snow samples. SD for fresh snow deposition samples. SM accounts for snowmelt samples.

Sample	**PFHxS**	**ΣPFOS**	**PFDS**	**PFBA**	**PFPeA**	**PFHxA**	**PFHpA**	**PFOA**	**PFNA**	**PFDA**	**PFUnA**	**PFDoA**	**PFTrA**	**PFTeA**	**ΣPFAS**	**Snow age (days)**	**Snow density (Kg L^{-1})**	**Distance To JC1 (Km)**	**Snowfall mm and event duration (days)**
NS1	n.d.	110	n.d.	180	n.d.	25	160	300	63	130	11	20	1.7	n.d.	1000		0.69		
NS2	n.d.	5.7	1.3	68	n.d.	n.d.	n.d.	250	42	150	15	20	2.3	n.d.	550		0.64		
NS3	23	750	0.55	240	n.d.	63	79	680	170	300	21	48	3.6	n.d.	2400		0.65		
S1	0.43	8.1	n.d.	n.d.	53	230	33	66	14	9.1	5.3	2.9	0.92	n.d.	430	1	0.66	0.24	
S2	n.d.	2.7	n.d.	190	n.d.	11	39	54	20	23	2.0	0.51	n.d.	n.d.	340	1	0.66	0.1	
S3	n.d.	9.1	n.d.	13	n.d.	76	36	45	n.d.	7.4	n.d.	0.8	n.d.	n.d.	190	4	0.75	0.1	
S4	n.d.	15	n.d.	260	n.d.	6.5	52	47	n.d.	12	3.9	2.4	0.87	n.d.	400	1	0.40	0.5	
S5	n.d.	4.6	n.d.	200	n.d.	4.7	47	60	n.d.	6.1	2.6	1.5	n.d.	n.d.	320	1	0.35	0.5	
S6	n.d.	16	n.d.	n.d.	n.d.	7.5	50	60	26	12	5.7	5.0	1.1	n.d.	180	6	0.40	11	
S7	n.d.	15	n.d.	n.d.	n.d.	12	58	70	n.d.	11	3.7	2.3	n.d.	n.d.	170	6	0.55	11	
S8	4.2	31	n.d.	n.d.	n.d.	n.d.	36	93	40	29	3.3	0.81	n.d.	n.d.	240	6	0.50	0.28	
S9	0.13	2.1	n.d.	n.d.	1.5	2.3	23	32	n.d.	9.1	5.2	6.2	0.92	n.d.	82	1	0.65	4	
SD1	0.54	14	n.d.	240	n.d.	41	120	340	170	120	120	n.d.	n.d.	n.d.	1200				15(3)
SD2	0.12	1.3	n.d.	400	27	37	58	130	40	30	15	12	4.4	n.d.	760				4.3(2)
SD3	0.51	8.3	n.d.	190	12	33	80	290	84	100	100	43	9.8	n.d.	960				8(2)
SD4	0.13	14	n.d.	480	33	130	310	1300	330	600	150	180	32	20	3600				19(3)
SM1	7.3	17	1.2	530	n.d.	7.4	26	29	18	7.1	2.5	n.d.	n.d.	n.d.	640				
SM2	0.72	9.1	0.22	370	n.d.	6.7	27	39	n.d.	3.1	2.6	1.7	0.74	n.d.	460				
SM3	0.35	9.5	n.d.	360	n.d.	7.1	29	48	48	9.7	12	3.5	1.1	n.d.	530				
Detection Frequency(%)	58	100	21	74	26	90	95	100	68	100	95	90	63	5					

Table S7. Individual PFCAs concentrations correlations in snow samples

			PFBA	PFPeA	PFHxA	PFHpA	PFOA	PFNA	PFDA	PFUnA	PFDoA	PFTrA
Spearman's rho	**PFBA**	Correlation Coefficient	1.000	1.000**	-.093	-.192	-.130	.006	-.143	.060	.294	.133
		Sig. (2-tailed)			.762	.529	.659	.987	.626	.845	.354	.732
	PFPeA	Correlation Coefficient		1.000	1.000**	.300	.300	-.400	-.100	.300	-.100	.103
		Sig. (2-tailed)				.624	.624	.600	.873	.624	.873	.870
	PFHxA	Correlation Coefficient			1.000	.525*	.650**	.355	.498*	.638**	.354	.620*
		Sig. (2-tailed)				.031	.005	.285	.042	.008	.196	.042
	PFHpA	Correlation Coefficient				1.000	.880**	.776**	.839**	.686**	.597*	.788**
		Sig. (2-tailed)					.000	.003	.000	.002	.015	.004
	PFOA	Correlation Coefficient					1.000	.835**	.856**	.756**	.672**	.844**
		Sig. (2-tailed)						.000	.000	.000	.003	.001
	PFNA	Correlation Coefficient						1.000	.835**	.846**	.855**	.750*
		Sig. (2-tailed)							.000	.000	.001	.020
	PFDA	Correlation Coefficient							1.000	.734**	.701**	.816**
		Sig. (2-tailed)								.001	.002	.001
	PFUnA	Correlation Coefficient								1.000	.941**	.984**
		Sig. (2-tailed)									.000	.000
	PFDoA	Correlation Coefficient									1.000	.900**
		Sig. (2-tailed)										.000
	PFTrA	Correlation Coefficient										1.000
		Sig. (2-tailed)										

**. Correlation is significant at the 0.01 level (2-tailed).

*. Correlation is significant at the 0.05 level (2-tailed).

Table S8. Seawater PFAS (pg L^{-1}) concentrations. In the sample code. R and J account for the Raquelia and Johnsons sampling sites (Figure 1). The sampling date is also indicated in the sample code.

Sample	PFHxS	ΣPFOS	PFDS	PFHxA	PFHpA	PFOA	PFNA	PFDA	PFUnA	PFDoA	PFTrA	PFTeA	ΣPFAS
R.15/12/2014	n.d.	23	n.d.	n.d.	40	52	26	35	3.0	8.9	2.4	n.d.	190
R.18/12/2014	n.d.	23	n.d.	10	64	39	n.d.	27	6.8	n.d.	2.1	n.d.	170
R.24/12/2014	n.d.	26	n.d.	2.1	54	45	n.d.	6.3	2.3	2.1	n.d.	n.d.	140
R.29/12/2014	n.d.	14	0.23	15	62	140	18	14	2.5	2.1	0.67	n.d.	270
R.05/01/2015	n.d.	24	n.d.	4.1	43	37	110	13	6.1	4.8	2.1	n.d.	240
R.09/01/2015	n.d.	12	n.d.	30	45	59	79	9.3	20	1.4	n.d.	n.d.	260
R.12/01/2015	n.d.	n.d.	n.d.	4.5	44	78	n.d.	9.1	2.4	5.0	n.d.	n.d.	140
R.16/01/2015	n.d.	25	n.d.	3.8	19	43	32	26	12	n.d.	n.d.	n.d.	160
R.21/01/2015	n.d.	1.1	n.d.	3.1	77	41	n.d.	9.0	2.0	n.d.	n.d.	n.d.	130
R.26/01/2015	n.d.	12	n.d.	n.d.	80	55	n.d.	8.8	13	1.0	n.d.	n.d.	170
R.02/02/2015	n.d.	21	n.d.	7.9	44	41	n.d.	9.8	18	n.d.	n.d.	25	170
R.10/02/2015	n.d.	46	n.d.	12	47	140	n.d.	n.d.	27	n.d.	n.d.	n.d.	270
R.16/02/2015	n.d.	1.5	n.d.	5.2	40	55	18	5.4	2.6	7.0	1.6	n.d.	130
J.16/12/2014	n.d.	12	n.d.	14	74	83	n.d.	15	3.1	2.4	n.d.	n.d.	200
J.23/12/2014	n.d.	2.0	n.d.	2.1	62	74	n.d.	11	2.0	0.5	n.d.	n.d.	150
J.26/12/2014	1.8	180	n.d.	4.2	55	69	28	68	6.6	1.1	n.d.	n.d.	420
J.31/12/2014	0.6	13	n.d.	9.6	52	110	n.d.	22	3.8	2.3	n.d.	n.d.	220
J.02/01/2015	n.d.	10	n.d.	3.3	45	73	n.d.	13	4.8	4.4	0.68	n.d.	150
J.07/01/2015	n.d.	2.5	n.d.	n.d.	69	58	n.d.	6.6	n.d.	1.9	n.d.	n.d.	140
J.14/01/2015	n.d.	3.9	n.d.	13	31	100	n.d.	12	4.6	4.2	n.d.	n.d.	170
J.19/01/2015	n.d.	5.6	n.d.	7.2	68	60	15	19	12	n.d.	n.d.	n.d.	190
J.23/01/2015	n.d.	27	n.d.	14	87	180	44	30	13	n.d.	n.d.	n.d.	390
J.29/01/2015	5.3	10	n.d.	6.3	48	39	n.d.	14	3.8	n.d.	n.d.	n.d.	130
J.05/02/2015	n.d.	5.5	n.d.	5.1	22	24	21	14	n.d.	1.4	n.d.	n.d.	94
J.12/02/2015	n.d.	1.9	n.d.	4.6	24	42	15	12	2.8	n.d.	n.d.	n.d.	100

J.19/02/2015	1.7	1.4	n.d.	9.8	40	68	n.d.	12	3.9	6.6	2.1	n.d.	140
Detection frequency (%)	15	96	4	88	100	100	42	96	92	65	27	4	

Table S9. Plankton PFAS (ng g_{dw}^{-1}) concentrations. For sample code. refer to Table S5 legend.

Sample	ΣPFOS	PFBA	PFPeA	PFHxA	PFHpA	ΣPFOA	PFUnA	ΣPFAS
R.15/12/2014	0.16	0.94	5.9	n.d.	4.6	4.4	n.d.	16
R.24/12/2014	0.07	1.2	0.22	0.30	n.d.	2.6	n.d.	4.5
R.09/01/2015	0.088	2.0	n.d.	0.35	n.d.	2.5	0.0011	5.0
R.21/01/2015	0.040	0.42	1.2	0.26	1.6	1.0	n.d.	4.6
R.10/02/2015	0.038	0.38	0.40	0.045	n.d.	2.6	n.d.	3.4
R.19/02/2015	0.055	0.98	0.47	0.066	n.d.	3.5	n.d.	5.0
J.16/12/2014	0.14	0.68	n.d.	n.d.	n.d.	3.9	0.014	4.7
J.26/12/2014	0.087	0.93	n.d.	n.d.	n.d.	3.6	n.d.	4.7
J.14/01/2015	0.13	0.43	0.031	n.d.	n.d.	3.2	n.d.	3.8
J.23/01/2015	0.079	n.d.	0.60	0.21	n.d.	2.2	n.d.	3.1
J.05/02/2015	0.17	1.8	1.5	0.46	0.13	4.9	n.d.	9.0
Detection Frequency(%)	100	89	67	67	33	100	22	

Table S10. Bioaccumulation factors (log BAFs) for the individual PFAS and for each sampling event.

Sample	n-PFOS	iso-PFOS	5m-PFOS	4m-PFOS	ΣPFOS	PFHxA	PFHpA	ΣPFOA	PFUnA
R.15/12/2014	3.1	2.8			3.0		4.2	4.1	
R.24/12/2014	3.8			2.0	3.7	3.7	2.2	3.7	
R.09/01/2015	3.3	3.6			3.2			3.8	2.8
R.21/01/2015	2.6	2.9	1.9	1.9	2.6	4.3		3.9	
R.10/02/2015	1.8	2.1	1.5	1.7	1.8			3.9	
R.19/02/2015	3.3	2.4	2.6	2.4	3.0	3.2		3.8	0.93
J.16/12/2014	3.6				3.7	4.1	2.9	4.5	
J.26/12/2014	3.8			2.6	3.8	3.0		3.9	
J.14/01/2015	3.6				3.7	4.1	3.5	3.6	
J.23/01/2015	2.6		2.0		2.6	3.3		3.3	
J.05/02/2015	2.1	2.4			2.1	2.7		3.5	

Table S11. Ratios of the average concentrations of individual PFAS between the different matrices.

PFAS	C_{SD}/C_{Snow}	C_{SD}/C_{SM}	C_{SD}/C_{SW}	C_{Snow}/C_{SM}	C_{Snow}/C_{SW}	C_{SM}/C_{SW}
PFSAs						
ΣPFOS	0.82	0.80	0.49	0.97	0.59	0.61
n-PFOS	0.82	0.82	0.49	1.0	0.46	0.60
iso-PFOS	1.0	0.63	0.48	0.60	0.39	0.77
5m-PFOS	1.1	0.75	0.44	0.67	0.86	0.59
4m-PFOS	0.62	0.85	0.53	1.4	0.17	0.63
PFCAs						
PFBA		0.78				
PFHxA	1.4	8.5	7.3	6.3	5.3	0.85
PFHpA	3.4	5.2	2.8	1.5	0.81	0.53
PFOA	8.8	13	7.5	1.5	0.84	0.56
PFNA		4.8				
PFDA	16	33	13	2.0	0.78	0.39
PFUnA	25	17	14	0.70	0.55	0.79
PFDoA	31	30	23	1.0	0.74	0.78
PFTrA		16			0.95	

Compounds with detectability below 50% were excluded.

Table S12. Estimated monthly snow deposition (MSD) of individual PFAS, their seawater column inventories, and the time that would be needed to accumulate the measured water column concentrations due to snow deposition inputs only.

PFAS	MSD (ng m^{-2} $month^{-1}$)	Seawater inventories (ng m^{-2})	Time (years)
PFOS	0.38	300	67
PFHxA	2.4	100	3.5
PFHpA	5.6	730	11
PFOA	20	1100	4.3
PFNA	6.2	130	1.8
PFDA	8.5	270	2.7
PFUnA	3.9	65	1.4
PFDoA	2.3	26	1.0
PFTrA	0.46	2.9	0.53
ΣPFAS	64	2700	3.7

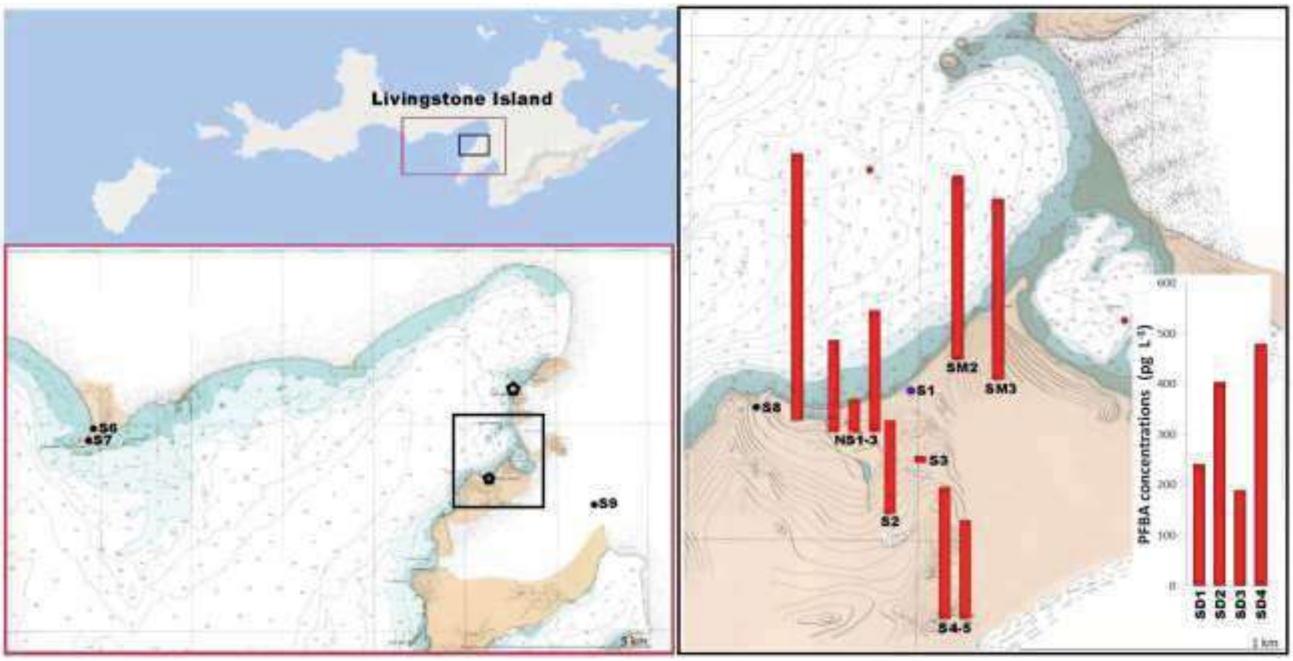

Figure S1. Near-field snow(NS), far-field snow(S), snow-melt(SM) and snow deposition (SD) PFBA concentrations (pg L^{-1})

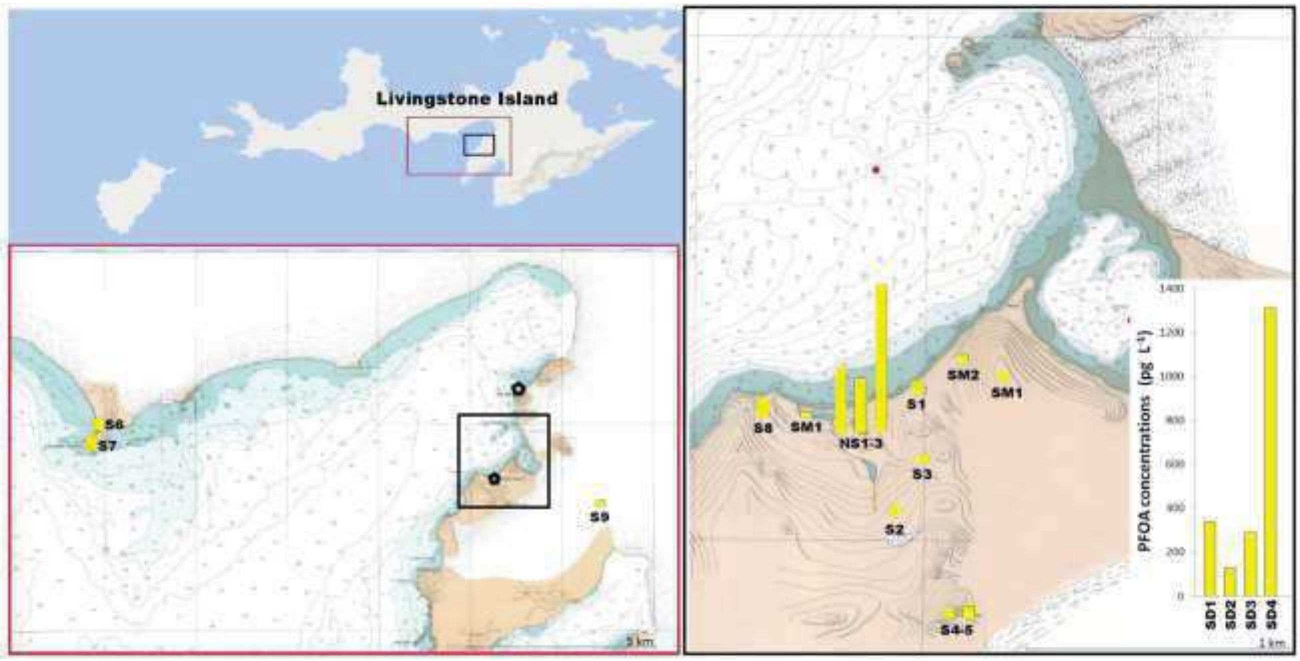

Figure S2. Near-field snow(NS), far-field snow(S), snow-melt(SM) and snow deposition (SD) PFOA concentrations (pg L^{-1})

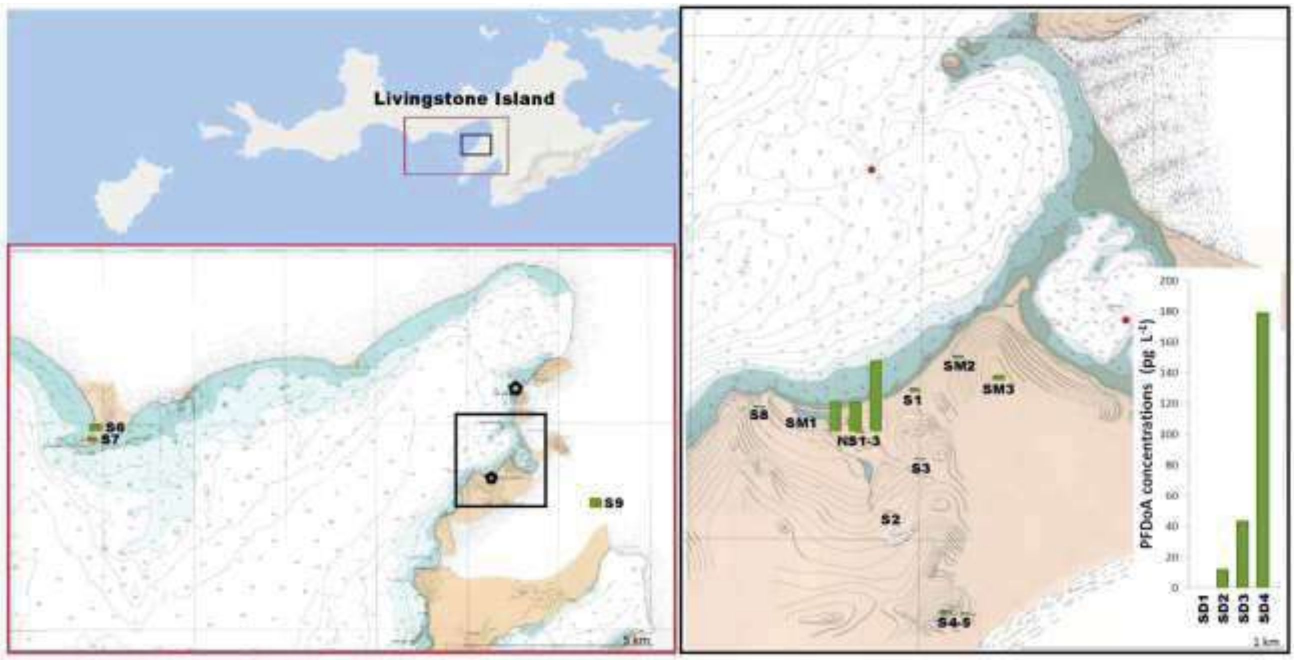

Figure S3. Near-field snow(NS), far-field snow(S), snow-melt(SM) and snow deposition (SD) PFDoA concentrations (pg L^{-1})

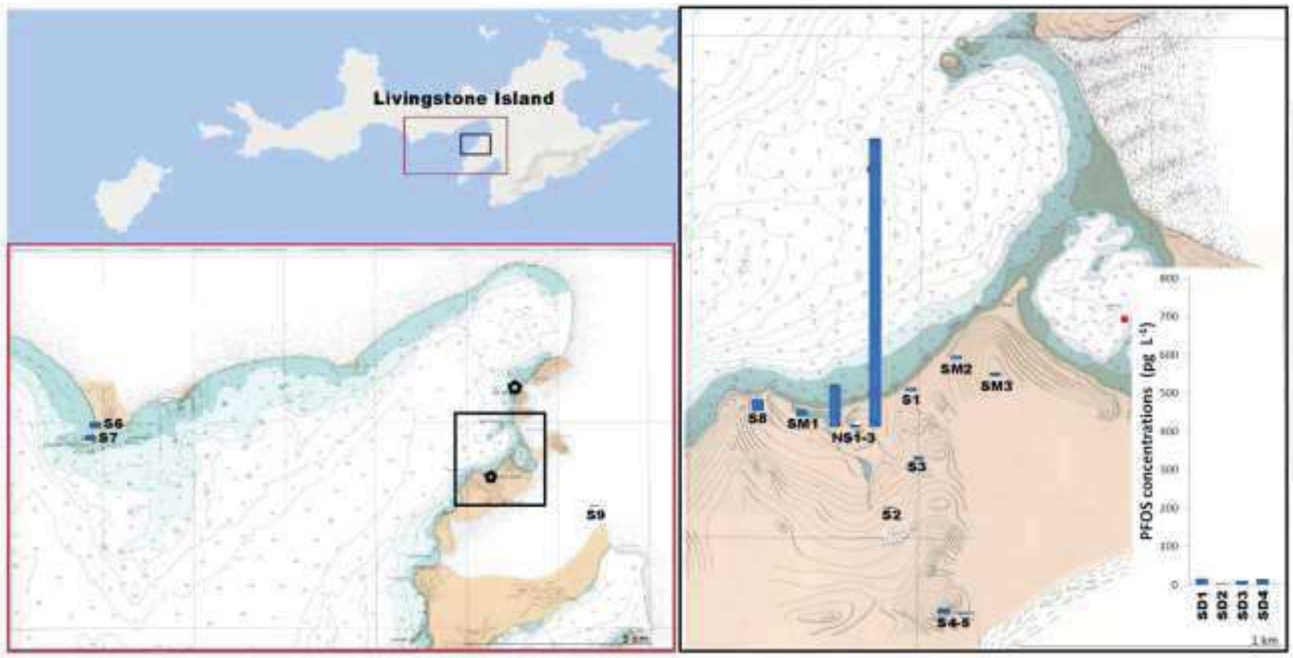

Figure S4. Near-field snow(NS), far-field snow(S), snow-melt(SM) and snow deposition (SD) PFOS concentrations (pg L^{-1})

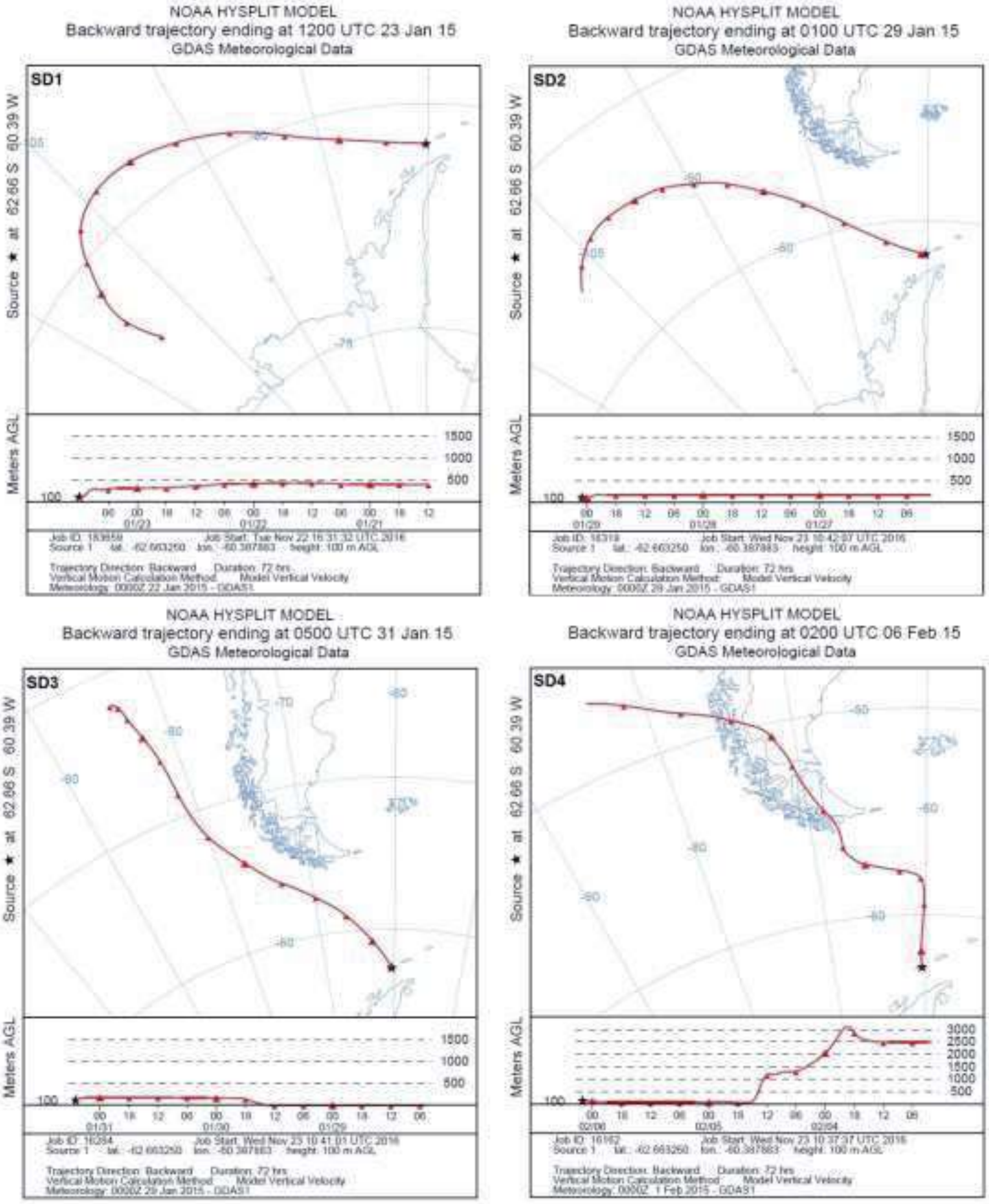
NOAA HYSPLIT MODEL
Backward trajectory ending at 1200 UTC 23 Jan 15
GDAS Meteorological Data

NOAA HYSPLIT MODEL
Backward trajectory ending at 0100 UTC 29 Jan 15
GDAS Meteorological Data

NOAA HYSPLIT MODEL
Backward trajectory ending at 0500 UTC 31 Jan 15
GDAS Meteorological Data

NOAA HYSPLIT MODEL
Backward trajectory ending at 0200 UTC 06 Feb 15
GDAS Meteorological Data

Figure S5. 72 hours air-mass backtrajectories for the four fresh snow deposition samples (SD) analyzed for PFAS.

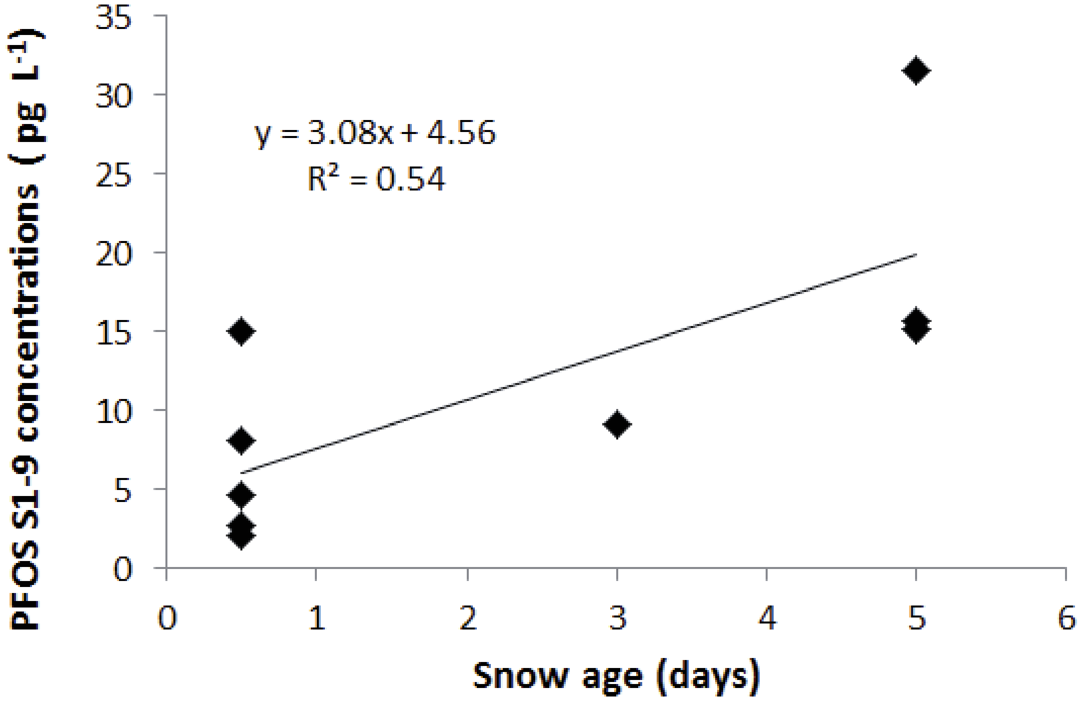

Figure S6. Least squares linear regression between surface snow PFOS concentration and snow age ($p = 0.025$).

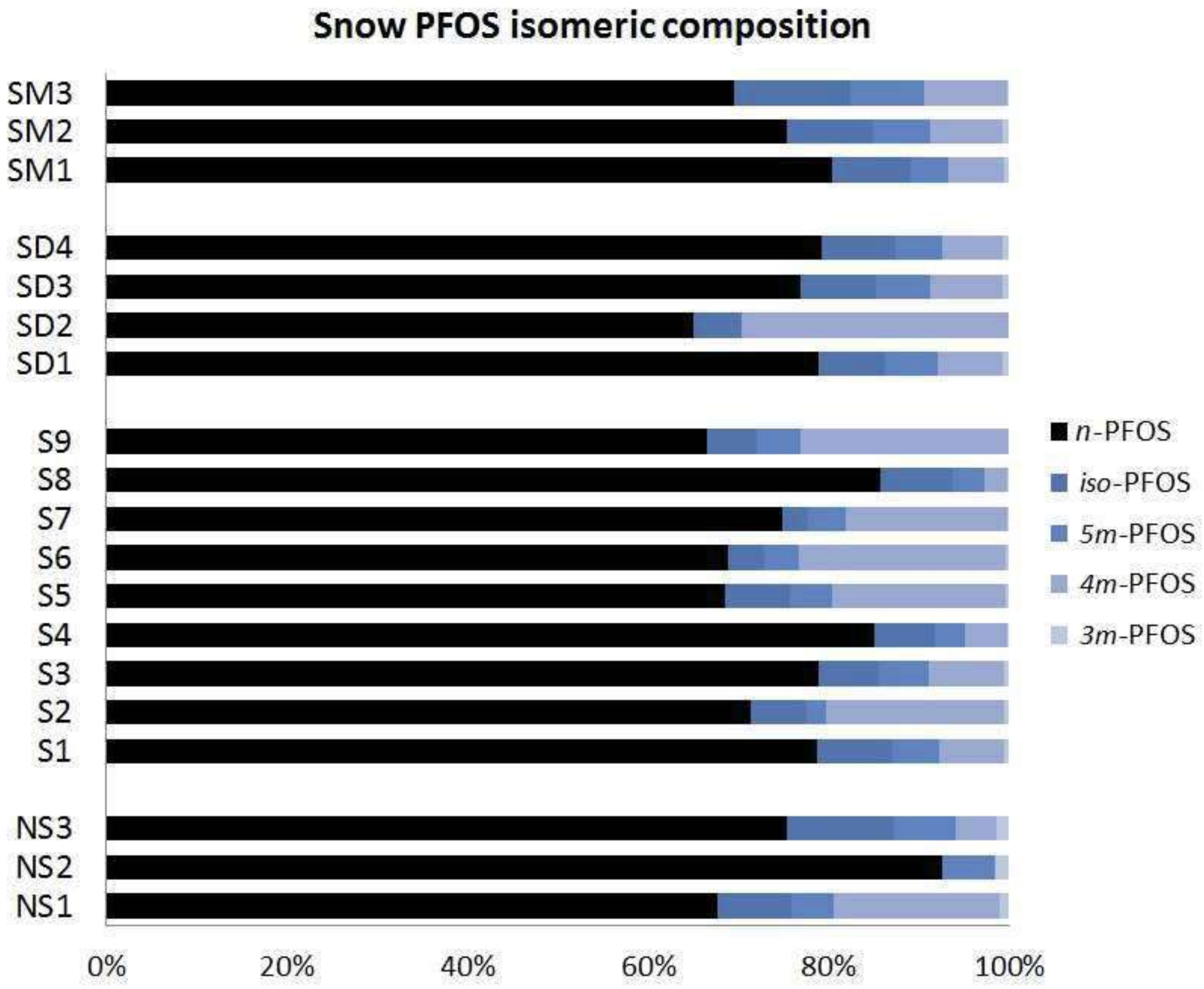

Figure S7. PFOS isomeric composition for the snow samples.

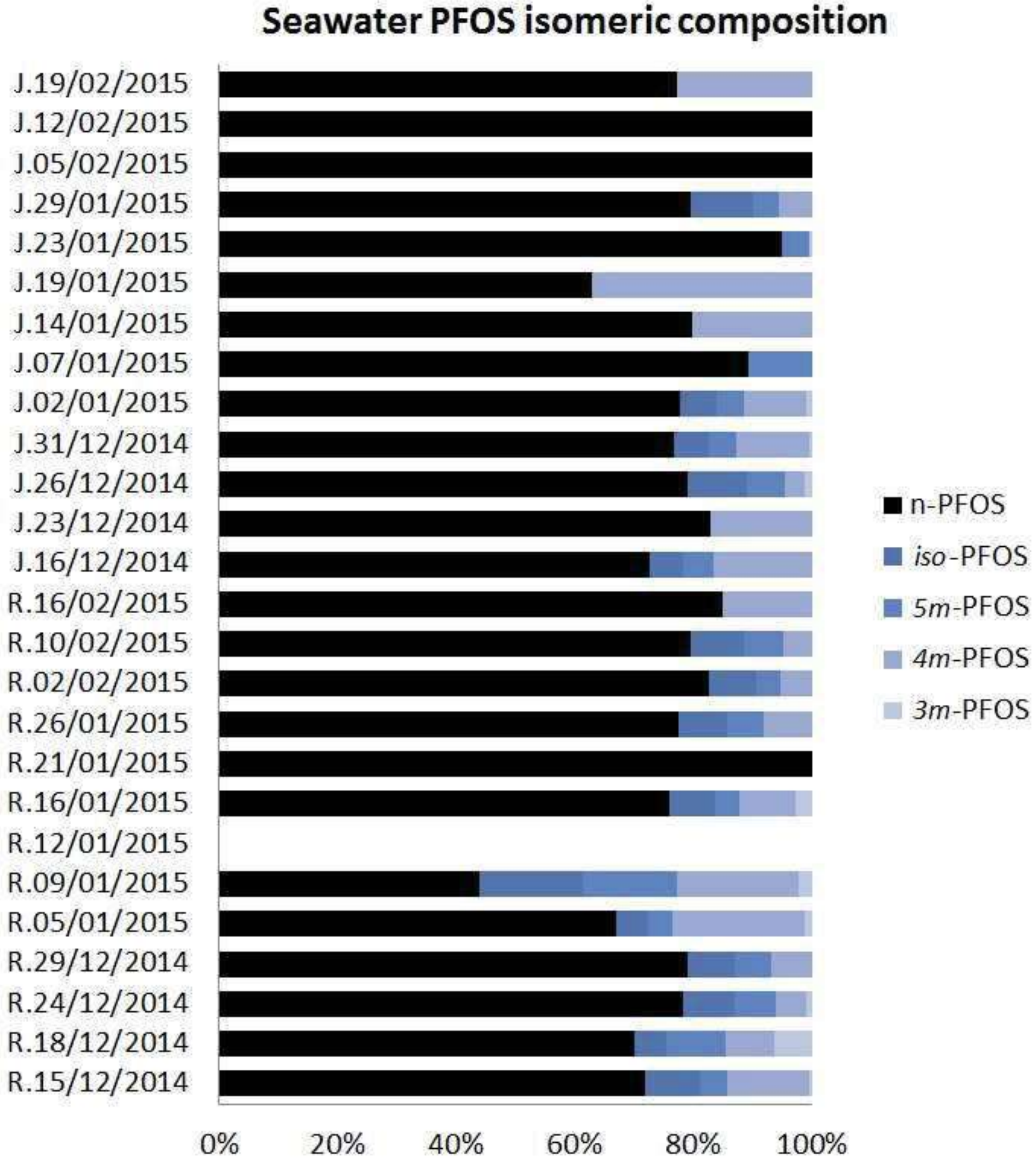

Figure S8. PFOS isomeric composition in the seawater samples. For samplers code refer to Table S5 legend.

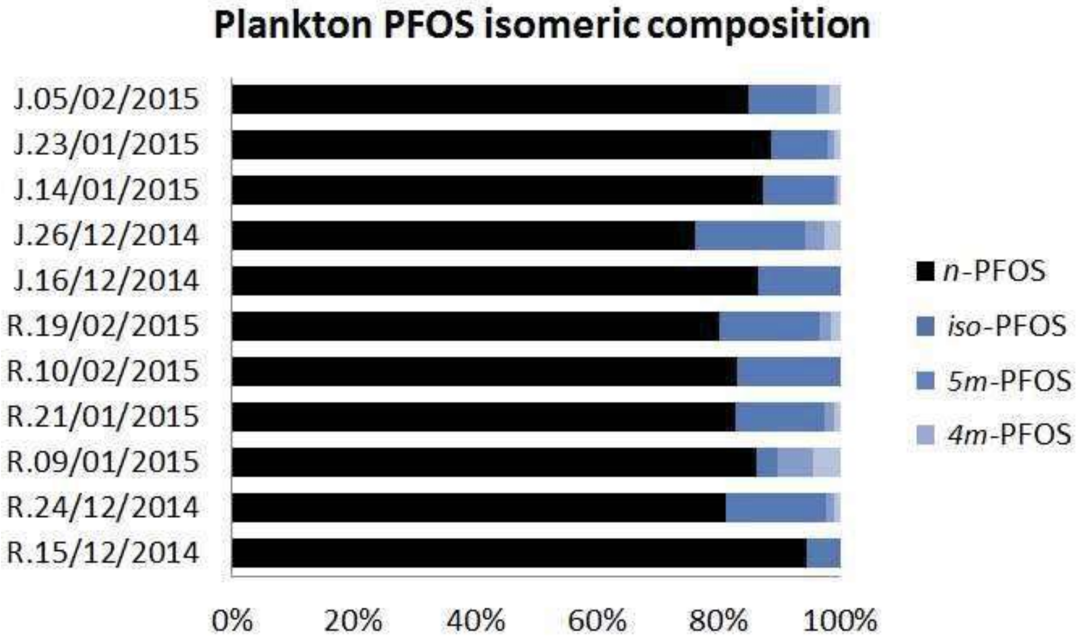

Figure S9. PFOS isomeric composition for the plankton samples. For sample code. refer to Table S5 legend.

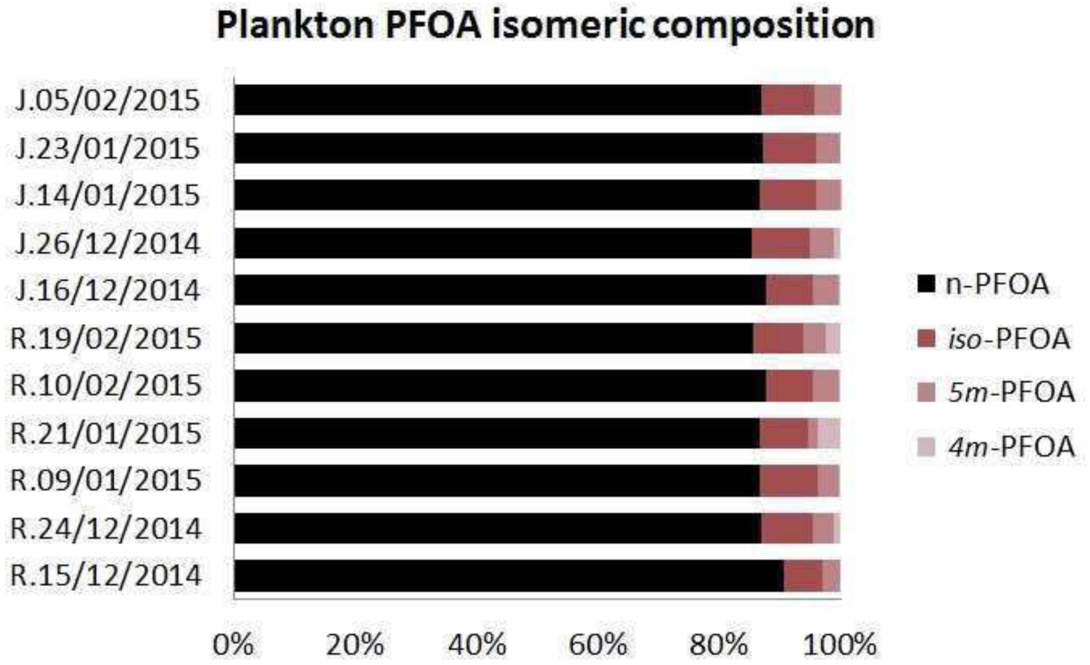

Figure S10. PFOA isomeric composition for the plankton samples. For sample code. refer to Table S5 legend.

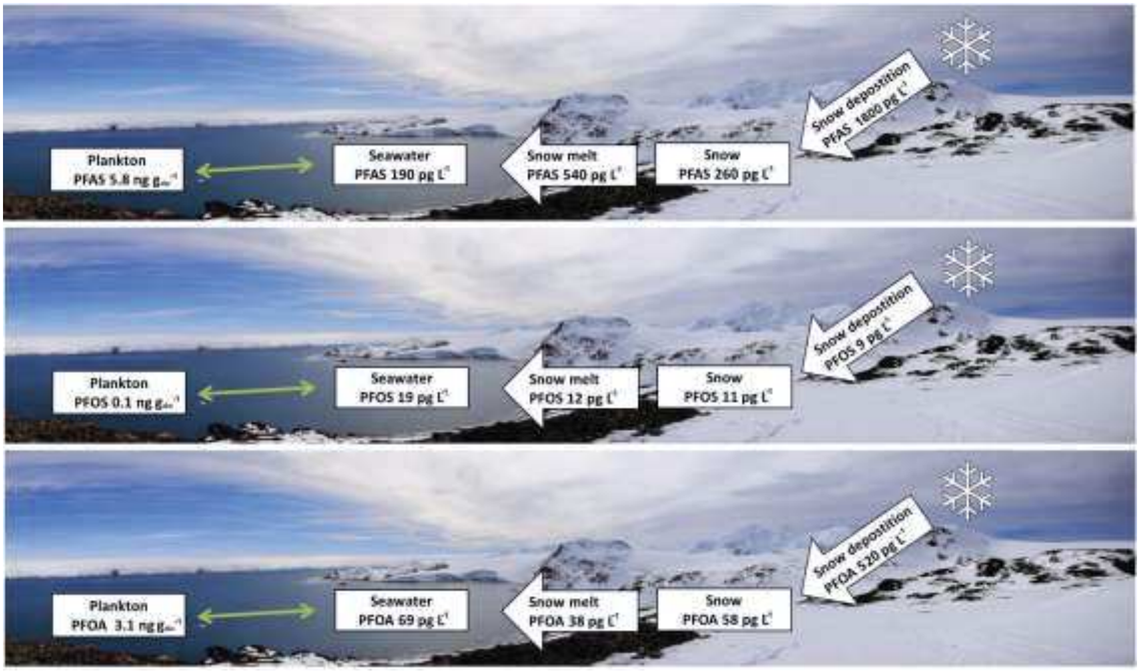

Figure S11. Diagram of ΣPFAS. PFOS and PFOA in snow deposition. surface snow. snowmelt. seawater and plankton phases. These schematics allow to see the differences in concentrations of PFAS from fresh snow deposition until PFAS reach coastal seawater in the maritime Antarctica.

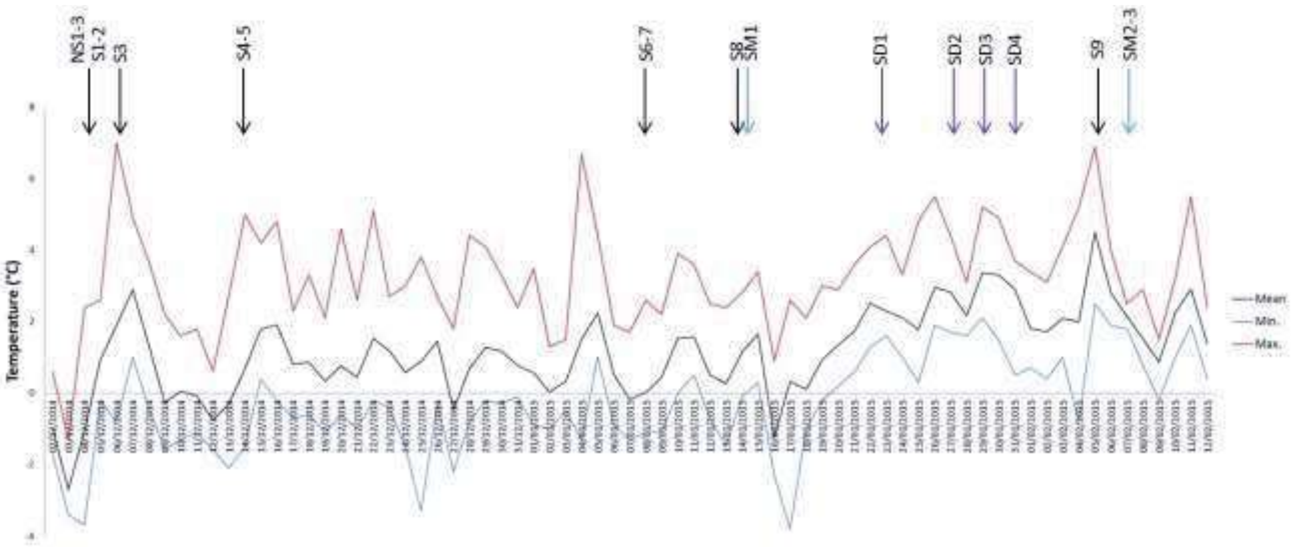

Figure S12. Daily mean, minimum and maximum temperatures (°C) during the sampling campaign

8.3 Capítol 4. Supporting Information

SUPPLEMENTARY MATERIAL

PIVOTAL ROLE OF SNOW DEPOSITION AND MELTING DRIVING FLUXES OF POLYCYCLIC AROMATIC HYDROCARBONS AT COASTAL LIVINGSTON ISLAND (ANTARCTICA)

Paulo Casal[1], Ana Cabrerizo[1], Maria Vila-Costa[1], Mariana Pizarro[1], Begoña Jiménez[2], Jordi Dachs[1]*

[1]Institute of Environmental Assessment and Water Research, Spanish National Research Council (IDAEA-CSIC), Barcelona, Catalonia 08034, Spain

[2]Department of Instrumental Analysis and Environmental Chemistry, Institute of Organic Chemistry, Spanish National Research Council (IQOG-CSIC), Madrid 28006, Spain.

This supplementary material contains 14 Tables and 5 Figures.

Table S1. Average surface (from 0.2 to 5 m depth) CTD data from the Raquelias and Johnson sampling sites.

Table S2. Surface seawater PAH concentrations (ng L^{-1}).

Table S3. Plankton PAH concentrations (ng g_{dw}^{-1}).

Table S4. Surface snow PAH concentrations (ng L^{-1}, water equivalent).

Table S5. Ambient air PAH concentrations (pg m^{-3}).

Table S6. PAH concentrations (pg m^{-3}) in the air equilibrated in-situ with the soil/snow surface PAHs concentrations (directly proportional to soil and snow fugacity).

Table S7. Ancillary data for the fugacity samples. Sample positions (F1-F5) are indicated in Figure 1.

Table S8. Air, snow, seawater and plankton phases surrogate recoveries.

Table S9. Soil/snow-air fugacity ratios for individual PAHs (Ln f_s/f_a ratios).

Table S10. Gross diffusive absorption fluxes of PAHs to coastal seawater (ng m^{-2} d^{-1}).

Table S11. Gross diffusive volatilization fluxes of PAHs from coastal seawater (ng m^{-2} d^{-1}).

Table S12. Net diffusive air-water exchange fluxes of PAHs (ng m^{-2} d^{-1}). Negative values mean net absorption fluxes.

Table S13. Correlations of PAHs diffusive net air-water fluxes with seawater temperature.

Table S14. Correlations of PAHs diffusive net air-water fluxes correlations with seawater salinity.

Figure S1. 4-5 ringed PAHs seawater concentrations (ng L^{-1}) at coastal Livingston Island, and ambient temperature during the austral summer.

Figure S2. Seawater nitrate vs temperature and salinity

Figure S3. Seawater phospate vs turbidity

Figure S4. Seawater ∑PAHs concentrations vs ammonia

Figure S5. Phenanthrene (Phe) and Fluorene (Flu) concentrations in plankton (ng g_{dw}^{-1}) versus plankton biomass (g L^{-1}).

Table S1. Average surface (from 0.2 to 5 m depth) CTD data from the Raquelias and Johnson sampling sites.

Date	Sampling station	Temperature (°C)	Salinity (PSU)	PAR	Fluorescence (RFU)	Turbidity (NTU)	Seawater and Plankton samples	NOxT ΣNO_3^- $+NO_2^-$ (µmol L^{-1})	NH_4^+ (µmol L^{-1})	PO_4^{3-} (µmol L^{-1})	Bacterial abundance (copies16S L^{-1})
15/12/2014	Raquelia	0.46	34.01	129.51	0.52	4.86	SW1-P1	29.129	1.342	2.029	2.08E+09
16/12/2014	Johnson	0.82	33.68	161.21	0.33	5.97	SW2-P2	24.839	3.771	1.742	3.54E+09
18/12/2014	Raquelia	0.70	33.81	207.84	0.68	5.50	SW3-P3	16.175	2.068	1.436	1.25E+09
23/12/2014	Johnson	1.24	33.70	203.10	0.50	3.90	SW4-P4	23.465	3.940	1.783	6.86E+09
24/12/2014	Raquelia	0.20	34.00	367.00	0.22	3.18	SW5-P5	24.018	4.681	1.646	6.60E+09
26/12/2014	Johnson	1.24	33.70	203.10	0.50	3.90	SW6-P6	18.490	12.602	1.456	5.09E+09
29/12/2014	Raquelia	0.48	33.99	295.60	0.41	3.59	SW7-P7	27.674	22.620	1.831	6.34E+09
31/12/2014	Johnson	1.33	33.84	431.20	0.28	3.92	SW8-P8	23.997	22.401	1.768	1.09E+10
02/01/2015	Johnson	1.52	33.77	294.90	0.25	2.65	SW9-P9	23.829	10.652	1.859	5.78E+08
05/01/2015	Raquelia	1.34	33.55	259.30	0.59	4.87	SW10-P10	15.386	22.747	1.350	8.08E+09
07/01/2015	Johnson	1.32	33.59	550.20	0.43	4.92	SW11-P11	17.270	22.483	1.639	5.73E+09
09/01/2015	Raquelia	1.12	33.95	126.04	0.57	2.27	SW12-P12	15.464	22.512	1.346	2.00E+10
12/01/2015	Raquelia	1.64	33.81	307.60	0.43	3.13	SW13-P13	21.490	7.954	1.613	1.23E+10
14/01/2015	Johnson	1.97	33.36	154.07	1.21	3.68	SW14-P14	14.870	21.409	1.359	1.42E+10
16/01/2015	Raquelia	1.26	33.91	68.30	1.91	3.02	SW15-P15	22.884	8.841	1.636	4.21E+09
19/01/2015	Johnson	1.23	33.69	176.72	1.01	5.95	SW16-P16	19.506	22.954	1.716	1.64E+10
21/01/2015	Raquelia	0.40	33.55	179.76	0.91	5.70	SW17-P17	25.825	22.636	1.813	5.90E+09
23/01/2015	Johnson	1.15	33.34	49.63	1.57	6.65	SW18-P18	21.415	1.657	1.746	7.27E+09
26/01/2015	Raquelia	1.55	33.55	81.98	1.12	5.79	SW19-P19	20.178	23.211	1.663	5.70E+09
29/01/2015	Johnson	1.51	33.29	29.67	1.63	10.55	SW20-P20	14.157	21.756	1.755	1.34E+09
02/02/2015	Raquelia	1.83	33.73	67.37	1.21	5.07	SW21-P21	12.001	22.768	1.715	1.15E+09
05/02/2015	Johnson	1.71	33.19	67.40	1.04	12.38	SW22-P22	18.363	8.589	1.870	1.33E+09
10/02/2015	Raquelia	1.66	33.58	46.30	1.62	7.24	SW23-P23	21.866	23.152	1.948	4.78E+10
12/02/2015	Johnson	1.83	33.33	42.01	1.52	10.46	SW24-P24	12.973	22.832	2.193	7.85E+09
16/02/2015	Raquelia	1.82	33.52	305.40	0.68	6.15	SW25-P25	23.917	22.861	1.958	2.98E+09
19/02/2015	Johnson	1.91	33.39	137.83	0.92	8.23	SW26-P26	20.656	14.476	2.109	1.29E+09

Table S2. Surface seawater PAH concentrations (ng L^{-1}).

PAH	SW1	SW2	SW3	SW4	SW5	SW6	SW7	SW8	SW9	SW10	SW11	SW12	SW13	SW14	SW15	SW16	SW17	SW18	SW19	SW20	SW21	SW22	SW23	SW24	SW25	SW26
Ace	0.011	0.011	0.003	0.017	0.010	0.058	0.036	0.004	0.031	0.026	0.003	0.005	0.005	0.004	0.024	0.012	0.058	0.012	0.007	0.014	0.005	0.031	0.022	0.022	0.011	0.018
Flu	0.022	<loq	<loq	<loq	<loq	0.017	0.018	<loq	0.015	0.020	<loq	<loq	<loq	0.014	<loq	0.015	<loq	0.020	<loq	0.028	0.015	0.018	<loq	0.020	0.016	<loq
Phe	0.26	<loq	0.093	<loq	<loq	0.11	<loq	0.098	0.12	0.11	<loq	0.093	<loq	0.12	0.093	0.15	0.10	0.23	<loq	0.24	0.28	0.24	0.17	0.21	0.20	0.11
ΣMP	<loq	<loq	<loq	<loq	<loq	<loq	<loq	0.14	0.12	0.12	0.11	0.11	<loq	0.12	<loq	0.32	<loq	<loq	<loq	0.42	0.61	0.44	0.32	0.45	0.40	<loq
ΣDMP	<loq	<loq	<loq	<loq	<loq	<loq	<loq	0.54	0.43	0.47	0.40	0.46	<loq	0.31	<loq	0.57	<loq	<loq	<loq	0.24	0.72	0.65	0.48	0.49	0.64	<loq
Ant	0.015	<loq	<loq	<loq	0.011	0.015	0.012	<loq	0.014	0.020	0.021	0.017	0.013	0.019	0.025	<loq	0.025	0.015	0.019	0.022	0.020	0.026	0.019	0.014	0.026	0.015
ΣMDBT	0.10	0.093	<loq	<loq	0.043	<loq	<loq	0.037	0.013	<loq	<loq	<loq	<loq	<loq	<loq	0.090	<loq	<loq	<loq	0.051	0.12	0.098	0.094	0.11	0.12	<loq
Flt	<loq	<loq	<loq	<loq	<loq	<loq	<loq	<loq	<loq	<loq	<loq	<loq	<loq	<loq	<loq	<loq	<loq	<loq	<loq	<loq	0.069	<loq	0.082	<loq	<loq	<loq
Pyr	0.054	<loq	<loq	<loq	<loq	<loq	<loq	0.058	0.050	0.052	0.065	0.078	<loq	0.060	<loq	0.068	<loq	<loq	<loq	0.065	0.16	0.094	0.21	0.087	0.086	<loq
ΣMPyr	0.021	0.013	0.013	0.004	0.020	0.024	0.015	0.14	0.097	0.10	0.12	0.12	0.023	0.12	0.022	0.13	0.042	0.027	0.019	0.050	0.15	0.14	0.13	0.15	0.16	0.018
ΣDMPyr	0.013	0.007	0.009	0.002	0.017	0.022	0.005	0.15	0.11	0.12	0.13	0.13	0.022	0.14	0.008	0.16	0.011	0.023	0.007	0.027	0.15	0.14	0.13	0.16	0.17	0.008
B[g,h,i]f	0.034	0.020	0.026	0.012	0.028	0.036	0.022	0.015	0.013	0.012	0.010	0.012	0.005	0.007	0.010	0.009	0.010	0.008	0.010	0.007	0.015	<loq	0.018	0.012	<loq	0.020
B[a]ant	0.004	<loq	0.003	<loq	0.004	0.003	0.003	0.010	0.006	0.009	0.008	0.007	<loq	0.007	<loq	0.009	<loq	0.006	0.004	0.002	0.010	0.008	0.006	0.010	0.009	<loq
Cry	0.014	0.010	0.009	0.006	0.018	0.019	0.010	0.15	0.097	0.10	0.11	0.12	0.012	0.13	0.010	0.14	0.016	0.018	0.010	0.016	0.11	0.11	0.11	0.14	0.15	0.008
ΣMCry	0.005	0.003	0.004	0.002	0.008	0.010	0.004	0.18	0.11	0.12	0.13	0.14	0.007	0.15	0.004	0.17	0.005	0.018	0.005	0.009	0.13	0.13	0.12	0.17	0.18	0.003
B[b]f	0.002	0.001	0.001	0.001	0.002	0.002	0.001	0.006	0.005	0.006	0.006	0.006	0.001	0.007	0.001	0.006	0.002	0.003	0.002	0.001	0.007	0.005	0.006	0.005	0.006	0.001
B[k]f	<loq	<loq	0.003	<loq	<loq	<loq	<loq	0.001	0.002	0.002	0.002	0.002	0.002	0.002	<loq	0.002	0.001	0.001	<loq	<loq	0.002	0.002	0.001	0.002	0.001	<loq
B[a]pyr	<loq	<loq	0.001	<loq	<loq	<loq	<loq	<loq	<loq	0.002	<loq	<loq	<loq	<loq	<loq	<loq	<loq	0.002	<loq	<loq	<loq	<loq	<loq	<loq	<loq	<loq
In[1,2,3-cd]pyr	<loq	<loq	0.025	<loq	0.026	0.021	<loq	0.019	0.018	<loq	0.052	0.028	<loq	0.023	0.051	<loq	0.060	<loq	<loq	<loq	<loq	<loq	0.019	0.038	0.031	0.018
Dib[a,h]ant	0.029	0.028	0.039	0.023	0.049	0.044	0.028	0.032	0.032	<loq	0.102	0.075	0.041	0.055	0.10	<loq	0.11	0.021	0.044	0.030	0.041	0.061	0.033	0.067	0.058	0.032
B[g,h,i]pery	0.012	<loq	0.009	<loq	0.009	0.013	0.006	0.020	0.019	0.009	0.024	0.023	0.018	0.027	0.015	0.006	0.011	0.009	0.016	0.021	0.026	0.026	0.022	0.011	0.040	0.009

Table S3. Plankton PAH concentrations (ng g_{dw}^{-1}).

PAH	P1	P2	P3	P4	P5	P6	P7	P8	P9	P10	P11	P12	P13	P14	P15	P16	P17	P18	P19	P20	P21	P22	P23	P24	P25	P26
Act	0.69	0.97	<loq	<loq	<loq	<loq	0.13	0.57	0.60	0.17	0.34	0.68	0.98	0.69	1.2	0.35	<loq	0.29	0.58	<loq	0.31	<loq	<loq	<loq	<loq	<loq
Ace	5.8	13	3.0	<loq	4.1	<loq	1.7	5.1	5.3	2.7	3.4	<loq	15	6.3	16	3.1	<loq	<loq	4.7	<loq	<loq	<loq	<loq	<loq	<loq	<loq
Flu	3.1	7.2	1.9	2.2	4.3	5.4	1.4	3.3	3.6	2.2	2.1	2.6	5.5	3.9	6.0	2.0	1.1	1.6	2.1	1.9	1.9	<loq	4.5	1.4	<loq	<loq
Phe	14	23	13	18	31	25	9.5	14	10	15	11	8.9	17	16	20	8.1	9.9	7.2	7.7	14	11	9.4	30	15	26	16
ΣMP	6.2	12	8.2	12	26	12	6.4	8.1	8.7	9.7	10	3.3	11	7.1	9.9	5.9	18	5.5	3.3	6.3	6.3	6.0	20	16	47	17
ΣDMP	4.8	8.2	7.2	8.3	20	10	7.6	5.4	8.6	10	11	2.7	9.6	6.0	7.6	4.9	28	5.9	2.6	4.5	5.3	4.3	16	13	42	14
Ant	1.5	1.3	0.57	0.16	1.3	1.8	0.78	1.7	1.0	1.0	0.98	0.09	1.6	1.0	1.5	0.45	0.40	0.19	0.74	1.6	1.0	1.1	1.1	0.43	0.02	<loq
DBT	0.34	1.3	<loq	0.50	0.27	2.4	1.4	0.95	1.2	3.6	1.3	0.43	2.3	0.74	2.2	1.8	1.3	0.58	1.0	0.88	0.95	0.85	2.1	0.85	1.2	2.0
ΣMDBT	<loq	<loq	2.3	1.1	1.2	1.9	1.1	0.90	0.94	6.2	1.6	<loq	2.9	<loq	2.1	3.1	1.6	0.18	0.74	0.33	0.34	0.17	2.3	0.93	1.4	1.7
ΣDMDBT	<loq	2.6	7.4	6.4	12	6.4	2.9	3.4	3.0	21	5.3	<loq	9.1	<loq	7.7	7.9	5.7	1.1	1.8	0.40	2.2	1.9	13	3.5	5.4	1.0
Flt	2.5	4.1	1.7	2.2	3.3	3.0	1.0	2.6	3.5	1.1	3.3	<loq	3.8	1.65	4.6	1.5	1.4	1.2	0.85	1.2	1.6	<loq	<loq	<loq	1.5	<loq
Pyr	3.4	4.7	3.0	2.9	6.4	6.7	2.3	2.8	5.3	4.1	4.5	1.8	4.7	2.8	4.7	2.3	4.4	3.1	2.5	3.2	2.8	2.1	4.7	2.4	4.4	2.4
ΣMPyr	1.3	0.95	0.46	0.80	1.2	0.67	2.2	0.70	1.2	0.99	2.1	0.69	1.5	0.80	1.4	0.80	5.8	0.98	0.45	0.83	1.2	0.93	3.5	0.78	4.4	0.58
ΣDMPyr	0.31	<loq	<loq	0.16	<loq	<loq	1.3	<loq	0.98	0.66	2.3	<loq	0.28	<loq	0.43	0.26	3.1	0.29	0.08	0.08	0.28	<loq	<loq	<loq	1.7	<loq
B[a]ant	2.7	4.3	2.1	2.7	2.6	4.9	0.76	3.3	2.6	0.76	1.2	5.2	2.6	4.5	2.0	1.3	1.3	2.4	1.7	3.8	2.6	5.4	9.5	2.3	1.8	5.2
Cry	2.5	2.3	1.1	1.3	0.99	1.8	2.6	1.3	2.4	0.87	3.1	0.85	2.3	1.4	2.5	0.86	3.3	1.1	0.98	0.59	1.3	0.84	1.8	1.6	5.7	2.2
B[b]f	1.3	2.4	0.92	1.6	1.2	3.1	0.49	1.2	1.0	0.35	0.37	1.6	0.82	1.6	0.66	0.43	0.54	0.85	0.70	1.32	0.85	1.9	2.6	0.99	0.77	2.7
B[k]f	1.9	1.1	0.96	<loq	<loq	<loq	0.44	<loq	0.54	0.19	0.91	<loq	0.50	<loq	0.88	0.27	0.54	<loq	<loq	<loq	0.37	<loq	<loq	<loq	<loq	<loq
Pery	4.3	<loq	<loq	<loq	<loq	8.2	2.2	<loq	4.6	1.7	<loq	5.8	<loq	<loq	1.7	2.1	2.5	4.3	3.3	5.5	3.7	6.1	10	3.0	3.3	<loq
In[1,2,3-cd]pyr	0.46	<loq	<loq	0.16	<loq	<loq	0.17	0.18	0.19	<loq	0.50	<loq	0.09	<loq	0.35	0.10	0.20	0.12	0.09	<loq	0.22	0.11	<loq	<loq	0.07	<loq
Dib[a,h]ant	<loq	<loq	<loq	<loq	<loq	<loq	<loq	<loq	<loq	<loq	0.08	<loq	<loq	<loq	<loq	<loq	<loq	<loq	<loq	<loq	0.05	<loq	<loq	<loq	<loq	<loq
B[g,h,i]pery	2.1	0.99	0.45	0.46	0.47	1.9	0.42	0.48	0.66	0.24	1.6	0.36	0.73	0.36	0.68	0.35	0.56	0.50	0.66	0.34	0.68	0.28	0.61	0.18	0.34	0.13
B[g,h,i]f	0.43	0.26	<loq	0.14	0.20	0.74	0.29	0.25	0.76	0.18	1.2	<loq	0.37	<loq	0.34	0.15	0.07	0.14	0.24	0.10	0.16	<loq	<loq	<loq	<loq	<loq
B[e]pyr	1.7	3.7	<loq	5.1	2.5	<loq	1.9	4.0	0.81	<loq	0.54	10	3.7	2.3	4.2	0.73	2.8	<loq	<loq	3.1	3.0	6.04	31	1.6	<loq	<loq

Table S4. Surface snow PAH concentrations (ng L^{-1}, water equivalent).

PAH	**S1**	**S2**	**S3**	**S4**	**S5**	**S6**	**S7**	**S8**	**S9**	**S10**
Act	0.031	<loq	0.023	0.040	0.19	0.045	0.022	0.14	0.027	0.050
Flu	0.032	0.031	0.093	0.052	0.17	0.075	0.14	0.17	0.063	0.084
Phe	0.71	0.21	0.78	0.70	1.8	0.69	1.6	1.3	0.60	0.75
ΣMP	0.59	<loq	0.55	<loq	1.3	0.35	1.0	0.79	0.64	0.45
ΣDMP	0.37	<loq	0.32	<loq	0.98	0.23	0.52	0.71	1.0	0.31
Ant	0.023	0.006	0.017	0.040	0.057	0.035	0.056	0.062	0.018	0.023
DBT	<loq	<loq	0.060	0.056	<loq	0.045	0.12	0.090	0.043	0.047
ΣMDBT	0.11	<loq	0.40	0.102	1.4	0.10	0.28	0.57	0.19	0.12
Flt	0.19	0.040	0.14	2.1	0.36	0.53	0.25	0.95	0.39	0.69
Pyr	0.14	0.041	0.099	2.7	0.26	2.2	0.15	3.4	1.5	2.9
ΣMPyr	0.035	0.008	0.023	0.081	0.085	0.046	0.039	0.10	0.20	0.043
ΣDMPyr	0.019	<loq	0.014	0.011	0.035	0.039	0.033	0.086	0.25	0.016
B[g,h,i]f	0.013	0.003	0.004	0.54	0.019	0.22	0.007	0.28	0.15	0.26
B[a]ant	0.005	0.005	0.005	<loq	0.020	<loq	0.005	<loq	<loq	<loq
Cry	0.018	0.004	0.015	0.012	0.044	0.022	0.029	0.061	0.18	0.018
ΣMCry	0.006	0.002	0.006	0.008	0.013	0.032	0.009	0.035	0.24	0.008
B[b]f	0.003	0.001	0.001	<loq	0.009	0.025	0.002	0.011	<loq	<loq
B[k]f	<loq	0.001	0.001	<loq	<loq	0.002	<loq	<loq	<loq	<loq
B[a]pyr	<loq	0.002	<loq	<loq	0.023	<loq	<loq	0.036	0.003	<loq
In[1,2,3-cd]pyr	0.024	0.014	0.015	0.014	0.039	0.045	0.028	0.10	0.071	0.070
Dib[a,h]ant	0.049	0.010	0.025	0.056	0.10	0.061	0.058	0.11	0.11	0.11
B[g,h,i]pery	0.025	0.010	0.006	<loq	0.039	0.087	0.010	0.18	0.063	0.084
Water vol.(L)	22.37	21.42	23.78	18.59	6.07	20	19.73	8	24.75	29.9
Snow density(%)	65	50	67	55.6	11	40	41	40	55	65

Table S5. Ambient air PAH concentrations (pg m^{-3}).

Sample	Act	Ace	Flu	Phe	ΣMP	ΣDMP	Ant	DBT	ΣMDBT	ΣDMDBT	Flt	Pyr	ΣMPyr	ΣDMPyr	B[a]ant	Cry	B[b]f
F1A1	0.17	2.4	12	26	24	11	0.47	0.61	0.77	5.6	5.6	4.2	0.77	0.42	1.1	0.65	<loq
F1A2	0.42	1.7	25	669	18	13	0.46	1.4	0.69	6.5	4.4	2.2	0.49	0.20	0.91	0.29	4.7
F1A3	6.8	<loq	12	69	44	76	<loq	<loq	0.29	230	18	1.2	0.51	0.44	3.0	0.88	13
F1A4	1.7	2.7	5.9	32	11	13	0.98	1.2	0.05	7.0	5.3	2.2	0.31	<loq	0.79	<loq	17
F1A6	<loq	0.54	2.0	17	6.5	6.1	0.24	0.29	0.36	3.4	2.4	1.7	0.94	2.2	0.88	<loq	<loq
F1A7	<loq	0.20	1.2	6.8	3.1	2.5	<loq	<loq	0.10	1.4	0.82	0.45	0.12	0.40	0.82	<loq	<loq
F1A8	2.3	0.70	2.2	19	4.9	3.5	0.35	0.32	0.28	3.2	24	15	0.87	1.5	1.0	0.61	<loq
F1A9	<loq	0.48	2.2	9.5	6.0	3.9	<loq	0.28	0.21	1.8	1.3	0.71	0.11	0.25	0.84	0.16	12
F1A10	<loq	<loq	1.5	7.9	2.4	2.8	0.26	0.22	0.11	1.4	1.0	0.69	<loq	0.21	6.92	<loq	6.6
F1A11	<loq	0.33	1.9	8.6	8.5	2.9	0.17	0.17	0.24	1.7	1.2	0.62	<loq	0.22	0.89	<loq	1.4
F2A1	<loq	5.0	22	91	220	260	2.2	3.2	0.65	47	27	3.2	1.6	0.53	0.96	0.52	<loq
F2A2	1.0	10	27	140	130	61	14	4.6	<loq	74	20	6.9	0.77	5.0	3.3	1.9	14
F2A3	0.21	1.4	11	74	71	40	2.6	1.4	1.1	11	14	8.2	2.9	0.25	0.80	0.92	8.5
F2A4	0.88	6.6	15	53	41	25	1.0	1.1	0.47	8.7	5.9	2.6	2.8	3.3	0.90	0.42	7.2
F2A6	3.8	28	14	44	22	15	2.4	<loq	<loq	13	7.7	1.1	<loq	5.8	0.44	<loq	<loq
F2A7	8.0	4.7	13	43	48	29	1.5	1.3	0.57	11	7.1	4.6	2.2	4.1	0.96	0.57	<loq
F2A8	0.22	4.3	18	38	37	20	1.3	0.93	0.79	10	5.6	4.0	1.7	3.2	1.1	0.21	<loq
F2A9	0.65	5.6	16	41	30	17	1.7	0.93	0.61	8.3	3.6	2.1	2.6	1.9	1.0	0.22	<loq
F2A10	0.72	9.0	24	46	19	15	1.3	1.0	0.44	5.8	28	18	1.2	0.22	0.87	0.39	<loq
F2A11	0.29	5.4	22	50	45	23	1.7	1.4	1.1	9.1	9.1	5.9	0.63	0.56	0.88	0.18	<loq
F3A1	3.7	10	33	90	140	82	3.0	4.0	2.2	26	17	9.6	2.3	0.37	1.2	0.65	<loq
F3A2	5.9	4.3	13	53	58	33	2.4	1.8	0.96	11	7.4	4.5	1.7	0.24	1.0	0.52	5.0
F3A3	0.77	0.86	10	52	22	15	2.4	0.58	0.23	3.9	23	9.7	0.64	<loq	0.84	0.24	5.0
F3A4	0.49	<loq	3.1	14	10	6.4	<loq	0.36	0.11	1.9	3.7	1.6	0.48	0.51	0.85	0.17	8.1
F3A5	<loq	1.8	5.1	32	12	7.2	0.84	0.59	0.32	5.6	3.8	2.3	2.1	4.5	0.92	<loq	4.8

F3A6	2.3	4.1	11	70	55	34	2.3	1.7	0.78	21	4.8	2.6	6.3	12	1.3	<loq	<loq
F3A7	1.4	1.8	5.6	21	17	15	0.71	0.92	0.41	5.2	3.6	2.3	0.57	0.81	1.0	0.23	<loq
F3A8	6.2	2.7	17	77	42	24	4.3	1.5	0.68	8.3	120	87	1.7	1.6	1.2	1.3	<loq
F3A9	0.37	1.4	9.2	25	30	18	0.62	1.3	0.67	5.7	3.8	2.8	0.33	0.30	0.83	0.17	<loq
F3A10	<loq	2.6	6.8	23	35	14	<loq	<loq	<loq	<loq	5.2	0.70	<loq	<loq	0.82	<loq	<loq
F3A11	0.93	3.6	10	27	41	24	0.79	1.2	0.55	7.5	3.7	2.2	0.22	0.26	0.95	<loq	<loq
F4A1	0.12	1.1	27	47	39	24	3.3	1.5	0.22	2.0	18	10	1.4	0.20	0.83	0.16	<loq
F5A1	0.76	2.3	48	670	61	31	7.6	2.6	0.50	5.4	18	14	2.7	0.18	1.2	0.36	<loq
F4A2	0.83	1.4	2.6	5.7	1.9	1.0	<loq	0.24	0.07	0.51	1.8	1.0	0.28	0.20	0.87	0.12	4.6
F5A2	0.33	1.2	16	73	20	8.4	1.7	1.8	<loq	6.4	4.9	1.5	0.28	0.15	1.2	0.36	5.1
F4A3	0.37	0.32	1.5	7.8	2.0	2.0	0.27	0.18	0.07	0.63	19	11	0.74	0.14	0.62	0.25	3.5
F5A3	<loq	0.54	5.0	19	5.3	2.1	<loq	0.46	0.25	1.9	0.90	0.43	<loq	0.12	0.74	0.11	4.4
F4A4	0.45	0.78	1.3	15	1.9	2.1	0.58	0.24	<loq	2.6	0.44	0.29	2.4	5.2	1.0	0.13	7.6
F5A4	0.51	0.42	3.2	34	5.3	4.4	1.2	0.50	0.05	6.3	1.7	0.79	3.2	6.6	1.5	0.34	9.4
F4A5	0.13	1.1	2.4	18	2.3	3.5	0.38	0.31	0.11	3.0	1.7	0.97	1.4	3.0	1.3	0.49	5.9
F5A5	<loq	2.4	2.2	8.8	1.8	2.9	0.44	0.24	0.01	1.2	1.6	0.79	0.19	0.25	1.1	0.10	5.7
F4A6	<loq	0.51	2.2	9.2	1.2	10	<loq	1.0	<loq	9.1	0.91	0.37	0.40	0.85	0.82	<loq	<loq
F5A6	<loq	0.65	5.0	29	8.8	7.3	0.82	0.48	0.29	6.6	2.6	1.6	2.2	5.0	0.85	<loq	<loq
F4A7	<loq	1.3	3.0	180	68	33	10	1.4	<loq	53	8.2	1.6	7.1	19	2.0	<loq	<loq
F5A7	0.64	1.8	5.0	53	18	13	2.2	0.70	0.51	17	5.4	2.8	5.3	13	1.2	<loq	0.47
F4A8	0.99	1.6	5.6	8.9	2.6	2.9	0.37	0.30	0.17	1.7	1.4	0.89	<loq	0.18	0.95	0.29	6.3
F5A8	<loq	0.58	10	44	23	7.2	0.76	0.96	1.4	7.6	5.2	3.1	0.16	0.30	1.0	0.34	3.5
F4A9	3.9	2.9	5.6	8.9	5.4	5.6	0.98	0.29	0.07	1.1	2.2	1.3	0.18	0.21	0.80	0.15	3.7
F5A9	3.8	3.2	11	23	9.0	7.2	2.2	0.35	0.37	3.0	5.8	3.6	<loq	0.27	1.4	0.37	2.3
F4A10	3.1	0.38	8.7	13	2.5	<loq	0.69	0.44	<loq	<loq	3.3	2.2	<loq	0.37	1.6	<loq	1.8
F5A10	<loq	<loq	6.7	35	12	18	2.2	0.94	<loq	178	20	7.1	<loq	<loq	1.1	<loq	<loq

Table S6. PAH concentrations (pg m^{-3}) in the air equilibrated in-situ with the soil/snow surface PAHs concentrations (directly proportional to soil and snow fugacity).

Sample	Act	Ace	Flu	Phe	ΣMP	ΣDMP	Ant	DBT	ΣMDBT	ΣDMDBT	Flt	Pyr	ΣMPyr	ΣDMPyr	B[a]ant	Cry	B[b]f
F1S1	1.5	11	250	2300	1100	4000	260	26	21	150	270	170	11	0.97	1.3	1.2	<loq
F1S2	0.80	12	270	3500	1200	430	400	33	24	160	340	210	19	1.2	1.1	0.88	4.7
F1S3	1.4	9.2	260	3200	1200	520	340	26	20	170	400	220	21	1.5	1.2	1.1	5.7
F1S4	1.3	3.4	78	1100	390	160	100	10	2.8	40	120	64	5.2	0.47	2.7	0.69	11
F1S5	0.54	5.0	180	3700	1500	640	300	29	20	210	520	260	26	6.1	0.85	1.0	6.8
F1S6	0.33	6.5	210	3800	2100	930	380	35	36	240	770	460	30	3.1	0.85	1.9	<loq
F1S7	0.32	3.2	120	1900	1200	580	220	15	19	180	490	250	17	1.9	0.85	1.6	<loq
F1S8	3.2	11	270	3100	1700	710	300	27	36	220	560	380	25	3.6	0.77	1.9	<loq
F1S9	0.16	5.1	180	2100	860	340	160	17	18	110	230	160	13	2.0	0.72	1.7	<loq
F1S10	0.12	0.58	62	860	370	170	38	7.0	6.5	53	120	74	6.4	1.8	0.89	0.84	<loq
F1S11	0.55	2.9	160	1900	870	310	180	20	12	110	250	120	6.8	0.79	0.89	0.72	<loq
F2S1	0.55	13	21	88	120	67	1.4	2.4	2.2	25	12	7.0	1.1	0.30	0.85	0.21	<loq
F2S2	1.1	8.7	28	90	85	50	2.8	2.6	1.5	20	7.6	4.7	4.8	6.1	1.1	0.76	4.6
F2S3	<loq	2.7	18	130	190	87	2.7	1.7	0.87	130	33	7.5	3.1	1.2	3.9	0.10	<loq
F2S4	1.1	5.8	19	71	56	20	1.4	1.6	1.2	13	6.7	3.4	0.40	0.77	0.82	0.21	7.2
F2S5	<loq	3.6	19	100	77	52	1.8	2.7	1.0	33	9.9	4.6	27	6.8	8.2	<loq	6.5
F2S6	<loq	16	32	99	68	26	1.9	1.7	1.9	27	8.8	4.4	3.5	11	0.96	<loq	<loq
F2S7	2.2	62	21	68	64	24	2.0	2.1	1.8	20	8.6	4.4	0.45	1.1	0.94	0.29	<loq
F2S8	0.41	5.9	25	70	68	24	2.4	1.8	2.9	25	10	6.6	1.1	1.9	0.96	0.14	<loq
F2S9	0.47	6.9	27	66	50	17	1.7	1.7	2.0	16	5.8	3.2	0.20	0.23	0.90	0.11	<loq
F2S11	13	<loq	41	280	190	160	9.1	<loq	0.46	97	340	8.7	<loq	0.42	0.86	<loq	<loq
F3S1	2.4	8.5	22	57	78	54	2.4	2.2	0.87	14	30	13	3.0	0.74	1.4	0.69	<loq
F3S2	1.8	5.1	11	42	38	23	0.93	1.6	0.67	7.4	4.9	2.8	1.1	0.23	0.95	0.26	<loq
F3S3	1.1	0.73	7.4	48	21	34	2.8	<loq	<loq	13	31	9.1	0.56	0.58	1.5	0.68	<loq

F3S4	0.82	1.4	5.2	17	8.9	6.8	0.30	0.68	0.18	2.1	4.1	2.4	0.48	0.59	1.0	0.41	10
F3S5	<loq	<loq	4.3	24	1.0	<loq	<loq	<loq	<loq	<loq	<loq	33	<loq	<loq	<loq	<loq	<loq
F3S6	<loq	4.0	4.3	130	24	48	6.9	16	1.5	320	6.5	1.2	5.0	11	1.4	<loq	<loq
F3S7	2.8	2.9	4.4	16	4.8	4.9	0.21	0.40	<loq	3.7	1.7	0.93	0.44	1.3	1.0	<loq	<loq
F3S8	6.4	4.1	20	60	39	20	6.0	1.3	0.46	7.2	40	18	1.4	0.34	0.95	0.34	<loq
F3S9	0.40	1.1	8.0	24	35	19	0.65	1.2	0.43	5.8	4.4	2.7	0.48	0.34	0.83	0.28	0.31
F3S10	1.2	2.3	5.9	18	18	9.6	0.39	0.80	0.22	3.8	2.8	1.8	0.14	0.20	0.95	0.21	2.4
F3S11	1.4	5.2	14	22	24	14	0.46	1.5	0.29	4.1	2.7	1.8	0.20	0.18	0.98	0.14	0.24
F4S1	<loq	2.0	19	34	32	18	1.8	0.82	0.29	2.3	8.0	3.5	0.31	0.14	0.80	0.17	<loq
F5S1	0.38	4.0	44	83	55	19	4.6	2.3	0.54	4.9	9.1	5.6	0.84	0.33	1.3	0.18	7.4
F4S2	0.30	2.9	5.6	14	3.5	6.7	0.23	0.31	0.07	1.6	1.7	0.99	0.66	0.20	0.85	0.18	<loq
F5S2	0.25	1.6	5.7	26	11	4.7	<loq	0.44	0.35	2.5	2.7	1.3	0.10	0.22	0.97	0.12	<loq
F4S3	6.8	2.0	5.7	17	4.7	5.5	2.6	1.0	<loq	4.0	33	6.0	0.65	0.34	0.59	0.30	7.9
F5S3	<loq	0.56	1.9	9.9	4.9	2.9	<loq	0.32	<loq	1.7	1.4	0.65	<loq	0.16	0.73	0.11	5.3
F4S4	0.78	0.91	3.3	16	2.8	3.8	0.27	0.37	0.10	2.0	1.1	0.74	1.3	2.5	1.1	0.30	9.9
F4S5	<loq	1.1	2.2	11	2.7	1.4	<loq	0.15	0.09	1.4	1.1	0.57	0.49	0.99	0.97	0.08	4.6
F5S5	<loq	3.6	5.8	19	9.8	2.9	<loq	0.97	0.21	1.9	8.6	4.4	0.36	0.23	1.3	0.20	6.5
F4S6	<loq	1.1	3.7	8.2	2.5	2.0	0.34	0.18	0.10	0.89	1.1	0.60	<loq	0.15	0.69	<loq	<loq
F5S6	0.32	1.9	9.3	30	15	12	<loq	0.47	0.31	3.7	3.7	1.9	<loq	0.37	1.3	<loq	<loq
F4S7	<loq	1.8	5.2	51	13	8.9	2.6	0.64	0.17	16	2.5	1.4	5.9	15	1.4	<loq	1.7
F5S7	<loq	2.2	5.8	33	10	13	1.5	1.3	0.78	13	3.3	2.1	4.5	10	1.7	<loq	10
F4S8	0.27	0.88	4.0	8.1	4.6	2.1	0.43	0.23	0.14	0.85	1.1	0.74	<loq	0.19	0.95	<loq	2.3
F5S8	0.46	1.4	4.8	23	19	10	0.66	0.72	0.42	5.7	11	5.1	<loq	0.21	1.0	0.33	12
F4S9	3.6	2.7	8.0	11	4.3	2.7	0.88	0.18	0.10	0.96	6.3	4.0	0.18	0.23	0.86	0.15	5.4
F5S9	0.44	1.3	3.4	9.8	5.5	3.4	0.20	0.20	0.21	2.3	1.9	1.3	<loq	0.23	1.1	<loq	38
F4S10	2.8	3.8	20	110	90	60	26	4.1	12	45	35	29	4.9	15	0.51	2.2	<loq
F5S10	<loq	0.59	8.6	23	14	6.1	0.36	0.39	0.20	5.5	5.9	2.8	0.14	0.33	0.93	0.12	3.1

Table S7. Ancillary data for the fugacity samples. Sample positions (F1-F5) is indicated in Figure 1.

Sampling start	Sampling End	Samples	mean T.(°C)	min. T.(°C)	max. T.(°C)	Surface
03/12/14	09/12/14	F1-1	0.4	-3.7	7	Soil with vegetation
09/12/14	16/12/14	F1-2	0.4	-2.1	5	Soil with vegetation
16/12/14	22/12/14	F1-3	1.0	-1.1	5.1	Soil with vegetation
22/12/14	29/12/14	F1-4	0.9	-3.3	5.1	Soil with vegetation
29/12/14	05/01/15	F1-5	1.0	-1.3	6.7	Soil with vegetation
05/01/15	12/01/15	F1-6	0.8	-1.3	4.4	Soil with vegetation
12/01/15	19/01/15	F1-7	0.5	-3.8	3.4	Soil with vegetation
19/01/15	26/01/15	F1-8	2.0	-0.2	5.5	Soil with vegetation
26/01/15	02/02/15	F1-9	2.6	0.4	5.5	Soil with vegetation
02/02/15	09/02/15	F1-10	2.2	-0.8	6.9	Soil with vegetation
09/02/15	16/02/15	F1-11	2.1	-0.2	5.5	Soil with vegetation
02/12/14	09/12/14	F2-1	0.3	-3.7	7	Snow
09/12/14	16/12/14	F2-2	0.4	-2.1	5	Snow
16/12/14	23/12/14	F2-3	1.0	-1.1	5.1	Snow
23/12/14	30/12/14	F2-4	0.8	-3.3	4.4	Snow
30/12/14	06/01/15	F2-5	0.9	-1.3	6.7	Snow
06/01/15	13/01/15	F2-6	0.6	-1.5	3.9	Snow
13/01/15	20/01/15	F2-7	0.6	-3.8	3.4	Snow
20/01/15	27/01/15	F2-8	2.2	0.2	5.5	Bare soil
27/01/15	03/02/15	F2-9	2.5	0.4	5.2	Bare soil
03/02/15	10/02/15	F2-10	2.3	-0.8	6.9	Bare soil
10/02/15	17/02/15	F2-11	2.3	0.4	5.5	Bare soil
03/12/14	10/12/14	F3-1	0.4	-3.7	7	Snow
10/12/14	17/12/14	F3-2	0.5	-2.1	5	Snow
17/12/14	24/12/14	F3-3	0.8	-1.5	5.1	Snow
24/12/14	31/12/14	F3-4	0.8	-3.3	4.4	Snow
31/12/14	07/01/15	F3-5	0.7	-1.3	6.7	Snow
07/01/15	14/01/15	F3-6	0.7	-1.5	3.9	Snow
14/01/15	21/01/15	F3-7	0.7	-3.8	3.6	Bare soil
21/01/15	28/01/15	F3-8	2.3	0.3	5.5	Bare soil
28/01/15	04/02/15	F3-9	2.4	-0.8	5.2	Bare soil
04/02/15	11/02/15	F3-10	2.4	-0.8	6.9	Bare soil
11/02/15	18/02/15	F3-11	2.4	0.4	5.5	Bare soil
05/12/14	12/12/14	F4-1	0.8	-1.6	7	Snow
12/12/14	19/12/14	F4-2	0.7	-2.1	5	Snow
19/12/14	28/12/14	F4-3	0.7	-3.3	5.1	Snow
28/12/14	02/01/15	F4-4	0.7	-1	4.4	Snow
02/01/15	09/01/15	F4-5	0.6	-1.3	6.7	Snow
09/01/15	17/01/15	F4-6	0.7	-3.8	3.9	Snow
17/01/15	23/01/15	F4-7	1.3	-3.8	4.4	Snow
23/01/15	30/01/15	F4-8	2.6	0.3	5.5	Snow
30/01/15	06/02/15	F4-9	2.6	-0.8	6.9	Snow
06/02/15	13/02/15	F4-10	2.0	-0.2	5.5	Snow
05/12/14	12/12/14	F5-1	0.8	-1.6	7	Snow
12/12/14	19/12/14	F5-2	0.7	-2.1	5	Snow
19/12/14	28/12/14	F5-3	0.7	-3.3	5.1	Snow
28/12/14	02/01/15	F5-4	0.7	-1	4.4	Snow
02/01/15	09/01/15	F5-5	0.6	-1.3	6.7	Snow
09/01/15	17/01/15	F5-6	0.7	-3.8	3.9	Snow
17/01/15	23/01/15	F5-7	1.3	-3.8	4.4	Snow
23/01/15	30/01/15	F5-8	2.6	0.3	5.5	Snow
30/01/15	06/02/15	F5-9	2.6	-0.8	6.9	Snow
06/02/15	13/02/15	F5-10	2.0	-0.2	5.5	Snow

Table S8. Air, snow, seawater and plankton phases surrogate recoveries.

Surrogate	Air	Snow	Seawater	Plankton
acenaphthene-d10	52±24%	74±7.7%	63±9.5%	65±18%
phenanthrene-d10	70±29%	72±8.1%	96±17%	72±12%
crysene-d12	110±35%	100±8.9%	85±25%	85±14%
perylene-d12	110±50%	120±30%	100±17%	100±25%

Table S9. Soil/snow-air fugacity ratios for individual PAHs (Ln f_s/f_a ratios).

Ln f_s/f_a	**Act**	**Ace**	**Flu**	**Phe**	**ΣMP**	**ΣDMP**	**Ant**	**DBT**	**ΣMDBT**	**ΣDMDBT**	**Flt**	**Pyr**	**ΣMPyr**	**ΣDMPyr**	**B[a]ant**	**Cry**	**B[b]f**
F2-1		0.91	-0.03	-0.03	-0.57	-1.37	-0.45	-0.29	1.23	-0.62	-0.79	0.77	-0.37	-0.57	-0.13	-0.89	
F2-2	0.05	-0.15	0.03	-0.45	-0.44	-0.20	-1.62	-0.56		-1.29	-0.99	-0.39	1.84	0.18	-1.10	-0.91	
F2-3		0.65	0.55	0.57	1.00	0.79	0.06	0.15	-0.24	2.49	0.87	-0.09	0.06	1.57	1.59	-2.22	-0.58
F2-4	0.25	-0.12	0.22	0.29	0.31	-0.22	0.32	0.36	0.96	0.41	0.13	0.25	-1.95	-1.46	-0.09	-0.69	0.00
F2-6		-0.55	0.80	0.80	1.12	0.55	-0.22			0.73	0.13	1.38		0.62	0.77		
F2-7	-1.31	2.56	0.45	0.46	0.28	-0.19	0.26	0.47	1.17	0.61	0.20	-0.03	-1.60	-1.33	-0.02	-0.67	
F2-8	0.63	0.31	0.36	0.62	0.61	0.16	0.63	0.66	1.30	0.92	0.59	0.49	-0.48	-0.50	-0.12	-0.41	
F2-9	-0.31	0.21	0.49	0.46	0.51	-0.04	-0.02	0.61	1.18	0.68	0.48	0.43	-2.57	-2.09	-0.15	-0.72	
F2-11	3.79		0.62	1.72	1.41	1.93	1.68		-0.87	2.37	3.64	0.39		-0.31	-0.02		
F3-1	-0.45	-0.18	-0.42	-0.46	-0.59	-0.42	-0.26	-0.59	-0.91	-0.61	0.56	0.30	0.25	0.68	0.15	0.06	
F3-2	-1.22	0.17	-0.12	-0.24	-0.43	-0.37	-0.94	-0.14	-0.36	-0.38	-0.41	-0.46	-0.45	-0.05	-0.07	-0.68	
F3-3	0.32	-0.15	-0.35	-0.07	-0.08	0.83	0.16			1.22	0.30	-0.06	-0.13		0.60	1.03	
F3-4	0.51		0.52	0.22	-0.12	0.07		0.63	0.47	0.08	0.09	0.39	0.00	0.14	0.20	0.86	0.25
F3-5			-0.17	-0.30	-2.52							2.64					
F3-6		-0.04	-0.98	0.64	-0.80	0.35	1.08	2.26	0.63	2.74	0.30	-0.76	-0.24	-0.07	0.05		
F3-7	0.68	0.45	-0.23	-0.31	-1.26	-1.11	-1.23	-0.83		-0.35	-0.77	-0.90	-0.26	0.51	0.01		
F3-8	0.02	0.39	0.19	-0.24	-0.07	-0.15	0.34	-0.16	-0.40	-0.15	-1.06	-1.56	-0.20	-1.56	-0.24	-1.33	
F3-9	0.09	-0.20	-0.14	-0.03	0.15	0.10	0.05	-0.03	-0.44	0.01	0.14	-0.03	0.37	0.13	-0.01	0.53	
F3-10		-0.12	-0.14	-0.22	-0.65	-0.40					-0.62	0.94			0.14		
F3-11	0.40	0.38	0.31	-0.21	-0.54	-0.54	-0.55	0.19	-0.62	-0.59	-0.32	-0.20	-0.09	-0.33	0.03		
F1-1	2.19	1.54	3.08	4.49	3.84	3.63	6.34	3.74	3.32	3.27	3.88	3.68	2.64	0.84	0.18	0.59	
F1-2	0.65	1.96	2.41	3.96	4.21	3.52	6.78	3.20	3.55	3.20	4.34	4.56	3.67	1.79	0.22	1.09	-0.01
F1-3	-1.55		3.05	3.83	3.30	1.92			4.25	-0.32	3.08	5.23	3.71	1.21	-0.92	0.26	-0.83
F1-4	-0.26	0.23	2.58	3.56	3.53	2.53	4.67	2.09	4.13	1.73	3.14	3.35	2.83		1.23		-0.39
F1-6		2.48	4.69	5.41	5.80	5.03	7.39	4.78	4.63	4.25	5.77	5.57	3.45	0.36	-0.03		

F1-7		2.75	4.62	5.66	5.92	5.47			5.27	4.81	6.39	6.32	4.92	1.55	0.04		
F1-8	0.32	2.73	4.83	5.12	5.85	5.31	6.76	4.44	4.85	4.24	3.15	3.25	3.36	0.84	-0.30	1.16	
F1-9		2.36	4.40	5.38	4.97	4.47		4.13	4.47	4.14	5.19	5.40	4.82	2.06	-0.16	2.35	
F1-10			3.72	4.69	5.03	4.13	5.00	3.47	4.08	3.67	4.75	4.68		2.17	-0.04		
F1-11		2.15	4.43	5.41	4.63	4.70	6.95	4.76	3.86	4.21	5.38	5.28		1.29	-0.01		
F4-1		0.63	-0.33	-0.31	-0.22	-0.29	-0.61	-0.63	0.28	0.13	-0.79	-1.06	-1.50	-0.36	-0.03	0.02	
F5-1	-0.70	0.55	-0.09	0.21	-0.10	-0.47	-0.49	-0.13	0.07	-0.09	-0.68	-0.93	-1.17	0.64	0.06	-0.72	
F4-2	-1.01	0.71	0.76	0.88	0.61	1.89		0.25	-0.10	1.16	-0.04	-0.04	0.84	0.01	-0.03	0.44	
F5-2	-0.29	0.26	-1.05	-1.04	-0.60	-0.58		-1.43		-0.93	-0.60	-0.14	-1.02	0.37	-0.23	-1.13	
F4-3	2.90	1.82	1.33	0.78	0.85	0.99	2.28	1.71		1.84	0.56	-0.57	-0.12	0.87	-0.04	0.21	0.80
F5-3		0.04	-0.95	-0.65	-0.06	0.34		-0.37		-0.11	0.46	0.41		0.29	-0.02	-0.01	0.18
F4-4	0.54	0.15	0.94	0.06	0.37	0.58	-0.76	0.44		-0.24	0.95	0.94	-0.63	-0.72	0.12	0.82	0.26
F4-5		0.04	-0.08	-0.51	0.15	-0.91		-0.71	-0.23	-0.76	-0.42	-0.53	-1.09	-1.11	-0.32	-1.76	-0.25
F5-5		0.39	0.98	0.78	1.68	0.00		1.40	3.03	0.42	1.71	1.71	0.66	-0.09	0.14	0.65	0.13
F4-6		0.74	0.50	-0.11	0.73	-1.64		-1.70		-2.32	0.17	0.48		-1.72	-0.17		
F5-6		1.06	0.62	0.04	0.55	0.45		-0.01	0.05	-0.59	0.34	0.21		-2.61	0.47		
F4-7		0.28	0.56	-1.24	-1.65	-1.30	-1.38	-0.76		-1.22	-1.17	-0.11	-0.19	-0.22	-0.37		
F5-7		0.21	0.15	-0.49	-0.59	-0.02	-0.41	0.64	0.43	-0.27	-0.51	-0.28	-0.17	-0.22	0.37		3.06
F4-8	-1.31	-0.58	-0.33	-0.09	0.57	-0.33	0.15	-0.26	-0.22	-0.72	-0.25	-0.18		0.03	0.00		-1.01
F5-8		0.91	-0.73	-0.65	-0.23	0.37	-0.15	-0.28	-1.23	-0.30	0.74	0.50		-0.39	-0.04	-0.02	1.23
F4-9	-0.09	-0.08	0.35	0.18	-0.24	-0.73	-0.11	-0.46	0.39	-0.12	1.03	1.12	-0.01	0.10	0.07	-0.03	0.38
F5-9	-2.16	-0.87	-1.15	-0.83	-0.49	-0.75	-2.40	-0.57	-0.57	-0.26	-1.14	-1.03		-0.15	-0.23		2.80
F4-10	-0.12	2.30	0.83	2.15	3.58		3.61	2.23			2.37	2.60		3.71	-1.14		
F5-10			0.25	-0.43	0.14	-1.08	-1.82	-0.88		-1.10	-1.19	-0.92			-0.22		

Table S10. Gross diffusive absorption fluxes of PAHs to coastal seawater (ng m^{-2} d^{-1}).

PAH	SW1	SW2	SW3	SW4	SW5	SW6	SW7	SW8	SW9	SW10	SW11	SW12	SW13	SW14	SW15	SW16	SW17	SW18	SW19	SW20	SW21	SW22	SW23	SW24	SW25	SW26
Ace	-1.2	-0.38	-1.6	-0.87	-0.12	-0.069	-0.045	-0.037	-0.040	-0.037				-0.26	-0.53	-0.37	-0.30	-0.91	-0.71	-0.45	-0.37	-0.61	-0.12	-0.034	-0.092	-0.062
Flu	-1.1	-0.61		-5.1	-0.77	-1.5	-1.0	-0.53	-0.57	-0.53	-1.1	-0.22	-0.33	-1.2	-2.3	-1.6	-0.65	-1.9	-1.5	-2.5	-2.1	-3.4	-3.1	-0.91	-2.1	-1.4
Phe	-20	-14	-15	-32	-6.6	-13	-9.3	-3.2	-3.4	-3.2	-9.6	-2.4	-3.4	-8.0	-14	-11	-3.6	-8.7	-7.1	-12	-10	-15	-10	-3.8	-6.7	-4.9
ΣMP	-28	-17		-25	-4.1	-7.2	-4.8	-1.6	-1.7	-1.6	-2.9	-0.58	-0.88	-3.8	-7.2	-5.2	-2.51	-6.9	-5.5	-6.3	-5.3	-8.3	-7.6	-2.4	-3.9	-2.7
ΣDMP	-31	-29		-13	-2.1	-4.4	-3.0	-1.0	-1.1	-1.0	-1.7	-0.35	-0.53	-2.5	-4.8	-3.4	-1.8	-4.9	-3.9	-3.7	-3.1	-4.8	-4.6	-1.4	-2.2	-1.5
Ant	-1.1	-1.5	-1.8	-2.5	-0.45	-0.46	-0.32	-0.081	-0.087	-0.082	-0.23	-0.051	-0.075	-0.29	-0.53	-0.39	-0.11	-0.27	-0.22	-0.52	-0.44	-0.68	-0.34	-0.11	-0.23	-0.16
Flt				-5.0	-1.2	-4.4	-3.2	-0.57	-0.60	-0.57	-1.2	-0.36	-0.49	-1.0	-1.7	-1.3	-0.74	-1.6	-1.4	-15	-13	-18	-1.3	-0.53	-3.7	-2.8
Pyr	-12	-8.9		-2.2	-0.59	-2.3	-1.7	-0.29	-0.30	-0.29	-0.80	-0.26	-0.35	-0.34	-0.55	-0.43	-0.54	-1.1	-0.93	-12	-10	-14	-0.90	-0.39	-2.3	-1.8
ΣMPyr	-20	-16	-3.4	-0.46	-0.13	-0.45	-0.34	-0.22	-0.23	-0.22	-0.72	-0.23	-0.31	-1.2	-1.9	-1.5	-0.22	-0.45	-0.38	-0.45	-0.40	-0.55	-0.54	-0.23	-0.30	-0.23
ΣDMPyr	-22	-17	-1.5	-1.0	-0.27	-0.064	-0.048	-0.26	-0.27	-0.26	-1.5	-0.49	-0.67	-1.7	-2.6	-2.1	-0.38	-0.78	-0.66	-0.62	-0.55	-0.76	-0.40	-0.17	-0.054	-0.042
B[a]ant	-1.7	-1.4		-0.87	-0.32	-0.24	-0.19	-0.16	-0.16	-0.16	-0.34	-0.14	-0.17	-0.20	-0.29	-0.24	-0.19	-0.34	-0.30	-0.34	-0.30	-0.40	-0.37	-0.19	-0.25	-0.19
Cry	-30	-28	-2.0	-0.50	-0.22	-0.18	-0.15	-0.061	-0.062	-0.061							-0.091	-0.15	-0.13	-0.24	-0.22	-0.27	-0.078	-0.044	-0.12	-0.099
B[b]f	-1.0	-1.1	-0.22	-3.9	-1.7	-2.0	-1.6	-1.6	-1.6	-1.6	-1.8	-0.89	-1.0													
ΣPAHs	-170	-140	-26	-93	-19	-36	-26	-9.6	-10	-9.7	-22	-6.0	-8.3	-20	-37	-27	-11	-28	-23	-54	-46	-68	-30	-10	-22	-16

Table S11. Gross diffusive volatilization fluxes of PAHs from coastal seawater (ng m^{-2} d^{-1}).

PAH	**SW1**	**SW2**	**SW3**	**SW4**	**SW5**	**SW6**	**SW7**	**SW8**	**SW9**	**SW10**	**SW11**	**SW12**	**SW13**	**SW14**	**SW15**	**SW16**	**SW17**	**SW18**	**SW19**	**SW20**	**SW21**	**SW22**	**SW23**	**SW24**	**SW25**	**SW26**
Ace	0.60	0.40	0.29	4.6	0.38	8.5	3.5	0.23	1.8	1.5	0.78	0.18	0.34	0.39	4.3	1.6	4.3	2.6	1.2	2.3	0.69	7.0	6.1	1.7	1.6	1.9
Flu	1.1					2.2	1.6		0.83	1.1				1.2		1.7		4.0		4.3	1.8	3.6		1.5	2.2	
Phe	10		5.5			9.9		3.9	4.9	4.5		2.8		6.9	9.6	12	5.4	29		25	24	30	26	11	19	7.3
ΣMP								6.7	6.2	5.9	18	4.0		9.1		32				55	66	75	67	29	48	
ΣDMP								27	23	23	72	17		23		60				33	82	110	100	33	80	
Ant	0.64				0.33	1.5	0.87		0.66	0.89	3.1	0.57	0.64	1.3	3.0		1.5	2.3	2.3	2.6	2.0	3.9	3.5	0.8	2.8	1.1
Flt																					4.167		8.139			
Pyr	1.4							1.5	1.4	1.4	4.3	1.7		2.1		3.1				3.7	8.3	6.4	17	3.0	4.6	
ΣMPyr	0.54	0.25	0.49	0.33	0.40	1.2	0.55	3.7	2.7	2.7	8.2	2.6	0.66	4.5	1.3	6.1	1.4	1.8	1.1	2.8	7.4	9.4	10	5.1	8.3	0.75
ΣDMPyr	0.33	0.13	0.33	0.18	0.33	1.1	0.21	4.0	3.0	3.1	8.8	2.7	0.63	4.9	0.44	7.0	0.35	1.6	0.38	1.5	7.7	9.4	10	5.7	8.9	0.33
B[a]ant	0.036		0.036		0.037	0.049	0.036	0.11	0.066	0.097	0.18	0.067		0.095		0.14		0.14	0.082	0.052	0.18	0.20	0.17	0.14	0.19	
Cry	0.021	0.013	0.017	0.021	0.026	0.046	0.021	0.24	0.16	0.16	0.32	0.17	0.019	0.24	0.026	0.31	0.034	0.064	0.031	0.050	0.31	0.41	0.42	0.32	0.46	0.020
B[b]f	0.003	0.001	0.003	0.002	0.004	0.006	0.003	0.011	0.011	0.012	0.021	0.009	0.002	0.015	0.004	0.015	0.005	0.009	0.005	0.004	0.018	0.018	0.022	0.011	0.019	0.002
ΣPAHs	15	0.80	6.7	5.1	1.5	25	6.8	47	45	44	120	31	2.3	54	19	120	13	41	5.1	130	200	260	250	91	180	11

Table S12. Net diffusive air-water exchange fluxes of PAHs (ng m^{-2} d^{-1}). Negative values mean net absorption fluxes.

PAH	SW1	SW2	SW3	SW4	SW5	SW6	SW7	SW8	SW9	SW10	SW11	SW12	SW13	SW14	SW15	SW16	SW17	SW18	SW19	SW20	SW21	SW22	SW23	SW24	SW25	SW26
Ace	-0.55	0.015	-1.3	3.7	0.25	8.4	3.4	0.20	1.8	1.4	0.78	0.18	0.34	0.13	3.8	1.2	4.0	1.7	0.52	1.8	0.32	6.4	5.9	1.7	1.5	1.8
Flu	-0.044	-0.61		-5.1	-0.77	0.66	0.60	-0.53	0.27	0.52	-1.1	-0.22	-0.33	-0.012	-2.3	0.094	-0.65	2.1	-1.5	1.8	-0.27	0.25	-3.1	0.55	0.11	-1.4
Phe	-9.7	-14	-9.7	-32	-6.6	-3.3	-9.3	0.71	1.6	1.3	-9.6	0.47	-3.4	-1.1	-4.6	1.1	1.8	20	-7.1	13	14	15	16	7.5	12	2.4
ΣMP	-28	-17		-25	-4.1	-7.2	-4.8	5.1	4.5	4.3	16	3.4	-0.88	5.4	-7.2	27	-2.5	-6.9	-5.5	49	61	66	60	27	44	-2.7
ΣDMP	-31	-29		-13	-2.1	-4.4	-3.0	26	22	22	70	16	-0.53	21	-4.8	57	-1.8	-4.9	-3.9	30	79	110	100	31	78	-1.5
Ant	-0.44	-1.5	-1.8	-2.5	-0.12	1.1	0.55	-0.081	0.57	0.81	2.9	0.52	0.56	1.0	2.5	-0.39	1.4	2.0	2.1	2.1	1.6	3.3	3.2	0.72	2.6	0.96
Flt				-5.0	-1.3	-4.4	-3.2	-0.57	-0.60	-0.57	-1.2	-0.36	-0.49	-1.0	-1.7	-1.3	-0.74	-1.6	-1.4	-15	-8.6	-18	6.8	-0.53	-3.7	-2.8
Pyr	-10	-8.9		-2.2	-0.59	-2.3	-1.7	1.2	1.1	1.1	3.5	1.4	-0.35	1.8	-0.55	2.7	-0.54	-1.1	-0.93	-8.2	-2.2	-8.0	16	2.6	2.2	-1.8
ΣMPyr	-19	-16	-2.9	-0.13	0.28	0.75	0.2	3.4	2.5	2.5	7.4	2.3	0.35	3.3	-0.59	4.6	1.2	1.4	0.71	2.4	7.0	8.8	9.6	4.9	8.0	0.51
ΣDMPyr	-22	-17	-1.1	-0.82	0.063	1.0	0.16	3.8	2.8	2.8	7.3	2.2	-0.032	3.2	-2.2	4.9	-0.029	0.80	-0.28	0.90	7.1	8.6	9.8	5.5	8.8	0.29
B[a]ant	-1.7	-1.4	0.036	-0.87	-0.28	-0.19	-0.15	-0.049	-0.095	-0.059	-0.15	-0.076	-0.17	-0.10	-0.29	-0.098	-0.19	-0.20	-0.21	-0.28	-0.12	-0.20	-0.20	-0.051	-0.051	-0.19
Cry	-30	-28	-2.0	-0.48	-0.19	-0.13	-0.13	0.18	0.095	0.10	0.32	0.17	0.019	0.24	0.026	0.31	-0.057	-0.083	-0.099	-0.19	0.092	0.13	0.34	0.28	0.34	-0.080
B[b]f	-1.0	-1.1	-0.22	-3.9	-1.7	-2.0	-1.6	-1.6	-1.6	-1.6	-1.79	-0.88	-1.0	0.015	0.004	0.015	0.005	0.009	0.005	0.004	0.018	0.018	0.022	0.011	0.019	0.002
ΣPAHs	-150	-130	-19	-87	-17	-12	-19	38	34	35	94	25	-6.0	34	-18	97	1.9	13	-18	76.	159	190	220	81	150	-4.6

Table S13. Correlations of PAHs diffusive net air-water fluxes with seawater temperature.

Spearman's rho	**Volatilization Fluxes**	**Net Air-water exchange Fluxes**
ΣPAHs	0.535**	0.593**
Act		
Flu		
Phe		0.517**
ΣMP		0.600**
ΣDMP	0.564**	0.594**
Ant		0.511**
Flt		
Pyr	0.521**	
ΣMPyr	0.595**	0.605**
ΣDMPyr	0.567**	0.579**
B[a]ant	0.632**	
Cry	0.488*	0.562**
B[b]f	0.434*	0.494*

**. Correlation is significant at the 0.01 level (2-tailed).

*. Correlation is significant at the 0.05 level (2-tailed).

Table S14. Correlations of PAHs diffusive net air-water fluxes correlations with seawater salinity.

Spearman's rho	**Volatilization Fluxes**	**Net Air-water exchange Fluxes**
ΣPAHs	-0.460*	-0.504**
Act		
Flu	-0.555*	
Phe	-0.537*	-0.595**
ΣMP		-0.445*
ΣDMP		
Ant	-0.516*	-0.563**
Flt		
Pyr		
ΣMPyr	-0.496*	-0.520*
ΣDMPyr	-0.392*	-0.430*
B[a]ant	-0.579**	
Cry	-0.419*	
B[b]f		-0.516**

**. Correlation is significant at the 0.01 level (2-tailed).

*. Correlation is significant at the 0.05 level (2-tailed

Figure S1. 4-5 ringed PAHs seawater concentrations (ng) at coastal Livingston Island, and ambient temperature during the austral summer.

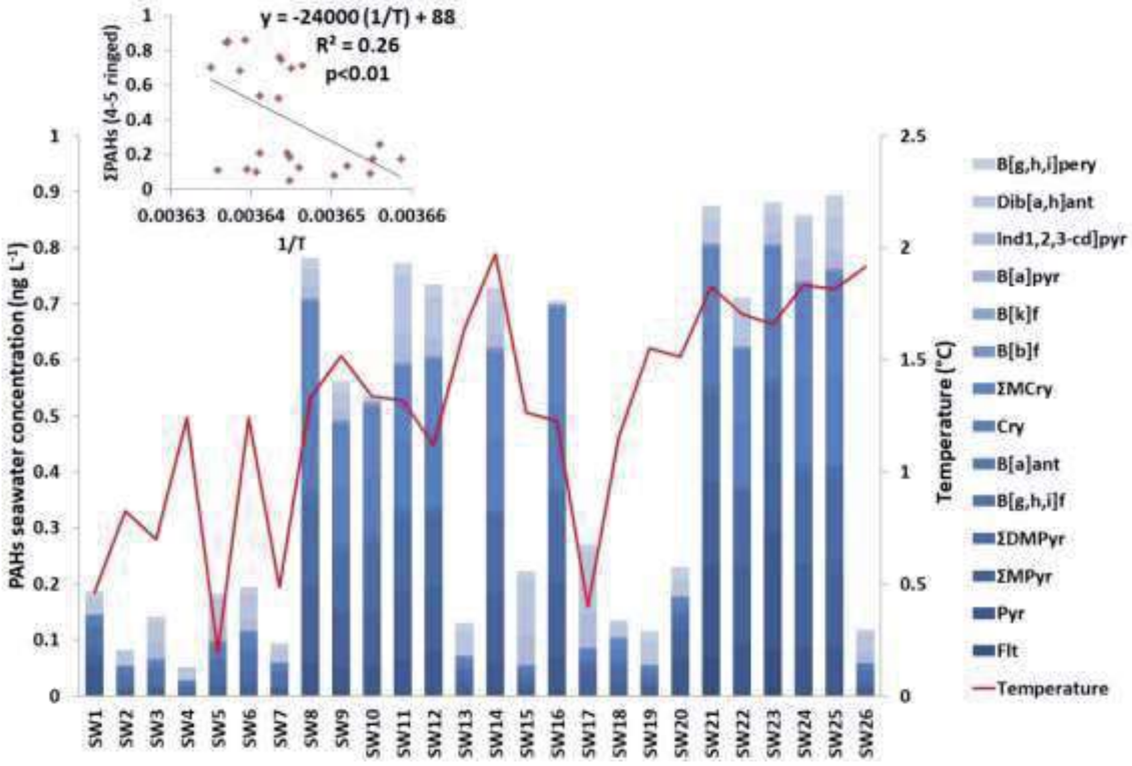

Figure S2. Seawater nitrate vs temperature and salinity

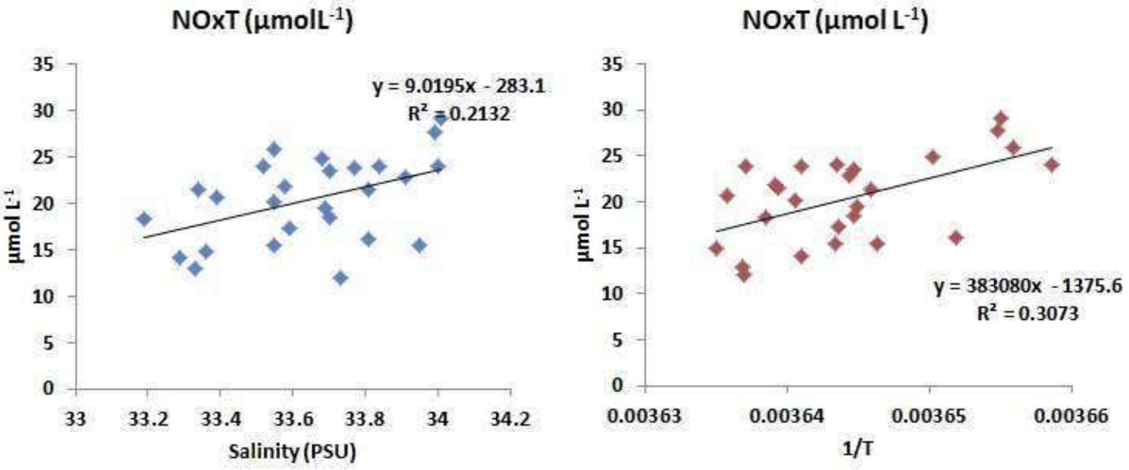

Figure S3. Seawater phospate vs turbidity

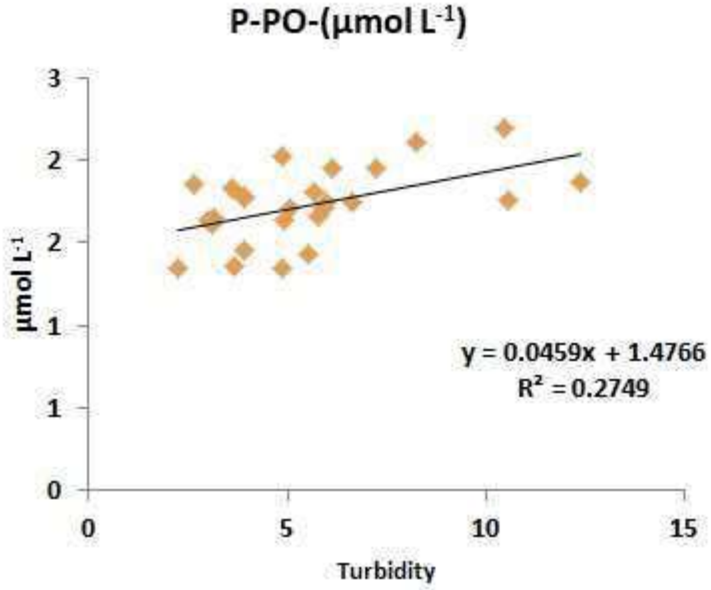

Figure S4. Seawater ∑PAHs concentrations vs ammonium and nitrate

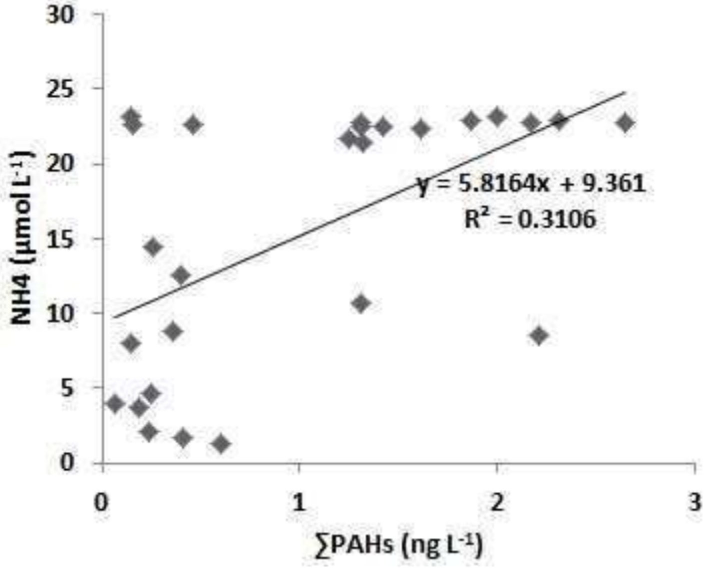

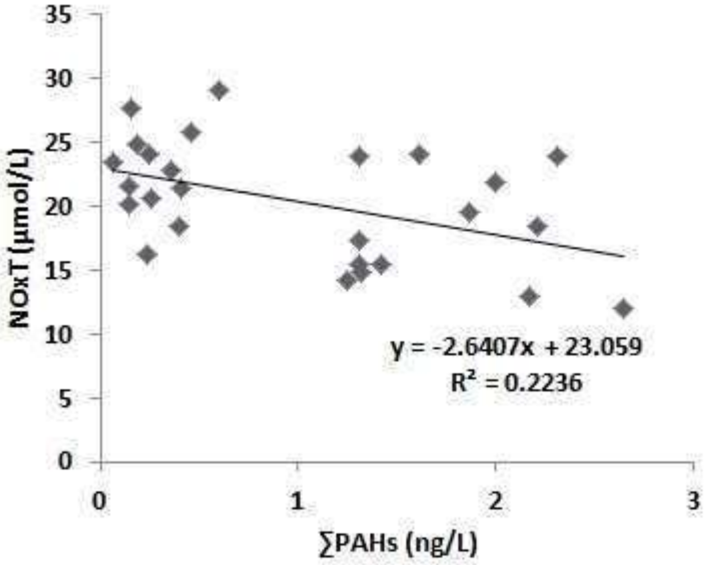

Figure S5. Phenanthrene (Phe) and Fluorene (Flu) concentrations in plankton (ng g_{dw}^{-1}) versus plankton biomass (g L^{-1}).

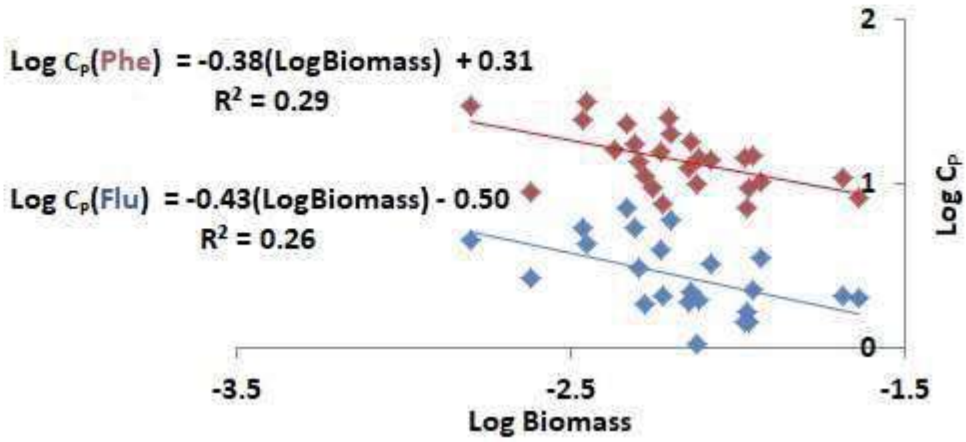

8.4 Capítol 5. Supporting Information

SUPPLEMENTARY INFORMATION

Snow Deposition Enhances the Net Volatilization of Polychlorinated Biphenyls and Organochlorine Pesticides from Antarctic Coastal Soils and Waters

Paulo Casal[1], Ana Cabrerizo[1], Maria Vila-Costa[1], Mariana Pizarro[1], Begoña Jiménez[2], Jordi Dachs[1]*

[1]Institute of Environmental Assessment and Water Research, Spanish National Research Council (IDAEA-CSIC), Barcelona, Catalonia 08034, Spain

[2]Department of Instrumental Analysis and Environmental Chemistry, Institute of Organic Chemistry, Spanish National Research Council (IQOG-CSIC), Madrid 28006, Spain

Figure S1. PCB-149 and PCB-187 ambient air and air equilibrated in-situ with soil/snow correlations with temperature

Figure S2. PCBs Ln f_s/f_a ratios versus Log K_{OA} bare soil and soil with vegetation

Figure S3. HCB Ln f_s/f_a ratios versus Log K_{OA}

Text S1. Air-snow gas exchange flux calculations

The exchange velocity (m d^{-1}) was calculated following Hansen et al. (2006)

$$v^{-1} = (v_{air})^{-1} + (v_{snow}K_{SA})^{-1}$$

The air side exchange velocity is calculated by:

$$v_{air} = k^2 U \left(\ln\left(\frac{Z_W}{Z_0}\right) \ln\left(\frac{Z_{ref}}{Z_0}\right) \right)^{-1}$$

where k is von Karman’s constant (0.4), U is the wind speed, Z_W is the height of the wind (10 m), Z_{ref} is the reference height (2 m), and Z_0 is the surface roughness for snow (0.001 m). v_{snow} is given by the snow diffusion coefficient, D_{snow}, divided by half the thickness of the snowpack, which represents the average diffusion path given the evolution of the snowpack depth over the course of a winter season. D_{snow} is calculated as follows:

$$D_{snow} = D_{air}(1 - \frac{\rho_{snow}}{\rho_{ice}})^{1.5}$$

where D_{air} is the air diffusion coefficient, calculated acording to Schwarzenbach et al. (2005), ρ_{snow} is the sample snow density and ρ_{ice} is the ice density (0.917 g cm^{-3}).

Table S1. Average surface (at 0.2 to 5 m depth) CTD data from the Raquelia and Johnson sampling sites.

Date	**Sampling station**	**Temperature (°C)**	**Salinity (PSU)**	**PAR**	**Fluorescence (RFU)**	**Turbidity (NTU)**	**Seawater and Plankton samples**	**$\sum NO_x$ (µmol L^{-1})**	**NH_4^+ (µmol L^{-1})**	**PO_4^{3-} (µmol L^{-1})**
15/12/2014	Raquelia	0.46	34.01	129.51	0.52	4.86	SW1-P1	29.129	1.342	2.029
16/12/2014	Johnson	0.82	33.68	161.21	0.33	5.97	SW2-P2	24.839	3.771	1.742
18/12/2014	Raquelia	0.70	33.81	207.84	0.68	5.50	SW3-P3	16.175	2.068	1.436
23/12/2014	Johnson	1.24	33.70	203.10	0.50	3.90	SW4-P4	23.465	3.940	1.783
24/12/2014	Raquelia	0.20	34.00	367.00	0.22	3.18	SW5-P5	24.018	4.681	1.646
26/12/2014	Johnson	1.24	33.70	203.10	0.50	3.90	SW6-P6	18.490	12.602	1.456
29/12/2014	Raquelia	0.48	33.99	295.60	0.41	3.59	SW7-P7	27.674	22.620	1.831
31/12/2014	Johnson	1.33	33.84	431.20	0.28	3.92	SW8-P8	23.997	22.401	1.768
02/01/2015	Johnson	1.52	33.77	294.90	0.25	2.65	SW9-P9	23.829	10.652	1.859
05/01/2015	Raquelia	1.34	33.55	259.30	0.59	4.87	SW10-P10	15.386	22.747	1.350
07/01/2015	Johnson	1.32	33.59	550.20	0.43	4.92	SW11-P11	17.270	22.483	1.639
09/01/2015	Raquelia	1.12	33.95	126.04	0.57	2.27	SW12-P12	15.464	22.512	1.346
12/01/2015	Raquelia	1.64	33.81	307.60	0.43	3.13	SW13-P13	21.490	7.954	1.613
14/01/2015	Johnson	1.97	33.36	154.07	1.21	3.68	SW14-P14	14.870	21.409	1.359
16/01/2015	Raquelia	1.26	33.91	68.30	1.91	3.02	SW15-P15	22.884	8.841	1.636
19/01/2015	Johnson	1.23	33.69	176.72	1.01	5.95	SW16-P16	19.506	22.954	1.716
21/01/2015	Raquelia	0.40	33.55	179.76	0.91	5.70	SW17-P17	25.825	22.636	1.813
23/01/2015	Johnson	1.15	33.34	49.63	1.57	6.65	SW18-P18	21.415	1.657	1.746
26/01/2015	Raquelia	1.55	33.55	81.98	1.12	5.79	SW19-P19	20.178	23.211	1.663
29/01/2015	Johnson	1.51	33.29	29.67	1.63	10.55	SW20-P20	14.157	21.756	1.755
02/02/2015	Raquelia	1.83	33.73	67.37	1.21	5.07	SW21-P21	12.001	22.768	1.715
05/02/2015	Johnson	1.71	33.19	67.40	1.04	12.38	SW22-P22	18.363	8.589	1.870
10/02/2015	Raquelia	1.66	33.58	46.30	1.62	7.24	SW23-P23	21.866	23.152	1.948
12/02/2015	Johnson	1.83	33.33	42.01	1.52	10.46	SW24-P24	12.973	22.832	2.193
16/02/2015	Raquelia	1.82	33.52	305.40	0.68	6.15	SW25-P25	23.917	22.861	1.958
19/02/2015	Johnson	1.91	33.39	137.83	0.92	8.23	SW26-P26	20.656	14.476	2.109

Table S2. PCBs and OCPs surface seawater concentrations (pg L^{-1})

pg L^{-1}	SW1	SW2	SW3	SW4	SW5	SW6	SW7	SW8	SW9	SW10	SW11	SW12	SW13	SW14	SW15	SW16	SW17	SW18	SW19	SW20	SW21	SW22	SW23	SW24	SW25	SW26
∑OCPs	2.5	0.6	4.6	6.4	3.0	3.4	2.4	2.0	1.9	2.3	2.4	3.4	3.5	0.8	3.6	2.3	17.1	3.5	5.0	2.6	6.2	4.1	4.4	6.5	2.2	2.5
HCB	2.5	<LOQ	2.8	1.7	1.9	2.8	1.9	2.0	1.9	1.9	1.6	2.0	2.0	<LOQ	2.8	1.8	10.4	2.2	3.6	2.2	1.7	3.0	3.4	3.3	2.2	2.1
∑HCHs		0.6	1.9	4.7	1.1	0.6	0.6			0.4	0.8	1.3	1.6	0.8	0.8	0.5	6.6	1.3	1.5	0.4	4.5	1.1	1.0	3.2		0.4
a-HCH	<LOQ	<LOQ	<LOQ	0.5	0.3	<LOQ	<LOQ	<LOQ	<LOQ	<LOQ	<LOQ	<LOQ	<LOQ	<LOQ	<LOQ	<LOQ	0.7	<LOQ	0.5	<LOQ	<LOQ	<LOQ	<LOQ	<LOQ	<LOQ	<LOQ
b-HCH	<LOQ	<LOQ	0.9	0.5	<LOQ	<LOQ	0.6	<LOQ	<LOQ	<LOQ	<LOQ	<LOQ	<LOQ	<LOQ	<LOQ	<LOQ	1.1	<LOQ	<LOQ	<LOQ	<LOQ	<LOQ	<LOQ	0.7	<LOQ	<LOQ
g-HCH	<LOQ	0.6	0.6	3.7	<LOQ	<LOQ	<LOQ	<LOQ	<LOQ	0.4	0.8	0.9	0.9	0.8	<LOQ	0.5	1.4	0.8	1.0	0.4	4.5	<LOQ	1.0	0.7	<LOQ	0.4
d-HCH	<LOQ	<LOQ	0.5	<LOQ	0.8	0.6	<LOQ	<LOQ	<LOQ	<LOQ	<LOQ	0.5	0.7	<LOQ	0.8	<LOQ	3.5	0.5	<LOQ	<LOQ	<LOQ	1.1	<LOQ	1.8	<LOQ	<LOQ
∑PCBs	34.3	13.6	117.5	31.3	71.8	68.7	48.0	71.0	41.5	29.8	61.4	62.6	50.5	35.6	60.0	47.6	109.4	56.0	109.4	42.6	57.5	93.8	50.4	72.4	59.0	35.8
PCB18	<LOQ	<LOQ	0.1	<LOQ	<LOQ	0.5	<LOQ	0.2	<LOQ	<LOQ	0.5	<LOQ	1.0	<LOQ	1.0	0.7	1.2	<LOQ	<LOQ	<LOQ	7.6	0.9	1.1	4.2	<LOQ	1.0
PCB17	<LOQ	<LOQ	0.7	4.2	0.6	0.3	0.2	0.2	0.1	0.2	0.8	1.2	0.7	1.6	2.1	1.8	3.3	0.9	1.4	0.7	0.8	3.3	0.9	6.5	1.0	0.7
PCB31+28	<LOQ	<LOQ	1.7	<LOQ	<LOQ	<LOQ	<LOQ	<LOQ	<LOQ	<LOQ	<LOQ	<LOQ	<LOQ	<LOQ	1.0	<LOQ	2.7	1.5	2.2	<LOQ	1.3	2.1	<LOQ	1.6	1.3	<LOQ
PCB33	<LOQ	<LOQ	0.6	<LOQ	0.4	0.3	<LOQ	<LOQ	<LOQ	<LOQ	0.4	0.5	0.4	0.4	0.5	0.3	15.3	1.6	0.9	1.0	1.1	0.5	0.8	<LOQ	<LOQ	<LOQ
PCB52	2.8	0.6	7.0	2.1	3.0	3.5	2.6	2.4	3.2	3.1	3.8	3.3	2.6	2.0	3.7	3.6	4.5	7.3	16.8	15.3	5.5	5.1	4.7	6.1	4.9	2.9
PCB49	0.3	<LOQ	1.0	<LOQ	0.7	0.7	<LOQ	<LOQ	<LOQ	<LOQ	<LOQ	<LOQ	<LOQ	<LOQ	<LOQ	<LOQ	5.3	<LOQ	0.9	0.5	0.7	0.6	<LOQ	0.6	0.6	<LOQ
PCB44	<LOQ	<LOQ	<LOQ	0.3	0.8	0.6	0.3	0.3	0.2	<LOQ	0.4	0.4	0.4	0.1	0.4	0.3	<LOQ	0.2	15.3	0.2	0.6	0.4	0.3	0.3	0.5	0.2
PCB74	<LOQ	<LOQ	0.9	<LOQ	0.4	0.5	<LOQ	<LOQ	0.4	<LOQ	<LOQ	0.4	<LOQ	<LOQ	<LOQ	<LOQ	<LOQ	0.5	0.8	<LOQ	<LOQ	<LOQ	<LOQ	<LOQ	<LOQ	<LOQ
PCB70	0.8	<LOQ	2.3	<LOQ	1.5	1.6	0.8	1.0	0.8	0.5	1.1	1.1	1.1	0.5	0.9	0.7	1.0	1.1	2.4	0.5	1.0	1.2	0.7	0.8	0.9	0.6
PCB95	<LOQ	<LOQ	6.5	<LOQ	3.2	3.4	1.8	2.7	1.5	0.8	3.2	2.9	2.4	1.6	3.0	1.9	2.9	1.4	3.0	1.1	1.7	3.4	1.4	2.5	2.2	1.2
PCB99+101	10.6	4.1	23.0	7.5	13.3	14.9	10.0	13.2	10.1	7.2	11.4	10.5	9.1	6.5	10.7	8.4	12.9	6.3	9.9	5.8	6.7	12.4	6.8	9.1	8.9	6.9
PCB87	<LOQ	<LOQ	1.3	<LOQ	0.9	1.0	<LOQ	<LOQ	<LOQ	<LOQ	<LOQ	<LOQ	<LOQ	<LOQ	<LOQ	<LOQ	<LOQ	<LOQ	<LOQ	<LOQ	<LOQ	<LOQ	<LOQ	<LOQ	<LOQ	<LOQ
PCB110	<LOQ	<LOQ	2.2	<LOQ	1.5	1.3	0.7	1.0	0.5	0.2	1.3	1.1	0.9	0.6	1.1	0.8	1.6	0.7	1.1	0.5	0.7	1.2	0.5	0.9	1.0	0.5
PCB82	<LOQ	<LOQ	1.4	<LOQ	0.6	0.6	<LOQ	0.6	<LOQ	<LOQ	0.8	0.8	0.6	<LOQ	0.7	<LOQ	1.0	<LOQ	0.8	<LOQ	<LOQ	0.9	<LOQ	0.6	0.6	<LOQ
PCB151	2.1	1.1	6.5	1.5	4.2	4.2	2.8	4.6	2.2	1.6	3.4	3.3	2.5	2.1	3.8	2.6	4.5	2.4	3.9	1.7	2.3	5.6	2.9	3.7	3.5	2.3
PCB149	3.5	2.2	18.0	3.8	11.1	10.2	7.2	12.0	5.5	3.5	9.7	10.4	7.2	6.3	9.3	7.4	15.2	7.6	11.7	4.8	7.3	15.0	8.2	10.7	9.6	5.6
PCB118	<LOQ	<LOQ	2.7	<LOQ	1.5	1.5	1.1	1.5	1.1	<LOQ	1.6	1.7	1.3	<LOQ	1.2	1.1	3.4	<LOQ	6.6	<LOQ	1.1	1.8	<LOQ	1.2	1.3	<LOQ

PCB153	8.7	<LOQ	16.1	6.5	11.0	10.3	8.7	12.8	8.0	6.9	8.4	9.3	7.8	6.0	8.4	7.1	12.3	8.5	13.3	5.2	7.2	14.7	8.9	9.2	9.1	6.4
PCB132	<LOQ	3.4	2.7	<LOQ	1.2	1.0	0.8	1.4	0.3	<LOQ	2.1	2.2	1.5	1.1	1.6	1.3	3.0	1.4	2.6	0.5	1.3	2.9	0.7	1.9	1.5	0.3
PCB105	<LOQ	1.0	0.5	<LOQ	0.2	0.2	0.2	0.2	0.1	<LOQ	0.4	0.4	0.3	0.2	0.3	0.3	0.8	0.2	0.3	0.1	0.2	0.5	<LOQ	0.3	0.2	<LOQ
PCB138	1.2	<LOQ	7.2	1.6	4.4	4.0	3.2	4.9	2.3	1.2	4.1	4.5	3.5	2.5	3.4	3.1	6.4	3.8	5.3	1.7	3.2	6.4	3.0	4.2	3.8	2.2
PCB158	<LOQ	<LOQ	0.8	<LOQ	0.5	0.5	0.4	0.6	0.3	<LOQ	0.4	0.5	0.4	0.3	0.4	0.4	0.8	0.4	0.5	<LOQ	0.4	0.7	0.3	0.4	0.5	0.3
PCB187	1.5	<LOQ	3.4	1.2	2.7	2.2	1.9	3.2	1.5	1.6	2.1	2.1	1.7	1.3	1.9	1.6	3.0	2.4	2.5	1.1	1.8	3.7	2.7	2.2	2.2	1.5
PCB183	0.7	<LOQ	1.6	0.6	1.2	0.9	0.8	1.4	0.7	0.7	0.9	0.9	0.8	<LOQ	0.8	0.7	1.2	1.0	1.0	<LOQ	0.8	1.6	1.2	1.0	1.0	0.7
PCB128	<LOQ	<LOQ	0.3	<LOQ	0.1	0.1	0.1	0.1	<LOQ	<LOQ	0.2	0.3	0.2	0.1	0.1	0.1	0.4	0.2	0.3	<LOQ	0.2	0.4	<LOQ	0.2	0.2	<LOQ
PCB177	0.1	0.1	1.3	0.2	1.0	0.7	0.6	1.0	0.4	0.2	0.8	0.8	0.6	0.4	0.6	0.6	1.2	1.0	1.0	0.3	0.7	1.4	0.7	0.8	0.8	0.4
PCB156	0.1	<LOQ	0.4	<LOQ	0.3	0.2	0.2	0.3	0.1	<LOQ	0.2	0.2	0.2	0.1	0.2	0.2	0.3	0.3	0.3	0.1	0.2	0.4	0.2	0.2	0.2	0.1
PCB171	<LOQ	<LOQ	0.7	<LOQ	0.5	0.4	0.3	0.4	0.2	<LOQ	0.4	0.5	0.4	0.2	0.3	0.4	0.5	0.4	0.5	<LOQ	0.3	0.5	0.2	0.4	0.4	0.2
PCB180	1.9	0.9	4.2	1.6	3.3	2.3	2.5	3.7	1.8	1.8	2.1	2.3	2.0	1.3	1.8	1.8	3.2	3.3	3.0	1.2	2.1	4.3	3.0	2.2	2.3	1.5
PCB191	<LOQ	0.1	<LOQ	<LOQ	<LOQ	<LOQ	<LOQ	<LOQ	<LOQ	<LOQ	<LOQ	<LOQ	<LOQ	<LOQ	<LOQ	<LOQ	<LOQ	<LOQ	<LOQ	<LOQ	<LOQ	0.1	<LOQ	<LOQ	<LOQ	<LOQ
PCB169	<LOQ	<LOQ	0.4	<LOQ	<LOQ	<LOQ	<LOQ	<LOQ	<LOQ	<LOQ	<LOQ	<LOQ	<LOQ	<LOQ	<LOQ	<LOQ	<LOQ	<LOQ	<LOQ	<LOQ	<LOQ	<LOQ	<LOQ	<LOQ	<LOQ	<LOQ
PCB170	<LOQ	0.1	1.3	0.1	1.0	0.7	0.6	1.0	0.3	0.1	0.8	0.8	0.7	0.4	0.5	0.5	1.2	1.1	1.0	0.2	0.6	1.3	0.8	0.7	0.7	0.4
PCB201/199	0.1	0.1	0.4	0.1	0.4	0.2	0.2	0.3	0.1	0.1	0.1	0.1	0.1	0.1	0.1	0.1	0.2	0.3	0.2	0.1	0.1	0.3	0.3	0.1	0.1	0.1
PCB208	<LOQ	<LOQ	<LOQ	<LOQ	<LOQ	<LOQ	<LOQ	<LOQ	<LOQ	<LOQ	<LOQ	<LOQ	<LOQ	<LOQ	0.1	0.1	0.1	<LOQ	<LOQ	<LOQ	<LOQ	<LOQ	<LOQ	<LOQ	<LOQ	<LOQ
PCB195	<LOQ	<LOQ	0.1	<LOQ	0.1	0.1	<LOQ	0.1	<LOQ	<LOQ	<LOQ	0.1	<LOQ	<LOQ	<LOQ	<LOQ	<LOQ	0.1	<LOQ	<LOQ	<LOQ	0.1	0.1	<LOQ	0.1	<LOQ
PCB194	<LOQ	<LOQ	0.3	<LOQ	0.3	0.1	0.1	0.2	0.1	0.1	0.1	0.1	0.1	<LOQ	0.1	0.1	0.1	0.2	<LOQ	<LOQ	0.1	0.2	0.2	<LOQ	0.1	<LOQ
PCB205	<LOQ	<LOQ	<LOQ	<LOQ	<LOQ	<LOQ	<LOQ	<LOQ	<LOQ	<LOQ	<LOQ	<LOQ	<LOQ	<LOQ	<LOQ	<LOQ	<LOQ	<LOQ	<LOQ	<LOQ	<LOQ	<LOQ	<LOQ	<LOQ	<LOQ	<LOQ
PCB206	<LOQ	<LOQ	<LOQ	<LOQ	0.2	<LOQ	<LOQ	<LOQ	<LOQ	<LOQ	<LOQ	<LOQ	<LOQ	<LOQ	<LOQ	<LOQ	<LOQ	<LOQ	<LOQ	<LOQ	<LOQ	<LOQ	<LOQ	<LOQ	<LOQ	<LOQ
PCB209	<LOQ	<LOQ	<LOQ	<LOQ	<LOQ	<LOQ	<LOQ	<LOQ	<LOQ	<LOQ	<LOQ	<LOQ	<LOQ	<LOQ	<LOQ	<LOQ	<LOQ	<LOQ	<LOQ	<LOQ	<LOQ	<LOQ	<LOQ	<LOQ	<LOQ	<LOQ

Table S3. Fugacity sampling ancillary data

Sampling start	Sampling end	Samples	mean T.(°C)	min. T.(°C)	max. T.(°C)	Surface
03/12/14	09/12/14	F1-1	0.4	-3.7	7	Soil with vegetation
09/12/14	16/12/14	F1-2	0.4	-2.1	5	Soil with vegetation
16/12/14	22/12/14	F1-3	1.0	-1.1	5.1	Soil with vegetation
22/12/14	29/12/14	F1-4	0.9	-3.3	5.1	Soil with vegetation
29/12/14	05/01/15	F1-5	1.0	-1.3	6.7	Soil with vegetation
05/01/15	12/01/15	F1-6	0.8	-1.3	4.4	Soil with vegetation
12/01/15	19/01/15	F1-7	0.5	-3.8	3.4	Soil with vegetation
19/01/15	26/01/15	F1-8	2.0	-0.2	5.5	Soil with vegetation
26/01/15	02/02/15	F1-9	2.6	0.4	5.5	Soil with vegetation
02/02/15	09/02/15	F1-10	2.2	-0.8	6.9	Soil with vegetation
09/02/15	16/02/15	F1-11	2.1	-0.2	5.5	Soil with vegetation
02/12/14	09/12/14	F2-1	0.3	-3.7	7	Snow
09/12/14	16/12/14	F2-2	0.4	-2.1	5	Snow
16/12/14	23/12/14	F2-3	1.0	-1.1	5.1	Snow
23/12/14	30/12/14	F2-4	0.8	-3.3	4.4	Snow
30/12/14	06/01/15	F2-5	0.9	-1.3	6.7	Snow
06/01/15	13/01/15	F2-6	0.6	-1.5	3.9	Snow
13/01/15	20/01/15	F2-7	0.6	-3.8	3.4	Snow
20/01/15	27/01/15	F2-8	2.2	0.2	5.5	Bare soil
27/01/15	03/02/15	F2-9	2.5	0.4	5.2	Bare soil
03/02/15	10/02/15	F2-10	2.3	-0.8	6.9	Bare soil
10/02/15	17/02/15	F2-11	2.3	0.4	5.5	Bare soil
03/12/14	10/12/14	F3-1	0.4	-3.7	7	Snow
10/12/14	17/12/14	F3-2	0.5	-2.1	5	Snow
17/12/14	24/12/14	F3-3	0.8	-1.5	5.1	Snow
24/12/14	31/12/14	F3-4	0.8	-3.3	4.4	Snow
31/12/14	07/01/15	F3-5	0.7	-1.3	6.7	Snow
07/01/15	14/01/15	F3-6	0.7	-1.5	3.9	Snow
14/01/15	21/01/15	F3-7	0.7	-3.8	3.6	Bare soil
21/01/15	28/01/15	F3-8	2.3	0.3	5.5	Bare soil
28/01/15	04/02/15	F3-9	2.4	-0.8	5.2	Bare soil
04/02/15	11/02/15	F3-10	2.4	-0.8	6.9	Bare soil
11/02/15	18/02/15	F3-11	2.4	0.4	5.5	Bare soil
05/12/14	12/12/14	F4-1	0.8	-1.6	7	Snow
12/12/14	19/12/14	F4-2	0.7	-2.1	5	Snow
19/12/14	28/12/14	F4-3	0.7	-3.3	5.1	Snow
28/12/14	02/01/15	F4-4	0.7	-1	4.4	Snow
02/01/15	09/01/15	F4-5	0.6	-1.3	6.7	Snow
09/01/15	17/01/15	F4-6	0.7	-3.8	3.9	Snow
17/01/15	23/01/15	F4-7	1.3	-3.8	4.4	Snow
23/01/15	30/01/15	F4-8	2.6	0.3	5.5	Snow
30/01/15	06/02/15	F4-9	2.6	-0.8	6.9	Snow
06/02/15	13/02/15	F4-10	2.0	-0.2	5.5	Snow
05/12/14	12/12/14	F5-1	0.8	-1.6	7	Snow
12/12/14	19/12/14	F5-2	0.7	-2.1	5	Snow
19/12/14	28/12/14	F5-3	0.7	-3.3	5.1	Snow
28/12/14	02/01/15	F5-4	0.7	-1	4.4	Snow
02/01/15	09/01/15	F5-5	0.6	-1.3	6.7	Snow
09/01/15	17/01/15	F5-6	0.7	-3.8	3.9	Snow
17/01/15	23/01/15	F5-7	1.3	-3.8	4.4	Snow
23/01/15	30/01/15	F5-8	2.6	0.3	5.5	Snow
30/01/15	06/02/15	F5-9	2.6	-0.8	6.9	Snow
06/02/15	13/02/15	F5-10	2.0	-0.2	5.5	Snow

Table S4. Air, snow, seawater and plankton recoveries

Surrogate	PUFs	Snow	Seawater	Plankton
PCB65	110±44%	90±14%	57±23%	71±17%
PCB200	84±24%	96±16%	63±23%	94±5.6%

Table S5. Ambient air PCBs and OCPs concentrations (pg m^{-3})

pg m^{-3}	F1A1	F1A2	F1A3	F1A6	F1A7	F1A8	F1A9	F1A10	F1A11	F2A1	F2A2	F2A3	F2A4	F2A5	F2A7	F2A8	F2A9	F2A10	F2A11
∑OCPs	13.52	14.49	4.93	10.95	13.55	18.97	14.12	11.12	12.36	2.38	11.80	10.03	10.37	11.33	12.01	14.34	10.44	15.57	11.91
HCB	13.52	14.49	4.93	10.95	13.55	17.04	14.12	11.12	12.36	2.38	11.80	10.03	10.37	11.33	12.01	14.34	10.44	14.10	11.91
∑HCH						1.93												1.47	
a-HCH	<LOQ	<LOQ	<LOQ	<LOQ	<LOQ	<LOQ	<LOQ	<LOQ	<LOQ	<LOQ	<LOQ	<LOQ	<LOQ	<LOQ	<LOQ	<LOQ	<LOQ	<LOQ	<LOQ
b-HCH	<LOQ	<LOQ	<LOQ	<LOQ	<LOQ	<LOQ	<LOQ	<LOQ	<LOQ	<LOQ	<LOQ	<LOQ	<LOQ	<LOQ	<LOQ	<LOQ	<LOQ	<LOQ	<LOQ
g-HCH	<LOQ	<LOQ	<LOQ	<LOQ	<LOQ	1.93	<LOQ	<LOQ	<LOQ	<LOQ	<LOQ	<LOQ	<LOQ	<LOQ	<LOQ	<LOQ	<LOQ	1.47	<LOQ
d-HCH	<LOQ	<LOQ	<LOQ	<LOQ	<LOQ	<LOQ	<LOQ	<LOQ	<LOQ	<LOQ	<LOQ	<LOQ	<LOQ	<LOQ	<LOQ	<LOQ	<LOQ	<LOQ	<LOQ
∑PCBs	33.39	46.87	50.01	15.67	7.73	44.85	48.19	35.97	23.96	37.84	75.97	69.89	63.00	44.56	3.67	42.33	13.30	47.25	80.32
PCB18	2.11	5.04	<LOQ	2.07	1.98	4.66	<LOQ	4.29	1.92	2.57	<LOQ	<LOQ	<LOQ	1.35	<LOQ	4.43	1.22	3.00	<LOQ
PCB17	0.51	0.67	1.57	0.42	0.25	1.32	0.33	<LOQ	<LOQ	1.64	0.31	1.21	<LOQ	<LOQ	<LOQ	2.00	<LOQ	0.68	<LOQ
PCB31+28	0.44	1.53	1.10	<LOQ	<LOQ	0.17	<LOQ	3.51	1.32	1.30	1.12	1.50	1.92	0.78	<LOQ	0.25	0.26	<LOQ	<LOQ
PCB52	6.53	9.53	3.49	<LOQ	1.87	<LOQ	<LOQ	<LOQ	<LOQ	13.54	22.82	24.54	8.89	22.86	<LOQ	17.65	<LOQ	<LOQ	49.41
PCB49	1.98	3.33	<LOQ	<LOQ	<LOQ	1.45	<LOQ	1.92	1.73	4.45	1.40	5.22	<LOQ	3.52	<LOQ	2.64	<LOQ	1.65	<LOQ
PCB44	<LOQ	<LOQ	<LOQ	<LOQ	<LOQ	<LOQ	<LOQ	<LOQ	<LOQ	<LOQ	<LOQ	<LOQ	<LOQ	<LOQ	<LOQ	<LOQ	<LOQ	<LOQ	<LOQ
PCB74	<LOQ	<LOQ	<LOQ	<LOQ	<LOQ	<LOQ	<LOQ	<LOQ	<LOQ	<LOQ	<LOQ	<LOQ	5.88	<LOQ	<LOQ	<LOQ	<LOQ	<LOQ	<LOQ
PCB70	<LOQ	<LOQ	<LOQ	<LOQ	<LOQ	<LOQ	<LOQ	<LOQ	<LOQ	2.94	13.82	3.52	<LOQ	<LOQ	<LOQ	<LOQ	<LOQ	<LOQ	<LOQ
PCB95	<LOQ	<LOQ	<LOQ	<LOQ	<LOQ	<LOQ	<LOQ	<LOQ	<LOQ	<LOQ	<LOQ	<LOQ	2.51	<LOQ	<LOQ	<LOQ	<LOQ	<LOQ	<LOQ
PCB99+101	0.78	<LOQ	<LOQ	0.36	<LOQ	3.10	0.77	<LOQ	<LOQ	1.71	7.25	<LOQ	0.61	0.49	<LOQ	1.30	<LOQ	1.76	1.85
PCB87	<LOQ	2.53	2.81	<LOQ	<LOQ	1.25	<LOQ	<LOQ	0.25	<LOQ	3.62	2.36	2.69	1.17	<LOQ	<LOQ	<LOQ	<LOQ	<LOQ
PCB110	<LOQ	0.37	0.56	<LOQ	<LOQ	<LOQ	<LOQ	<LOQ	<LOQ	0.63	<LOQ	<LOQ	<LOQ	<LOQ	<LOQ	<LOQ	<LOQ	<LOQ	<LOQ
PCB82	<LOQ	<LOQ	<LOQ	<LOQ	<LOQ	<LOQ	<LOQ	<LOQ	<LOQ	<LOQ	<LOQ	<LOQ	<LOQ	<LOQ	<LOQ	<LOQ	<LOQ	<LOQ	<LOQ
PCB151	0.94	7.86	14.81	0.72	<LOQ	<LOQ	<LOQ	<LOQ	<LOQ	0.56	7.09	11.21	14.66	5.58	<LOQ	0.34	<LOQ	0.45	<LOQ
PCB149	8.69	5.66	2.35	3.05	3.22	13.63	27.43	18.96	15.58	2.76	3.11	1.49	1.80	0.93	1.22	2.95	3.44	23.73	19.27
PCB118	<LOQ	<LOQ	9.97	<LOQ	<LOQ	<LOQ	<LOQ	<LOQ	<LOQ	<LOQ	<LOQ	<LOQ	<LOQ	<LOQ	<LOQ	<LOQ	<LOQ	<LOQ	<LOQ
PCB153	<LOQ	1.02	1.15	<LOQ	<LOQ	<LOQ	<LOQ	<LOQ	<LOQ	<LOQ	1.19	<LOQ	<LOQ	<LOQ	<LOQ	<LOQ	3.25	<LOQ	<LOQ

PCB132	6.97	4.67	<LOQ	8.64	<LOQ	<LOQ	<LOQ	<LOQ	<LOQ	2.76	3.34	3.30	7.37	<LOQ	2.19	6.50	3.44	2.43	9.27
PCB105	<LOQ	<LOQ	<LOQ	<LOQ	<LOQ	0.45	0.48	<LOQ	<LOQ	<LOQ	<LOQ	<LOQ	4.50	<LOQ	<LOQ	<LOQ	<LOQ	<LOQ	<LOQ
PCB138	<LOQ	<LOQ	<LOQ	<LOQ	<LOQ	2.31	<LOQ	<LOQ	<LOQ	<LOQ	0.06	0.03	<LOQ	<LOQ	<LOQ	<LOQ	<LOQ	<LOQ	<LOQ
PCB158	0.08	<LOQ	<LOQ	<LOQ	<LOQ	0.55	0.08	<LOQ	0.05	<LOQ	0.13	0.05	<LOQ	<LOQ	<LOQ	<LOQ	<LOQ	0.02	<LOQ
PCB187	3.06	<LOQ	1.42	<LOQ	<LOQ	6.08	11.27	4.57	1.94	<LOQ	1.05	0.96	6.38	4.29	<LOQ	2.65	1.02	7.36	<LOQ
PCB183	<LOQ	0.65	0.84	<LOQ	<LOQ	<LOQ	<LOQ	<LOQ	<LOQ	1.19	0.77	<LOQ	<LOQ	<LOQ	<LOQ	<LOQ	<LOQ	<LOQ	<LOQ
PCB128	<LOQ	0.29	0.21	<LOQ	<LOQ	0.21	0.17	<LOQ	<LOQ	<LOQ	0.27	0.19	0.24	<LOQ	<LOQ	<LOQ	<LOQ	0.15	<LOQ
PCB177	<LOQ	1.32	2.36	0.27	0.20	2.72	0.12	<LOQ	<LOQ	0.93	2.54	3.49	0.44	0.24	<LOQ	0.18	0.06	0.29	<LOQ
PCB156	<LOQ	<LOQ	<LOQ	<LOQ	<LOQ	0.92	<LOQ	<LOQ	<LOQ	<LOQ	<LOQ	<LOQ	<LOQ	<LOQ	<LOQ	<LOQ	<LOQ	0.71	<LOQ
PCB171	<LOQ	<LOQ	<LOQ	<LOQ	<LOQ	0.08	<LOQ	<LOQ	<LOQ	<LOQ	0.17	<LOQ	<LOQ	<LOQ	0.05	<LOQ	<LOQ	0.11	<LOQ
PCB180	<LOQ	0.86	3.38	0.14	<LOQ	3.34	1.16	0.66	0.31	0.73	3.52	4.99	1.09	0.14	<LOQ	0.52	<LOQ	<LOQ	<LOQ
PCB191	<LOQ	0.91	1.73	<LOQ	<LOQ	0.99	<LOQ	<LOQ	<LOQ	<LOQ	0.78	2.06	<LOQ	<LOQ	<LOQ	<LOQ	<LOQ	<LOQ	<LOQ
PCB169	1.30	0.65	<LOQ	<LOQ	0.22	0.96	6.13	2.06	0.81	<LOQ	1.40	3.78	3.42	3.20	0.21	0.71	0.61	4.44	0.52
PCB170	<LOQ	<LOQ	0.30	<LOQ	<LOQ	0.65	0.24	<LOQ	0.04	0.13	0.22	<LOQ	0.60	<LOQ	<LOQ	0.20	<LOQ	0.45	<LOQ
PCB201/199	<LOQ	<LOQ	1.98	<LOQ	<LOQ	<LOQ	<LOQ	<LOQ	<LOQ	<LOQ	<LOQ	<LOQ	<LOQ	<LOQ	<LOQ	<LOQ	<LOQ	<LOQ	<LOQ

Table S5. Ambient air PCBs and OCPs concentrations (pg m^{-3}) (continuation)

pg m^{-3}	F3A1	F3A2	F3A3	F3A4	F3A5	F3A6	F3A7	F3A8	F3A9	F3A10	F3A11	F4A1	F4A2	F4A3	F4A4	F4A5	F4A6	F4A7	F4A8	F4A9	F4A10
∑OCPs	14.93	12.50	10.89	10.72	13.59	12.99	16.47	18.24	14.18	3.40	12.22	10.63	14.53	15.84	10.30	8.47	6.40	2.18	11.01	10.81	9.42
HCB	14.93	12.50	10.89	10.72	13.59	12.99	16.47	15.25	14.18	3.40	12.22	10.63	14.53	13.66	10.30	8.47	6.40	2.18	11.01	10.81	9.42
∑HCH								2.99						2.18							
a-HCH	<LOQ	<LOQ	<LOQ	<LOQ	<LOQ	<LOQ	<LOQ	<LOQ	<LOQ	<LOQ	<LOQ	<LOQ	<LOQ	<LOQ	<LOQ	<LOQ	<LOQ	<LOQ	<LOQ	<LOQ	<LOQ
b-HCH	<LOQ	<LOQ	<LOQ	<LOQ	<LOQ	<LOQ	<LOQ	<LOQ	<LOQ	<LOQ	<LOQ	<LOQ	<LOQ	<LOQ	<LOQ	<LOQ	<LOQ	<LOQ	<LOQ	<LOQ	<LOQ
g-HCH	<LOQ	<LOQ	<LOQ	<LOQ	<LOQ	<LOQ	<LOQ	2.99	<LOQ	<LOQ	<LOQ	<LOQ	<LOQ	2.18	<LOQ	<LOQ	<LOQ	<LOQ	<LOQ	<LOQ	<LOQ
d-HCH	<LOQ	<LOQ	<LOQ	<LOQ	<LOQ	<LOQ	<LOQ	<LOQ	<LOQ	<LOQ	<LOQ	<LOQ	<LOQ	<LOQ	<LOQ	<LOQ	<LOQ	<LOQ	<LOQ	<LOQ	<LOQ
∑PCBs	37.87	44.96	39.09	55.44	44.31	26.10	29.08	57.08	17.13	34.82	10.13	9.87	37.58	76.27	27.86	47.76	15.56	39.33	75.67	60.32	22.73
PCB18	<LOQ	<LOQ	<LOQ	<LOQ	<LOQ	<LOQ	<LOQ	9.35	<LOQ	<LOQ	2.32	0.99	<LOQ	7.95	<LOQ	<LOQ	1.60	4.27	<LOQ	<LOQ	<LOQ
PCB17	<LOQ	0.33	<LOQ	0.78	0.44	0.94	0.39	0.24	<LOQ	<LOQ	<LOQ	<LOQ	0.44	1.09	0.49	<LOQ	1.59	0.90	<LOQ	<LOQ	<LOQ
PCB31+28	0.51	0.18	0.24	<LOQ	1.07	<LOQ	0.33	0.85	<LOQ	<LOQ	<LOQ	0.17	0.56	1.03	0.69	1.68	<LOQ	1.72	0.19	1.08	<LOQ
PCB52	10.11	6.28	11.44	16.05	4.19	3.60	<LOQ	<LOQ	5.49	<LOQ	0.29	0.48	2.55	<LOQ	0.48	<LOQ	1.64	<LOQ	<LOQ	<LOQ	1.20
PCB49	<LOQ	2.13	<LOQ	5.18	<LOQ	<LOQ	<LOQ	3.21	0.98	<LOQ	<LOQ	1.75	<LOQ	2.81	2.47	<LOQ	1.19	<LOQ	<LOQ	<LOQ	1.77
PCB44	<LOQ	<LOQ	<LOQ	<LOQ	<LOQ	<LOQ	<LOQ	<LOQ	<LOQ	<LOQ	<LOQ	<LOQ	<LOQ	<LOQ	<LOQ	<LOQ	<LOQ	<LOQ	<LOQ	1.27	<LOQ
PCB74	<LOQ	<LOQ	<LOQ	<LOQ	<LOQ	<LOQ	<LOQ	7.93	<LOQ	<LOQ	<LOQ	<LOQ	<LOQ	11.36	4.35	3.03	<LOQ	<LOQ	<LOQ	12.26	<LOQ
PCB70	5.54	11.24	<LOQ	<LOQ	<LOQ	<LOQ	<LOQ	<LOQ	<LOQ	<LOQ	<LOQ	<LOQ	8.21	4.63	<LOQ	<LOQ	<LOQ	<LOQ	<LOQ	<LOQ	<LOQ
PCB95	<LOQ	<LOQ	2.34	<LOQ	<LOQ	3.87	<LOQ	<LOQ	<LOQ	<LOQ	<LOQ	<LOQ	<LOQ	<LOQ	<LOQ	<LOQ	<LOQ	<LOQ	<LOQ	3.92	<LOQ
PCB99+101	0.48	0.91	<LOQ	<LOQ	0.49	<LOQ	2.20	1.48	1.17	<LOQ	<LOQ	<LOQ	<LOQ	0.90	1.23	1.85	1.40	0.99	4.30	3.12	2.26
PCB87	<LOQ	1.64	2.39	3.15	1.65	<LOQ	0.87	<LOQ	<LOQ	<LOQ	<LOQ	<LOQ	1.77	2.26	2.43	1.76	0.40	<LOQ	0.22	<LOQ	<LOQ
PCB110	<LOQ	<LOQ	<LOQ	<LOQ	<LOQ	<LOQ	<LOQ	<LOQ	<LOQ	<LOQ	<LOQ	<LOQ	<LOQ	1.48	<LOQ	<LOQ	0.52	0.48	0.43	<LOQ	<LOQ
PCB82	<LOQ	<LOQ	<LOQ	<LOQ	<LOQ	<LOQ	<LOQ	<LOQ	<LOQ	<LOQ	<LOQ	<LOQ	<LOQ	<LOQ	<LOQ	<LOQ	<LOQ	<LOQ	<LOQ	<LOQ	<LOQ
PCB151	0.41	7.48	13.08	17.39	7.75	<LOQ	<LOQ	<LOQ	<LOQ	<LOQ	<LOQ	0.35	8.12	5.06	10.35	7.28	0.81	1.28	<LOQ	<LOQ	<LOQ
PCB149	4.27	5.09	4.46	3.43	6.80	3.15	3.91	9.87	7.65	21.72	7.43	1.48	2.27	3.72	2.33	1.52	3.13	7.95	57.45	29.13	13.34
PCB118	<LOQ	<LOQ	<LOQ	<LOQ	<LOQ	<LOQ	<LOQ	<LOQ	<LOQ	<LOQ	<LOQ	<LOQ	<LOQ	<LOQ	<LOQ	<LOQ	<LOQ	<LOQ	1.16	<LOQ	<LOQ
PCB153	<LOQ	3.26	<LOQ	<LOQ	<LOQ	<LOQ	<LOQ	0.99	<LOQ	<LOQ	<LOQ	<LOQ	2.68	1.73	<LOQ	<LOQ	<LOQ	<LOQ	<LOQ	<LOQ	<LOQ

PCB132	1.44	4.94	4.90	6.03	5.32	13.42	<LOQ	2.60	<LOQ	2.17	<LOQ	4.12	9.02	<LOQ	<LOQ	1.41	1.99	11.32	<LOQ	5.49	2.85
PCB105	<LOQ	<LOQ	<LOQ	<LOQ	<LOQ	<LOQ	<LOQ	<LOQ	<LOQ	<LOQ	<LOQ	<LOQ	<LOQ	0.82	<LOQ	<LOQ	<LOQ	<LOQ	0.31	<LOQ	<LOQ
PCB138	0.16	<LOQ	0.02	<LOQ	0.56	<LOQ	2.79	0.74	<LOQ	<LOQ	<LOQ	<LOQ	<LOQ	0.85	<LOQ	<LOQ	<LOQ	0.05	0.62	0.49	<LOQ
PCB158	0.03	0.02	<LOQ	<LOQ	<LOQ	<LOQ	<LOQ	0.99	<LOQ	0.74	<LOQ	<LOQ	<LOQ	0.27	<LOQ	<LOQ	0.43	0.29	0.16	<LOQ	<LOQ
PCB187	<LOQ	0.98	<LOQ	<LOQ	0.99	<LOQ	1.08	4.57	1.36	3.20	<LOQ	<LOQ	<LOQ	0.75	<LOQ	<LOQ	<LOQ	1.74	3.01	2.79	1.08
PCB183	<LOQ	<LOQ	<LOQ	<LOQ	0.43	<LOQ	<LOQ	<LOQ	<LOQ	<LOQ	<LOQ	<LOQ	<LOQ	1.23	<LOQ	<LOQ	<LOQ	<LOQ	<LOQ	<LOQ	<LOQ
PCB128	0.57	<LOQ	<LOQ	<LOQ	0.00	0.13	0.49	0.98	<LOQ	0.69	<LOQ	<LOQ	<LOQ	0.77	<LOQ	0.27	<LOQ	0.80	0.24	<LOQ	<LOQ
PCB177	5.41	0.08	<LOQ	0.58	5.41	0.41	6.65	3.35	<LOQ	0.54	0.09	0.33	0.20	2.32	1.23	10.85	0.49	1.70	2.37	<LOQ	<LOQ
PCB156	<LOQ	<LOQ	<LOQ	<LOQ	<LOQ	<LOQ	<LOQ	1.72	<LOQ	<LOQ	<LOQ	<LOQ	<LOQ	3.98	<LOQ	0.37	<LOQ	<LOQ	0.28	<LOQ	<LOQ
PCB171	0.46	0.04	<LOQ	<LOQ	0.22	<LOQ	0.43	0.08	<LOQ	0.34	<LOQ	0.06	0.56	4.92	0.12	0.52	<LOQ	<LOQ	0.35	<LOQ	<LOQ
PCB180	5.78	0.04	<LOQ	1.43	5.91	0.58	7.23	5.06	<LOQ	0.54	<LOQ	0.15	0.77	0.93	1.24	12.13	0.38	3.88	2.67	<LOQ	<LOQ
PCB191	1.05	<LOQ	<LOQ	<LOQ	1.41	<LOQ	1.49	1.26	<LOQ	<LOQ	<LOQ	<LOQ	<LOQ	0.73	<LOQ	2.54	<LOQ	1.19	<LOQ	<LOQ	<LOQ
PCB169	1.42	0.32	0.21	1.02	1.33	<LOQ	1.10	0.97	0.48	3.79	<LOQ	<LOQ	<LOQ	1.40	0.34	1.90	<LOQ	0.78	1.91	0.76	0.22
PCB170	0.21	<LOQ	<LOQ	0.42	0.34	<LOQ	0.13	0.84	<LOQ	1.08	<LOQ	<LOQ	0.42	4.29	0.12	0.65	<LOQ	<LOQ	<LOQ	<LOQ	<LOQ
PCB201/199	<LOQ	<LOQ	<LOQ	<LOQ	<LOQ	<LOQ	<LOQ	<LOQ	<LOQ	<LOQ	<LOQ	<LOQ	<LOQ	8.98	<LOQ	<LOQ	<LOQ	<LOQ	<LOQ	<LOQ	<LOQ

Table S5. Ambient air PCBs and OCPs concentrations (pg m^{-3}) (continuation)

pg m^{-3}	F5A1	F5A2	F5A3	F5A4	F5A5	F5A6	F5A7	F5A8	F5A9	F5A10
∑OCPs	39.64	11.10	17.37	9.58	9.00	12.68	10.76	17.95	7.67	9.76
HCB	17.15	11.10	17.37	9.58	9.00	12.68	10.76	15.71	7.67	7.29
∑HCH	22.49							2.24		2.46
a-HCH	1.73	<LOQ	<LOQ	<LOQ	<LOQ	<LOQ	<LOQ	2.24	<LOQ	<LOQ
b-HCH	11.72	<LOQ	<LOQ	<LOQ	<LOQ	<LOQ	<LOQ	<LOQ	<LOQ	<LOQ
g-HCH	5.18	<LOQ	<LOQ	<LOQ	<LOQ	<LOQ	<LOQ	<LOQ	<LOQ	<LOQ
d-HCH	3.85	<LOQ	<LOQ	<LOQ	<LOQ	<LOQ	<LOQ	<LOQ	<LOQ	2.46
∑PCBs	129.52	66.52	36.89	72.07	23.69	7.69	36.36	39.44	23.86	19.45
PCB18	10.51	2.20	1.81	<LOQ	<LOQ	2.17	<LOQ	<LOQ	1.24	1.29
PCB17	14.08	<LOQ	0.16	<LOQ	0.90	0.61	0.50	0.90	<LOQ	<LOQ
PCB31+28	4.77	0.51	0.12	1.96	0.65	<LOQ	0.75	<LOQ	0.56	<LOQ
PCB52	9.52	8.33	2.68	4.82	0.77	0.22	<LOQ	<LOQ	1.52	<LOQ
PCB49	<LOQ	<LOQ	<LOQ	<LOQ	<LOQ	<LOQ	<LOQ	1.86	<LOQ	<LOQ
PCB44	44.09	<LOQ	<LOQ	<LOQ	<LOQ	<LOQ	<LOQ	<LOQ	<LOQ	<LOQ
PCB74	<LOQ	<LOQ	<LOQ	5.74	<LOQ	<LOQ	<LOQ	<LOQ	<LOQ	<LOQ
PCB70	16.18	9.68	9.97	<LOQ	<LOQ	<LOQ	<LOQ	<LOQ	<LOQ	<LOQ
PCB95	<LOQ	<LOQ	<LOQ	<LOQ	<LOQ	<LOQ	<LOQ	<LOQ	<LOQ	<LOQ
PCB99+101	5.08	<LOQ	<LOQ	0.91	<LOQ	0.48	2.48	<LOQ	<LOQ	2.08
PCB87	2.02	3.18	2.40	3.06	1.64	<LOQ	0.79	<LOQ	<LOQ	<LOQ
PCB110	0.43	<LOQ	<LOQ	<LOQ	0.75	<LOQ	<LOQ	<LOQ	<LOQ	0.69
PCB82	<LOQ	<LOQ	<LOQ	<LOQ	<LOQ	<LOQ	<LOQ	<LOQ	<LOQ	<LOQ
PCB151	1.25	15.64	12.94	17.13	7.46	0.29	<LOQ	0.43	<LOQ	<LOQ
PCB149	3.91	2.14	2.72	2.44	0.96	1.44	6.07	15.80	9.11	5.34
PCB118	1.15	<LOQ	<LOQ	<LOQ	2.01	<LOQ	<LOQ	<LOQ	<LOQ	<LOQ
PCB153	<LOQ	<LOQ	1.87	1.75	<LOQ	<LOQ	<LOQ	<LOQ	<LOQ	<LOQ

PCB132	2.32	1.76	<LOQ	<LOQ	<LOQ	1.96	<LOQ	5.63	2.26	1.58
PCB105	0.55	<LOQ	<LOQ	<LOQ	<LOQ	<LOQ	<LOQ	<LOQ	<LOQ	<LOQ
PCB138	0.16	0.02	<LOQ	0.01	<LOQ	<LOQ	0.07	0.21	0.77	4.01
PCB158	0.56	0.02	<LOQ	0.03	<LOQ	<LOQ	0.02	<LOQ	<LOQ	<LOQ
PCB187	1.44	<LOQ	0.92	<LOQ	<LOQ	<LOQ	2.74	9.08	6.05	2.91
PCB183	0.93	<LOQ	<LOQ	<LOQ	<LOQ	<LOQ	<LOQ	<LOQ	<LOQ	<LOQ
PCB128	0.66	0.55	<LOQ	0.51	<LOQ	<LOQ	0.70	<LOQ	<LOQ	<LOQ
PCB177	2.88	6.84	<LOQ	10.43	2.51	0.13	9.61	0.43	<LOQ	<LOQ
PCB156	<LOQ	<LOQ	<LOQ	<LOQ	<LOQ	<LOQ	<LOQ	<LOQ	<LOQ	<LOQ
PCB171	0.18	0.39	0.30	0.52	<LOQ	<LOQ	0.51	<LOQ	<LOQ	<LOQ
PCB180	3.13	8.41	<LOQ	12.40	3.86	0.20	10.33	1.36	0.24	<LOQ
PCB191	<LOQ	1.51	<LOQ	2.82	1.65	<LOQ	<LOQ	<LOQ	<LOQ	<LOQ
PCB169	3.00	3.76	1.00	3.82	<LOQ	0.18	1.33	3.14	2.10	1.55
PCB170	0.72	0.16	<LOQ	1.19	0.54	<LOQ	0.46	0.59	<LOQ	<LOQ
PCB201/199	<LOQ	1.41	<LOQ	2.53	<LOQ	<LOQ	<LOQ	<LOQ	<LOQ	<LOQ

Table S6. Air equilibrated in-situ with soil/snow PCBs and OCPs concentrations (pg m^{-3})

pg m^{-3}	**F1S1**	**F1S2**	**F1S3**	**F1S4**	**F1S5**	**F1S6**	**F1S7**	**F1S8**	**F1S9**	**F1S10**	**F1S11**	**F2S1**	**F2S3**	**F2S4**	**F2S5**	**F2S6**	**F2S7**	**F2S8**	**F2S9**	**F2S11**
∑OCPs	90.18	171.02	145.93	43.89	64.58	104.75	59.42	136.15	109.03	37.64	83.93	7.21	6.89	10.22	7.99	13.66	13.89	13.82	13.38	3.54
HCB	72.40	128.46	81.01	38.29	52.90	86.57	49.36	105.65	70.53	37.64	63.68	7.21	6.89	10.22	7.99	13.66	13.89	13.82	13.38	0.44
∑HCH	8.89	21.28	32.46	2.80	5.84	9.09	5.03	15.25	19.25		10.12									1.55
a-HCH	8.89	15.79	11.10	2.80	5.84	9.09	5.03	9.46	6.72	<LOQ	4.86	<LOQ	<LOQ	<LOQ	<LOQ	<LOQ	<LOQ	<LOQ	<LOQ	<LOQ
b-HCH	<LOQ	5.49	6.41	<LOQ	<LOQ	<LOQ	<LOQ	5.79	12.53	<LOQ	5.26	<LOQ	<LOQ	<LOQ	<LOQ	<LOQ	<LOQ	<LOQ	<LOQ	<LOQ
g-HCH	<LOQ	<LOQ	2.20	<LOQ	<LOQ	<LOQ	<LOQ	<LOQ	<LOQ	<LOQ	<LOQ	<LOQ		<LOQ	<LOQ	<LOQ	<LOQ	<LOQ	<LOQ	1.55
d-HCH	<LOQ	<LOQ	12.75	<LOQ	<LOQ	<LOQ	<LOQ	<LOQ	<LOQ	<LOQ	<LOQ	<LOQ	<LOQ	<LOQ	<LOQ	<LOQ	<LOQ	<LOQ	<LOQ	<LOQ
∑PCBs	47.24	108.98	139.29	117.60	100.93	111.63	57.05	73.67	48.74	21.85	43.31	25.47	234.50	48.22	57.49	49.53	48.98	45.79	30.17	25.29
PCB18	5.35	10.78	12.59	1.86	7.00	12.12	4.15	8.66	8.38	2.99	7.71	4.38	9.52	4.19	9.75	9.20	7.69	6.89	9.31	2.77
PCB17	1.22	2.06	4.73	1.18	1.62	1.27	1.19	2.74	1.95	1.08	1.26	0.85	2.14	2.40	3.98	2.08	2.64	2.36	2.24	<LOQ
PCB31+28	7.52	10.23	9.63	5.27	10.56	12.50	7.04	10.53	6.89	1.93	5.32	4.26	16.97	7.10	10.51	10.54	9.79	10.55	7.68	1.00
PCB52	9.81	8.40	8.04	16.45	12.47	15.03	15.43	17.06	9.84	2.49	2.88	5.05	4.44	8.41	5.35	6.13	6.70	13.84	<LOQ	3.15
PCB49	<LOQ	<LOQ	36.06	1.73	33.43	49.30	<LOQ	<LOQ	<LOQ	<LOQ	<LOQ	0.90	1.57	1.74	2.55	3.00	1.67	1.54	1.63	1.11
PCB44	4.02	7.50	9.17	3.98	6.28	6.44	5.66	9.86	4.07	<LOQ	5.32	<LOQ	<LOQ	<LOQ	1.60	<LOQ	<LOQ	<LOQ	<LOQ	<LOQ
PCB74	<LOQ	<LOQ	5.02	<LOQ	3.56	<LOQ	<LOQ	<LOQ	<LOQ	<LOQ	<LOQ	<LOQ	4.56	<LOQ	<LOQ	3.76	<LOQ	<LOQ	<LOQ	<LOQ
PCB70	<LOQ	<LOQ	8.40	<LOQ	<LOQ	<LOQ	<LOQ	<LOQ	<LOQ	<LOQ	<LOQ	2.97	<LOQ	<LOQ	<LOQ	<LOQ	<LOQ	<LOQ	<LOQ	<LOQ
PCB95	<LOQ	<LOQ	3.42	17.43	2.86	2.55	<LOQ	<LOQ	<LOQ	<LOQ	<LOQ	<LOQ	7.71	<LOQ	<LOQ	4.54	<LOQ	<LOQ	<LOQ	<LOQ
PCB99+101	3.25	6.08	6.75	2.13	2.06	2.85	2.81	2.01	1.48	0.69	0.96	1.14	11.34	1.55	<LOQ	1.40	2.38	1.89	2.20	0.77
PCB87	<LOQ	3.74	5.38	5.21	2.19	<LOQ	0.72	<LOQ	<LOQ	<LOQ	<LOQ	<LOQ	4.17	2.25	7.77	0.77	0.86	0.31	<LOQ	<LOQ
PCB110	<LOQ	0.43	0.68	<LOQ	<LOQ	<LOQ	0.42	0.24	0.35	<LOQ	<LOQ	0.40	<LOQ	0.24	<LOQ	<LOQ	0.31	0.33	0.30	<LOQ
PCB82	<LOQ	<LOQ	<LOQ	<LOQ	<LOQ	<LOQ	<LOQ	<LOQ	<LOQ	<LOQ	<LOQ	<LOQ	2.47	<LOQ	<LOQ	<LOQ	<LOQ	<LOQ	<LOQ	<LOQ
PCB151	0.56	9.05	11.71	19.73	8.69	<LOQ	0.34	<LOQ	<LOQ	<LOQ	<LOQ	0.26	14.38	11.01	7.87	<LOQ	<LOQ	<LOQ	<LOQ	<LOQ
PCB149	5.78	10.10	6.72	4.01	4.30	4.84	5.64	7.79	8.07	5.92	7.91	1.58	<LOQ	1.40	1.40	1.75	1.22	2.95	3.03	9.80
PCB118	1.15	<LOQ	2.29	1.71	<LOQ	<LOQ	<LOQ	<LOQ	<LOQ	<LOQ	<LOQ	<LOQ	5.39	<LOQ	0.82	<LOQ	<LOQ	<LOQ	<LOQ	<LOQ
PCB153	1.22	2.03	2.27	<LOQ	<LOQ	<LOQ	<LOQ	0.98	<LOQ	<LOQ	<LOQ	<LOQ	3.07	1.60	1.40	<LOQ	0.71	<LOQ	<LOQ	<LOQ

PCB132	1.77	1.52	1.87	<LOQ	4.90	2.25	<LOQ	4.08	<LOQ	<LOQ	9.03	3.50	1.21	4.24	<LOQ	4.09	<LOQ	1.45	<LOQ	<LOQ
PCB105	<LOQ	0.48	<LOQ	<LOQ	<LOQ	<LOQ	<LOQ	<LOQ	<LOQ	<LOQ	<LOQ	<LOQ	<LOQ	<LOQ	<LOQ	<LOQ	<LOQ	<LOQ	<LOQ	<LOQ
PCB138	0.62	0.07	0.52	<LOQ	<LOQ	0.11	0.45	1.89	0.13	0.09	0.07	0.16	<LOQ	0.40	<LOQ	0.28	0.23	1.65	0.11	1.33
PCB158	<LOQ	<LOQ	0.10	<LOQ	<LOQ	<LOQ	0.42	<LOQ	0.02	<LOQ	0.01	0.01	5.25	0.20	0.57	<LOQ	0.24	<LOQ	<LOQ	<LOQ
PCB187	1.25	1.94	<LOQ	2.76	0.93	1.58	1.09	5.29	4.38	3.59	1.26	<LOQ	3.82	0.77	<LOQ	1.10	0.90	1.06	2.27	1.88
PCB183	<LOQ	<LOQ	<LOQ	<LOQ	<LOQ	0.45	<LOQ	<LOQ	<LOQ	<LOQ	<LOQ	<LOQ	2.75	<LOQ	2.33	0.51	<LOQ	<LOQ	<LOQ	0.89
PCB128	0.34	0.73	0.06	1.16	<LOQ	<LOQ	0.03	<LOQ	<LOQ	<LOQ	<LOQ	<LOQ	2.14	<LOQ	0.78	<LOQ	0.69	<LOQ	0.04	<LOQ
PCB177	1.16	11.92	1.52	12.84	<LOQ	<LOQ	5.22	0.32	<LOQ	<LOQ	0.30	<LOQ	43.57	<LOQ	0.56	<LOQ	5.52	<LOQ	<LOQ	0.22
PCB156	<LOQ	0.45	<LOQ	1.26	<LOQ	<LOQ	0.29	<LOQ	<LOQ	<LOQ	<LOQ	<LOQ	1.66	<LOQ	<LOQ	<LOQ	<LOQ	<LOQ	<LOQ	<LOQ
PCB171	0.08	0.61	0.06	1.94	<LOQ	<LOQ	0.26	0.13	0.19	0.11	0.16	0.03	5.44	<LOQ	<LOQ	<LOQ	0.28	0.11	0.13	0.33
PCB180	1.70	13.57	1.74	12.78	0.08	0.07	5.90	1.16	0.24	<LOQ	0.12	<LOQ	50.74	0.42	0.25	0.37	6.01	0.25	0.45	0.44
PCB191	<LOQ	2.82	<LOQ	2.55	<LOQ	<LOQ	<LOQ	<LOQ	<LOQ	<LOQ	<LOQ	<LOQ	9.77	<LOQ	<LOQ	<LOQ	0.84	<LOQ	<LOQ	<LOQ
PCB169	0.33	3.76	0.45	<LOQ	<LOQ	0.27	<LOQ	<LOQ	2.53	2.53	0.86	<LOQ	10.86	0.30	<LOQ	<LOQ	0.17	0.33	0.62	1.33
PCB170	0.10	0.72	0.12	1.62	<LOQ	<LOQ	<LOQ	0.94	0.24	0.44	0.15	<LOQ	3.81	<LOQ	<LOQ	<LOQ	0.12	0.27	0.15	0.28
PCB201/199	<LOQ	<LOQ	<LOQ	<LOQ	<LOQ	<LOQ	<LOQ	<LOQ	<LOQ	<LOQ	<LOQ	<LOQ	5.73	<LOQ	<LOQ	<LOQ	<LOQ	<LOQ	<LOQ	<LOQ

Table S6. Air equilibrated in-situ with soil/snow PCBs and OCPs concentrations (pg m^{-3}) (continuation)

pg m^{-3}	F3S1	F3S2	F3S3	F3S4	F3S5	F3S6	F3S7	F3S8	F3S9	F3S10	F3S11	F4S1	F4S2	F4S3	F4S4	F4S5	F4S6	F4S7	F4S8	F4S9
∑OCPs	15.78	13.67	3.49	11.91	5.28	1.72	5.00	16.65	12.57	12.33	14.04	9.50	10.17	2.01	9.77	6.70	6.49	12.16	10.66	18.12
HCB	10.50	13.67	3.49	11.91	5.28	1.72	5.00	16.65	12.57	12.33	14.04	9.50	10.17	2.01	9.77	6.70	6.49	9.38	10.66	8.19
∑HCH	2.64																	1.39		4.96
a-HCH	<LOQ	<LOQ	<LOQ	<LOQ	<LOQ	<LOQ	<LOQ	<LOQ	<LOQ	<LOQ	<LOQ	<LOQ	<LOQ	<LOQ	<LOQ	<LOQ	<LOQ	<LOQ	<LOQ	<LOQ
b-HCH	<LOQ	<LOQ	<LOQ	<LOQ	<LOQ	<LOQ	<LOQ	<LOQ	<LOQ	<LOQ	<LOQ	<LOQ	<LOQ	<LOQ	<LOQ	<LOQ	<LOQ	<LOQ	<LOQ	4.96
g-HCH	<LOQ	<LOQ	<LOQ	<LOQ	<LOQ	<LOQ	<LOQ	<LOQ	<LOQ	<LOQ	<LOQ	<LOQ	<LOQ	<LOQ	<LOQ	<LOQ	<LOQ	1.39	<LOQ	<LOQ
d-HCH	2.64	<LOQ	<LOQ	<LOQ	<LOQ	<LOQ	<LOQ	<LOQ	<LOQ	<LOQ	<LOQ	<LOQ	<LOQ	<LOQ	<LOQ	<LOQ	<LOQ	<LOQ	<LOQ	<LOQ
∑PCBs	20.01	38.18	56.82	53.83	17.84	65.87	18.52	22.91	29.57	45.54	31.66	32.50	34.53	57.41	112.37	58.04	15.21	46.85	55.16	43.40
PCB18	<LOQ	2.37	3.15	<LOQ	<LOQ	<LOQ	<LOQ	<LOQ	2.17	<LOQ	2.47	1.50	3.46	2.05	<LOQ	<LOQ	1.10	3.39	<LOQ	1.51
PCB17	<LOQ	<LOQ	2.58	<LOQ	<LOQ	5.55	<LOQ	<LOQ	0.36	<LOQ	<LOQ	<LOQ	1.03	1.45	<LOQ	0.47	<LOQ	<LOQ	<LOQ	<LOQ
PCB31+28	0.14	0.48	4.39	0.13	0.27	1.15	0.28	<LOQ	<LOQ	0.01	<LOQ	<LOQ	1.20	1.45	1.77	0.54	1.24	0.33	0.23	<LOQ
PCB52	3.40	6.08	1.03	4.46	1.08	4.24	<LOQ	<LOQ	1.96	1.67	<LOQ	13.40	11.97	<LOQ	50.53	40.31	<LOQ	<LOQ	<LOQ	<LOQ
PCB49	<LOQ	2.11	3.56	<LOQ	1.16	1.06	<LOQ	<LOQ	1.89	<LOQ	<LOQ	1.57	<LOQ	<LOQ	0.90	<LOQ	<LOQ	<LOQ	0.93	<LOQ
PCB44	<LOQ	<LOQ	<LOQ	<LOQ	<LOQ	2.56	<LOQ	<LOQ	<LOQ	<LOQ	<LOQ	<LOQ	<LOQ	10.01	<LOQ	<LOQ	<LOQ	<LOQ	<LOQ	<LOQ
PCB74	<LOQ	<LOQ	<LOQ	<LOQ	<LOQ	<LOQ	<LOQ	<LOQ	<LOQ	<LOQ	<LOQ	<LOQ	<LOQ	6.02	2.86	<LOQ	2.76	4.83	<LOQ	<LOQ
PCB70	4.72	<LOQ	<LOQ	<LOQ	<LOQ	5.18	<LOQ	<LOQ	<LOQ	<LOQ	<LOQ	<LOQ	<LOQ	<LOQ	<LOQ	<LOQ	<LOQ	<LOQ	<LOQ	<LOQ
PCB95	<LOQ	<LOQ	<LOQ	<LOQ	<LOQ	<LOQ	<LOQ	<LOQ	<LOQ	<LOQ	<LOQ	<LOQ	<LOQ	<LOQ	<LOQ	<LOQ	<LOQ	<LOQ	<LOQ	<LOQ
PCB99+101	<LOQ	1.30	3.77	2.39	0.84	<LOQ	1.15	<LOQ	<LOQ	1.96	<LOQ	0.48	1.05	<LOQ	1.58	<LOQ	0.44	1.60	2.75	1.28
PCB87	<LOQ	2.04	4.87	3.73	0.99	0.25	<LOQ	<LOQ	<LOQ	0.89	<LOQ	<LOQ	1.90	2.38	2.50	1.19	<LOQ	0.92	<LOQ	<LOQ
PCB110	<LOQ	<LOQ	1.06	<LOQ	0.63	1.50	<LOQ	<LOQ	<LOQ	<LOQ	<LOQ	0.26	0.34	0.33	<LOQ	<LOQ	<LOQ	<LOQ	<LOQ	<LOQ
PCB82	<LOQ	<LOQ	<LOQ	<LOQ	<LOQ	<LOQ	<LOQ	<LOQ	<LOQ	<LOQ	<LOQ	<LOQ	<LOQ	<LOQ	<LOQ	<LOQ	<LOQ	<LOQ	<LOQ	<LOQ
PCB151	<LOQ	6.65	10.53	13.39	4.27	<LOQ	<LOQ	<LOQ	<LOQ	<LOQ	<LOQ	0.31	5.55	10.30	10.56	6.05	<LOQ	0.71	0.61	<LOQ
PCB149	4.20	6.73	7.47	6.02	3.67	9.77	4.22	12.10	19.17	34.63	27.30	6.00	2.93	2.27	3.84	3.68	3.16	14.34	39.26	34.64
PCB118	<LOQ	<LOQ	<LOQ	1.18	1.60	1.84	<LOQ	<LOQ	<LOQ	<LOQ	<LOQ	<LOQ	<LOQ	<LOQ	<LOQ	1.34	2.57	<LOQ	<LOQ	<LOQ
PCB153	<LOQ	3.88	1.22	2.00	1.03	6.96	<LOQ	0.93	<LOQ	<LOQ	<LOQ	0.93	1.15	2.17	0.98	1.60	<LOQ	<LOQ	<LOQ	<LOQ

PCB132	3.02	4.79	4.05	<LOQ	<LOQ	6.21	<LOQ	4.97	<LOQ	<LOQ	<LOQ	6.42	1.88	<LOQ	<LOQ	2.60	1.47	<LOQ	5.59	1.62
PCB105	<LOQ	<LOQ	<LOQ	<LOQ	<LOQ	<LOQ	<LOQ	<LOQ	<LOQ	<LOQ	<LOQ	<LOQ	<LOQ	<LOQ	<LOQ	<LOQ	<LOQ	<LOQ	<LOQ	<LOQ
PCB138	0.11	0.20	<LOQ	0.20	0.11	0.81	<LOQ	0.40	0.14	0.55	0.07	0.31	0.25	0.73	<LOQ	0.11	0.17	1.76	0.16	<LOQ
PCB158	0.05	<LOQ	1.20	<LOQ	<LOQ	0.62	<LOQ	<LOQ	<LOQ	<LOQ	<LOQ	<LOQ	<LOQ	<LOQ	<LOQ	<LOQ	<LOQ	0.17	<LOQ	<LOQ
PCB187	<LOQ	1.07	<LOQ	1.38	0.94	<LOQ	1.82	2.55	2.22	3.10	0.86	<LOQ	0.84	0.87	<LOQ	<LOQ	1.01	1.69	3.45	2.47
PCB183	<LOQ	<LOQ	3.98	<LOQ	<LOQ	<LOQ	<LOQ	<LOQ	<LOQ	<LOQ	<LOQ	<LOQ	<LOQ	2.03	<LOQ	<LOQ	0.93	<LOQ	<LOQ	<LOQ
PCB128	0.32	<LOQ	0.34	0.15	0.28	<LOQ	0.25	<LOQ	<LOQ	<LOQ	<LOQ	0.30	0.07	<LOQ	0.57	<LOQ	0.03	0.43	<LOQ	0.29
PCB177	1.61	0.29	1.17	6.69	0.33	<LOQ	4.38	<LOQ	<LOQ	<LOQ	<LOQ	0.31	0.43	2.43	11.88	<LOQ	<LOQ	4.24	0.03	0.06
PCB156	<LOQ	<LOQ	0.42	<LOQ	<LOQ	<LOQ	<LOQ	<LOQ	<LOQ	<LOQ	<LOQ	<LOQ	<LOQ	1.06	<LOQ	<LOQ	<LOQ	0.31	<LOQ	0.42
PCB171	<LOQ	<LOQ	0.90	0.32	<LOQ	0.50	0.34	0.10	0.09	<LOQ	0.14	0.17	<LOQ	<LOQ	0.57	<LOQ	<LOQ	0.21	0.19	<LOQ
PCB180	2.26	0.06	1.13	7.67	0.64	11.51	4.14	0.49	0.44	<LOQ	0.31	0.54	0.47	4.19	13.41	0.16	<LOQ	5.39	0.42	0.16
PCB191	<LOQ	<LOQ	<LOQ	1.73	<LOQ	<LOQ	0.89	<LOQ	<LOQ	<LOQ	<LOQ	<LOQ	<LOQ	3.96	2.42	<LOQ	<LOQ	1.09	<LOQ	<LOQ
PCB169	<LOQ	0.12	<LOQ	1.87	<LOQ	<LOQ	0.90	0.93	1.04	2.44	0.38	<LOQ	<LOQ	<LOQ	5.56	<LOQ	0.34	4.81	1.44	0.91
PCB170	0.19	<LOQ	<LOQ	0.51	<LOQ	6.15	0.15	0.44	0.08	0.28	0.13	<LOQ	<LOQ	0.69	1.29	<LOQ	<LOQ	0.63	0.11	0.05
PCB201/199	<LOQ	<LOQ	<LOQ	<LOQ	<LOQ	<LOQ	<LOQ	<LOQ	<LOQ	<LOQ	<LOQ	<LOQ	<LOQ	3.00	1.16	<LOQ	<LOQ	<LOQ	<LOQ	<LOQ

Table S6. Air equilibrated in-situ with soil/snow PCBs and OCPs concentrations (pg m^{-3}) (continuation)

pg m^{-3}	**F5S1**	**F5S2**	**F5S3**	**F5S4**	**F5S5**	**F5S6**	**F5S7**	**F5S8**	**F5S9**	**F5S10**
∑OCPs	9.66	8.52	11.07	11.13	17.64	9.15	8.71	22.70	6.40	10.76
HCB	9.66	8.52	11.07	11.13	11.16	9.15	8.71	18.67	6.40	10.76
∑HCH					3.24			2.01		
a-HCH	<LOQ	<LOQ	<LOQ	<LOQ	<LOQ	<LOQ	<LOQ	2.01	<LOQ	<LOQ
b-HCH	<LOQ	<LOQ	<LOQ	<LOQ	<LOQ	<LOQ	<LOQ	<LOQ	<LOQ	<LOQ
g-HCH	<LOQ	<LOQ	<LOQ	<LOQ	<LOQ	<LOQ	<LOQ	<LOQ	<LOQ	<LOQ
d-HCH	<LOQ	<LOQ	<LOQ	<LOQ	3.24	<LOQ	<LOQ	<LOQ	<LOQ	<LOQ
∑PCBs	49.36	31.38	44.14	66.01	45.43	9.96	42.05	73.42	27.29	14.04
PCB18	1.24	1.35	<LOQ	<LOQ	1.26	3.24	<LOQ	<LOQ	<LOQ	1.91
PCB17	<LOQ	0.45	0.19	0.32	2.76	0.41	0.17	0.75	<LOQ	<LOQ
PCB31+28	0.53	1.16	0.93	1.06	3.50	1.19	0.76	1.89	0.58	0.23
PCB52	9.95	11.02	12.31	15.04	<LOQ	<LOQ	25.20	58.98	<LOQ	<LOQ
PCB49	2.08	2.09	<LOQ	3.14	2.16	1.75	1.37	1.45	1.01	<LOQ
PCB44	<LOQ	<LOQ	<LOQ	<LOQ	<LOQ	<LOQ	<LOQ	1.81	<LOQ	<LOQ
PCB74	<LOQ	<LOQ	<LOQ	4.35	<LOQ	<LOQ	<LOQ	4.88	<LOQ	<LOQ
PCB70	20.36	<LOQ	<LOQ	<LOQ	<LOQ	<LOQ	<LOQ	<LOQ	<LOQ	<LOQ
PCB95	<LOQ	<LOQ	<LOQ	<LOQ	<LOQ	<LOQ	<LOQ	3.67	<LOQ	<LOQ
PCB99+101	0.83	0.57	2.69	1.87	3.27	0.68	1.92	<LOQ	1.60	1.26
PCB87	1.81	1.67	3.60	2.65	2.56	<LOQ	<LOQ	<LOQ	<LOQ	<LOQ
PCB110	<LOQ	<LOQ	0.28	<LOQ	<LOQ	<LOQ	<LOQ	<LOQ	<LOQ	<LOQ
PCB82	<LOQ	<LOQ	<LOQ	<LOQ	<LOQ	<LOQ	<LOQ	<LOQ	<LOQ	<LOQ
PCB151	8.35	8.18	14.87	8.77	11.41	<LOQ	0.69	<LOQ	<LOQ	<LOQ
PCB149	<LOQ	<LOQ	1.34	<LOQ	0.97	0.80	3.37	<LOQ	14.76	3.51
PCB118	<LOQ	<LOQ	<LOQ	<LOQ	<LOQ	1.11	<LOQ	<LOQ	<LOQ	<LOQ
PCB153	<LOQ	<LOQ	<LOQ	<LOQ	1.14	<LOQ	<LOQ	<LOQ	<LOQ	<LOQ

PCB132	3.97	3.12	<LOQ	<LOQ	4.86	<LOQ	<LOQ	<LOQ	<LOQ	<LOQ
PCB105	<LOQ	<LOQ	0.42	<LOQ	0.54	<LOQ	<LOQ	<LOQ	<LOQ	<LOQ
PCB138	0.05	0.06	0.06	<LOQ	<LOQ	<LOQ	<LOQ	<LOQ	2.58	0.41
PCB158	<LOQ	0.05	0.10	<LOQ	<LOQ	<LOQ	0.08	<LOQ	<LOQ	<LOQ
PCB187	<LOQ	0.84	1.31	0.87	1.03	<LOQ	3.90	<LOQ	4.09	3.66
PCB183	<LOQ	<LOQ	<LOQ	<LOQ	<LOQ	0.50	<LOQ	<LOQ	<LOQ	<LOQ
PCB128	<LOQ	<LOQ	0.12	0.30	0.53	<LOQ	0.10	<LOQ	<LOQ	0.05
PCB177	<LOQ	0.29	2.28	8.64	0.54	0.03	1.28	<LOQ	<LOQ	0.12
PCB156	<LOQ	<LOQ	<LOQ	<LOQ	2.43	<LOQ	<LOQ	<LOQ	0.40	<LOQ
PCB171	<LOQ	<LOQ	0.22	0.42	<LOQ	<LOQ	<LOQ	<LOQ	<LOQ	<LOQ
PCB180	<LOQ	0.20	2.16	9.95	0.96	0.24	1.58	<LOQ	<LOQ	0.12
PCB191	<LOQ	<LOQ	<LOQ	2.30	<LOQ	<LOQ	<LOQ	<LOQ	<LOQ	<LOQ
PCB169	0.17	0.33	0.90	3.55	0.63	<LOQ	1.62	<LOQ	2.10	2.46
PCB170	<LOQ	<LOQ	0.37	1.21	2.04	<LOQ	<LOQ	<LOQ	0.16	0.31
PCB201/199	<LOQ	<LOQ	<LOQ	1.56	2.84	<LOQ	<LOQ	<LOQ	<LOQ	<LOQ

Table S7. PCBs and OCPs Ln f_s/f_a ratios

Ln f_s/f_a	**F1-1**	**F1-2**	**F1-4**	**F1-6**	**F1-7**	**F1-8**	**F1-9**	**F1-10**	**F1-11**	**F2-1**	**F2-3**	**F2-4**	**F2-5**	**F2-7**	**F2-8**	**F2-9**	**F2-11**
HCB	1.68	2.18	2.05	2.07	1.29	1.82	1.61	1.22	1.64	1.11	-0.38	-0.01	-0.35	0.14	-0.04	0.25	-3.29
PCB18	0.93	0.76		1.77	0.74	0.62		-0.36	1.39	0.53			1.98		0.44	2.03	
PCB17	0.88	1.13	-0.29	1.10	1.58	0.73	1.77			-0.66	0.57				0.16		
PCB31+28	2.84	1.90	1.57			4.13		-0.60	1.40	1.18	2.42	1.31	2.60		3.73	3.39	
PCB52	0.41	-0.13	1.55		2.11					-0.99	-1.71	-0.06	-1.45		-0.24		-2.75
PCB49										-1.60	-1.20		-0.32		-0.54		
PCB74																	
PCB70										0.01							
PCB99+101	1.43			2.07		-0.43	0.65			-0.41		0.93			0.37		-0.87
PCB87		0.39	0.62								0.57	-0.18	1.89				
PCB110		0.17								-0.46							
PCB151	-0.52	0.14	0.29							-0.77	0.25	-0.29	0.34				
PCB149	-0.41	0.58	0.54	0.46	0.56	-0.56	-1.22	-1.16	-0.68	-0.56		-0.25	0.41	0.00	0.00	-0.13	-0.68
PCB118			-1.76														
PCB153		0.69															
PCB132	-1.37	-1.12		-1.35						0.24	-1.01	-0.55			-1.50		
PCB138						-0.20											
PCB158							-1.66		-1.26								
PCB187	-0.90		0.66			-0.14	-0.94	-0.24	-0.44		1.38	-2.11			-0.92	0.80	
PCB183																	
PCB128		0.94	1.71								2.44						
PCB177		2.20	1.69		3.28	-2.14					2.53		0.87				
PCB156																	
PCB171						0.46								1.78			
PCB180		2.76	1.33	-0.74		-1.05	-1.60		-0.97		2.32	-0.97	0.54		-0.73		

PCB191		1.13	0.39								1.56						
PCB169	-1.38	1.75					-0.89	0.20	0.06		1.06	-2.45		-0.18	-0.76	0.02	0.93
PCB170			1.70			0.37	0.00		1.33						0.30		
PCB201/199																	

Table S7. PCBs and OCPs Ln f_s/f_a ratios (continuation)

Ln f_s/f_a	**F3-1**	**F3-2**	**F3-3**	**F3-4**	**F3-5**	**F3-6**	**F3-7**	**F3-8**	**F3-9**	**F3-10**	**F3-11**	**F4-1**	**F4-2**	**F4-3**	**F4-4**	**F4-5**	**F4-6**	**F4-7**	**F4-8**	**F4-9**
HCB	1.11	0.09	-1.14	0.11	-0.94	-2.02	-1.19	0.09	-0.12	1.29	0.14	-0.11	-0.36	-1.92	-0.05	-0.23	0.01	1.46	-0.03	-0.28
PCB18	0.53										0.06	0.41		-1.36			-0.38	-0.23		
PCB17	-0.66					1.78							0.85	0.29						
PCB31+28	1.18	0.98	2.89		-1.38		-0.18						0.76	0.34	0.94	-1.13		-1.65	0.17	
PCB52	-0.99	-0.03	-2.41	-1.28	-1.36	0.16			-1.03			3.34	1.55		4.67					
PCB49	-1.60	-0.01							0.66			-0.11			-1.01					
PCB74														-0.64	-0.42					
PCB70	0.01																			
PCB99+101	-0.41	0.36			0.54		-0.65								0.25		-1.16	0.48	-0.45	-0.89
PCB87		0.22	0.71	0.17	-0.51								0.07	0.05	0.03	-0.39				
PCB110	-0.46													-1.49						
PCB151	-0.77	-0.12	-0.22	-0.26	-0.60							-0.11	-0.38	0.71	0.02	-0.18		-0.59		
PCB149	-0.56	0.28	0.52	0.56	-0.62	1.13	0.08	0.20	0.92	0.47	1.30	1.40	0.25	-0.49	0.50	0.88	0.01	0.59	-0.38	0.17
PCB118																				
PCB153		0.17						-0.06					-0.84	0.22						
PCB132	0.24	-0.03	-0.19			-0.77		0.65				0.44	-1.57			0.61	-0.30			-1.22
PCB138					-1.65			-0.61						-0.15				3.59	-1.36	
PCB158																		-0.51		
PCB187		0.09			-0.05		0.52	-0.58	0.49	-0.03				0.15				-0.03	0.14	-0.12
PCB183														0.50						
PCB128							-0.66											-0.61		
PCB177		1.23		2.44	-2.79		-0.42					-0.05	0.75	0.05	2.27			0.92	-4.32	
PCB156														-1.32						
PCB171							-0.24	0.19				1.05							-0.60	
PCB180		0.28		1.68	-2.23	2.99	-0.56	-2.33				1.30	-0.49	1.50	2.38	-4.30		0.33	-1.85	

PCB191						-0.51							1.69				-0.08		
PCB169	-0.95		0.61			-0.20	-0.04	0.77	-0.44					2.81			1.83	-0.28	0.19
PCB170			0.20			0.16	-0.64		-1.35				-1.82						
PCB201/199													-1.10						

Table S7. PCBs and OCPs Ln f_s/f_a ratios (continuation)

Ln f_s/f_a	**F5-1**	**F5-2**	**F5-3**	**F5-4**	**F5-5**	**F5-6**	**F5-7**	**F5-8**	**F5-9**	**F5-10**
HCB	-0.57	-0.26	-0.45	0.15	0.22	-0.33	-0.21	0.17	-0.18	0.39
PCB18	-2.13	-0.49				0.40				0.39
PCB17			0.21		1.12	-0.38	-1.05	-0.19		
PCB31+28	-2.20	0.82	2.01	-0.62	1.68		0.01		0.03	
PCB52	0.04	0.28	1.52	1.14						
PCB49								-0.25		
PCB74				-0.28						
PCB70	0.23									
PCB99+101	-1.81			0.73		0.36	-0.25			-0.50
PCB87	-0.11	-0.64	0.40	-0.15	0.45					
PCB110										
PCB151	1.90	-0.65	0.14	-0.67	0.43					
PCB149			-0.70		0.01	-0.59	-0.59		0.48	-0.42
PCB118										
PCB153										
PCB132	0.54	0.57								
PCB138	-1.06	1.09							1.21	-2.28
PCB158		0.86					1.55			
PCB187			0.35				0.36		-0.39	0.23
PCB183										
PCB128				-0.55			-1.91			
PCB177		-3.16		-0.19	-1.53	-1.37				
PCB156										
PCB171			-0.31	-0.22			-1.85			
PCB180		-3.75		-0.22	-1.40	0.15	-1.88			

PCB191				-0.20						
PCB169	-2.85	-2.45	-0.11	-0.07			0.20		0.00	0.46
PCB170				0.02	1.33					
PCB201/199				-0.48						

Table S8. PCBs and OCPs surface snow concentrations (pg L^{-1})

pg L^{-1}	**S1**	**S2**	**S3**	**S4**	**S5**	**S6**	**S7**	**S8**	**S9**	**S10**
∑OCPs	8.36	32.26	6.60	25.66	44.32	25.2	29.4	36.75	21.33	36.29
HCB	6.26	8.59	4.96	11.94	15.49	5.50	8.87	11.00	5.74	5.32
∑HCH	2.10	23.67	1.64	13.72	28.83	19.70	20.53	25.75	15.60	30.97
a-HCH	<LOQ	<LOQ	<LOQ	<LOQ	<LOQ	<LOQ	<LOQ	<LOQ	<LOQ	1.10
b-HCH	2.10	19.05	<LOQ	9.36	<LOQ	13.95	17.99	25.75	15.60	23.58
g-HCH	<LOQ	4.62	1.64	4.36	20.26	3.20	2.53	<LOQ	<LOQ	2.61
d-HCH	<LOQ	<LOQ	<LOQ	<LOQ	8.57	2.55	<LOQ	<LOQ	<LOQ	3.68
∑PCBs	168.58	158.68	91.97	245.78	417.30	101.50	228.48	235.50	78.30	146.42
PCB18	<LOQ	3.59	<LOQ	5.54	<LOQ	<LOQ	<LOQ	<LOQ	<LOQ	<LOQ
PCB17	1.21	4.48	0.34	3.55	10.38	4.70	4.00	25.63	3.60	6.35
PCB31+28	6.84	8.54	3.62	6.51	<LOQ	1.05	10.95	3.63	3.88	9.87
PCB33	3.04	4.15	1.22	2.64	<LOQ	<LOQ	5.32	<LOQ	<LOQ	2.88
PCB52	23.37	25.68	27.33	45.94	140.20	18.80	31.88	54.50	13.45	16.35
PCB49	2.99	4.06	<LOQ	4.68	25.21	11.40	5.98	8.88	<LOQ	13.58
PCB44	5.05	9.48	3.07	9.74	42.50	10.50	11.81	30.88	9.33	37.42
PCB74	2.41	2.33	<LOQ	4.30	16.31	3.10	4.46	<LOQ	1.66	<LOQ
PCB70	8.09	8.82	3.45	15.55	11.53	4.50	14.19	9.63	3.11	2.41
PCB95	14.17	11.67	6.01	20.60	13.84	5.65	17.59	10.25	4.36	10.50
PCB99+101	34.50	33.94	15.43	49.76	67.55	20.35	51.80	41.13	14.22	17.66
PCB87	4.47	5.56	<LOQ	7.69	<LOQ	<LOQ	8.41	<LOQ	<LOQ	3.31
PCB110	6.44	5.37	2.35	9.68	8.07	2.80	8.36	4.25	2.75	2.34
PCB82	2.95	<LOQ	<LOQ	5.16	<LOQ	<LOQ	3.19	<LOQ	1.33	3.78
PCB151	4.92	2.47	2.27	4.46	5.27	1.95	3.95	2.88	1.58	1.17
PCB149	13.27	7.75	7.15	13.66	19.44	5.65	10.85	10.13	5.62	5.99
PCB118	7.46	6.91	3.11	12.37	12.03	3.45	9.93	7.50	3.60	3.38
PCB153	10.50	6.77	6.90	<LOQ	20.10	4.55	9.68	11.38	4.53	4.88
PCB132	2.86	1.21	1.22	<LOQ	3.95	1.10	1.57	2.00	1.09	1.34
PCB105	1.74	1.12	0.63	<LOQ	3.29	0.65	1.57	2.00	0.61	1.04
PCB138	5.59	<LOQ	3.07	7.53	<LOQ	<LOQ	5.12	5.00	<LOQ	<LOQ
PCB158	<LOQ	<LOQ	<LOQ	<LOQ	<LOQ	<LOQ	<LOQ	<LOQ	<LOQ	<LOQ
PCB187	1.79	0.89	2.06	1.78	5.11	<LOQ	1.52	<LOQ	0.97	0.74
PCB183	<LOQ	<LOQ	<LOQ	<LOQ	<LOQ	<LOQ	<LOQ	<LOQ	<LOQ	<LOQ
PCB128	<LOQ	2.15	<LOQ	2.96	0.66	<LOQ	1.42	3.00	0.73	0.17
PCB177	0.72	0.28	0.34	0.75	1.81	<LOQ	0.91	<LOQ	0.12	<LOQ
PCB156	<LOQ	<LOQ	<LOQ	<LOQ	<LOQ	<LOQ	<LOQ	<LOQ	<LOQ	0.13
PCB171	1.39	1.26	0.55	2.37	1.65	0.50	1.27	<LOQ	0.53	<LOQ
PCB180	2.32	<LOQ	1.85	2.69	8.40	0.80	2.23	2.63	1.09	1.14
PCB191	<LOQ	<LOQ	<LOQ	4.52	<LOQ	<LOQ	<LOQ	<LOQ	<LOQ	<LOQ
PCB169	<LOQ	<LOQ	<LOQ	<LOQ	<LOQ	<LOQ	<LOQ	<LOQ	<LOQ	<LOQ
PCB170	<LOQ	<LOQ	<LOQ	0.91	<LOQ	<LOQ	0.51	<LOQ	<LOQ	<LOQ
PCB201/199	<LOQ	<LOQ	<LOQ	<LOQ	<LOQ	<LOQ	<LOQ	<LOQ	<LOQ	<LOQ
PCB208	0.49	0.19	<LOQ	0.43	<LOQ	<LOQ	<LOQ	0.25	0.16	<LOQ
PCB195	<LOQ	<LOQ	<LOQ	<LOQ	<LOQ	<LOQ	<LOQ	<LOQ	<LOQ	<LOQ

PCB194	<LOQ	<LOQ	<LOQ	<LOQ	<LOQ	<LOQ	<LOQ	<LOQ	<LOQ	<LOQ
PCB205	<LOQ	<LOQ	<LOQ	<LOQ	<LOQ	<LOQ	<LOQ	<LOQ	<LOQ	<LOQ
PCB206	<LOQ	<LOQ	<LOQ	<LOQ	<LOQ	<LOQ	<LOQ	<LOQ	<LOQ	<LOQ
PCB209	<LOQ	<LOQ	<LOQ	<LOQ	<LOQ	<LOQ	<LOQ	<LOQ	<LOQ	<LOQ

Table S9. PCBs and OCPs correlations with snow density

Pearson Correlations

This study		Snow density
∑OCPs	Pearson Correlation	-,707*
	Sig. (2-tailed)	.022
	N	10
HCB	Pearson Correlation	-,761*
	Sig. (2-tailed)	.011
	N	10
g-HCH	Pearson Correlation	-,852*
	Sig. (2-tailed)	.015
	N	7
PCB33	Pearson Correlation	-,879*
	Sig. (2-tailed)	.021
	N	6
PCB52	Pearson Correlation	-,818**
	Sig. (2-tailed)	.004
	N	10
PCB49	Pearson Correlation	-,728*
	Sig. (2-tailed)	.041
	N	8
PCB74	Pearson Correlation	-,891**
	Sig. (2-tailed)	.007
	N	7
PCB99+101	Pearson Correlation	-,713*
	Sig. (2-tailed)	.021
	N	10
PCB153	Pearson Correlation	-,733*
	Sig. (2-tailed)	.025
	N	9
PCB105	Pearson Correlation	-,733*
	Sig. (2-tailed)	.025
	N	9
PCB187	Pearson Correlation	-,791*
	Sig. (2-tailed)	.020
	N	8
PCB177	Pearson Correlation	-,832*
	Sig. (2-tailed)	.020
	N	7
PCB180	Pearson Correlation	-,762*
	Sig. (2-tailed)	.017
	N	9
∑PCBs	Pearson Correlation	-,760*
	Sig. (2-tailed)	.011
	N	10

*. Correlation is significant at the 0.05 level (2-tailed).
**. Correlation is significant at the 0.01 level (2-tailed).

Pearson Correlations

Khairy et al., 2016		Snow density
a-HCH	Pearson Correlation	-,985**
	Sig. (2-tailed)	.000
	N	6
b-HCH	Pearson Correlation	-,997**
	Sig. (2-tailed)	.003
	N	4
g-HCH	Pearson Correlation	-,927**
	Sig. (2-tailed)	.008
	N	6
∑HCHs	Pearson Correlation	-,970**
	Sig. (2-tailed)	.001
	N	6
∑OCPs	Pearson Correlation	-,837*

	Sig. (2-tailed)	.019
	N	7
PCB11	Pearson Correlation	-,848*
	Sig. (2-tailed)	.016
	N	7
PCB28+31	Pearson Correlation	-,783*
	Sig. (2-tailed)	.037
	N	7
PCB66	Pearson Correlation	-,817*
	Sig. (2-tailed)	.025
	N	7
PCB77	Pearson Correlation	-,943**
	Sig. (2-tailed)	.001
	N	7
PCB118	Pearson Correlation	-,859*
	Sig. (2-tailed)	.013
	N	7
PCB114	Pearson Correlation	-,884**
	Sig. (2-tailed)	.008
	N	7
PCB105	Pearson Correlation	-,939**
	Sig. (2-tailed)	.002
	N	7
PCB126	Pearson Correlation	-,988**
	Sig. (2-tailed)	.001
	N	5
PCB182+187	Pearson Correlation	-,755*
	Sig. (2-tailed)	.050
	N	7
PCB180+193	Pearson Correlation	-,782*
	Sig. (2-tailed)	.038
	N	7
PCB169	Pearson Correlation	-,988*
	Sig. (2-tailed)	.012
	N	4

*. Correlation is significant at the 0.05 level (2-tailed).
**. Correlation is significant at the 0.01 level (2-tailed).

Table S10. PCBs and HCB net air-snow fluxes (ng m^{-2} d^{-1})

ng m^{-2} d^{-1}	S1	S2	S3	S4	S5	S6	S7	S8	S9	S10
HCB	0.34	0.97	0.07	-0.91	-1.58	-1.09	-0.83	-0.40	0.51	-0.51
PCB18		0.37								
PCB17		-0.16	0.41		0.56	0.60	0.07	-0.16		
PCB31+28	0.09	0.60	1.95	-0.08		1.22	0.16	0.29	0.05	-0.06
PCB52	-0.06	-1.76		-1.44	-2.25	0.33	1.48			
PCB49	-0.01	-0.73			0.77	0.43	0.51	0.13		0.28
PCB44						0.54				
PCB74						0.79				
PCB70		0.01		-0.18		1.09				
PCB95						0.14				
PCB99+101	0.12	-0.12	0.56		0.82	0.30	0.20	-0.09	-0.20	-0.47
PCB87	0.12						-0.17			
PCB110		-0.05			0.23	0.32	0.08			
PCB151	-0.26	-0.06	-0.07		-0.56		-1.24			
PCB149	0.51	-0.25	-0.03	-0.02	0.66	0.56	0.18	-0.07	-1.32	1.60
PCB118						0.39		0.44		
PCB153	0.19		0.59		0.27	1.50	-0.38			
PCB132	-0.05	0.16	0.35		-0.19	-1.78	-0.72	-0.12		-0.65
PCB138	0.06		0.13	-0.01			0.03	0.04		
PCB187	0.03		-0.07				0.21		0.38	-0.33
PCB128				-0.06	0.07		-0.12	0.01	0.01	0.08
PCB177	0.07			-0.86	0.26		-0.79		0.03	
PCB156										0.12
PCB171		0.01			0.20	0.11				
PCB180	0.004		-1.72	-0.80	0.25	1.17	-1.07	-0.01	0.03	-0.02
PCB170				-0.01						

Table S11. Plankton PCBs and OCPs concentrations (ng g_{dw}^{-1})

	P1	P2	P3	P4	P5	P6	P7	P8	P9	P10	P11	P12	P13	P14	P15	P16	P17	P18	P19	P20	P21	P22	P23	P24	P25	P26
∑OCPs	1.69	3.16	0.46	2.07	1.03	2.65	0.99	1.72	1.44	1.09	3.09	1.96	2.06	1.64	1.37	0.35	1.97	1.80	1.25	1.97	1.32	1.87	2.45	1.07	1.65	2.07
HCB	<LOQ	0.29	<LOQ	<LOQ	0.20	0.22	0.49	0.43	0.02	0.39	0.26	<LOQ	0.61	0.13	0.45	0.05	0.14	0.16	0.43	<LOQ	<LOQ	<LOQ	<LOQ	<LOQ	0.30	<LOQ
∑HCHs	1.69	2.87	0.46	2.07	0.83	2.43	0.50	1.28	1.42	0.70	2.83	1.96	1.44	1.51	0.92	0.30	1.83	1.64	0.82	1.97	1.32	1.87	2.45	1.07	1.36	2.07
a-HCH	0.53	0.86	<LOQ	0.55	<LOQ	<LOQ	0.26	0.59	0.49	0.29	0.22	0.77	0.58	<LOQ	0.41	<LOQ	0.32	0.43	<LOQ	0.57	0.52	0.92	1.11	0.49	0.60	<LOQ
b-HCH	<LOQ	<LOQ	<LOQ	<LOQ	<LOQ	<LOQ	<LOQ	<LOQ	<LOQ	<LOQ	<LOQ	<LOQ	<LOQ	<LOQ	<LOQ	<LOQ	<LOQ	<LOQ	<LOQ	<LOQ	<LOQ	<LOQ	<LOQ	<LOQ	<LOQ	<LOQ
g-HCH	0.50	0.90	<LOQ	0.68	<LOQ	1.05	<LOQ	<LOQ	0.45	0.16	2.36	<LOQ	0.38	0.71	<LOQ	<LOQ	1.18	0.68	0.36	0.47	0.34	<LOQ	<LOQ	<LOQ	0.36	0.93
d-HCH	0.66	1.11	0.46	0.84	0.83	1.38	0.25	0.69	0.47	0.25	0.26	1.18	0.49	0.80	0.51	0.30	0.33	0.52	0.46	0.92	0.46	0.95	1.34	0.58	0.40	1.15
∑PCBs	28.67	40.82	14.55	71.00	14.38	15.08	4.90	6.91	40.63	11.72	67.67	5.13	111.75	46.20	15.10	3.08	3.78	5.43	4.31	7.68	12.55	17.07	27.91	3.50	6.92	82.47
PCB18	<LOQ	<LOQ	<LOQ	0.50	<LOQ	<LOQ	<LOQ	<LOQ	<LOQ	<LOQ	2.81	<LOQ	<LOQ	<LOQ	<LOQ	<LOQ	1.15	0.20	<LOQ	<LOQ	<LOQ	<LOQ	<LOQ	<LOQ	<LOQ	<LOQ
PCB17	1.29	0.78	0.17	0.68	0.58	0.77	0.32	0.41	0.30	0.18	0.19	0.59	0.31	0.22	0.28	<LOQ	0.32	0.29	0.18	0.00	0.39	0.31	2.06	0.11	0.27	0.48
PCB31+28	<LOQ	<LOQ	<LOQ	0.05	<LOQ	<LOQ	<LOQ	<LOQ	<LOQ	0.03	0.08	<LOQ	<LOQ	<LOQ	<LOQ	<LOQ	<LOQ	<LOQ	<LOQ	<LOQ	<LOQ	<LOQ	<LOQ	<LOQ	<LOQ	<LOQ
PCB33	0.69	<LOQ	0.45	1.02	<LOQ	<LOQ	0.21	<LOQ	<LOQ	0.19	<LOQ	<LOQ	0.72	<LOQ	0.55	0.20	<LOQ	<LOQ	<LOQ	0.97	<LOQ	<LOQ	<LOQ	0.62	<LOQ	3.39
PCB52	2.79	<LOQ	2.10	3.86	4.46	3.48	<LOQ	1.72	2.46	0.81	1.55	<LOQ	2.47	4.27	1.08	1.01	<LOQ	<LOQ	<LOQ	3.67	1.12	6.12	12.09	1.09	1.85	9.87
PCB49	0.03	0.16	<LOQ	1.08	0.30	<LOQ	0.05	<LOQ	0.17	0.02	0.25	<LOQ	0.34	<LOQ	0.10	0.51	<LOQ	<LOQ	<LOQ	<LOQ	0.02	0.03	0.45	0.02	0.06	<LOQ
PCB44	0.05	<LOQ	<LOQ	0.39	0.10	<LOQ	<LOQ	0.53	0.13	0.00	0.15	<LOQ	0.14	0.10	0.08	<LOQ	<LOQ	<LOQ	<LOQ	<LOQ	0.10	0.07	0.22	<LOQ	<LOQ	0.31
PCB74	0.18	<LOQ	<LOQ	<LOQ	<LOQ	<LOQ	<LOQ	<LOQ	<LOQ	<LOQ	<LOQ	<LOQ	<LOQ	0.22	<LOQ	<LOQ	<LOQ	<LOQ	<LOQ	<LOQ	<LOQ	0.58	1.39	<LOQ	<LOQ	0.44
PCB70	0.32	0.57	0.74	0.68	0.35	0.61	0.07	0.21	0.21	0.14	0.17	0.48	0.34	0.32	0.28	<LOQ	0.16	0.02	0.19	0.07	0.32	3.78	0.22	0.24	0.21	0.44
PCB95	1.34	<LOQ	<LOQ	2.78	<LOQ	<LOQ	<LOQ	0.18	0.89	<LOQ	1.89	<LOQ	1.25	2.25	0.58	<LOQ	<LOQ	<LOQ	<LOQ	<LOQ	0.74	<LOQ	6.57	<LOQ	0.61	2.69
PCB99+101	2.29	<LOQ	<LOQ	8.87	<LOQ	<LOQ	0.57	<LOQ	<LOQ	0.96	7.31	<LOQ	3.83	<LOQ	1.51	<LOQ	<LOQ	1.28	<LOQ	<LOQ	1.39	<LOQ	<LOQ	<LOQ	<LOQ	<LOQ
PCB87	<LOQ	<LOQ	<LOQ	0.63	<LOQ	<LOQ	<LOQ	<LOQ	<LOQ	0.06	0.30	<LOQ	<LOQ	<LOQ	0.03	<LOQ	<LOQ	0.02	0.24	<LOQ	0.03	<LOQ	<LOQ	<LOQ	0.03	<LOQ
PCB110	0.21	0.08	0.11	1.44	0.18	<LOQ	0.06	0.05	0.23	0.14	0.59	0.11	0.14	0.06	0.15	<LOQ	0.04	0.13	0.04	<LOQ	0.27	<LOQ	<LOQ	0.02	0.17	<LOQ
PCB82	0.11	0.12	0.04	0.89	0.05	0.11	0.05	0.05	0.11	0.09	0.38	0.07	0.16	0.19	0.14	0.02	0.04	0.11	0.06	0.05	0.17	0.07	0.11	0.04	0.09	0.13
PCB151	0.74	1.35	0.39	1.65	0.35	0.17	0.18	0.11	1.06	0.33	3.83	0.15	4.31	2.02	0.58	0.05	0.07	0.20	0.19	0.05	0.30	0.24	0.33	0.05	0.20	1.06
PCB149	2.48	4.02	1.51	6.61	3.17	0.94	0.58	0.66	3.92	1.09	10.72	0.81	11.28	8.76	1.87	0.41	0.25	0.68	0.61	0.35	1.27	2.72	2.17	0.53	0.86	5.64
PCB118	<LOQ	0.04	<LOQ	2.83	0.05	0.11	0.02	0.02	0.15	0.27	0.96	0.11	0.36	<LOQ	0.25	<LOQ	0.01	0.11	0.04	<LOQ	0.30	0.20	<LOQ	<LOQ	0.07	0.09

PCB153	2.45	5.04	1.39	7.40	1.18	1.22	0.55	0.66	6.08	1.26	10.11	0.55	10.70	7.13	1.56	<LOQ	0.35	0.58	0.73	0.37	1.20	0.44	0.11	0.02	0.61	8.37
PCB132	0.34	0.41	0.04	2.05	<LOQ	0.11	0.09	0.02	0.89	0.26	1.62	0.11	1.44	1.22	0.39	0.01	0.05	0.09	0.04	<LOQ	0.34	<LOQ	<LOQ	<LOQ	0.09	0.48
PCB105	<LOQ	0.12	<LOQ	0.55	<LOQ	0.28	0.15	0.11	0.06	0.10	0.14	0.18	<LOQ	0.10	0.08	<LOQ	0.05	0.05	0.06	0.35	0.15	0.17	0.17	0.11	0.09	<LOQ
PCB138	1.21	2.62	0.72	5.64	0.48	0.66	0.30	0.32	3.35	0.88	4.89	0.22	4.91	3.31	0.92	0.14	0.20	0.36	0.31	0.22	0.76	0.27	<LOQ	0.02	0.39	5.11
PCB158	0.21	0.45	0.15	0.71	0.25	0.17	0.06	0.18	0.42	0.12	0.50	0.07	0.69	0.45	0.27	0.04	0.07	0.09	0.07	0.10	0.17	0.17	0.11	0.02	0.10	0.57
PCB187	1.82	3.81	1.17	2.41	0.45	0.99	0.36	0.34	4.26	0.64	4.86	0.22	11.50	3.56	0.90	0.15	0.20	0.31	0.37	0.42	0.69	0.37	0.22	0.11	0.31	7.00
PCB183	0.87	1.89	0.46	1.31	0.23	0.28	0.15	0.14	2.01	0.40	2.17	<LOQ	4.91	1.80	0.45	0.19	0.04	0.09	0.12	0.05	0.27	0.10	<LOQ	<LOQ	0.10	3.22
PCB128	0.05	0.04	<LOQ	1.08	<LOQ	<LOQ	0.01	<LOQ	0.17	0.11	0.30	<LOQ	0.22	0.13	0.08	<LOQ	<LOQ	<LOQ	<LOQ	<LOQ	0.07	<LOQ	<LOQ	<LOQ	<LOQ	0.13
PCB177	0.92	1.68	0.39	1.42	<LOQ	<LOQ	0.12	<LOQ	2.03	0.34	1.98	<LOQ	5.31	1.57	0.37	<LOQ	<LOQ	<LOQ	<LOQ	<LOQ	0.24	<LOQ	<LOQ	<LOQ	<LOQ	3.92
PCB156	0.32	0.66	0.15	0.66	<LOQ	<LOQ	<LOQ	<LOQ	0.72	0.15	0.71	<LOQ	1.79	0.55	0.13	<LOQ	<LOQ	<LOQ	<LOQ	<LOQ	<LOQ	<LOQ	<LOQ	<LOQ	<LOQ	1.32
PCB171	0.13	0.37	0.07	0.94	<LOQ	<LOQ	<LOQ	0.02	0.28	0.19	0.33	<LOQ	0.40	0.16	0.07	<LOQ	<LOQ	0.04	<LOQ	0.02	<LOQ	0.03	<LOQ	<LOQ	<LOQ	0.44
PCB180	3.87	7.46	2.06	7.09	1.03	2.38	0.49	0.48	6.27	1.45	5.25	0.33	20.65	4.21	1.20	0.20	0.32	0.32	0.46	0.30	1.05	0.37	0.39	0.07	0.34	15.59
PCB191	0.16	0.04	0.06	<LOQ	0.15	<LOQ	<LOQ	<LOQ	0.04	<LOQ	0.06	<LOQ	0.34	<LOQ	<LOQ	<LOQ	<LOQ	<LOQ	<LOQ	<LOQ	<LOQ	<LOQ	<LOQ	<LOQ	<LOQ	0.26
PCB169	<LOQ	<LOQ	<LOQ	<LOQ	<LOQ	<LOQ	<LOQ	<LOQ	<LOQ	<LOQ	<LOQ	<LOQ	<LOQ	<LOQ	<LOQ	<LOQ	<LOQ	<LOQ	<LOQ	0.02	<LOQ	<LOQ	<LOQ	<LOQ	<LOQ	<LOQ
PCB170	1.58	3.03	0.78	2.89	0.25	0.83	0.17	0.14	2.14	0.70	1.85	0.11	7.98	1.41	0.45	0.04	0.08	0.07	0.13	0.05	0.44	0.03	<LOQ	<LOQ	0.11	5.55
PCB201/199	0.95	1.68	0.46	0.84	0.05	0.22	0.07	0.00	0.97	0.27	0.77	<LOQ	5.70	0.51	0.17	<LOQ	<LOQ	<LOQ	0.03	<LOQ	0.14	<LOQ	<LOQ	<LOQ	<LOQ	2.38
PCB208	0.00	2.09	0.50	0.71	0.55	1.38	0.16	0.53	0.49	0.18	0.25	1.00	0.81	1.25	0.39	0.11	0.30	0.41	0.36	0.60	0.44	0.99	1.28	0.45	0.36	1.54
PCB195	0.34	0.61	0.17	0.39	0.03	0.06	0.02	0.00	0.32	0.10	0.26	<LOQ	2.51	0.19	0.06	<LOQ	<LOQ	<LOQ	0.03	<LOQ	0.05	<LOQ	<LOQ	<LOQ	<LOQ	0.84
PCB194	0.92	1.68	0.46	0.92	0.13	0.33	0.08	0.02	0.49	0.28	0.43	<LOQ	5.27	0.22	0.11	<LOQ	0.11	<LOQ	0.03	<LOQ	0.12	<LOQ	<LOQ	<LOQ	<LOQ	1.19
PCB205	<LOQ	<LOQ	<LOQ	<LOQ	<LOQ	<LOQ	<LOQ	<LOQ	<LOQ	<LOQ	<LOQ	<LOQ	0.20	<LOQ	<LOQ	<LOQ	<LOQ	<LOQ	<LOQ	<LOQ	<LOQ	<LOQ	<LOQ	<LOQ	<LOQ	<LOQ
PCB206	<LOQ	<LOQ	<LOQ	<LOQ	<LOQ	<LOQ	<LOQ	<LOQ	<LOQ	<LOQ	<LOQ	<LOQ	0.76	<LOQ	<LOQ	<LOQ	<LOQ	<LOQ	<LOQ	<LOQ	<LOQ	<LOQ	<LOQ	<LOQ	<LOQ	<LOQ
PCB209	<LOQ	<LOQ	<LOQ	<LOQ	<LOQ	<LOQ	<LOQ	<LOQ	<LOQ	<LOQ	<LOQ	<LOQ	<LOQ	<LOQ	<LOQ	<LOQ	<LOQ	<LOQ	<LOQ	<LOQ	<LOQ	<LOQ	<LOQ	<LOQ	<LOQ	<LOQ

Table S12. Gross diffusive absorption fluxes of PCBs and HCB to coastal seawater (pg m^{-2} d^{-1})

pg m^{-2} d^{-1}	**SW1**	**SW2**	**SW3**	**SW4**	**SW5**	**SW6**	**SW7**	**SW8**	**SW9**	**SW10**	**SW11**	**SW12**	**SW13**	**SW14**	**SW15**	**SW16**	**SW17**	**SW18**	**SW19**	**SW20**	**SW21**	**SW22**	**SW23**	**SW24**	**SW25**	**SW26**
PCB18																	-182	-666	-490					-47	-101	-64
PCB17	-4.5	-2.9			-7.0	-34	-20	-6.2	-6.7	-6.2	-70	-9.3	-15	-9.3	-22	-14	-4.2	-16	-11							
PCB28	-1.8	-1.2	-4.3	-17				-11	-12	-11				-5.8	-14	-8.9	-11	-42	-31							
PCB52	-66	-43	-213	-815	-109	-544	-320	-45	-49	-45	-212	-27	-44							-194	-153			-4.1	-9.1	-5.7
PCB49	-14	-9			-23	-116	-67										-29	-113	-81	-23	-18					
PCB44																										
PCB74																	-71	-278	-200							
PCB70	-106	-69																								
PCB95			-20	-80							-107	-13	-21													
PCB99	-3	-2						-1.9	-2.0	-1.9				-15	-37	-23	-7.6	-30	-22	-16	-13					
PCB87	-16	-10	-40	-155	-19	-97	-57	-16	-17	-16				-15	-35	-22										
PCB110																										
PCB82																										
PCB151	-41	-26	-127	-512	-61	-314	-182	-43	-47	-43																
PCB149	-41	-26	-63	-246	-18	-89	-52	-55	-60	-56	-144	-18	-30	-55	-134	-85	-100	-385	-278	-200	-157	-833	-1101	-78	-173	-107
PCB118																										
PCB153	-64	-42															-23	-82	-61							
PCB132	-75	-50	-128	-468	-59	-284	-170	-82	-89	-83	-1077	-147	-239				-48	-175	-128			-143	-186			
PCB105																										
PCB138			-1.1	-3.3				-24	-26	-24				-195	-396	-277	-36	-110	-85							
PCB158	-0.69	-0.46															-37	-121	-92			-88	-111			
PCB187	-40	-27						-40	-43	-41				-72	-146	-102	-206	-638	-491	-136	-112	-439	-548			
PCB183								-21	-22	-21																
PCB128											-36	-11	-15	-73	-120	-94	-113	-253	-210			-176	-206			
PCB177	-6.3	-4.5			-30	-97	-67	-402	-426	-403	-99	-24	-34	-739	-1331	-988	-266	-690	-556			-110	-132	-7.2	-13	-9.2

PCB156																-168	-405	-331								
PCB171	-2.1	-1.5						-11	-12	-11				-34	-68	-48	-4.6	-14	-11			-55	-67			
PCB180	-6.0	-4.8			-160	-349	-272	-837	-871	-839	-183	-69	-88	-1335	-2010	-1626	-754	-1471	-1256			-156	-179			
PCB191								-222	-230	-223				-295	-431	-354	-208	-384	-331							
PCB169	-56	-48	-46	-80	-152	-280	-227	-236	-243	-236				-240	-340	-283	-183	-317	-276	-133	-121	-1230	-1390			
PCB170					-63	-114	-93	-61	-63	-61				-28	-39	-33	-159	-271	-237			-348	-393			
PCB201/199																										
∑PCBs	-543	-369	-643	-2376	-701	-2318	-1529	-2116	-2218	-2122	-1929	-318	-487	-3112	-5123	-3957	-2610	-6461	-5179	-703	-573	-3579	-4313	-136	-297	-186
HCB	-165	-108	-251	-944	-91	-449	-266	-182	-197	-183	-937	-123	-201	-381	-904	-579	-252	-943	-689	-595	-469	-207	-270	-209	-458	-287

Table S13. Gross diffusive volatilization fluxes of PCBs and HCB from coastal seawater (pg m^{-2} d^{-1})

pg m^{-2} d^{-1}	SW1	SW2	SW3	SW4	SW5	SW6	SW7	SW8	SW9	SW10	SW11	SW12	SW13	SW14	SW15	SW16	SW17	SW18	SW19	SW20	SW21	SW22	SW23	SW24	SW25	SW26
PCB18			13			95		12			138		64		236	111	99				1234	272	434	354		113
PCB17			68	1596	23	61	22	13	3.8	11	254	49	45	159	498	282	268	265	298	141	132	987	335	552	180	85
PCB28			183												251		224	463	502		213	652		137	240	
PCB52	159	24	714	838	113	645	281	141	202	182	1210	135	176	199	906	549	359	2219	3745	3208	915	1544	1849	514	901	337
PCB49	17		107		27	128											441		211	118	127	204		47	116	
PCB44				125	31	110	33	20	14		135	18	25	14	95	39		61	3403	33	98	130	123	25	84	20
PCB74			90		15	95			23			17						145	188							
PCB70	43		241		57	302	86	57	51	27	364	44	72	54	231	105	84	353	529	101	165	367	274	68	169	69
PCB95			683		119	653	206	157	98	46	1090	120	160	165	771	299	239	461	707	244	281	1080	585	211	418	141
PCB99	604	152	2424	3245	498	2924	1126	785	651	431	3967	431	619	673	2764	1363	1055	2085	2326	1285	1148	4033	2964	774	1731	815
PCB87			135		33	188																				
PCB110			217		53	231	75	58	32	12	416	46	62	58	262	118	125	208	241	101	119	366	196	70	188	59
PCB82			143		23	113		34			244	32	42		165		81		165			267		51	113	
PCB151	115	38	666	604	151	786	307	262	139	94	1107	134	165	213	932	399	360	748	879	364	377	1729	1185	309	648	261
PCB149	190	77	1793	1476	400	1863	767	683	338	201	3061	412	471	621	2224	1114	1192	2305	2560	986	1176	4496	3240	872	1748	634
PCB118			253		54	257	113	82	63		437	64	83		265	151	257		1342		160	485		91	215	
PCB153	448		1467	2067	379	1649	847	684	461	371	2210	352	473	535	1708	953	904	2210	2575	955	1057	3786	2960	706	1487	665
PCB132		117	259		42	165	80	74	18		587	86	94	106	342	180	227	394	526	88	199	790	244	151	252	33
PCB105		31	42		6.8	30	13	12	5.7		70	13	18	16	43	29	52	41	43	18	29	94		19	30	
PCB138	54		544	343	136	487	256	226	116	56	759	152	182	187	504	323	408	731	801	246	382	1243	715	275	500	195
PCB158			63		15	68	33	28	15		93	17	22	24	67	41	51	86	79		46	160	86	30	65	26
PCB187	65		256	274	83	268	153	146	71	75	381	70	89	92	290	170	192	472	376	166	217	718	646	143	287	127
PCB183	29		110	109	34	106	62	61	32	32	150	29	38		112	71	72	187	144		89	285	268	60	116	54
PCB128			12		1.2	3.8	2.0	2.7			17	5.8	6.2	4.2	8.7	5.3	14	14	22		10	34		8.0	10	
PCB177	4.8	3.0	74	27	24	58	37	35	13	6.2	94	22	25	21	60	41	61	132	109	31	60	183	111	42	73	24

PCB156	1.5		20	4.5	7.1	15	8.9	9.4	2.7	1.3	22	5.5	6.7	4.6	14	10	12	34	22	6.6	17	44	31	11	18	7.0
PCB171			45		13	43	23	16	9.2		69	15	18	14	45	35	30	68	67		35	94	41	22	50	19
PCB180	28	11	91	67	43	66	55	59	30	29	76	31	34	26	56	44	77	152	121	49	75	201	163	53	85	44
PCB191		0.45	0.61		0.29							0.19										1.0				
PCB169			3.3																							
PCB170		0.58	8.3	1.6	4.6	5.4	3.9	5.3	1.5	0.6	7.5	3.7	3.7	2.3	4.5	3.8	9.7	16	12	2.8	6.8	18	12	5.9	7.7	3.5
PCB201/199	0.40	0.15	1.6	0.52	1.22	1.01	0.83	0.94	0.37	0.44	0.93	0.44	0.48	0.22	0.72	0.50	1.2	3.0	1.4	0.80	1.11	3.1	3.0	0.78	1.1	0.61
∑PCBs	1757	454	10724	10778	2388	11417	4592	3666	2392	1574	16958	2304	2996	3190	12854	6437	6894	13854	21997	8146	8368	24268	16464	5606	9732	3729
HCB	145		295	692	76	540	215	124	124	118	539	88	140		707	294	885	682	825	486	297	928	1387	295	430	249

Table S14. PCBs and HCB net air-seawater diffusive fluxes (pg m^{-2} d^{-1}). Negative values mean net absorption fluxes.

pg m^{-2} d^{-1}	SW1	SW2	SW3	SW4	SW5	SW6	SW7	SW8	SW9	SW10	SW11	SW12	SW13	SW14	SW15	SW16	SW17	SW18	SW19	SW20	SW21	SW22	SW23	SW24	SW25	SW26
PCB18			13			95		12			138		64		236	111	-83	-666	-490		1234	272	434	308	-101	49
PCB17	-4.5	-2.9	68	1596	16	27	1.7	6.9	-2.8	4.5	184	40	30	150	476	267	264	250	287	141	132	987	335	552	180	85
PCB28	-1.8	-1.2	179	-17				-11	-12	-11				-5.8	237	-8.9	213	421	472		213	652		137	240	
PCB52	93	-19	501	24	3.8	101	-39	96	153	137	998	108	132	199	906	549	359	2219	3745	3014	762	1544	1849	510	892	331
PCB49	3.0	-9.3	107		4.3	12	-67										412	-113	130	95	108	204		47	116	
PCB44				125	31	110	33	20	14		135	18	25	14	95	39		61	3403	33	98	130	123	25	84	20
PCB74			90		15	95			23			17					-71	-133	-12							
PCB70	-64	-69	241		57	302	86	57	51	27	364	44	72	54	231	105	84	353	529	101	165	367	274	68	169	69
PCB95			663	-80	119	653	206	157	98	46	982	107	139	165	771	299	239	461	707	244	281	1080	585	211	418	141
PCB99	601	150	2424	3245	498	2924	1126	783	649	429	3967	431	619	659	2727	1340	1047	2055	2305	1269	1135	4033	2964	774	1731	815
PCB87	-16	-10	95	-155	14	91	-57	-16	-17	-16				-15	-35	-22										
PCB110			217		53	231	75	58	32	12	416	46	62	58	262	118	125	208	241	101	119	366	196	70	188	59
PCB82			143		23	113		34			244	32	42		165		81		165			267		51	113	
PCB151	74	12	539	92	90	471	125	219	92	51	1107	134	165	213	932	399	360	748	879	364	377	1729	1185	309	648	261
PCB149	149	51	1730	1229	383	1774	715	628	278	146	2917	394	441	566	2090	1030	1092	1920	2281	786	1019	3663	2139	795	1574	526
PCB118			253		54	257	113	82	63		437	64	83		265	151	257		1342		160	485		91	215	
PCB153	384	-42	1467	2067	379	1649	847	684	461	371	2210	352	473	535	1708	953	881	2128	2514	955	1057	3786	2960	706	1487	665
PCB132	-75	67	130	-468	-17	-119	-90	-7.7	-71	-83	-491	-61	-145	106	342	180	180	219	398	88	199	647	58	151	252	33
PCB105		31	42		6.8	30	13	12	5.7		70	13	18	16	43	29	52	41	43	18	29	94		19	30	
PCB138	54		543	339	136	487	256	201	90	31	759	152	182	-8.7	108	46	372	621	716	246	382	1243	715	275	500	195
PCB158	-0.69	-0.46	63		15	68	33	28	15		93	17	22	24	67	41	14	-34	-13		46	72	-25	30	65	26
PCB187	25	-27	256	274	83	268	153	106	28	34	381	70	89	20	143	68	-14	-166	-116	30	105	279	99	143	287	127
PCB183	29		110	109	34	106	62	40	10	11	150	29	38		112	71	72	187	144		89	285	268	60	116	54
PCB128			12		1.2	3.8	2.0	2.7			-19	-5.1	-8.8	-69	-112	-88	-99	-239	-188		10	-142	-206	8.0	9.8	
PCB177	-1.5	-1.6	74	27	-5.9	-39	-31	-367	-413	-397	-6	-1.6	-9.5	-718	-1271	-947	-205	-558	-446	31	60	73	-21	35	60	15

PCB156	1.5		20	4.5	7.1	15	8.9	9.4	2.7	1.3	22	5.5	6.7	4.6	14	9.7	-156	-371	-309	6.6	17	44	31	11	18	7
PCB171	-2.1	-1.5	45		13	43	23	5.0	-2.9	-11	69	15	18	-20	-23	-13	26	55	56		35	39	-27	22	50	19
PCB180	22	5.9	91	67	-117	-283	-217	-778	-840	-810	-108	-38	-53	-1309	-1953	-1582	-676	-1320	-1135	49	75	45	-17	53	85	44
PCB191		0.45	0.61		0.3			-222	-230	-223		0.19		-295	-431	-354	-208	-384	-331			0.97				
PCB169	-56	-48	-43	-80	-152	-280	-227	-236	-243	-236				-240	-340	-283	-183	-317	-276	-133	-120.68	-1230	-1390			
PCB170		0.58	8.3	1.6	-59	-108	-89	-56	-61	-61	7.5	3.7	3.7	-26	-35	-29	-150	-256	-225	2.8	6.8	-331	-381	5.9	7.7	3.5
PCB201/199	0.40	0.15	1.6	0.52	1.2	1.0	0.83	0.94	0.37	0.44	0.93	0.44	0.48	0.22	0.72	0.50	1.22	3.00	1.4	0.80	1.1	3.1	3.0	0.78	1.1	0.61
∑PCBs	1214	85	10082	8402	1687	9100	3063	1550	174	-548	15029	1987	2510	78	7731	2480	4285	7393	16818	7443	7795	20688	12151	5470	9435	3543
HCB	-20	-110	44	-250	-15	91	-50	-59	-73	-65	-400	-35	-61	-380	-200	-290	630	-260	140	-110	-170	720	1100	86	-28	-38

Figure S1. PCB-149 and PCB-187 ambient air and air equilibrated in-situ with soil/snow correlations with temperature

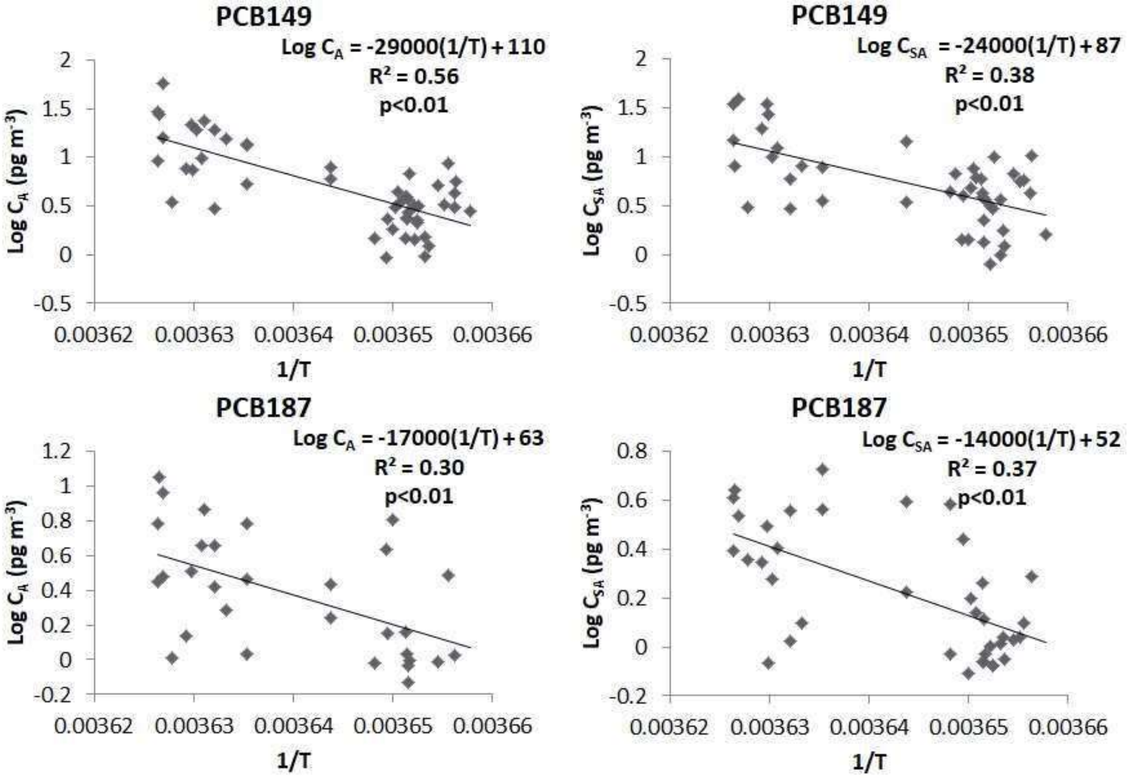

Figure S2. PCBs Ln f_s/f_a ratios versus Log K_{OA} bare soil and soil with vegetation

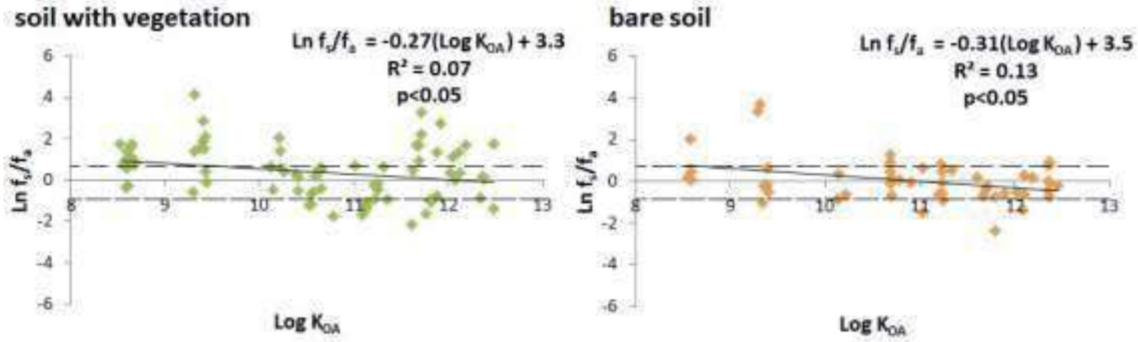

Figure S3. HCB Ln f_s/f_a ratios versus Log K_{OA}

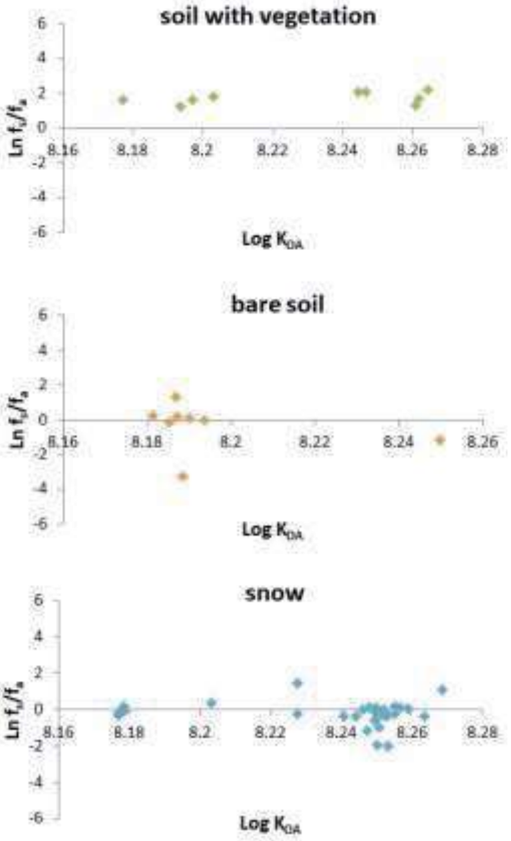

References

Hansen, K.M., Halsall, C.J., Christensen, J.H., 2006. A Dynamic Model To Study the Exchange of Gas-Phase Persistent Organic Pollutants between Air and a Seasonal Snowpack. Environ. Sci. Technol. 40, 2644–2652. doi:10.1021/es051685b

Schwarzenbach, R.P., Gschwend, P.M., Imboden, D.M., 2005. Environmental Organic Chemistry. John Wiley & Sons.

8.5 Bibliografia

Ahrens, L.; Marusczak, N.; Rubarth, J.; Dommergue, A.; Nedjai, R.; Ferrari, C.; Ebinghaus, R. **2010**. Distribution of perfluoroalkyl compounds and mercury in fish liver from high-mountain lakes in France originating from atmospheric deposition. *Environ. Chem*. 7, 422

Armitage, J.; Cousins, I. T.; Buck, R.C.; Prevedouros, K.; Russell, M.H.; Macleod, M.; Korzeniowski, S.H. **2006**. Modeling global-scale fate and transport of perfluorooctanoate emitted from direct sources. *Environ. Sci. Technol*. 40, 6969

Arnot, J.; Gobas, F. **2006**. A review of bioconcentration factor (BCF) and bioaccumulation factor (BAF) assessments for organic chemicals in aquatic organisms. *Environ. Rev*. 14 (4), 257-297.

Bamford, H.; Poster, D.; Backer, J. **1999**. Temperature dependence of Henry's law constant of thirteen polycyclic aromatic hydrocarbons between 4ºC and 31ºC. *Environ. Tox. Chem.* 18 (9) 1905-1912.

Baker, J.I.; Hites, R.A. **1999**. Polychlorinated Dibenzo-p-dioxins and Dibenzofurans in the Remote North Atlantic Marine Atmosphere. *Environ. Sci. Tech*. 33 (1),14-20.

Barber, J.L.; Sweetman, A.J.; Van Wijk, D.; Jones, K.C. **2005**. Hexachlorobenzene in the global environment: Emissions, levels, distribution, trends and processes. *Sci. Total Environ*. 349(1-3), 1-44.

Bogdal, C.; Schmid, P.; Zennegg, M.; Anselmetti, F.S.; Scheringer, M.; Hungerbühler, K. **2009**. Blast from the past: melting glaciers as a relevant source for persistent organic pollutants. *Environ. Sci. Technol*., 43(21), 8173-8177.

Borgå, K.; Fisk, A.T.; Hoekstra, P.F.; Muir, D.C.G. **2004**. Biological and chemical factors of importance in the bioaccumulation and trophic transfer of persistent organochlorine contaminants in arctic marine food webs. *Environ. Tox. Chem.* 23 (10), 2367–2385.

Cabrerizo, A.; Dachs, J.; Barcelo, D. **2009**. Development of a soil fugacity sampler for determination of airsoil partitioning of persistent organic pollutants under field controlled conditions. *Environ. Sci. Technol*. 43 (21), 8257–8263.

Cabrerizo, A.; Dachs, J.; Barceló, D.; Jones, K.C. **2013**. Climatic and biogeochemical controls on the remobilization and reservoirs of persistent organic pollutants in Antarctica. *Environ. Sci. Technol*. 47(9), 4299-4306.

Cabrerizo, A.; Galbán-Malagón, C.; Del Vento, S.; Dachs, J. **2014**. Sources and fate of polycyclic aromatic hydrocarbons in the Antarctic and Southern Ocean atmosphere. *Glob. Biogeochem. Cycles*, 28, 1424–1436.

Casal, P.; González-Gaya, B.; Zhang, Y.; Reardon, A.J.; Martin, J.W.; Jiménez, B.; Dachs, J. **2017**. Accumulation of perfluoroalkylated substances in oceanic plankton. *Environ. Sci. Technol.* 51(5), 2766-2775.

Dachs, J.; Bayona, J.M.; Fowler, S.W.; Miquel, J.C.; Albaiges, J. **1996**. Vertical fluxes of polycyclic aromatic hydrocarbons and organochlorine compunds in the western Alboran Sea (southwestern Mediterranean). *Mar. Chem*. 52, 75-86.

Dachs, J.; Bayona, J.M.; Albaiges, J. **1997a**. Spatial distribution, vertical profiles and budget of organochlorine compounds in Western Mediterranean seawater. *Mar. Chem*. 57, 313- 324.

Dachs, J.; Bayona, J.M.; Raoux, C.; Albaiges, J. **1997b**. Spatial, vertical distribution and budget of polycyclic aromatic hydrocarbons and organochlorine compounds in the western Mediterranean seawater. *Environ. Sci.Technol*., 31, 682-688.

Dachs, J.; Lohmann, R.; Ockenden, W.A.; Méjanelle, L.; Eisenreich, S.J.; Jones, K.C. **2002**. Oceanic biogeochemical controls on global dynamics of persistent organic pollutants. *Environ. Sci. Technol*. 36, 4229-4237

Dachs J.; Méjanelle L. **2010**. Organic pollutants in coastal waters, sediments, biota: a relevant driver for ecosystems during the anthropocene? *Estuaries Coasts*, 33, 1–14.

Ferreira, M. **2001**. Polycyclic aromatic hydrocarbons: a QSPR study. *Chemosphere* 44, (2), 125-146

Dalla Valle, M.; Jurado, E.; Dachs, J.; Sweetman, A.J.; Jones, K. **2005**. The maximum reservoir capacity of soils for persistent organic pollutans: implications for the global cycling. *Environ. Pollut*. 134, 153–164.

DEFRA. **2004**. Perfluorooctane Sulphonate; Risk Reduction Strategy, Analysis of Advantages, Drawbacks. Department for Environment, Food, Rural Affairs

Del Vento, S.; Halsall, C.; Gioia, R.; Jones, K.; Dachs, J. **2012**. Volatile per- and polyfluoroalkyl compounds in the remote atmosphere of the western Antarctic Peninsula: an indirect source of perfluoroalkyl acids to Antarctic waters. *Atmos. Pollut. Res*. 3 (4), 450−455.

Domine, F.; Cabanes, A.; Legagneux, L. **2002**. Structure, microphysics, and surface area of the Arctic snowpack near Alert during the ALERT 2000 campaign. *Atmos. Environ*. 36(15-16): p. 2753-2765.

EPA. **2003**. Health Effects of PCBs. U.S. Environmental Protection Agency.

Ellis, D.A.; Martin, J.W.; Mabury, S.A.; De Silva, A.O.; Hurley, M.D.; Sulbaek Anderson, M.D.; Wallington, T.J. **2004**. Degradation of fluorotelomer alcohols: a likely atmospheric source of perfluorinated carboxylic acids. *Environ. Sci. Technol*. 38, 3316–3321.

Galbán-Malagón, C.; Berrojalbiz, N.; Ojeda, M.J.; Dachs, J. **2012**. The oceanic biological pump modulates the atmospheric transport of persistent organic pollutants to the Arctic. *Nature comm*. 3, 862.

Galbán-Malagón, C.; Del Vento, S.; Cabrerizo, A.; Dachs, J. **2013**. Factors affecting the atmospheric occurrence and deposition of polychlorinated biphenyls in the Southern Ocean. *Atmos. Chem. Phys*. 13(23), 12029-12041.

Geisz, H.N.; Dickhut, R.M.; Cochran, M.A.; Fraser, W.R.; Ducklow, H.W. **2008**. Melting Glaciers: A Probable Source of DDT to the Antarctic Marine Ecosystem. *Environ. Sci. Technol*. 42, (11), 3958-3962

Giesy, J.P.; Kannan, K. **2001**. Global distribution of perfluorooctane sulfonate in wildlife, *Environ. Sci. Technol*. 35, 1339–1342.

Gioia, R.; Lohmann, R.; Dachs, J.; Temme, Lakaschus, S.; Schulz-Bull, D.; Hand, I.; Jones, K.C. **2008**. Polychlorinated biphenyls in air and water of the North Atlantic and Arctic Ocean. *J. Geophys. Res*. 113, D19302

Gobas, F.A.; de Wolf, W.; Burkhard, L.P.; Verbruggen, E.; Plotzke, K. **2009**. Revisiting bioaccumulation criteria for POPs and PBT assessments. Integrated Environ. Assess. Manag. 5(4), 624-637.

Gregor, D.J.; Gummer, W.D. **1989**. Evidence of atmospheric transport anddeposition of organochlorine pesticidesandpolychlorinated biphenyls in Canadian Arctic snow. *Environ. Sci. Technol*.; 23, 561-565.

Grimalt, J. O.; Fernandez, P.; Berdie, L.; Vilanova, R. M.; Catalan, J.; Psenner, R.; Hofer, R.; Appleby, P. G.; Rosseland, B. O.; Lien, L.; Massabuau, J. C.; Battarbee, R. W. **2001**. Selective Trapping of Organochlorine Compounds in Mountain Lakes of Temperate Areas. *Environ. Sci. Technol*. 35, 2690–2697.

Halsall, C. J.; Barrie, L. A.; Fellin, P.; Muir, D. C. G.; Billeck, B. N.; Lockhart, L.; Rovinsky, F. Y.; Kononov, E. Y.; Pastukhov, B. Spatial and temporal variation of polycyclic aromatic hydrocarbons in the Arctic atmosphere, *Environ. Sci. Technol*. **1997**, 31(12), 3593–3599.

Halsall, C. J.; Bailey, R.; Stern, G. A.; Barrie, L. A.; Fellin, P.; Muir, D. C. G.; Rosenberg F.; Rovinsky, E.; Pastukhov, B. **1998**. Multi-year observations of organohalogen pesticides in the Arctic atmosphere. *Environ. Pollut*. 102(1), 51-62.

Harner, T.; Bidleman, T.F.; Jantunen, L.M.; Mackay, D. **2001**. Soil-Air exchange model of persistent pesticides in the United States Cotton Belt. *Environ. Toxicol. Chem*. 20, 1612–1621.

Harner, T.; Mackay, D. **1995**. Measurement of octanol - air partition coefficients for chlorobenzenes, PCBs, and DDT. *Environ. Sci. Technol*. 29(6), 1599-1606.

Harner, T.; Bidleman, T.F. **1998**. Measurement of Octanol-Air Partition Coefficients for Polycyclic Aromatic Hydrocarbons, Polychlorinated Naphthalenes. *J. Chem. Eng. Data*, 43, (1), 40-46.

Harvey, R.G. **1991**. Polycyclic aromatic hydrocarbons: chemistry and carcinogenicity. CUP Archive: 1991

Head, I. M.; Jones, D. M.; Röling, W. F. M. **2006**. Marine microorganisms make a meal of oil. Nature Reviews Microbiology 4, 173, doi:10.1038/nrmicro1348

Herbert, B.M.J.; Halsall, C.J.; Villa, S.; Jones, K.C.; Kallenborn, R. **2005**. Rapid changes in PCB and OC pesticide concentrations in Arctic snow. *Environ. Sci. Technol*. 39(9), 2998-3005.

Herbert, B.M.J.; Villa, S.; Halsall, C.J. **2006**. Chemical interactions with snow: Understanding the behavior and fate of semi-volatile organic compounds in snow. *Ecotox. Environ. Saf*. 63(1), 3-16.

Hekster, F.M.; Laane, R.W.P.M.; de Voogt, P. **2003**. Environmental and toxicity effects of perfluoroalkylated substances. *Rev. Environ. Contam. Toxicol*. 179, 99−121.

Hinckley, D.A.; Bidleman, T.F.; Foreman, W.T.; Tuschall, J.R. **1990**. Determination of vapor pressures for nonpolar and semipolar organic compounds from gas chromatographic retention data. *J. Chem. Eng. Data*, 35(3), 232-237.

Hulscher, T.E.M.T.; Van der Velde, L.E.; Bruggeman, W.A. **1992**. Temperature dependence of Henry’s law constants for selected chlorobenzenes, polychlorinated biphenyls, polycyclic aromatic hydrocarbons. *Environ. Tox. Chem*. 11, 1595-1603.

Hung, H.; Lee, S.C.; Wania, F.; Blancharda, P.; Briceet, K. **2005**. Measuring and simulating atmospheric concentration trends of polychlorinated biphenyls in the Northern Hemisphere. *Atmos. Environ*. 39, 6502– 6512.

Hung, H.; Katsoyiannis, A. A.; Brorström-Lundén, E.; Olafsdottir, K.; Aas, W.; Breivik, K.; Bohlin-Nizzetto, P.; Sigurdsson, A.; Hakola, H.; Bossi, R.; Skov, H.; Sverko, E.; Enzo, B.; Fellin, P.; Wilson, S. **2016**. Temporal trends of Persistent Organic Pollutants (POPs) in arctic air: 20 years of monitoring under the Arctic Monitoring and Assessment Programme (AMAP). *Environ. Pollut*. 217, 52-61.

Jahnke, A.; Berger, U.; Ebinghaus, R.; Temme, C. **2007**. Latitudinal gradient of airborne polyfluorinated alkyl substances in the marine atmosphere between Germany, South Africa (53 N–S). *Environ. Sci. Technol*. 41, 3055–3061.

Jonker, M.T.; Koelmans A.A. **2001**. Polyoxymethylene Solid Phase Extraction as a Partitioning Method for Hydrophobic Organic Chemicals in Sediment, Soot. *Environ. Sci. Technol.* 35, (18), 3742-3748.

Jonker, M.T.; Koelmans, A.A. **2002**. Sorption of Polycyclic Aromatic Hydrocarbons, Polychlorinated Biphenyls to Soot, Soot-like Materials in the Aqueous Environment: Mechanistic Considerations. *Environ. Sci. Technol*. 36, (17), 3725-3734.

Jurado, E.; Lohmann, R.; Meijer, S.; Jones, K.C.; Dachs, J. **2004**. Latitudinal and seasonal capacity of the surface oceans as a reservoir of polychlorinated biphenyls. *Environ. Pollut*. 128, 149-162

Jurado, E.; Dachs, J. **2008**. Seasonality in the, "grasshopping" and atmospheric residence times of Persistent Organic Pollutants over the oceans. *Geophys. Res. Lett*. 2008GL034698R ,

Kallenborn, R.; Breivik, K.; Eckhardt, S.; Lunder, C.R.; Manø, S.; Schlabach, M.; Stohl, A. **2013**. Long-term monitoring of persistent organic pollutants (POPs) at the Norwegian Troll station in Dronning Maud Land, Antarctica. *Atmos. Chem. Phys*. 13, 6983e6992.

Kallenborn, R.; Oehme, M.; Wynn-Williams, D.D.; Schlabach, M.; Harris, J.; **1998**. Ambient air levels and atmospheric long-range transport of persistent organochlorines to Signy Island, Antarctica. *Sci. Total Environ*. 220, 167e180.

Kannan N.; Tanabe S.; Tatsukawa R. **1988**. Toxic potential of non-ortho, mono-ortho coplanar PCBs in commercial PCB preparations: 2,3,7, 8-T4CDD toxicity equivalence factors approach. *Bull. Environ. Tox. Chem*. 41, 267-276.

Kannan K.; Corsolini S.; Falandysz J.; Fillmann G.; Kumar K.S.; Loganathan B.G.; Ali Mohd M.; Olivero J.; Van Wouwe N.; Ho Yang J.; Aldous K.M. **2004**. Perfluorooctanesulfonate, related fluorochemicals in human blood from several countries. *Environ. Sci. Technol*. 38, 4489–4495.

LaFlamme, R.E.; Hites, R.A. **1978**. Global distribution of polycyclic aromatic hydrocarbons in recent. *Geochimica and Cosmochimica Acta*, 42, (3), 289-303.

Lei, Y.D.; Wania, F. **2004**. Is rain or snow a more efficient scavenger of organic chemicals? *Atmos. Environ*. 38(22), 3557-3571.

Letcher, R.J.; Bustnes, J.O.; Dietz, R.; Jenssen, B.M.; Jørgensen, E.H.; Sonne, C.; Verreault, J.; Vijayan, M.M.; Gabrielsen, G.W. **2010**. Exposure and effects assessment of persistent organohalogen contaminants in arctic wildlife and fish. *Sci. Total Environ.* 408, (15), 2995-3043.

Li, Y.F. **1999**. Global technical hexachlorocyclohexane usage and its contamination consequences in the environment: From 1948 to 1997. *Sci. Total Environ.* 232(3), 121-158.

Li, Y.F.; Bidleman, T.F. **2003**. Correlation between Global Emissions of alpha-hexachlorocyclohexane and its Concentrations in the Arctic Air. *J. Environ. Inform*. 1(1), 52-57.

Li, Y.F.; Macdonald, R.W. **2005**. Sources and pathways of selected organochlorine pesticides to the arctic and the effect of pathway divergence on HCH trends in biota: A review. *Sci. Total Environ.* 342(1-3), 87-106.

Loewen M.; Wania F.; Wang F.; Tomy G. **2008**. Altitudinal transect of atmospheric, aqueous fluorinated organic compounds in western Canada. *Environ. Sci. Technol.* 42, 2374.

Lohmann, R.; Jurado, E.; Pilson, M.E.Q.; Dachs, J. **2006**. Oceanic deep water formation as a sink for persistent organic pollutants. *Geophys. Res. Lett*. 33, L12607

Lohmann, R.; Jurado, E.; Dijkstra, H. A.; Dachs, J. **2013**. Vertical eddy diffusion as a key mechanism for removing perfluorooctanoic acid (PFOA) from the global surface oceans. *Environ. Pollut*. 179, 88-94.

Macdonald, R. W.; Barrie, L. A.; Bidleman, T. F.; Diamond, M. L.; Gregor, D. J.; Semkin, R. G.; Strachan, W. M. J.; Li, Y. F.; Wania, F.; Alaee, M.; Alexeeva, L. B.; Backus, S. M.; Bailey, R.; Bewers, J. M.; Gobeil, C.; Halsall, C. J.; Harner, T.; Hoff, J. T.; Jantunen, L. M. M.; Lockhart, W. L.; Mackay, D.; Muir, D. C. G.; Pudykiewicz, J.; Reimer, K. J.; Smith, J. N.; Stern, G. A.; Schroeder, W. H.; Wagemann, R.; Yunker, M. B. **2000**. Contaminants in the Canadian Arctic: 5 years of progress in understanding sources, occurrence and pathways. *Sci. Total Environ.* 254, (2-3), 93-234.

Mackay, D. **1979**. Finding fugacity feasible. *Environ. Sci. Technol*. 13 (10), 1218–1223

Mackay, D.; Shiu, W.Y.; Ma, K. **1992**. Illustrated handbook of physical-chemical properties and environmental fate for organic chemicals. Volumes I: Monoaromatic Hydrocarbons, chlorobenzenes and PCBs, and II: Polynuclear aromatic Hydrocarbons, Polychlorinated Dioxins, and Benzofurans. Lewis Publishers.

Martin J.W.; Ellis, D.A.; Mabury, S.A.; Hurley, M.D.; Wallington, T.J. **2006**. Atmospheric chemistry of perfluoroalkanesulfonamides: kinetic, product studies of the OH radical, Cl atom initiated oxidation of n-ethyl perfluorobutanesulfonamide. *Environ. Sci. Technol*.; 40, 864– 872.

Martin, J.W.; Mabury, S.A.; Solomon, K.R.; Muir, D.C.G. **2003**. Bioconcentration, tissue distribution of perfluorinated acids in rainbow trout (Oncorhynchus mykiss). *Environ. Toxicol. Chem*. 22, 196–204.

Meyer, T.; Wania, F. **2008**. Organic contaminant amplification during snowmelt. *Water res*. 42(8-9), 1847-1865.

Muir, D.C.G.; Howard, P.H. **2006**. Are there new persistent organic pollutants? A challenge for environmental chemists. *Environ. Sci. Technol*. 40, 7157–7166.

Nash, S. B.; Rintoul, S. R.; Kawaguchi, S.; Staniland, I.; van den Hoff, J.; Tierney, M.; Bossi, R. **2010**. Perfluorinated compounds in the Antarctic region: ocean circulation provides prolonged protection from distant sources. *Environ. Pollut*. 158(9), 2985-2991.

Nash, S. 2011. Persistent organic pollutants in Antarctica: current and future research priorities. *J. Environ. Monit*. 13, (3), 497-504.

Nizzetto, L.; Lohmann, R.; Gioia, R.; Dachs, J.; Jones, K.C. **2010a**. Atlantic Ocean surface waters buffer declining atmospheric concentrations of persistent organic pollutants. *Environ. Sci. Technol*. 44, 6978-6984.

Nizzetto, L.; Macleod, M.; Borga, K.; Cabrerizo, A.; Dachs, J.; Guardo, A.D.; Ghirardello, D.; Hansen, K.M.; Jarvis, Av Lindroth, A.; Ludwig, B.; Monteith, D.; Perlinger, J.A.; Scheringer, M.; Schwendenmann, L.; Semple, K.T.; Wick, L.Y.; Zhang, G.; Jones, K.C. **2010b**. Past, present, and future controls on levels of persistent organic pollutants in the global environment. *Environ. Sci. Technol*. 44, 6526-6531.

Ostertag, S.K.; Tague, B.A.; Humphries, M.M.; Tittlemier, S.A.; Chan, H.M. **2009**. Estimated dietary exposure to fluorinated compounds from traditional foods among Inuit in Nunavut, Canada. *Chemosphere*, 75, 1165–1172.

Petrenko, V.; Whitworth, R. Physics of Ice. **1999**: Oxford University Press.

Rhoads, K.R.; Janssen, E.M.L.; Luthy, R.G.; Criddle, C.S. **2008**. Aerobic biotransformation, fate of n-ethyl perfluorooctane sulfonamidoethanol (n-EtFOSE) in activated sludge, *Environ. Sci. Technol*. 42, 2873–2878

Rigét, F., Bignert, A., Braune, B., Stow, J., Wilson, S. **2009**. Temporal trends of legacy POPs in Arctic biota, an update. *Sci. Total Environ.* 408(15), 2874-2884.

Russell, R.; Gobas, F.A.; Haffner, D. **1999**. Role of chemical and ecological factors in trophic transfer of organic chemicals in aquatic food webs. *Environ. Toxicol. Chem.* 18, 1250- 1257.

Shen, L.; Wania, F. **2005**. Compilation, evaluation, and selection of physicalchemical property data for organochlorine pesticides. *J. Chem. Eng. Data*, 50(3), 742-768.

Shiu W.Y; Mackay D. **1997**. Henry's Law Constants of Selected Aromatic Hydrocarbons, Alcohols, Ketones. *J. Chem. Eng. Data*, 42, (1), 27-30.

Shoeib, M.; Harner, T. **2002**. Using measured octanol-air partition coefficients to explain environmental partitioning of organochlorine pesticides, *Environ. Toxicol. Chem.* 21, 984–990,

Takamatsu, M.; Oki, M.; Maeda, K.; Inoue, Y.; Hirayama, H.; Yoshizuka, K. **1985**. Surveys of Workers Occupationally Exposed to PCBs, of Yusho Patients. *Environ. Health Perspectives,* 59, 91-97.

Vallack, H.W.; Bakker, D.J.; Brandt, I.; Brostrom-Lunden, E.; Brouwer, A.; Bull, K.R.; Gough, C.; Guardans, R.; Holoubek, I.; Jansson, B.; Koch, R.; Kuylenstierna, J.; Lecloux, A.; Mackay, D.; McCutcheon, P.; Mocarelli, P.; Taalman, R.D.F. **1998** Controlling persistent organic pollutants - what next? *Environ. Tox. Pharm.* 6(3), 143-175.

Van den Berg, M.; Birnbaum, L.; Bosveld, A.T.; Brunström, B.; Cook, P.; Feeley, M.; Giesy, J.P.; Hanberg, A.; Hasegawa, R.; Kennedy, S.W.; Kubiak, T.; Larsen, J.C.; van Leeuwen, F.X.; Liem, A.K.; Nolt, C.; Peterson, R.E.; Poellinger, L.; Safe, S.; Schrenk, D.; Tillitt, D.; Tysklind, M.; Younes, M.; Waern, F.; Zacharewski, T. **1998**. Toxic equivalency factors (TEFs) for PCBs, PCDDs, PCDFs for humans, wildlife. *Environ. Health Perspect*. 106, 775–792.

Voldner, E. C. **1995**. Global usage of selected persistent organochlorines. *Sci. Total Environ.* 160-161, 201-210.

Walker, K.; Vallero, D.A.; Lewis, R.G. **1999** actors influencing the distribution of lindane and other hexachlorocyclohexanes in the environment. *Environ. Science and Technology*. 33, 4373-4378.

Wang, Z.; MacLeod, M.; Cousins, I. T.; Scheringer, M.; Hungerbühler, K. **2011**. Using COSMOtherm to predict physicochemical properties of poly-and perfluorinated alkyl substances (PFASs). *Environ. Chem*. 8(4), 389-398.

Wang, Z.; Xie, Z. Y.; Mi, W. Y.; Möller, A.; Wolschke, H.; Ebinghaus, R. **2015**. Neutral poly/per-fluoroalkyl substances in air from the Atlantic to the Southern Ocean and in Antarctic snow. *Environ. Sci. Technol*. 49, 7770−7775.

Wania, F.; Mackay, D. **1993**. Global fractionation and cold condensation of low volatility organochlorine compounds in polar regions. *Ambio*. 10-18.

Wania, F.; Mackay, D. **1996**. Tracking the distribution of persistent organic pollutants. *Environ. Sci. Technol*. 30 (9), 390–396.

Wania, F. **1997**. Modelling the fate of nonpolar organic chemicals in an aging snowpack. *Chemosphere*, 35, 2345-2363.

Wania, F.; Hoff, J. T.; Jia, C. Q.; Mackay, D. **1998**. The effects of snow and ice on the environmental behaviour of hydrophobic organic chemicals. *Environ. Pollut*. 102, 25-41.

Wania, F.; Mackay, D. **1999**. The evolution of mass balance models of persistent organic pollutant fate in the environment. *Environ. Pollut*. 100, 223–240,

Wania, F. **2007**. A global mass balance analysis of the source of perfluorocarboxylic acids in the Arctic Ocean. *Environ. Sci. Technol.* 41, 4529. doi:10.1021/ES070124C

Wickström, K.; Tolonen, K. **1987**. The history of airborne polycyclic aromatic hydrocarbons (PAH) and perylene as recorded in dated lake sediments. *Water, Air Soil Pollution*, 32, 155-175.

Wilcke, W. **2007.** Global patterns of polycyclic aromatic hydrocarbons (PAHs) in soil. *Geoderma*, 141, (3-4), 157-166.

Xiao, H.; Li, N.; Wania, F. **2004**. Compilation, evaluation, and selection of physical-chemical property data for α-, β-, and γ-hexachlorocyclohexane. *J. Chem. Eng. Data*, 49(2), 173-185. DOI 10.1021/je034214i

Xie, Z.; Wang, Z.; Mi, W.; Möller, A.; Wolschke, H.; Ebinghaus, R. **2015**. Neutral poly-/perfluoroalkyl substances in air and snow from the Arctic. *Scientific reports*, 5, 8912.

Yamashita, N.; Kannan, K.; Taniyasu, S.; Horii, Y.; Petrick, G.; Gamo, T. **2005**. A global survey of perfluorinated acids in oceans. *Mar. Pollut. Bull*. 51, 658–668.

Young, C.J.; Furdui, V.I.; Franklin, J.; Koerner, R.M.; Muir, D.C.; Mabury, S.A. **2007**. Perfluorinated acids in arctic snow: new evidence for atmospheric formation. *Environ. Sci. Technol.* 41, 3455. doi:10.1021/ES0626234

Zhang, X. X.; Cheng, S. P.; Cheng-Jun, Z. H. U.; Shi-Lei, S. U. N. **2006**. Microbial PAH-Degradation in Soil: Degradation Pathways and Contributing Factors1. *Pedosphere*, 16(5), 555-565

8.6 Llista d'acrònims

BCF	Factor de bioconcentració
BAF	Factor de bioacumulació
C_A	Concentració a la fase gas
CLRTAP	Conveni sobre la Contaminació Atmosfèrica Transfronterera a Gran Distància
C_P	Concentració al plancton
C_S	Concentració al sòl
CTD	Conductivitat, temperatura, profunditat
C_W	Concentració a l’aigua
EPA	Agència de Protecció Ambiental
f_a	Fugacitat en el aire
F_{AW}	Flux d'aire-aigua
f_{oc}	Fracció de carboni orgànic
f_S	Fugacitat al sòl
F_{Snow}	Flux d'aire-neu
FTOHs	Alcohols de fluorotelomers
f_w	Fugacitat a l'aigua
GC/MS	Cromatografia de gasos acoblada a un espectròmetre de masses
GC-µ-ECD	Cromatografia de gasos acoblada a un detector de captura d’electrons
GF/F	Filtres de fibra de vidre
H’	Constant de Henry adimensional
HCHs	Hexaclorociclohexans
HCB	Hexaclorobencè
JC1	Juan Carlos I
K_{AW}	Coeficient de partició aire-aigua
K_{OA}	Coeficient de partició octanol-aire
K_{OW}	Coeficient de partició octanol-aigua
K_{SA}	Coeficient de partició sòl-aire
LOQs	Límits de quantificació
LRAT	Transport atmosfèric de llarg abast
MSD	Deposició mensual per neu
MW	Pes molecular
NOAA	Administració nacional atmosfèrica i oceànica
OCPs	Pesticides organoclorats
PAHS	Hidrocarburs aromàtics policíclics
PAR	Radiació fotosintéticamente activa
PCBs	Policlorobifenils
PFASs	Substàncies perfluoroalquilades
PFCAs	Àcids perfluoroalquilcarboxílics
PFSAs	Àcids perfluoroalquilsulfònics
PNUMA	Programa de les Nacions Unides per al Medi Ambient
POPS	Contaminants orgànics persistents
Pv	Pressió de vapor
SIM	Seguiment iònic seleccionat
SPE	Extracció en fase sòlida

S_{OCT}	Solubilitat en octanol
SOM	Matèria orgànica del sòl
SVOCs	Compostos orgànics semivolàtils
S_W	Solubilitat en aigua
T	Temperatura
UFLC-MS/MS	Cromatografia líquida ultraràpida acoblada a un espectròmetre de masses
UNECE	Comissió Econòmica de les Nacions Unides per a Europa
Z_A	Capacitat de fugacitat en el aire
Z_S	Capacitat de fugacitat del sòl

8.7 Llista de taules i figures

Agraïments

Serà molt difícil fer uns agraïments sense deixar-se a algú fora. No m'ho tingueu en compte.

Jo no sóc gaire fan del concepte de tesi, entre moltes altres raons perquè sembla donar la idea que tu, com a individu, has fet alguna cosa per la ciència, i no és del tot cert. Les tesis, les fan equips de persones amb un objectiu comú, i tu, com a individu, reculls el fruit del treball d'un equip. Ja sigui per suport logístic, teòric, i en molts casos, moral, aquesta tesi la heu fet possible vosaltres.

Per començar, òbviament, al jefe. Mil gràcies Jordi. Per mil coses. Perquè no em costa un pèl reconèixer que aquesta tesi té molt de "Dachs et al.,". Ha estat un plaer, Houston. Has estat un director de tesi extraordinari des del dia 1. Té mèrit.

Als meus camarades i excamarades d'equip, tant per establir les bases teòriques i pràctiques de la meva feina, com per formar-me i servir-me de referent a l'hora de fer-la. Cristóbal, Ana, Belenchu, Javi, Mari Ca, Maria, Naiara..., moltes gràcies a tots. He après de vosaltres fins a l'últim dia.

Especialment a les meves companyes de despatx, Elena, Gemma i Ali... No, espera, a l'Alicia millor no que em cau malament. Ja pensaves que no ho inclouria, eh? Per qui em prens? Trobaré molt a faltar El Gallinero, els pitis de la Gemma, els dinars, el naranjito, les birres, la guerra de bromes que vaig perdre per pallissa, “perdiendo el hilo” i molt més. Heu vingut a fer 3 tesis espectaculars, i a mi m'heu alegrat el final de la meva.

A Mariana, camarada, porque esta tesis no se hacía sin ti. Y punto. Lo tengo muy presente.

A SuperBego! Desde los muestreos en la Antártida a las revisiones de los papers. Que positivismo y que gustazo trabajar contigo camarada.

I would like to thank Professor Jonathan Martin for the opportunity to be part of his research group in Alberta, as well as for his support and insightful reviews on our

PFASs papers. And to Yifeng Zhang, I’ve said it before, but you know I couldn't have done it without your help. Many thanks.

I would also like to thank Ingjerd Sunde and Athanasios Katsoyiannis for their indispensable support from Tromsø, both in the sampling and comments on the manuscript.

Al personal de la BAE Juan Carlos 1, que segur que està en els agraïments de moltes tesis. Si és inviable fer una tesi sol, és impensable fer res sol a l'Antàrtida. Des del suport logístic tant al mar com a terra, fins al manteniment, la cuina, i alguna desafortunada visita a la infermeria. Gràcies a tots, si em poso a escriure noms aquí dóna per a una altra tesi.

Gracias a mis padres Anton y Esther, y a mi hermano Andrés, por el apoyo y por la paciencia durante todos estos años, que no ha sido poca.

Gracias a Ruxi, Lali, Yoshi, Nestorius, Arkos, Black, Estel, Angie, Smigol, Jaba... sin vosotros seguramente habría tardado menos en escribir esta tesis. O la habría abandonado. Una de las dos, no os pongais tiernos.

A Mar, contigo hasta el asilo, Lizana. A Bizcochito, por ser la primera persona en inspirarme a dedicarme a la ciencia. A Carmen, por todo el apoyo durante tantos años. A Marina, por que nuestro próximo proyecto sea codo con codo. Y a Terelu, por sacarme de más de un pozo, te prometo que te echaré un cabo siempre que caigas tú en alguno.

Gracias a todos.

UPC
idæa
INSTITUT DE DIAGNOSI AMBIENTAL I ESTUDIS DE L'AIGUA
CSIC
CONSEJO SUPERIOR DE INVESTIGACIONES CIENTÍFICAS